

# **FIELD HYDROLOGY AND MODEL PREDICTIONS FOR FINAL COVERS IN THE ALTERNATIVE COVER ASSESSMENT PROGRAM - 2002**

by

Arthur C. Roesler and Craig H. Benson  
University of Wisconsin-Madison

William H. Albright  
Desert Research Institute

Geo Engineering Report No. 02-08

Geo Engineering Program  
University of Wisconsin-Madison  
Madison, Wisconsin 53706 USA

September 20, 2002

## EXECUTIVE SUMMARY

The water balance of twenty-one landfill final cover test sections has been evaluated in this study. Each of the test sections is being monitored as part of the United States Environmental Protection Agency's Alternative Cover Assessment Program. The test sections are located at ten sites across the United States in climates ranging from arid to humid. Water balance predictions for seventeen of the test sections have been made using the models HELP and UNSAT-H, which are commonly used for evaluating the hydrology of final covers. Most of the climatic, soil, and vegetative inputs to the models were measured in the field or laboratory. For those inputs where measurements did not exist, estimates were made based on information in the literature.

The alternative covers in arid and semi-arid climates generally are transmitting significantly less percolation than the alternative covers in humid climates. Percolation rates for the alternative covers in arid and semi-arid climates typically are less than 1 mm/yr. The exception is the thin monolithic barrier in Sacramento, which has transmitted percolation at an average rate of 48 mm/yr. For the humid sites, percolation from the alternative covers typically is between 37 and 144 mm/yr. Percolation rates for the alternative covers in humid climates should decrease over time as the vegetation matures, and is capable of removing more soil water. For example, 170 mm of percolation was measured during the first nine months following construction of the alternative cover at Albany, GA. The percolation rate then decreased to less than 6 mm/yr as the poplar trees on the cover matured.

Data from the test sections simulating a composite cover (i.e., a geosynthetic clay liner or compacted clay barrier overlain by a geomembrane) indicate that these covers are very effective when constructed properly. Percolation rates for the composite covers are generally less than 1 mm/yr in semi-arid and arid regions, and 5 mm/yr in humid regions. Data from the test sections simulating compacted clay covers show that clay barriers are highly susceptible to desiccation cracking and can transmit percolation at large rates (several hundred mm/yr).

Predictions of the water balance made with HELP and UNSAT-H generally were not accurate even though the parameters used as input were well-defined. Discrepancies between field conditions and model predictions were related to the prediction of surface runoff, frozen ground conditions, preferential flow, and uncertainty in vegetation characteristics. Initial simulations that were conducted with "as constructed" input parameters (i.e. saturated hydraulic conductivity,

runoff curve number) greatly over-predicted surface runoff, which resulted in the subsequent flow processes being incorrect. Hydraulic conductivity of the surface layer was measured on specimens collected immediately after construction that probably did not include macroscopic features (desiccation and freeze-thaw cracks, root holes, worm holes, etc.) that affect the saturated hydraulic conductivity at field scale. Therefore, additional simulations were conducted using an “adjusted” saturated hydraulic conductivity and runoff curve number for the surface layer. Model predictions improved when the surface layer was more permeable, but the predictions were still inconsistent over time. Also, modeling of frozen ground conditions appears to be significant at sites in cooler climates if surface runoff due to melt water is to be predicted accurately.

Modeling of the long-term performance of compacted clay covers does not appear to be possible without significantly increasing the saturated hydraulic conductivity of the barrier layer to account for preferential flow through desiccation cracks. For composite covers, HELP predicted little percolation would occur, which is expected in arid and semi-arid climates. However, HELP under-predicted percolation from composite covers at sites in humid climates, even when placement conditions were degraded, and the defect frequency was increased. Also, HELP typically over-predicted lateral flow for covers that incorporated a drainage composite, and under-predicted lateral flow for covers that did not incorporate a drainage composite.

## **ACKNOWLEDGMENTS**

Financial support for this study was provided by the United States Environmental Protection Agency (USEPA) through a subcontract with the Bureau of Economic Geology of the State of Texas. Dr. Bridget Scanlon was the project director for the Bureau of Economic Geology of the State of Texas. Mr. David Carson was the program manager for USEPA. The field data were provided by USEPA's Alternative Cover Assessment Program, which is managed at USEPA by Mr. Steven Rock. This report has not been subjected to USEPA's review. Endorsement by USEPA is not implied, and should not be assumed. Each of the sites in ACAP has made considerable contributions to this effort. Assistance that has been provided by the site owners and managers is greatly appreciated.

## TABLE OF CONTENTS

EXECUTIVE SUMMARY .....	i
ACKNOWLEDGEMENTS .....	iii
TABLE OF CONTENTS .....	iv
LIST OF TABLES .....	vi
LIST OF FIGURES .....	xi
1.0 INTRODUCTION .....	1
2.0 TYPES OF FINAL COVERS .....	3
3.0 ALTERNATIVE COVER ASSESSMENT PROGRAM (ACAP) .....	8
3.1 ACAP Lysimeter .....	9
3.1.1 Cover Placement .....	9
3.1.2 Soil Monitoring Instrumentation .....	15
3.1.3 Water Flow Monitoring System .....	17
3.1.4 Meteorological Measurements .....	20
3.2 Test Facilities .....	20
3.2.1 Altamont Site .....	20
3.2.2 Cedar Rapids Site .....	28
3.2.3 Omaha Site .....	29
3.2.4 Boardman Site .....	30
3.2.5 Sacramento Site .....	31
3.2.6 Polson Site .....	31
3.2.7 Helena Site .....	32
3.2.8 Albany Site .....	33
3.2.9 Marina Site .....	34
3.2.10 Monticello Site .....	34
4.0 ACAP FIELD RESULTS .....	36
4.1 Altamont Site .....	39
4.2 Sacramento Site .....	44
4.3 Helena Site .....	49
4.4 Polson Site .....	54
4.5 Boardman Site .....	62
4.6 Marina Site .....	68
4.7 Albany Site .....	73
4.8 Cedar Rapids Site .....	79
4.9 Omaha Site .....	90
4.10 Monticello Site .....	99

5.0	EVALUATION OF WATER BALANCE MODELS .....	106
5.1	Water Balance Computations .....	106
5.2	HELP Model Formulation .....	107
5.3	UNSAT-H Model Formulation .....	111
5.4	Input Data .....	113
5.4.1	Meteorological Data .....	113
5.4.2	Initial Conditions .....	115
5.4.3	Hydraulic Properties .....	115
5.4.4	Geosynthetic Properties .....	122
5.4.5	Vegetation Data .....	124
5.4.6	Design Input .....	133
5.4.7	Simulation Control Parameters for UNSAT-H .....	133
5.5	Comparison Between Actual and Simulation Results .....	138
5.5.1	Alternative Covers .....	146
5.5.2	Conventional Covers .....	180
5.6	Parametric Study .....	200
5.6.1	Surface Runoff Curve Number in HELP .....	201
5.6.2	Saturated Hydraulic Conductivity of Barrier Layer in HELP .....	201
5.6.3	Geomembrane Properties in HELP .....	204
5.6.4	Maximum Leaf Area Index .....	208
5.6.5	Growing Season in HELP .....	213
6.0	SUMMARY AND CONCLUSIONS .....	216
6.1	Summary of Percolation Rates .....	216
6.1.1	Percolation from Alternative Covers .....	216
6.1.2	Percolation from Conventional Covers .....	218
6.2	Model Predictions .....	220
6.2.1	Prediction of Surface Runoff .....	221
6.2.2	Percolation from Alternative Covers .....	221
6.2.3	Lateral Flow and Percolation from Conventional Covers .....	222
6.3	Practical Implications .....	223
7.0	REFERENCES .....	225
APPENDICES		
A1.	CORRECTIONS TO ET CALCULATIONS .....	228
A2.	LAI GRAPHS FOR ACAP SITES .....	232
A3.	FACTORS AFFECTING SURFACE RUNOFF IN FIELD .....	241
A4.	WATER BALANCE GRAPHS OF ORIGINAL UNSAT-H SIMULATIONS .....	243
A5.	WATER BALANCE GRAPHS OF ORIGINAL HELP SIMULATIONS .....	255

## LIST OF TABLES

Table 2.1	Landfill Cover Designs Required by RCRA Subtitle D .....	4
Table 3.1	Profile of Each Cover Being Evaluated by ACAP .....	25
Table 3.2	Vegetation Mixture Used at Each Site .....	27
Table 4.1	Summary of Water Balance Data: Arid and Semi-Arid Sites.....	37
Table 4.2	Summary of Water Balance Data: Humid Sites .....	38
Table 4.3	Hydraulic Properties of the Alternative Cover at the Cedar Rapids Site ..	85
Table 4.4	Hydraulic Properties of the Compacted Clay Cover at the Cedar Rapids Site .....	85
Table 4.5	Hydraulic Properties of the Composite Cover at the Cedar Rapids Site ..	85
Table 4.6	Hydraulic Properties of the Composite Cover at the Monticello Site .....	104
Table 5.1	Meteorological Inputs for HELP .....	114
Table 5.2	Hydraulic Properties Input to UNSAT-H.....	116
Table 5.3	Hydraulic Properties Input to HELP .....	118
Table 5.4	Transpiration Parameters Input to UNSAT-H.....	120
Table 5.5	Vegetation Input Parameters for HELP.....	123
Table 5.6	Parameters for LAI Functions for UNSAT-H .....	126
Table 5.7	Rates of Root Growth Input to UNSAT-H.....	131
Table 5.8	RLD Function at ACAP Sites .....	132
Table 5.9	Runoff Curve Numbers Computed by HELP.....	135
Table 5.10	Design Inputs for HELP and UNSAT-H.....	136
Table 5.11	Surface Runoff Predictions From Original and Adjusted Simulations Using UNSAT.....	139
Table 5.12	Surface Runoff (SRO) Predictions From Original and Adjusted Simulations Using HELP .....	140

Table 5.13	Water Balance Quantities Predicted by HELP for Compacted Clay Cover at Albany Site for Various Surface Runoff Curve Numbers (CN) .....	202
Table 5.14	Water Balance Quantities Predicted by HELP for ECap Cover at Albany Site for Various Surface Runoff Curve Numbers (CN) .....	202
Table 5.15	Water Balance Quantities Predicted by HELP for Alternative Cover at Helena Site <sup>a</sup> for Various Surface Runoff Curve Numbers (CN) .....	203
Table 5.16	Water Balance Quantities Predicted by HELP for Compacted Clay Cover at Albany Site for Various Saturated Hydraulic Conductivities of the Barrier Layer .....	203
Table 5.17	Effect of Placement Condition and Hole Frequency for Geomembrane on Predictions Made with HELP for Composite Covers at Omaha .....	205
Table 5.18	Effect of Placement Condition and Hole Frequency for Geomembrane on Predictions Made with HELP for Composite Covers at Marina .....	206
Table 5.19	Water Balance Quantities Predicted by HELP for ECap Cover at Albany Site (Humid) for Various Maximum LAI .....	209
Table 5.20	Water Balance Quantities Predicted by HELP for Thick Monolithic Barrier Cover at Sacramento Site (Semi-Arid) for Various Maximum LAI .....	209
Table 5.21	Water Balance Quantities Predicted by HELP for Alternative Cover at Helena Site (Arid) for Various Maximum LAI .....	210
Table 5.22	Water Balance Quantities Predicted by UNSAT-H for Thin Monolithic Barrier Cover at Sacramento Site for Various Maximum LAI .....	212
Table 5.23	Water Balance Quantities Predicted by UNSAT-H for Alternative Cover at Helena Site (Arid) for Various Maximum LAI .....	212
Table 5.24	Water Balance Quantities Predicted by HELP for Thick Monolithic Barrier Cover at Sacramento Site (Semi-Arid) for Various Growing Season Dates .....	214
Table 5.25	Water Balance Quantities Predicted by HELP for Alternative Cover at Helena Site (Arid) for Various Growing Season Dates .....	214
Table 6.1	Summary of Percolation Rates: Alternative Covers .....	217
Table 6.2	Summary of Percolation Rates: Conventional Covers .....	219



## LIST OF FIGURES

Fig. 2.1	Typical Alternative Cover Designs: (a) Monolithic Barrier and (b) Capillary Barrier .....	7
Fig. 3.1	Schematic of ACAP Test Section and Lysimeter: (a) Plan View and (b) Cross-Section .....	10
Fig. 3.2	Photograph of Lysimeter “Box” Constructed with LLDPE Geomembrane at Cedar Rapids Site. Base is Covered with Geocomposite Drain.....	11
Fig. 3.3	Placement of Soil on Top of Geocomposite Drainage Layer at the Boardman Site.....	13
Fig. 3.4	Tow-Behind Tamping Foot Compactor Used to Compact a Clay Barrier Layer at the Cedar Rapids Site.....	14
Fig. 3.5	Placing Root Barrier on Top of Interim Cover Soil at the Sacramento Site ..	16
Fig. 3.6	Schematic of Collection Basin with Dosing Siphon Used to Monitor Flows .	18
Fig. 3.7	Typical Cross-Section of Sumps Used to Collect Percolation, Interflow, and Surface Runoff.....	19
Fig. 3.8	Weather Station Installed at the Cedar Rapids Site.....	21
Fig. 3.9	Locations of ACAP Test Sections .....	22
Fig. 3.10	Cover Profiles of Conventional Covers Being Evaluated by ACAP .....	23
Fig. 3.11	Cover Profiles of Alternative Covers Being Evaluated by ACAP .....	24
Fig. 4.1	Cumulative Water Balance for the Altamont Site: (a) Conventional Cover and (b) Alternative Cover .....	40
Fig. 4.2	Soil Water Storage in Test Covers at the Altamont Site.....	42
Fig. 4.3	Soil Water Storage of Individual Layers in (a) Conventional Cover and (b) Alternative Cover .....	43
Fig. 4.4	Cumulative Water Balance at the Sacramento Site: (a) “Thin” Monolithic Barrier and (b) “Thick” Monolithic Barrier .....	45
Fig. 4.5	Surface Runoff Occurring in Response to Topsoil Water Content: “Thin” Monolithic Barrier .....	47

Fig. 4.6	Soil Water Storage for the Monolithic Barriers: (a) “Thin” and (b) “Thick” ....	48
Fig. 4.7	Cumulative Water Balance at the Helena Site .....	50
Fig. 4.8	Soil Temperatures and Surface Runoff for Alternative Cover at the Helena Site.....	52
Fig. 4.9	Soil Water Storage for the Alternative Cover at the Helena Site .....	53
Fig. 4.10	Cumulative Water Balance at the Polson Site: (a) Alternative Cover and (b) Conventional Cover .....	55
Fig. 4.11	Soil Water Storage for the Covers at the Polson Site .....	57
Fig. 4.12	SWS in Each Layer at Polson Site: (a) Alternative Cover (b) Conventional Cover .....	58
Fig. 4.13	Percolation from the Alternative and Conventional Covers at Polson Site...	60
Fig. 4.14	Soil Water Suction Measurements Adjacent to Capillary Break in the Alternative Cover .....	61
Fig. 4.15	Cumulative Water Balance at the Boardman Site: (a) Conventional Cover and (b) “Thin” Monolithic Barrier .....	63
Fig. 4.16	Cumulative Water Balance at the Boardman Site: Thick Monolithic Barrier.	64
Fig. 4.17	Soil Water Storage for All Covers at the Boardman Site.....	66
Fig. 4.18	Volumetric Water of Soil Layers at Boardman Site: (a) Thin Monolithic Barrier and (b) “Thick” Monolithic Barrier.....	67
Fig. 4.19	Cumulative Water Balance at the Marina Site: (a) Conventional Cover and (b) Alternative Cover .....	69
Fig. 4.20	Soil Water Storage in (a) Conventional Cover and (b) Alternative Cover.....	71
Fig. 4.21	Soil Water Storage of Individual Soil Layers for the Alternative Cover .....	72
Fig. 4.22	Cumulative Water Balance at the Albany Site: (a) Conventional Cover and (b) Alternative Cover .....	75
Fig. 4.23	Soil Water Storage Record at the Albany Site: (a) Conventional Cover and (b) Alternative Cover .....	77
Fig. 4.24	Percolation at the Albany Site.....	78

Fig. 4.25	Cumulative Water Balance at the Cedar Rapids Site: (a) Composite Barrier and (b) Compacted Clay Barrier .....	80
Fig. 4.26	Cumulative Water Balance at the Cedar Rapids Site: Monolithic Barrier.....	81
Fig. 4.27	Soil Temperatures in Test Covers: (a) Monolithic Barrier and (b) Composite Barrier .....	83
Fig. 4.28	Soil Water Storage at Cedar Rapids Site.....	84
Fig. 4.29	Soil Water Storage of Topsoil Layer and Cumulative Percolation for the Composite Cover at the Cedar Rapids Site .....	87
Fig. 4.30	Soil Water Storage in Soil Layers at Cedar Rapids Site: (a) Compacted Clay Barrier and (b) Composite Barrier Soil Layers .....	88
Fig. 4.31	Percolation from Test Covers at Cedar Rapids Site .....	91
Fig. 4.32	Cumulative Water Balance at the Omaha Site: Conventional Cover .....	92
Fig. 4.33	Cumulative Water Balance at the Omaha Site: (a) Thin Capillary Barrier (760 mm) and (b) Thick Capillary Barrier (1060 mm).....	93
Fig. 4.34	Soil Temperature in Conventional Cover at the Omaha Site .....	96
Fig. 4.35	Soil Water Storage at the Omaha Site .....	97
Fig. 4.36	Soil Water Storage and Percolation at Omaha Site: (a) Thin Capillary Barrier (760 mm) and (b) Thick Capillary Barrier (1060 mm).....	98
Fig. 4.37	Percolation at the Omaha Site .....	100
Fig. 4.38	Cumulative Water Balance for the Alternative Cover at Monticello Site.....	101
Fig. 4.39	Alternative Cover at the Monticello Site: (a) Soil Water Storage, and (b) Water Content in the Individual Layers .....	103
Fig. 5.1	LAI Function Input to UNSAT-H for Polson Site.....	129
Fig. 5.2	Root Length Density Functions Measured at ACAP Sites with Upper and Lower Bounds Defined by Winkler (1999).....	134
Fig. 5.3	Schematic of Typical Nodal Spacing Used in UNSAT-H.....	137

Fig. 5.4	Surface Layer Adjustment for Alternative Covers at Sacramento Site Using UNSAT-H.....	143
Fig. 5.5.	Surface Layer Adjustment for ECap Cover at Albany Site: (a) UNSAT-H and (b) HELP .....	145
Fig. 5.6.	Comparison of Water Balance Data for the Altamont Site to Predictions Made with UNSAT-H and HELP: (a) Surface Runoff, (b) Soil Water Storage, (c) Evapotranspiration, and (d) Percolation.....	147
Fig. 5.7.	Comparison of Water Balance Data for the Sacramento Site (Thin Monolithic Barrier) to Predictions Made with UNSAT-H and HELP: (a) Surface Runoff, (b) Soil Water Storage, (c) Evapotranspiration, and (d) Percolation .....	150
Fig. 5.8.	Comparison of Water Balance Data for the Sacramento Site (Thick Monolithic Barrier) to Predictions Made with UNSAT-H and HELP: (a) Surface Runoff, (b) Soil Water Storage, (c) Evapotranspiration, and (d) Percolation.....	151
Fig. 5.9.	Soil Water Storage Predicted by HELP and Measured in Field for the Thin Monolithic Barrier at the Sacramento Site.....	153
Fig. 5.10.	Comparison of Water Balance Data for the Helena Site to Predictions Made with UNSAT-H and HELP: (a) Surface Runoff, (b) Soil Water Storage, (c) Evapotranspiration, and (d) Percolation.....	156
Fig. 5.11.	Comparison of Water Balance Data for the Polson Site to Predictions Made with UNSAT-H and HELP: (a) Surface Runoff, (b) Soil Water Storage, (c) Evapotranspiration, and (d) Percolation.....	159
Fig. 5.12.	Measured Surface Runoff and Predictions by HELP for the Alternative Cover at Polson Using Original and Adjusted Parameters for the Surface Layer.	160
Fig. 5.13.	Field Data and Predictions from HELP and UNSAT-H for the Thin Monolithic Barrier at the Boardman Site: (a) Evapotranspiration and (b) Soil Water Storage .....	163
Fig. 5.14.	Field Data and Predictions from HELP and UNSAT-H for the Thick Monolithic Barrier at the Boardman Site: (a) Evapotranspiration and (b) Soil Water Storage .....	164
Fig. 5.15.	Field Data and Predictions by HELP for the Thick Monolithic Barrier at the Boardman Site Using Adjusted Wilting Point and LAI Parameters: (a) Evapotranspiration and (b) Soil Water Storage.....	166

- Fig. 5.16. Comparison of Water Balance Data for the Marina Site to Predictions Made with UNSAT-H and HELP Using First Parameter Set: (a) Surface Runoff, (b) Soil Water Storage, (c) Evapotranspiration, and (d) Percolation..... 167
- Fig. 5.17. Comparison of Water Balance Data for the Alternative Cover at the Marina Site to Predictions Made with HELP Using Adjusted van Genuchten and LAI Parameters: (a) Soil Water Storage and (b) Percolation..... 170
- Fig. 5.18. Comparison of Water Balance Data at the Marina Site and Predictions Made with UNSAT-H Using Adjusted Parameters: (a) Surface Runoff, (b) Soil Water Storage, (c) Evapotranspiration, and (d) Percolation..... 172
- Fig. 5.19. Comparison of Water Balance Data for the Albany Site to Predictions Made with UNSAT-H and HELP: (a) Surface Runoff, (b) Soil Water Storage, (c) Evapotranspiration, and (d) Percolation..... 174
- Fig. 5.20. Comparison of Water Balance Data for the Omaha Site (Thin Monolithic Barrier) to Predictions Made with UNSAT-H and HELP: (a) Surface Runoff, (b) Soil Water Storage, (c) Evapotranspiration, and (d) Percolation ..... 177
- Fig. 5.21. Comparison of Water Balance Data for the Omaha Site (Thick Monolithic Barrier) to Predictions Made with UNSAT-H and HELP: (a) Surface Runoff, (b) Soil Water Storage, (c) Evapotranspiration, and (d) Percolation ..... 178
- Fig. 5.22. Comparison of Water Balance Data for the Altamont Site (Composite Cover) to Predictions Made with HELP: (a) Surface Runoff, (b) Soil Water Storage, (c) Evapotranspiration and (d) Lateral Flow ..... 181
- Fig. 5.23. Comparison of Water Balance Data for the Polson Site (Composite Cover) to Predictions Made with HELP: (a) Surface Runoff, (b) Evapotranspiration, (c) Lateral Flow, and (d) Percolation ..... 184
- Fig. 5.24. Comparison of Soil Water Storage Measured at Polson Site (Composite Cover) to Predictions Made with HELP ..... 186
- Fig. 5.25. Comparison of Water Balance Data for the Boardman Site (Composite Cover) to Predictions Made with HELP: (a) Surface Runoff, (b) Soil Water Storage, (c) Evapotranspiration, and (d) Lateral Flow..... 188
- Fig. 5.26. Comparison of Water Balance Data for the Marina Site (Composite Cover) to Predictions Made with HELP: (a) Surface Runoff, (b) Evapotranspiration, (c) Lateral Flow, and (d) Percolation ..... 191
- Fig. 5.27. Comparison of Soil Water Storage at the Marina Site (Composite Cover) and Predictions Made with HELP ..... 193

- Fig. 5.28. Comparison of Water Balance for the Albany Site (Compacted Clay Cover) to Predictions Made with UNSAT-H and HELP: (a) Surface Runoff, (b) Evapotranspiration, and (c) Percolation ..... 195
- Fig. 5.29. Comparison of Soil Water Storage for the at Albany Site (Compacted Clay Cover) to Predictions Made with (a) HELP and (b) UNSAT-H ..... 196
- Fig. 5.30. Comparison of Water Balance Data for the Omaha Site (Composite Cover) to Predictions Made with HELP: (a) Surface Runoff, (b) Evapotranspiration, (c) Lateral Flow, and (d) Percolation ..... 198
- Fig. 5.31. Comparison of Soil Water Storage at the Omaha Site (Composite Cover) and Predictions Made with HELP ..... 199

## **SECTION ONE INTRODUCTION**

The U.S. Environmental Protection Agency (USEPA) has developed guidance for design, construction, operation, and maintenance of final covers for landfills. Final covers constructed based on these guidelines (typically referred to as “conventional covers”) have traditionally relied on hydraulic barrier layers having low saturated hydraulic conductivity to reduce the amount of water percolating into the underlying waste. Due to the higher cost associated with prescriptive final covers, as well as their questionable performance in certain climates, alternative landfill cover designs are being explored.

Alternative covers typically rely on a combination of soil and vegetation to restrict percolation rather than relying on hydraulic barrier layers. For an alternative cover to perform as well as a prescriptive cover, the soil must be able to store water long enough to allow the atmosphere and vegetation to remove the water via evaporation and transpiration. Because evaporation and transpiration are important processes affecting their performance, alternative covers are often referred to as evapotranspiration (ET) covers. They are also referred to as “vegetative covers” or “store-and-release” covers.

This study relied on field data from USEPA’s Alternative Cover Assessment Program (ACAP), which is evaluating twenty-one cover designs throughout the United States in climates ranging from arid to humid. Each cover is being evaluated for 5 years. The purpose of ACAP is to collect field-scale data regarding the hydrology of prescriptive and alternative covers that can be used for model evaluations, development of design guidance, and improvement of regulations (Bolen et al. 2001). This study had

three objectives: (1) to analyze the ACAP field data and to make preliminary assessments, (2) to compare predictions made with two water balance models (UNSAT-H and HELP) to the field data for each cover, and (3) to perform a parametric study using the two water balance models to determine which parameters have a significant effect on water balance predictions. This report describes the findings of this study.



## **SECTION TWO TYPES OF FINAL COVERS**

Minimum standards for landfill liners and covers are listed in the United States Code of Federal Regulations (CFR), and are broken into two categories depending on the type of landfill. Subtitle D of the Resource Conservation and Recovery Act (RCRA) is for municipal solid waste (MSW) landfills, and Subtitle C is for hazardous waste landfills. The United States Environmental Protection Agency (USEPA) has also issued guidance on the design of landfills. The guidance is intended to clarify the regulations, and to assist the designer.

The cover designs described in RCRA depend on the design of the bottom liner, with the intention of preventing the “bath-tub” effect. The cover must have a hydraulic conductivity less than or equal to the hydraulic conductivity of any bottom liner or natural subsoils. Clarifications to the requirements of Subtitle D that were issued by USEPA match cover designs with liner designs (USEPA 1992). These cover designs are summarized in Table 2.1.

Subtitle D permits alternative covers if the alternative cover can be shown to be equally effective in reducing the rate of percolation into the underlying waste, as well as having equivalent resistance to erosion. Typical alternatives designs do not rely on a hydraulic barrier with a specific hydraulic conductivity, but rather on a combination of soil and vegetation to prevent water from percolating into the waste. This type of cover is also referred to as an evapotranspiration cover (or “ET” cover), a vegetative cover, or a store-and-release cover.

Table 2.1. Landfill Cover Designs Required by RCRA Subtitle D.

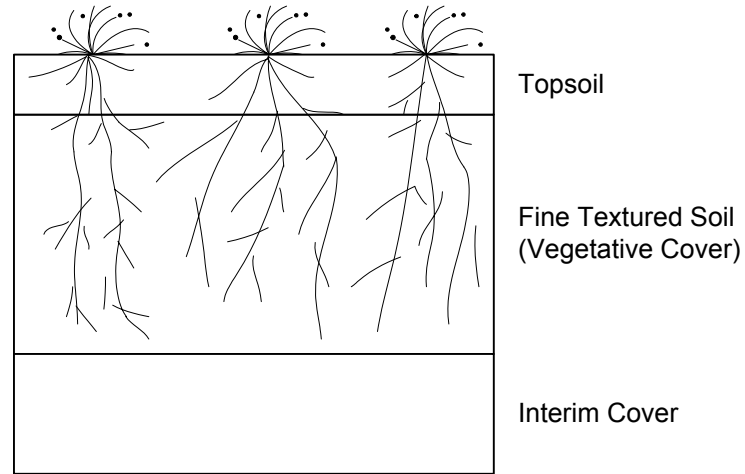
Category	Liner	Cover Requirement
A	No Liner.	150 mm erosion layer; 460 mm barrier layer with $K_s^a < 10^{-5}$ cm/s or $K_s$ of underlying soils, whichever is smaller.
B	Soil Liner with $K_s < 10^{-6}$ cm/s.	150 mm erosion layer; 460 mm barrier layer with $K_s < 10^{-6}$ cm/s.
C	Soil Liner with $K_s < 10^{-7}$ cm/s.	150 mm erosion layer; 460 mm barrier layer with $K_s < 10^{-7}$ cm/s.
D	Composite liner (soil layer having a $K_s < 10^{-7}$ cm/s overlain by geomembrane).	150 mm erosion layer; geomembrane; 460 mm barrier layer with $K_s < 10^{-5}$ cm/s.

<sup>a</sup> $K_s$  = saturated hydraulic conductivity

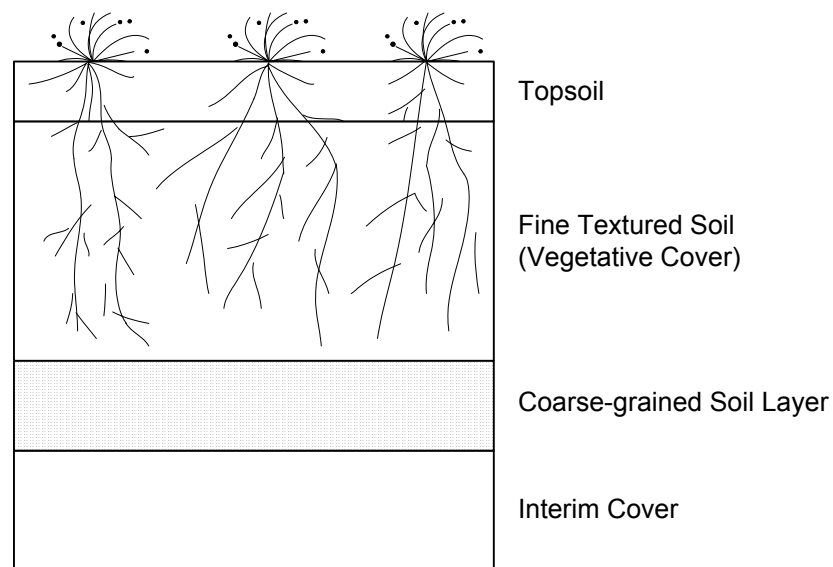
Alternative covers balance the hydrological processes (e.g., precipitation, surface runoff, soil water storage, evaporation, and transpiration) so as to limit percolation to an acceptable amount (Khire et al. 2000). Fine textured soils are used to store the infiltrating water, which is later removed by evaporation from the soil surface or by transpiration by plants. An effective alternative cover provides balance between the storage capacity of the soil and the water removal capabilities provided by the local climate and the vegetation. A mixture of native grasses, shrubs, and/or trees is used to take advantage of the varying growing seasons so that the number of days during which transpiration occurs is maximized.

In arid to semi-arid regions of the country, where potential ET typically exceeds precipitation, plants often are capable of using all the available moisture in the soil profile (Anderson et al. 1987, Hauser et al. 1994). As a result, the soil is rendered an empty reservoir to store infiltrating water in the cooler and wetter months. The type of soil plays an important role. Finer textured soils are generally suitable, because they can have substantial soil water storage capacity. In contrast, even under the most ideal plant and climatic scenario, soils with a low water storage capacity (e.g. coarse textured soils with little fines) are unlikely to be effective as a storage medium in an ET cover.

Several types of alternative cover designs have been evaluated. Two common designs (Fig. 2.1) are monolithic and capillary barriers. A monolithic barrier consists of a single layer of finer textured soil. A capillary barrier consists of finer textured layer overlying a coarse-grained soil. The contrast in unsaturated hydraulic properties between the two layers in a capillary barrier forms a capillary break that limits downward water movement in a capillary barrier (Khire et al. 2000).



(a)



(b)

Fig. 2.1. Typical Alternative Cover Designs: (a) Monolithic Barrier, (b) Capillary Barrier .

### **SECTION THREE ALTERNATIVE COVER ASSESSMENT PROGRAM**

USEPA's Alternative Cover Assessment Program (ACAP) was created to (i) provide data to support the development of an effective cover for each individual test site, (ii) provide data to support the development of guidelines for alternative cover designs throughout the country, and (iii) provide data to support the development of improved models for designers and regulators (Bolen et al. 2001).

During the initial phase of ACAP, twenty-one test sections were constructed at ten sites throughout the United States to evaluate similar cover designs in differing climates. Each site is proposing to use an alternative earthen final cover (AEFC). At least one AEFC test section was constructed at each site. The AEFC was designed by the owner, or an engineering consultant working for the owner, with input from the ACAP investigators. At eight of the sites, alternative and conventional cover designs are being compared side by side. Design of the conventional covers was based on regulations stipulated by the regulatory agencies having jurisdiction at each site. Each test section is to be monitored for a period of at least 5 years.

Performance of each cover is being evaluated by measuring the percolation rate. Other hydrological processes are also being measured, such as precipitation, surface runoff, lateral flow, and soil water content to calculate the water balance of each test section. Disturbed and undisturbed soil samples were collected during construction to determine the physical and hydraulic properties of the soils. A description of the testing that was conducted can be found in Bolen et al. (2001) and Gurdal (2002).

### **3.1 ACAP LYSIMETER**

To evaluate each cover design, a large-scale lysimeter was constructed using linear-low density polyethylene (LLDPE) geomembrane and a geocomposite drain (Benson et al. 2001). Each lysimeter had an areal extent of 10 m by 20 m (Fig. 3.1). The slope varied from site to site, and was between 5 and 25%. The lysimeter was constructed from several geomembrane panels that were welded together to form a “box” (Fig. 3.2).

Non-destructive testing was performed on each geomembrane seam to ensure the lysimeter was leak tight. A geocomposite drain was then placed above the base of the lysimeter on top of the geomembrane to direct any percolation through the cover to the sump. To ensure the drainage sump and associated plumbing was leak free, a leak test was performed by ponding water on the downstream end of the lysimeter, creating a small head on the drainage sump. The elevation of the water was monitored for any leaks for approximately one hour using a standpipe attached to the end of the drainage pipe. A description of the installation methods can be found in Benson et al. (1999).

#### **3.1.1 Cover Placement**

Soil was placed inside the test section using typical construction equipment (Fig. 3.3) following specifications described in Benson et al. (1999). A nuclear gauge was used to check compaction of each soil lift. Alternative cover soils typically were placed at 85% of maximum dry unit weight per standard Proctor, while compacted soil barriers were compacted as specified by the designer. To ensure uniform and adequate compaction, the maximum lift thickness was 460 mm, although thinner lifts were used for the conventional covers. Also, the surface elevation of each lift was surveyed to

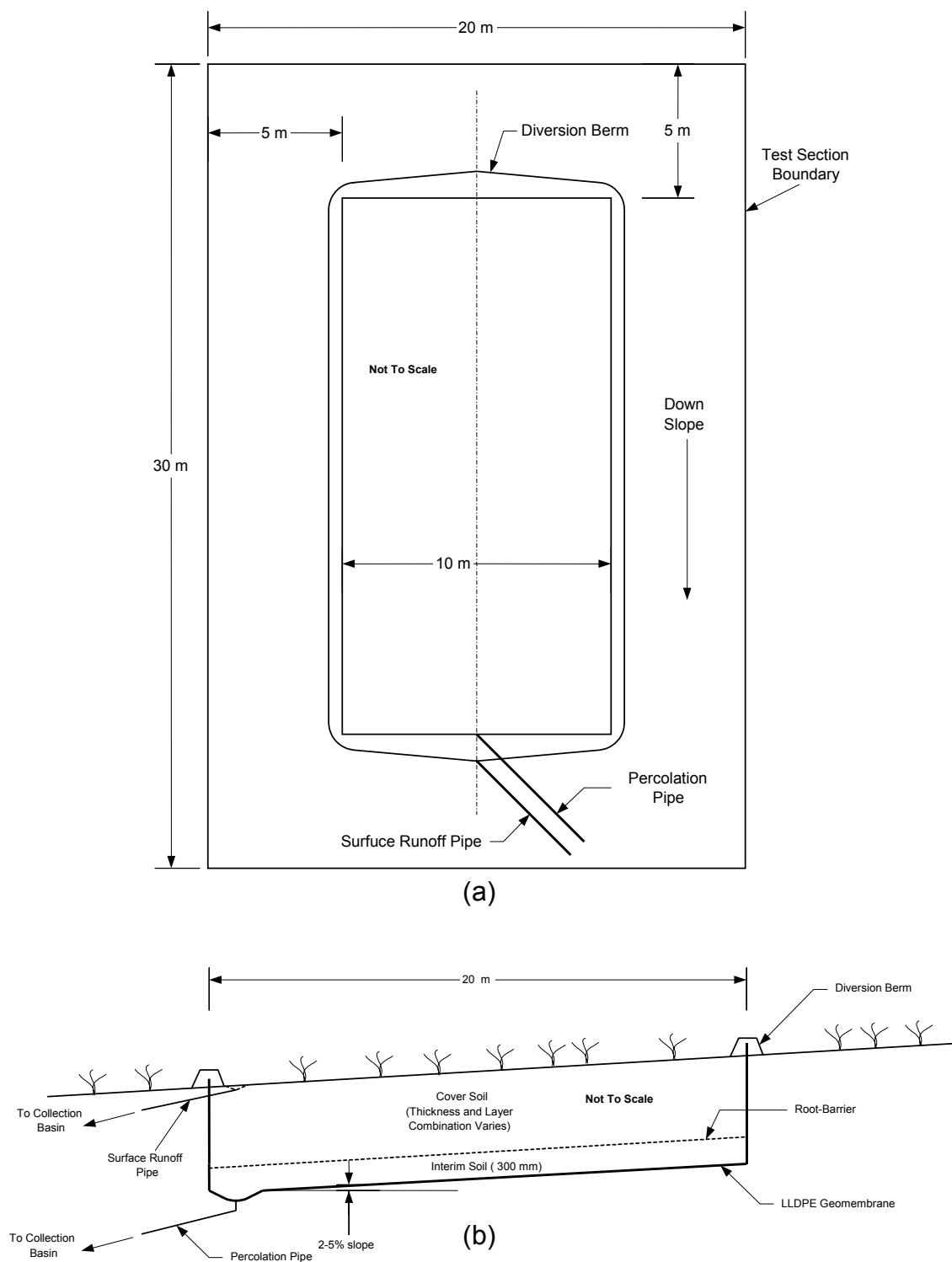


Fig. 3.1. Schematic of ACAP Test Section and Lysimeter: (a) Plan View and (b) Cross-Section.



Fig. 3.2. Photograph of Lysimeter “Box” Constructed with LLDPE Geomembrane at Cedar Rapids Site. Base is Covered with Geocomposite Drain.



replicate the level of control likely to exist during full-scale construction of final covers.

The first soil layer placed inside the lysimeter was an interim cover layer simulating the soil likely to exist over the waste prior to construction of the cover. A geosynthetic root barrier was placed on top of the interim cover soil (Fig. 3.5). The root barrier is a non-woven geotextile containing nodules impregnated with the root inhibitor trifluralin, which prevents penetration of roots into the geocomposite drain and other elements of the system used to collect percolation (Burton et al. 1986). Water in these elements would not normally be available for uptake by plants. The root barrier also provides a well-defined lower boundary for root penetration, since the root-barrier controls the rooting depth for all vegetation types (i.e. shrubs, trees, or grasses). The cover profile was constructed on top of the root barrier.

To achieve the necessary saturated hydraulic for barrier layers in the test sections simulating conventional covers, additional compactive effort and moisture conditioning generally were performed. To increase the compactive effort, a heavy tamping foot compactor was typically used (Fig. 3.4). Compaction was controlled using a compaction specification defined by the site owner. If a geomembrane was to be placed on top of a clay barrier layer, a smooth-drum roller was used to provide good contact between the soil layer and geomembrane. Once the cover geomembrane was installed, a single circular hole with a diameter of 11 mm (100 m<sup>2</sup> area) was placed in the center of the geomembrane to simulate an installation defect.

To prevent preferential flow along the sidewalls of the lysimeter, dry bentonite was placed along the geomembrane-soil interface during soil placement. A jumping-jack or vibrating plate compactor was also run along the inside of the sidewalls to ensure good compaction along the sidewall of the lysimeter.



Fig. 3.3. Placement of Soil on Top of Geocomposite Drainage Layer at the Boardman Site.



Fig. 3.4. Tow-Behind Tamping Foot Compactor Used to Compact a Clay Barrier Layer at the Cedar Rapids Site.

### 3.1.2 Soil Monitoring Instrumentation

Water content of the soils is measured using CS615 water content reflectometers (WCR) manufactured by Campbell Scientific Inc. (CSI). A WCR consists of two parallel rods (300 mm long, 32 mm spacing) attached to an electronic signal generator. The water content of material surrounding the conductors influences the speed of an electromagnetic wave displaced along the rods. As the dielectric constant of the soil increases, the wave propagates more slowly. Because the dielectric constant of water is much higher than that of most other materials, an electromagnetic wave propagates slower in a wet or moist soil than in the same soil when dry. A WCR measures the round-trip travel time of the electromagnetic wave, which is calibrated against water content (Campbell and Anderson 1998). Calibrations for the WCRs can be found in Kim (2002). Kim (2002) also found that the WCR measurements are sensitive to temperature, and that calibration equations should require a temperature correction. Temperature corrections were not incorporated in this study, will be in future work.

Soil matric suction is measured with heat dissipation units (HDU) manufactured by CSI. HDUs consist of a heat source and a temperature sensor contained within a porous ceramic housing (Phene et al. 1971). A thermocouple monitors dissipation of a heat pulse generated by a resistive heating element, and reports a temperature differential ( $\Delta T$ ) over a 29 s period. Heat dissipation is a function of the water content of the ceramic housing, which is assumed to be in equilibrium with the matric suction of the surrounding soil. A calibration relating soil matric suction and  $\Delta T$  was determined for each sensor by the Desert Research Institute. The initial temperature reading of the HDU was taken as ambient temperature of the soil.



Fig. 3.5. Placing Root Barrier on Top of Interim Cover Soil at the Sacramento Site.



### 3.1.3 Water Flow Monitoring System

The bottom of each test section is sloped ( $\geq 2\%$ ) toward the centerline. The primary axis of the lysimeter is aligned with the natural slope of the setting to allow percolation to collect in a sump. Collected water is conveyed through a boot in the geomembrane to a collection basin containing a redundant system with three devices to measure flow. Volume of percolation is measured by a tipping bucket, a pressure transducer, and a float switch. The float switch is used to identify when a collection basin is flushed. Each flush corresponds to the same volume of water ( $\sim 90$  L). A dosing siphon is used to flush the basin.

The primary means of measuring flow is with the float switch, because the tipping bucket is only able to measure low flows accurately. A pressure transducer located at the bottom of the collection basin measures the elevation (or stage) of the water (Fig. 3.6), and is used to confirm that a flush of the dosing siphon has occurred. The precision of the percolation measurements made with each instrument is described in Benson et al. (2001).

Surface runoff berms were constructed around the perimeter of each test section to prevent run-on, as well as to facilitate the collection of run-off (Fig. 3.7). Runoff is routed to a collection basin with a similar measurement system as the percolation basin, except that a tipping bucket is not used. For test sections with a drainage layer and/or a cover geomembrane, interflow is collected and measured using a system similar to that used for measuring runoff.

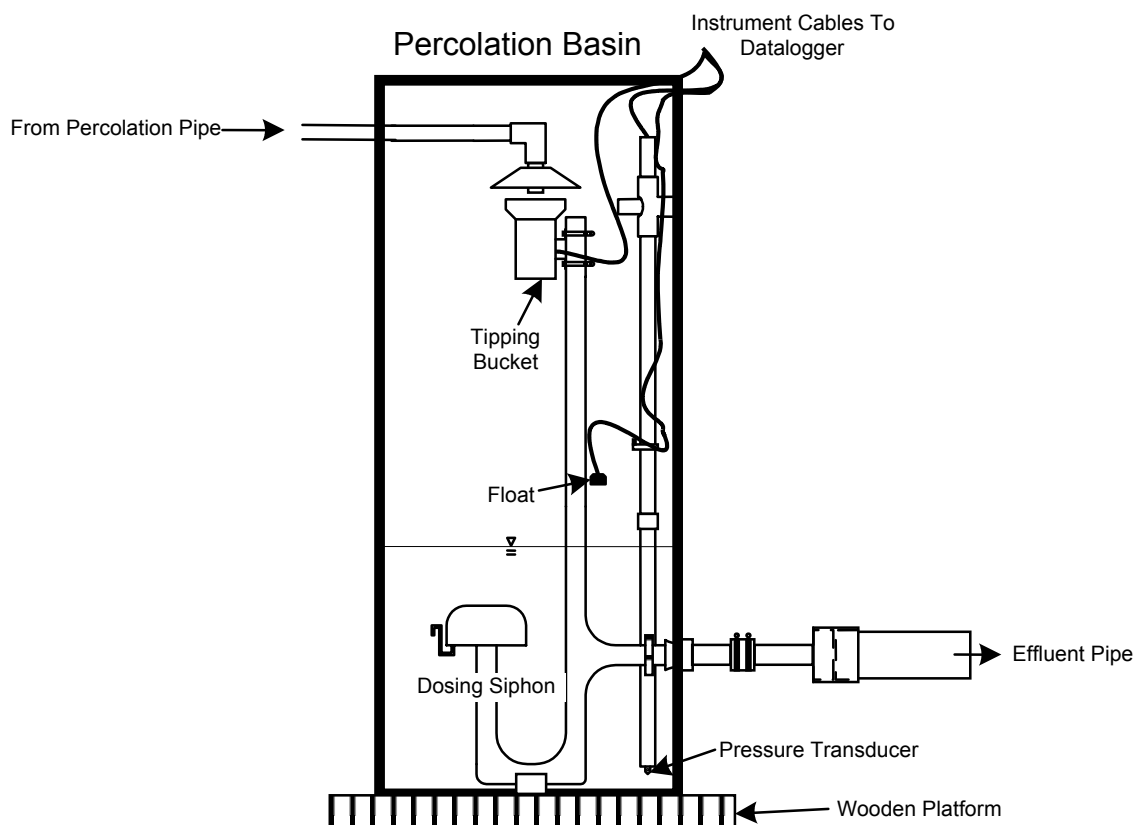


Fig. 3.6. Schematic of Collection Basin with Dosing Siphon Used to Monitor Flows.

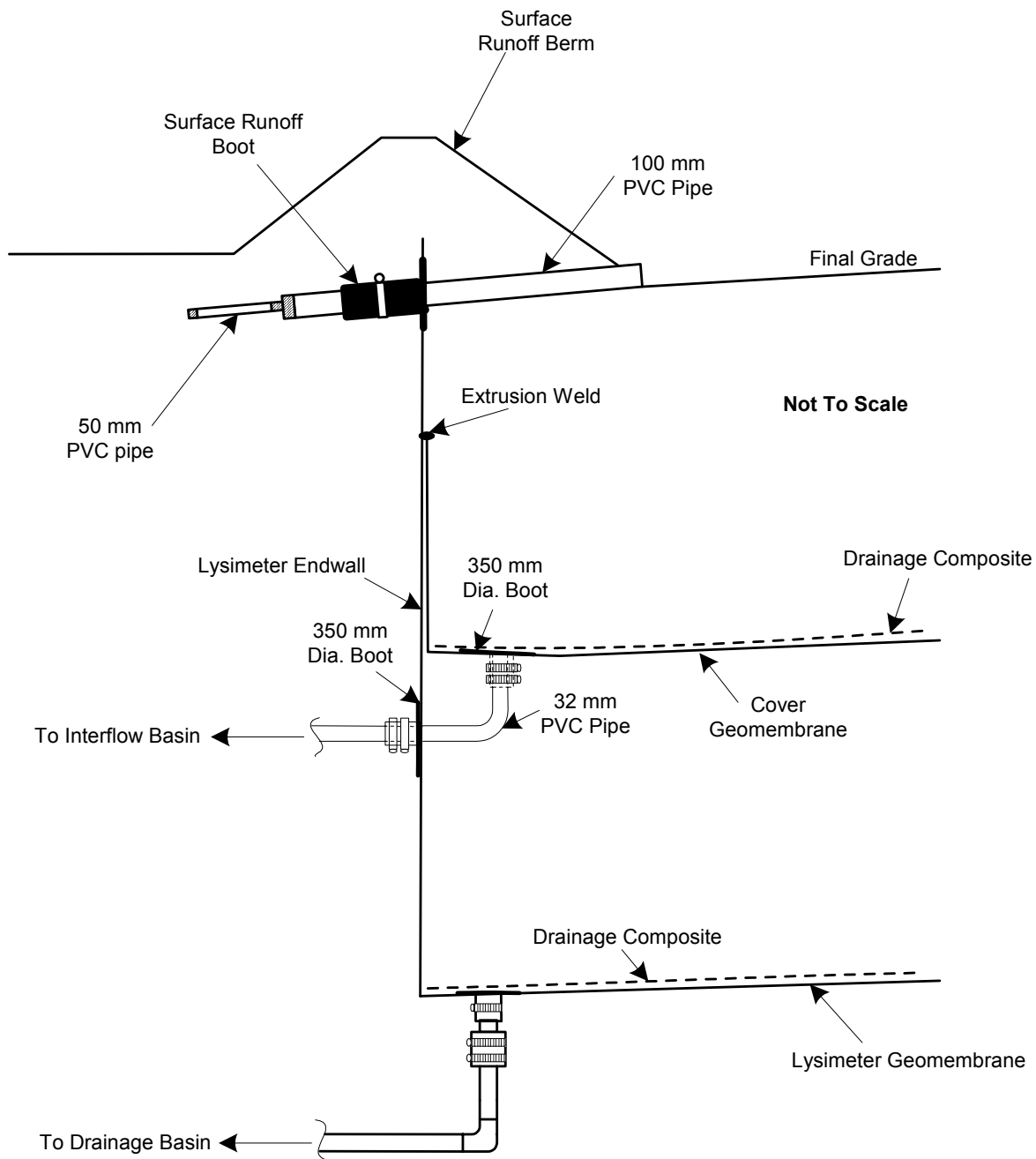


Fig. 3.7. Typical Cross-Section of Sumps Used to Collect Percolation, Interflow, and Surface Runoff.



### **3.1.4 Meteorological Measurements**

A CSI weather station (Fig. 3.8) was installed at each site to monitor local meteorological conditions. Wind speed and direction, air temperature, relative humidity, solar radiation, and precipitation are being measured.

## **3.2 TEST FACILITIES**

Twenty-one test sections were constructed at ten sites (Fig. 3.9) across the United States. At five of the sites, two test sections were constructed to compare a conventional cover and an alternative cover. At three of the sites, three test sections were constructed to compare multiple conventional and/or alternative covers. At two of the sites, only one test section (an alternative cover) was constructed.

The majority of the cover soils came from on-site borrow areas. The vegetation generally was chosen to be representative of native vegetation at the site. A detailed summary of all sites can be found in Bolen et al. (2001). An illustration of the cover profiles for each site is shown in Figures 3.10 and 3.11. A description of the profile of each test section is in Table 3.1. The seed mixtures for each site is in Table 3.1.

### **3.2.1 Altamont Site**

The Altamont site is located in the Altamont Hills near the City of Livermore, CA approximately 64 km east of the San Francisco Bay. The conventional final cover design, as dictated by Title 27 of the California Code of Regulations, is a composite barrier.



Fig. 3.8. Weather Station Installed at the Cedar Rapids Site.

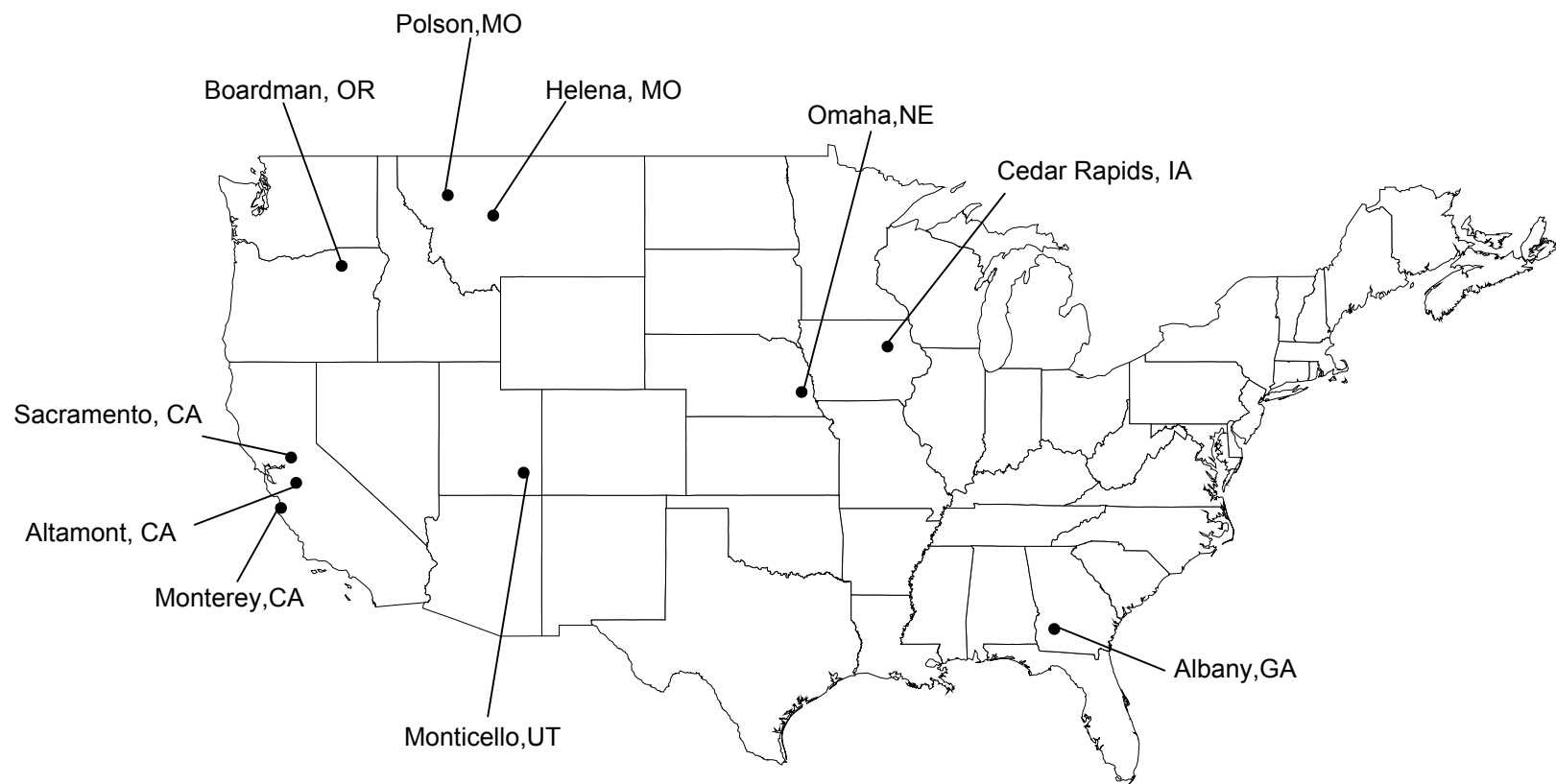


Fig. 3.9. Locations of ACAP Test Sections.

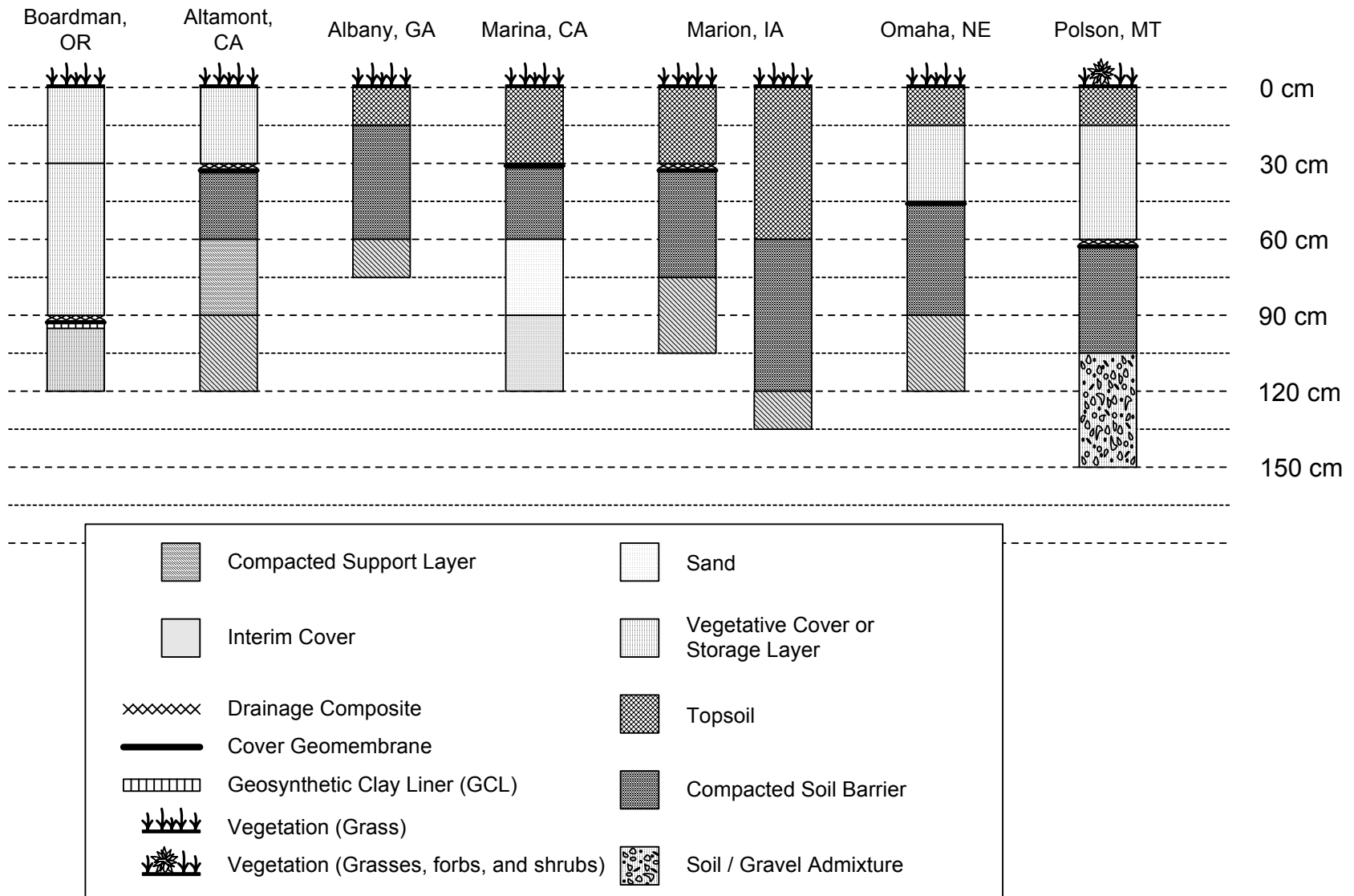


Fig. 3.10. Cover Profiles of Conventional Covers Being Evaluated by ACAP.

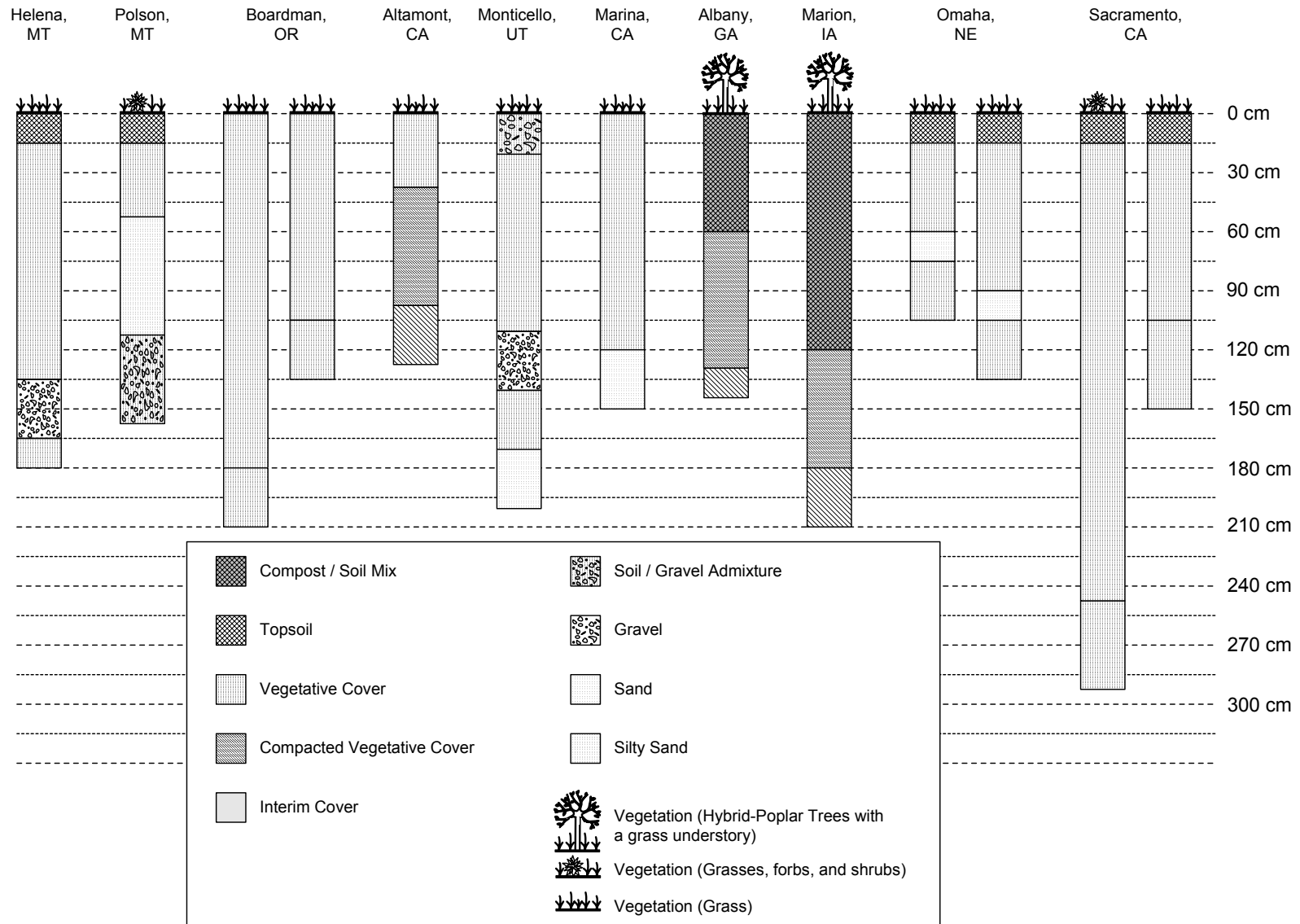


Fig. 3.11. Cover Profiles of Alternative Covers Being Evaluated by ACAP.

Table 3.1. Profile of Each Cover Being Evaluated by ACAP.

Site	Test Section	Layer	Description	Material <sup>a</sup>
Omaha Site	Capillary Barriers	Topsoil	Lean clay with organics	CL
		Storage Layer	Lean clay	CL
		Sand	Clean sand (Poorly graded)	SP
		Interim Cover	Lean clay	CL
	Composite Barrier	Topsoil	Lean Clay with organics	CL
		Vegetative Layer	Lean clay	CL
		Geomembrane	-	1.0 mm HDPE
		Compacted Soil Barrier	Lean clay	CL
Albany Site	Compacted Clay Barrier	Topsoil	Clayey sand	SC
		Compacted Soil Barrier	Clayey sand	SC
		Interim Cover	Clayey sand	SC
	Monolithic Barrier	Soil / Compost Mix	Clayey sand	SC
		Support Layer	Clayey sand	SC
		Interim Cover	Clayey sand	SC
Altamont Site	Composite Barrier	Topsoil	Lean clay	CL
		Drainage Composite	-	GT/GN/GT <sup>b</sup>
		Geomembrane	-	1.5 mm HDPE
		Compacted Soil Barrier	Lean clay	CL
		Foundation Layer	Lean clay	CL
	Monolithic Barrier	Interim Cover	Lean clay	CL
		Storage Layer	Lean clay	CL
		Support Layer	Lean clay	CL
Cedar Rapids Site	Composite Barrier	Topsoil	Lean clay with sand	CL w/ organic matter
		Drainage Composite	-	GT/GN/GT
		Geomembrane	-	1.0 mm LLDPE
		Compacted Soil Barrier	Sandy lean clay	CL
		Interim Cover	Sandy lean clay	CL
	Compacted Clay Barrier	Topsoil	Lean clay with sand	CL w/ organics matter
		Compacted Soil Barrier	Fat clay with sand	CH
		Interim Cover	Sandy lean clay	CL
	Monolithic Barrier	Soil / Compost Mix	Clayey sand	SC-CL w/ organic matter
		Support Layer	Sandy lean clay	CL
		Interim Cover	Sandy lean clay	CL

<sup>a</sup>Unified Soil Classification System, <sup>b</sup>GT/GN/GT corresponds to a geocomposite drainage layer consisting of a geonet between two non-woven geotextiles.

Table 3.1. Profile of Each Cover Being Evaluated by ACAP (*continued*).

Site	Test Section	Layer	Description	Material <sup>a</sup>
Boardman Site	Monolithic Barriers	Storage Layer	Silt with sand	ML
		Interim Cover	Silt with sand	ML
	Composite Barrier	Vegetative Layer	Silt with sand	ML
		Drainage Composite	-	GT/GN/GT
		Geomembrane	-	1.5 mm LLDPE
		Geosynthetic Clay Liner	-	Bentomat
		Interim Cover	Silt with sand	ML
Helena Site	Monolithic Barrier	Topsoil	Clayey sand with gravel	SC w/ organic matter
		Storage Layer	Clayey sand - Sandy fat clay	SC-CH
		Gas Vent Layer	Poorly graded gravel with silty clay	GP-GC
		Interim Cover	Clayey sand - Sandy fat clay	SC-CH
Sacramento Site	Monolithic Barriers	Topsoil	Sandy lean clay with gravel	SC-SM
		Storage Layer	Clayey sand, silty sand	CL, SC
		Interim Cover	Clayey sand	SC-CL
Marina Site	Composite Barrier	Vegetative Soil	Clayey sand	SC
		Geomembrane	-	1.5 mm LLDPE
		Compacted Soil Barrier	Fat clay	CH
	Monolithic Barrier	Interim Cover	Poorly graded sand w/ silt	SP-SM
		Storage Layer	Clayey sand	SC
		Interim Cover	Poorly graded sand w/ silt	SP-SM
Polson Site	Composite Barrier	Topsoil	Silty sand	SM
		Vegetative Layer	Silty sand	SM
		Drainage Composite	-	GT/GN/GT
		Geomembrane	-	1.5 mm LLDPE
		Compacted Soil Barrier	silty clay	CL-ML
		Interim Cover	Poorly graded gravel with sand	GP
	Capillary Barrier	Topsoil	Silty sand	SM
		Storage Layer	Silty clay	CL-ML
		Coarse-Grained Layer	Silty sand	SM
		Interim Cover	Poorly graded gravel with sand	GP
Monticello Site	Alternative	Soil / Gravel Admixture	Clayey gravel with sand	GC
		Storage Layer	Lean clay with sand	CL
		Bio-Intrusion Layer	Gravel	GC
		Fine-Grained Layer	Lean clay with sand	CL
		Coarse-Grained Layer	Clean sand (Poorly graded)	SP

<sup>a</sup>Unified Soil Classification System, <sup>b</sup>GT/GN/GT corresponds to a geocomposite drainage layer consisting of a geonet between two non-woven geotextiles.

Table 3.2. Vegetation Mixture Used at Each Site.

Site	Seed Mixture
Omaha	Cool Season Grasses: Brome and Switchgrasses
Albany	Bermuda Grass, Perennial Rye, and Eastern Cottonwood and Black Poplar, Imperial Carolina DN-34 (ECap only)
Altamont	Soft chess, slender oats, foxtail chess, Italian ryegrass, red-stemmed filaree, black mustard, yellow star-thistle, prickly lettuce, bull thistle, prickly sow-thistle, blue dicks, California poppy, purple owl's-clover, and miniature lupine
Cedar Rapids	Indian Grass, Little Bluestem, Big Bluestem, Side Oats, and Switch Grass, Tall Fescue Lawn Mix, and Crown Vetch
Boardman	Siberian, Bluebunch, and Thickspike Wheatgrasses, Alfalfa, and Yellow Blossom Sweetclover
Helena	Bluebunch, Slender, and West Wheatgrasses, Sandburg Bluegrass, Sheep Fescue, Blue Gamma, Green Needlegrass, and Needle-and-Thread
Sacramento	California Brome, Purple Needlegrass, Zorro Fescue, Arroyo Lupin, and Oleander bushes.
Marina	Blue Wild Rye, California Brome, Creeping Wild Rye, and Pacific Hairgrass
Polson	Thickspike, Bluebunch, Slender, and Crested Wheatgrasses, Mountain Brome, Idaho Fescue, Prairie Junegrass, Needle-and-Thread, Meadow Brome, Canada and Kentucky Bluegrasses, Yarrow, Fringed Sagewort, Alfalfa, Rubber Rabbitbrush, Prickly Rose, Arrowleaf Balsamroot, and Dolted Gayfeather, Lewis Flax, and Silky Lupine, and Cicer Milkvetch
Monticello	Western and Crested Wheatgrasses, Gray Rabittbrush, Sagebrush, Pinyon, and Juniper



The conventional cover was constructed with a 300 mm foundation layer and a 300 mm barrier layer (saturated hydraulic conductivity,  $K_s$ , less than  $1 \times 10^{-6}$  cm/s) underlying a 1.5 mm thick smooth HDPE geomembrane, drainage composite, and a 300 mm vegetative layer. The alternative cover was constructed with a 600-mm compacted “support layer” and a 460 mm “storage layer,” which effectively act together as a 1060 mm storage layer. Both covers overlay 300 mm of soil simulating interim cover.

All soil layers were constructed with crushed Panoche claystone from a nearby borrow area. To promote root growth, the storage, storage, and interim cover layers were compacted to 85% of maximum dry unit weight per standard Proctor. The support layer in the alternative cover was compacted between 90 and 95% of maximum dry unit weight per standard Proctor. The top layers of both test sections were seeded with grasses that currently exist on-site (see Table 3.2).

### **3.2.2 Cedar Rapids Site**

The Cedar Rapids site is located in Marion, IA, outside of Cedar Rapids. The bottom liner of the existing landfill consists of a compacted clay barrier, whereas the bottom liner of an expansion of the landfill will consist of a RCRA Subtitle D composite barrier. Therefore, two conventional covers that meet the RCRA Subtitle D criteria (as interpreted by the Iowa Department of Natural Resources) for the existing and expansion portions of the landfill were constructed, along with an alternative cover.

The composite cover consists of a 600 mm compacted clay layer ( $K_s \leq 1 \times 10^{-7}$  cm/s) overlain by a 1.0 mm thick textured LLDPE geomembrane, a drainage composite,

and a 150 mm layer of topsoil. The compacted clay cover consists of 600 mm of compacted clay ( $K_s \leq 1 \times 10^{-7}$  cm/s) and a 600 mm layer of topsoil. The alternative cover, also known as an ECap, consists of a 600 mm support layer and a 920 mm storage layer. All test sections overlay 300 mm of soil simulating interim cover.

All soil layers were constructed with soil (sandy lean clay) from a nearby borrow area. The soil used for the storage layer in the alternative cover is mixture of borrow soil (95%) and compost (5%). The compost consists of composted paper mill sludge, leaves, grass clippings, and corn hulls. The topsoil layers were stripped from the same borrow area as the clay, and had higher organic content.

Both covers were seeded with a mixture of native grasses (see Table 3.2). The alternative cover was also vegetated with two-year old hybrid poplar trees. The hybrid poplar trees were 4.5 m tall prior to planting, and were placed in 600 mm deep trenches. Additional rows of hybrid poplars were planted around the alternative test section as a perimeter buffer to minimize 'edge effects' caused by wind, humidity, and light, which makes the alternative test section more representative of a large-scale ECap.

### **3.2.3 Omaha Site**

The Omaha site is located in Bennington, NE, just outside of Omaha. The existing landfill employs two types of bottom liners that consist of a RCRA Subtitle D compacted clay barrier and a composite barrier. The final cover for the expansion of the Omaha site is a RCRA Subtitle D cover with a composite barrier. Therefore, a conventional cover with a composite barrier is being tested along side two alternative

covers. The two alternative covers contain a capillary break to enhance soil water storage in the storage layer.

The conventional cover consists of a 460 mm barrier layer ( $K_s \leq 1 \times 10^{-5}$  cm/s), a 1.0 mm thick smooth HDPE geomembrane, a 460 mm vegetative layer, and a 150 mm layer of topsoil. The two alternative covers were constructed with a 150 mm layer of clean sand, a storage layer (460 mm and 760 mm thick), and a 150-mm-thick layer of topsoil. All of the covers overlay 300 mm of soil simulating an interim cover.

The interim covers, storage layers, and compacted barrier layers were constructed from lean clay (Peorian Loess) from a nearby borrow area. The clean sand was delivered to the site from a local quarry. The topsoil layers were stripped from the same borrow area as the clay, and had higher organic content. Vegetation established on each test cover consisted of a mixture of native warm and cool season grasses (see Table 3.2).

### **3.2.4 Boardman Site**

The Boardman site is located 16 km south of Boardman, OR, in the vicinity of Finley Buttes. The existing landfill is lined with a RCRA Subtitle D conventional design consisting of a composite barrier. The soil component of the liner is a geosynthetic clay liner (GCL). The covers being tested at the Boardman site are a conventional cover (consisting of a composite barrier with a GCL), and two alternative covers.

The conventional cover consists of a GCL, 1.0 mm thick textured geomembrane, drainage composite, 600 mm of vegetative cover, and 300 mm of topsoil. The alternative covers tested at Boardman are monolithic barriers, consisting of a single

storage layer (1220 mm or 1840 mm). All cover profiles overlay a 300 mm soil layer simulating an interim cover.

All soil layers were constructed with Sagehill sandy silt from a nearby borrow area. All covers were seeded with indigenous grasses that are common in the non-irrigated rangelands in the area (see Table 3.2).

### **3.2.5 Sacramento Site**

The Sacramento site is located in eastern Sacramento County, approximately 24 km southeast of the Sacramento, CA metropolitan area. Older portions of the existing landfill are unlined, whereas newer portions are lined with a RCRA Subtitle D composite barrier.

The two covers being evaluated at the Sacramento site are alternative covers (monolithic barriers), and differ only in thickness (1.2 m and 2.4 m). Both covers were constructed using soil (interbedded sandy silts, clays, and fine sands) from a nearby borrow area, and are underlain by an interim cover layer 300 mm thick. A mixture of native grasses was used as the vegetation for both covers (see Table 3.2).

### **3.2.6 Polson Site**

The Polson site is located approximately 4.8 km southwest of Polson, MT, within the boundaries of the Flathead Indian Reservation. The existing landfill is unlined. Plans for an expansion included a liner system with a RCRA Subtitle D composite barrier using a GCL. Two covers are being tested at the Polson site, a conventional cover with a composite cover and an alternative cover containing a capillary barrier.

The conventional cover consists of 460 mm of compacted fine-grained soil ( $K_s \leq 10^{-5}$  cm/s), a 1.5 mm thick textured LLDPE textured geomembrane, a drainage composite, a 460 mm vegetative layer, and 150 mm of topsoil. The alternative cover consists of 600 mm of silty sand, 460 mm of silt, and 150 mm of topsoil. Both covers overlay 460 mm of sandy gravel that serves as interim cover and as a gas vent.

The vegetative layer for the conventional cover and the coarse-grained layer in the alternative cover were constructed with fine sand from a borrow area on-site. The compacted soil barrier and the storage layer (alternative cover) were constructed with non-plastic silt from a local source off-site. Both covers were seeded with a mixture of native and introduced grasses, forbs, and shrubs (see Table 3.2).

### **3.2.7 Helena Site**

The Helena site is located in southeastern Lewis and Clark County, approximately 16 km northeast of Helena, MT. The existing landfill is lined with a RCRA Subtitle D composite barrier. The alternative cover being tested at the Helena site is an alternative cover containing a capillary barrier. The cover consists of a 300 mm gravel gas-venting layer, 1200 mm of native soil, and 150 mm of topsoil. To simulate an interim cover, the final cover overlays 150 mm of native sandy clay from a nearby borrow area. The gravel was delivered to the site from a local quarry. The cover was seeded with a mixture of native grasses (see Table 3.2).

### 3.2.8 Albany Site

The Albany site is located about 850 m west of the western edge of the Indian Lake Refuge Area, in Albany, GA. There is no liner underlying the waste at the site. Approximately 700 mm of intermediate cover currently exists on top of the waste. The two covers being tested are a RCRA Subtitle D compacted clay barrier and an alternative cover. The compacted clay cover is the prescriptive remedy for the site, as required by the Georgia Environmental Protection Agency.

The conventional cover consists of a 460 mm barrier layer of compacted clay and a 150 mm topsoil layer. The clay was compacted to achieve  $K_s \leq 1 \times 10^{-7}$  cm/s. The alternative cover, also known as an ECap, consists of 700 mm of soil to simulate the interim cover and a 600 mm storage layer comprised of soil blended with organic amendments. Both covers overlay 150 mm of interim cover soil.

All soil layers were constructed with sandy clay that was stockpiled on-site during previous construction efforts. The storage layer in the alternative cover consists of a 4:1 ratio of soil and organic amendments, the latter being comprised of 75% peanut hulls and 25% composted municipal wastewater biosolids.

Both test covers were vegetated with Bermuda grass. The alternative cover was also vegetated with two-year old hybrid poplar trees. The hybrid poplar trees were 4.5 m tall prior to planting and were placed in 600 mm deep trenches. Tree rows were spaced 3 m apart with an in-row spacing of 1.2 m. Two rows of trees were also planted around the alternative test section as a perimeter buffer to minimize 'edge effects' caused by wind, humidity, and light, which makes the alternative test section more representative of a large-scale ECap.

### **3.2.9 Marina Site**

The Marina site is located approximately 3.2 km north of Marina, CA. Portions of the existing landfill are unlined, while other portions have a composite barrier. Two covers are being tested at the Marina site, a conventional cover with a composite barrier and an alternative cover.

The conventional cover consists of 600 mm of sand that serves as interim cover and as a gas vent, 300 mm of imported clay compacted to achieve a  $K_s \leq 1 \times 10^{-5}$  cm/s, a 1.5 mm thick textured LLDPE textured geomembrane, and a 300 mm vegetative layer. The alternative cover consists of a 300 mm intermediate cover and a 1220 mm storage layer.

The vegetative layer and the storage layer consist of heterogeneous clayey sand stockpiled on site as waste soil from nearby construction projects. The clay used for the compacted soil barrier was imported for a previous liner installation. The interim cover used for both covers is sand from a borrow area on site. Both covers were seeded with a mixture of native grasses (See Table 3.2). To improve vegetative growth in the alternative cover, compost was tilled into the top 75 mm of the storage layer November 2000, approximately five months after construction.

### **3.2.10 Monticello Site**

The Monticello site is a uranium mill tailings disposal cell located in Monticello, UT. A RCRA Subtitle C cover was installed at the site in 1999. A 3.0 ha portion of the cover was hydraulically isolated from the rest of the 32.4 ha cover to test an alternative cover design. The alternative cover being tested is a capillary barrier that consists of

300 mm of clean sand, a geotextile filter, 300 mm of fine-grained soil, a 300 mm bio-intrusion layer (gravel), a 920 mm storage layer (fine-grained soil), and a 200 mm soil/gravel admixture. The vegetative cover consists of a mixture of grasses, forbs, and shrubs (See Table 3.2).



## **SECTION FOUR ACAP WATER BALANCE DATA**

This section presents data collected from the ACAP test sections. The monitoring period presented in this study varies from site to site, depending on when the test sections were constructed. The monitoring period reported here ended on approximately April 10, 2002. The water balance parameters that are discussed are surface runoff, soil water storage, lateral flow (if applicable), and percolation. Evapotranspiration is not discussed because it is not a direct measurement, but rather is determined indirectly from the water balance equation (Section 5.1). A summary of the water balance quantities for each cover is in Tables 4.1 and 4.2. A summary of factors affecting surface runoff is in Appendix 3.

A summary of soil properties measured during construction is discussed along with the modeling in Section 5, with the exception of those the soil properties for the Cedar Rapids and Monticello sites. Model simulations were not conducted for Cedar Rapids and Monticello. Therefore, hydraulic properties of soils at these sites are presented in this section. A more detailed report on the soil properties can be found in Gurdal (2002).

In this section, soil water storage records from each site are compared to the soil water storage capacity of each cover. Soil water characteristic curves were measured for each soil (Gurdal 2002), and were used to calculate the field capacity and wilting points of each soil. The soil water storage (SWS) capacity for each test section was then calculated based on the field capacity of each layer, with the field capacity defined as the water content at a matric suction of 33 kPa. The total SWS capacity includes the cover profile and the interim cover.

Table 4.1. Summary of Water Balance Data: Arid and Semi-Arid Sites.  
Percentage of Precipitation in Parenthesis.

Site	Duration (Days)	Cover Type	Slope (%)	Total Precipitation (mm)	Avg. Annual Precipitation <sup>a</sup> (mm/yr)	Surface Runoff (mm/yr)	Lateral Flow (mm/yr)	Percolation (mm/yr)
Altamont, CA	517	Monolithic	5	486.7	358.4	18.6 (5.4%)	NA	1.0 (0.3%)
		Conventional Composite	5			10.4 (3.0%)	2.7 (0.8%)	0.0 (0.0%)
Sacramento, CA	987	Monolithic (1080-mm)	5	1142.5	434.3	44.4 (10.5%)	NA	48.4 (11.1%)
		Monolithic (2450-mm)	5			25.1 (5.9%)	NA	3.1 (0.7%)
Helena, MT	905	Capillary	5	385.3	288.8	28.4 (7.4%)	NA	0.0 (0.0%)
Polson, MT	847	Capillary	5	743.97	380.5	10.0 (3.1%)	NA	0.2 (0.1%)
		Conventional Composite	5			8.3 (2.6%)	10.9	0.2 (0.1%)
Boardman, OR	485	Monolithic (1220-mm)	25	180.8	225.3	0.0 (0.0%)	NA	0.0 (0.0%)
		Monolithic (1840-mm)	25			0.0 (0.0%)	NA	0.0 (0.0%)
		Conventional Composite	25			0.0 (0.0%)	0.0 (0.0%)	0.0 (0.0%)
Monticello, UT	607	Capillary	5	513.8		9.3 (1.8%)	NA	0.0 (0.0%)

NA = Not Applicable

Table 4.2. Summary of Water Balance Data: Humid Sites.  
Percentage of Precipitation in Parenthesis.

Site	Duration (Days)	Cover Type	Slope (%)	Total Precipitation (mm)	Avg. Annual Precipitation (mm/yr)	Surface Runoff (mm/yr)	Lateral Flow (mm/yr)	Percolation (mm/yr)
Marina, CA	684	Monolithic	25	605.0	466.1	0.0 (0%)	NA	61.8 (13.3%)
		Conventional Composite	25			45.7 (14.2%)	7.8 (1.7%)	18.1 (3.9%)
Albany, GA	722	Monolithic	5	1614.9 (1982.7) <sup>b</sup>	1263.4	7.8 (0.1%)	NA	91.3 (7.2%)
		Conventional Compacted Clay	5	1614.9 (1660.5) <sup>b</sup>		85.2 (10.4%)	NA	280.4 (22.2%)
Cedar Rapids, IA	381	Monolithic	5	772.1	914.7	25.7 (3.5%)	NA	143.1 (15.6%)
		Conventional Compacted Clay	5			14.2 (1.9%)	1.4 (0.2%)	15.5 (1.7%)
		Conventional Composite	5			21.0 (2.8%)	1.4 (0.2%)	0.9 (0.1%)
Omaha, NE	552	Capillary (760-mm)	25	719.1 <sup>c</sup>	760.2	47.8 (6.6%)	NA	62.9 (8.3%)
		Capillary (1060-mm)	25			36.0 (5.0%)	NA	36.8 (4.8%)
		Conventional Composite	25			45.5 (6.3%)	18.1 (2.4%)	3.7 (0.5%)

<sup>a</sup> Average Annual Precipitation from historical data.

<sup>b</sup> Total precipitation for Albany includes irrigation applied to each test section.

<sup>c</sup> Precipitation record at Omaha is from October 5, 2000 to mid December 2001.

NA = Not Applicable

## **4.1 ALTAMONT SITE**

Construction of two test sections at the Altamont site was completed on August 30, 2000. Data collection began on November 10, 2000. The total precipitation during the monitoring period is 487 mm. The majority of the precipitation occurred during the fall and winter.

The water balance for each test section is shown in Fig. 4.1. A datalogger error resulted in a large data gap between January 10, 2001 and March 29, 2001. However, meteorological data during this gap were obtained from a nearby weather station operated by the National Weather Service (Livermore, CA: station number 44997).

### **4.1.1 Surface Runoff**

Surface runoff during the monitoring period is shown in Fig. 4.1. Surface runoff was 14.8 mm from the conventional cover and 26.4 mm from the alternative cover, which corresponds to 3.5% and 6.1% of precipitation. Surface runoff was only recorded during two rain events. The majority of the runoff (14.3 mm for the conventional cover and 22.4 mm for the alternative cover) occurred between December 2, 2001 and January 2, 2001, when 128 mm of precipitation was recorded. The amount of surface runoff may be underestimated due to the data gap occurring during the winter, when most of the precipitation occurs.

The type of vegetation and the soil used for each cover are similar; therefore, the surface runoff from both covers should be similar. The difference in surface runoff that was measured is likely due to the conventional cover having a more permeable topsoil layer ( $2.0 \times 10^{-5}$  cm/s) than the alternative cover ( $2.8 \times 10^{-6}$  cm/s).

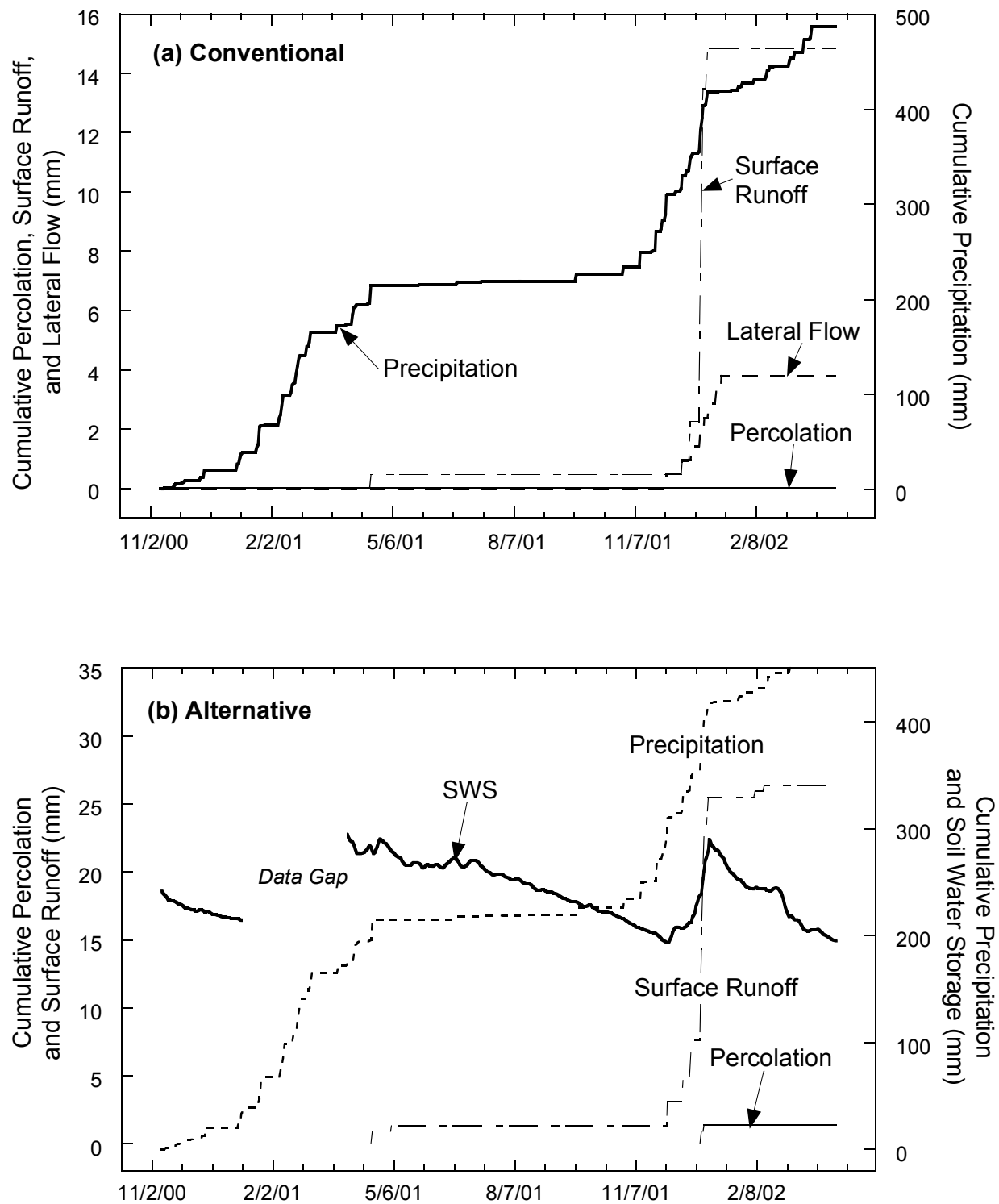


Fig. 4.1. Cumulative Water Balance for the Altamont Site: (a) Conventional Cover and (b) Alternative Cover.

#### **4.1.2 Lateral Flow from Conventional Cover**

Lateral flow was only recorded (3.8 mm) during the large rain event in December 2001. Lateral flow began on December 2, 2001, and ended on January 13, 2002. Approximately 18 mm of precipitation was measured during the four days prior to December 2, which slowly soaked into upper soil layer. On December 2, 20 mm of precipitation infiltrated the conventional cover and created lateral flow, even though surface runoff had not yet been recorded. This is likely due to the topsoil layer of the conventional cover being permeable, allowing for more infiltration than runoff.

#### **4.1.3 Soil Water Storage**

Soil water storage (Fig. 4.2) in the conventional and alternative covers increases during the winter due to the increase in precipitation, and then decreases due to evapotranspiration. During the winter, the soil water storage capacity was exceeded in the upper soil layers for short durations, but not in the lower soil layers (Fig. 4.3).

For the alternative cover, there is a delay in the increase in soil water storage (Fig. 4.3b) of the support layer and interim cover from the winter rains, which reflects the downward flow of water. Soil water storage initially peaked in the storage layer, which is followed by a peak in the support layer, and then the interim cover. The changes also occur more gradually with depth. During the first year, the soil water storage of the support layer rises sharply in Spring 2001, and slowly decreases during the following summer and fall. Water is primarily removed from the support layer by the vegetation.

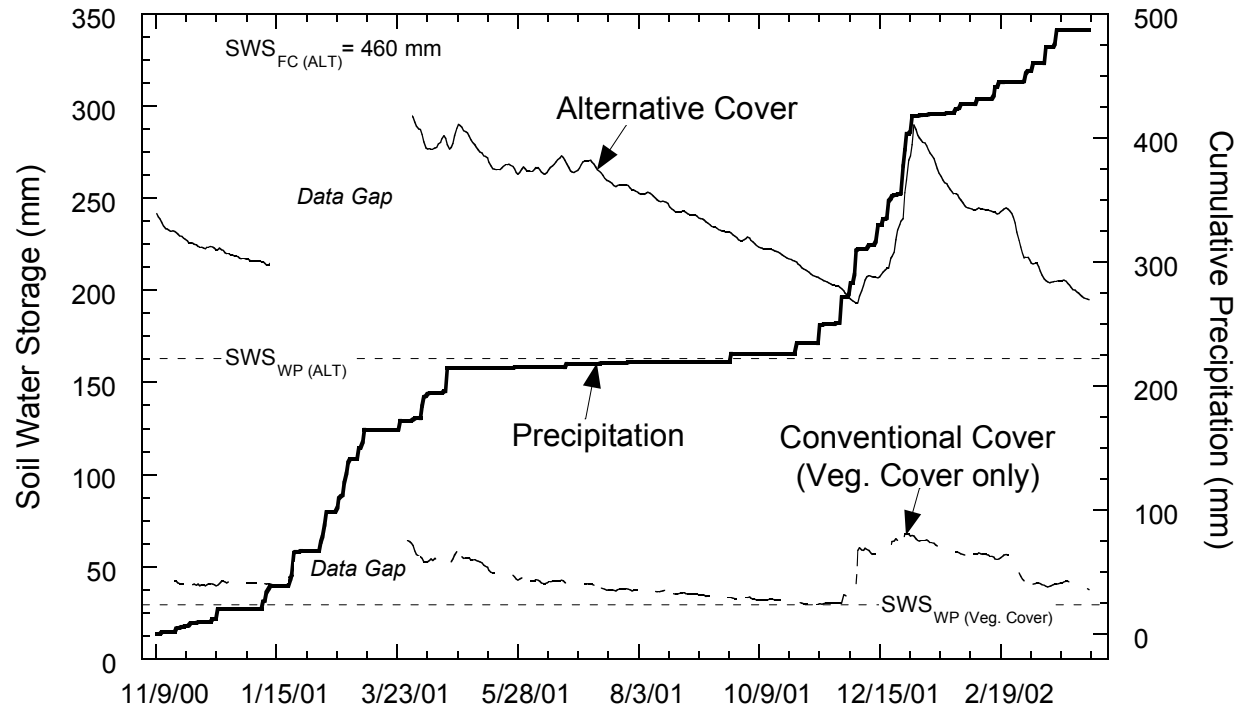


Fig. 4.2. Soil Water Storage in Test Sections at the Altamont Site.

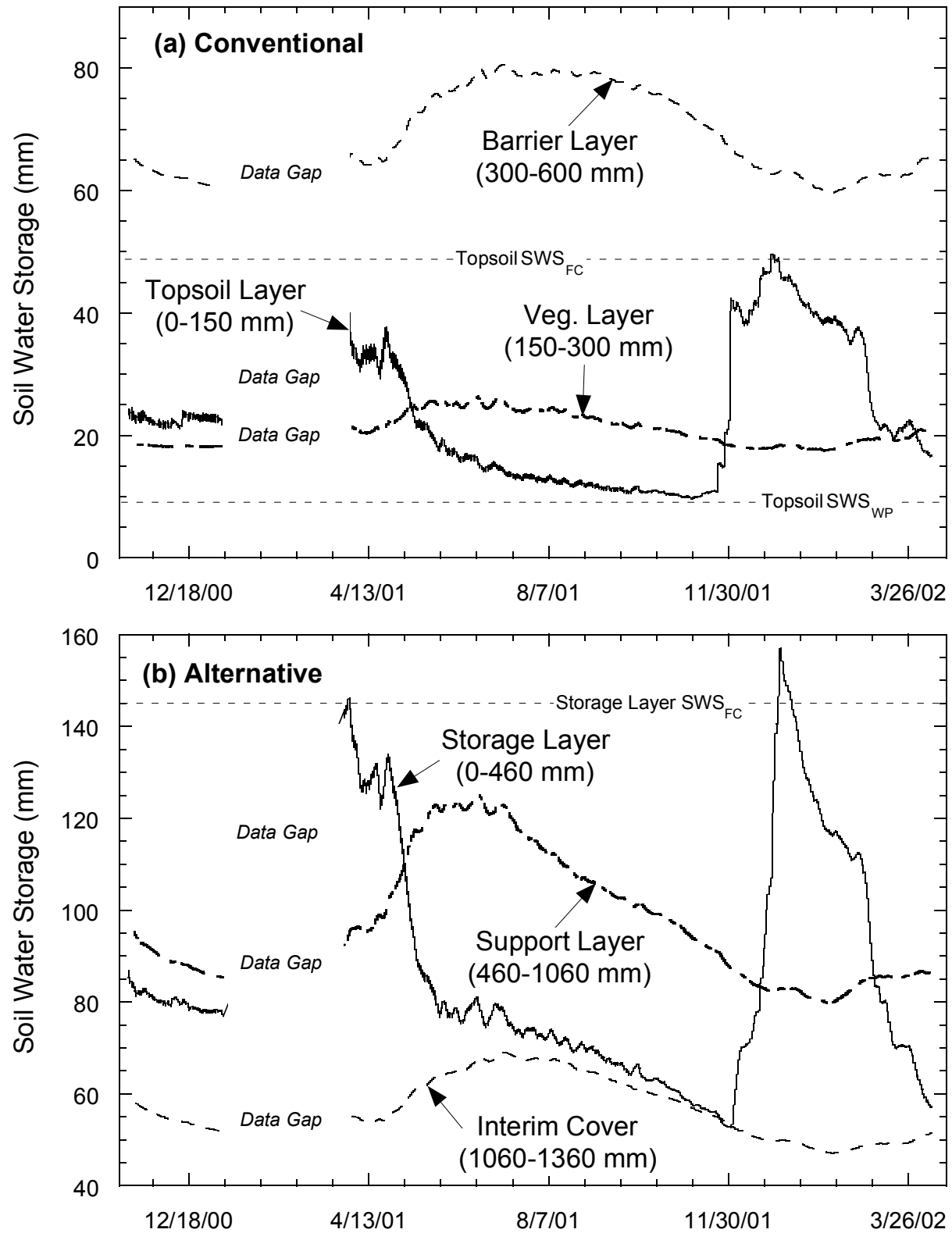


Fig. 4.3. Soil Water Storage of Individual Layers at the Altamont Site for the (a) Conventional Cover and (b) Alternative Cover.



The fluctuation of soil water storage in the interim cover of the alternative cover and the barrier layer of the conventional cover is likely due to either (1) water flux from a warmer to a cooler region caused by thermal gradients, or (2) is related to temperature effects on the WCR probes. Negative thermal gradients (upward water flow) were measured from mid August 2001 to end of March 2002.

#### **4.1.4 Percolation**

Percolation during the monitoring period is shown in Fig. 4.1. No percolation was recorded from the conventional cover. For the alternative cover, percolation was not recorded until December 28, 2001, which corresponds to the large rain event in December 2001. During this event, 1.4 mm of percolation was recorded. Soil water storage of the storage layer increased sharply during this rainy period (Fig. 4.3). However, the soil water storage of the support layer and interim cover did not increase at all. Thus, the percolation recorded between December 28-30 may be the result of preferential flow.

## **4.2 SACRAMENTO SITE**

Construction of two monolithic barrier covers (1070 and 2450 mm) at the Sacramento site was completed on July 25, 1999. Data collection also began on July 29 1999. The covers are referred to as “thick” (2450 mm) and “thin” (1070 mm) monolithic barriers throughout this section. Total precipitation during the monitoring period was 1143 mm.

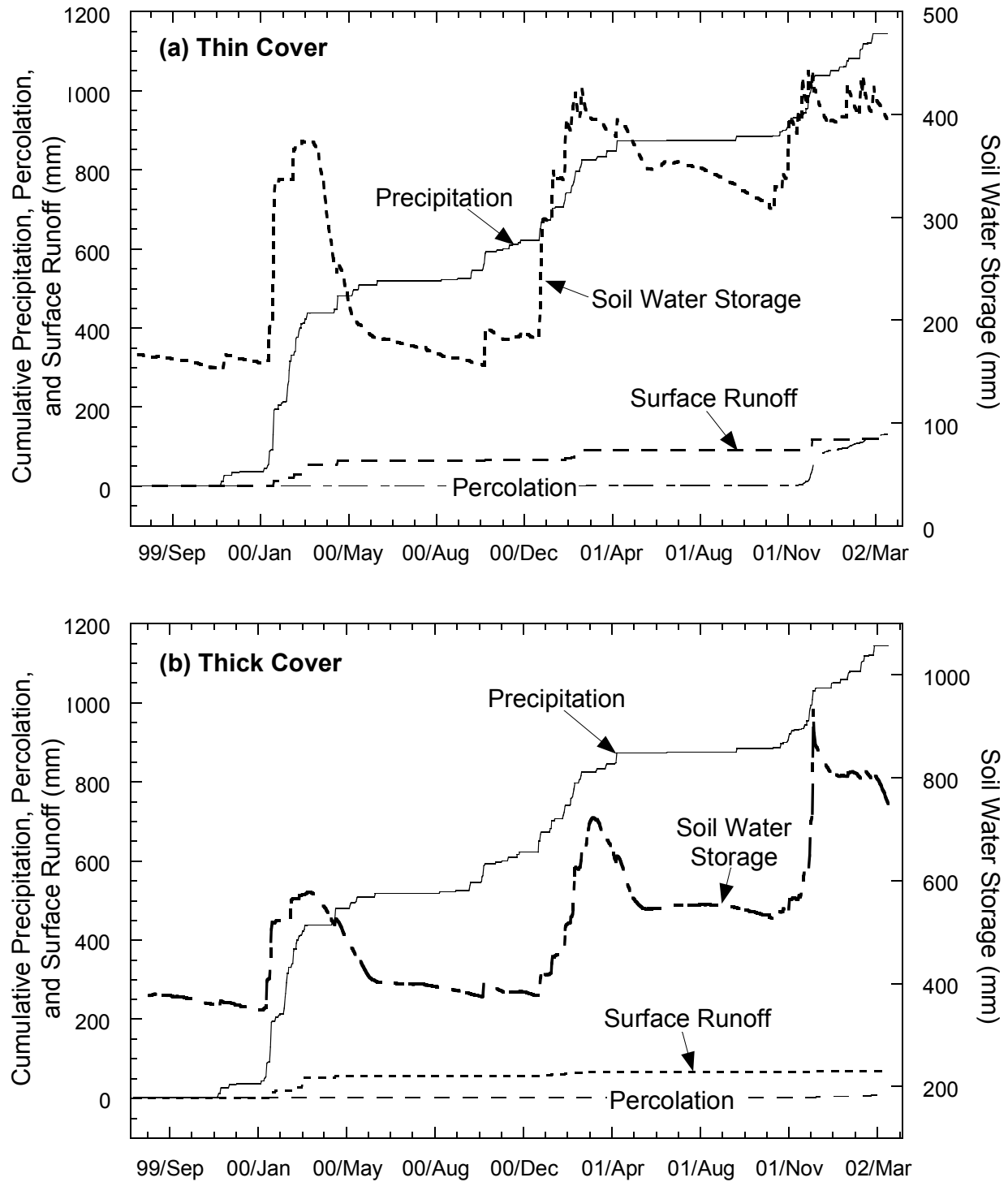


Fig. 4.4. Cumulative Water Balance at the Sacramento Site: (a) “Thin” Monolithic Barrier and (b) “Thick” Monolithic Barrier.

#### 4.2.1 Surface Runoff

Surface runoff during the monitoring period is shown in Fig. 4.4. Surface runoff measured from the “thick” monolithic barrier was 68 mm and from the “thin” monolithic barriers was 120 mm. These volumes correspond to 5.9 and 10.5% of precipitation.

Surface runoff only occurred during large rain events, at which time the volumetric water content of the topsoil layer exceeded the field capacity (Fig. 4.5). The topsoil layer needs to become nearly saturated before runoff begins because the vegetation on both covers is well established, trapping the water.

#### 4.2.2 Soil Water Storage

The rainy season at the Sacramento site occurs during the winter and spring, which is reflected in the trends in soil water storage. The water balance for each test section is shown in Fig. 4.4. Soil water storage increases during the rainy season (winter) and decreases during the summer. The soil water storage capacity for the “thin” monolithic barrier is exceeded twice during the monitoring period (February 5, 2001 and December 15, 2002). The soil water storage capacity for the “thick” monolithic barrier is exceeded once, which is towards the end of the monitoring period (January 1, 2002), as shown in Fig. 4.6.

During Summer 2000, the soil water “reservoir” for both covers was emptied by evapotranspiration, and the soil water storage reached the wilting point for both the “thin” monolithic barrier ( $\theta_{WP}=150$  mm) and the thick” monolithic barrier ( $\theta_{WP}= 351$  mm). However, during Summer 2001, the soil water storage of both covers only dropped approximately 100 mm.

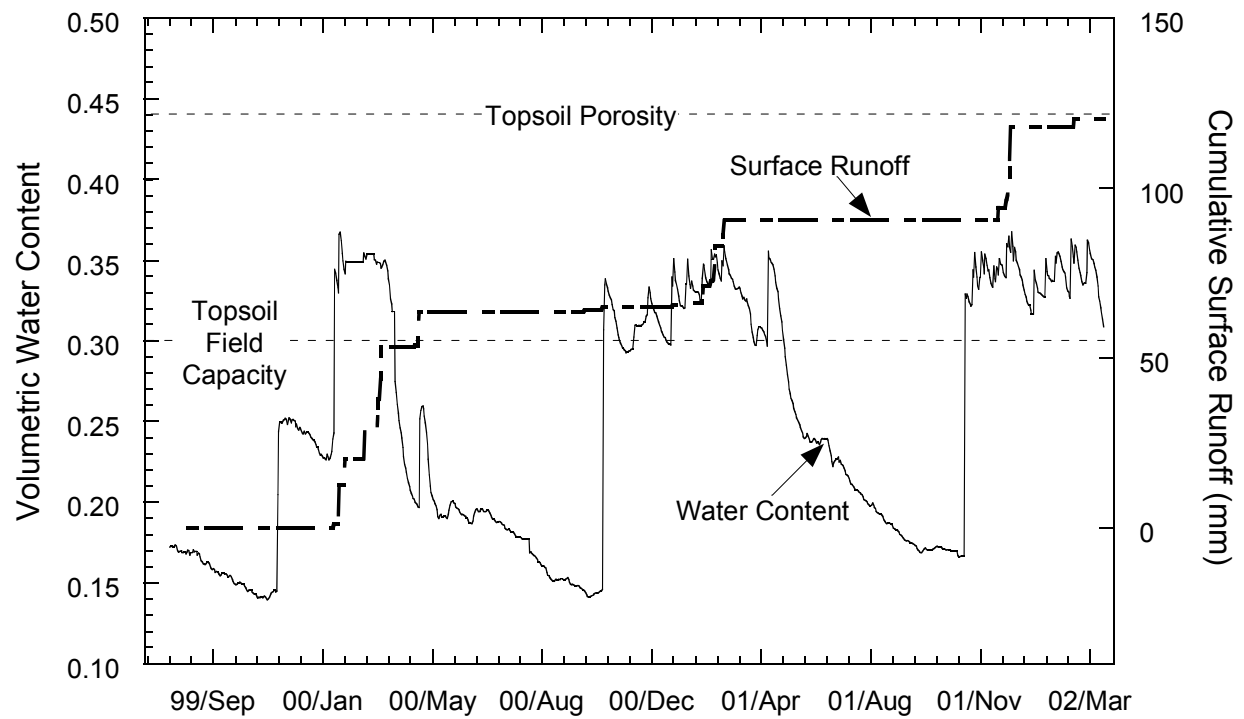


Fig. 4.5. Surface Runoff Occurring in Response to Topsoil Water Content: “Thin” Monolithic Barrier at the Sacramento Site.

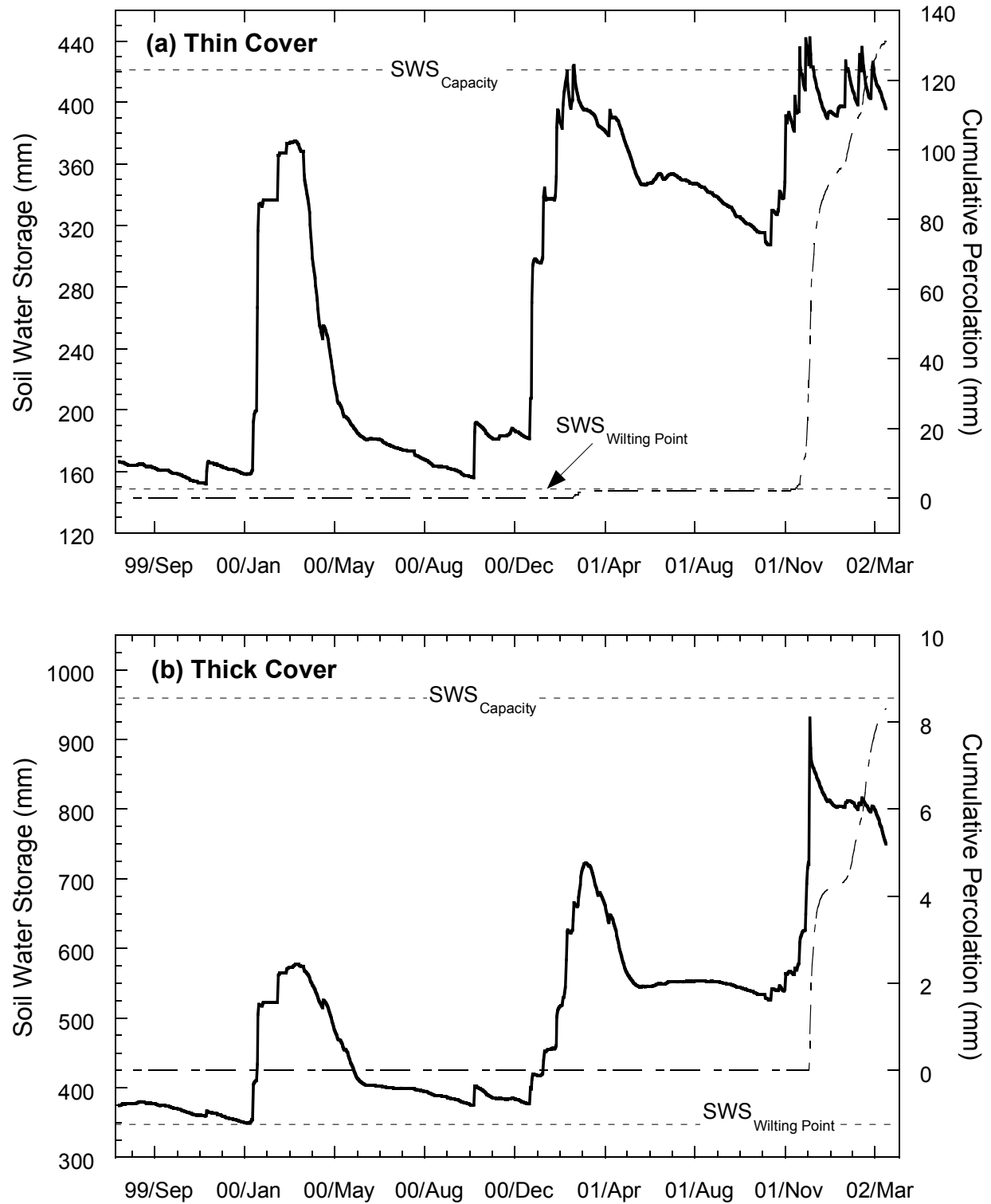


Fig. 4.6. Soil Water Storage for the Monolithic Barriers at the Sacramento Site: (a) "Thin" Cover and (b) "Thick" Cover.

### **4.2.3 Percolation**

Percolation during the monitoring period is shown in Fig. 4.5. Percolation was transmitted from both the “thick” (3.7 mm) and “thin” (79.9 mm) monolithic barriers. The “thick” monolithic barrier did not transmit percolation until Winter 2001. A small amount of percolation (2 mm) was transmitted by the “thin” monolithic barrier during Winter 2000, when the soil water storage capacity was exceeded. During Winter 2001, percolation transmitted by the “thin” monolithic barrier increased dramatically, resulting in an additional 129 mm of percolation. Percolation was transmitted by both covers during Winter 2001 because the soil water storage did not decrease sufficiently during Summer 2001.

The most likely cause for the inadequate depletion of soil water storage is the vegetation ceases to transpire during the summer. The typical harvest date for the vegetation at the Sacramento site is July 1, but the soil water storage for the “thick” monolithic barrier appears to stop decreasing at the end of May.

## **4.3 HELENA SITE**

Construction of the test section at the Helena site was completed on October 10, 1999. Data collection also began on October 10, 1999. Total precipitation during the monitoring period was 385 mm, 14.1% of which was frozen. Helena can be described as having wet summers and dry winters. The water balance for the test section is shown in Fig. 4.7.

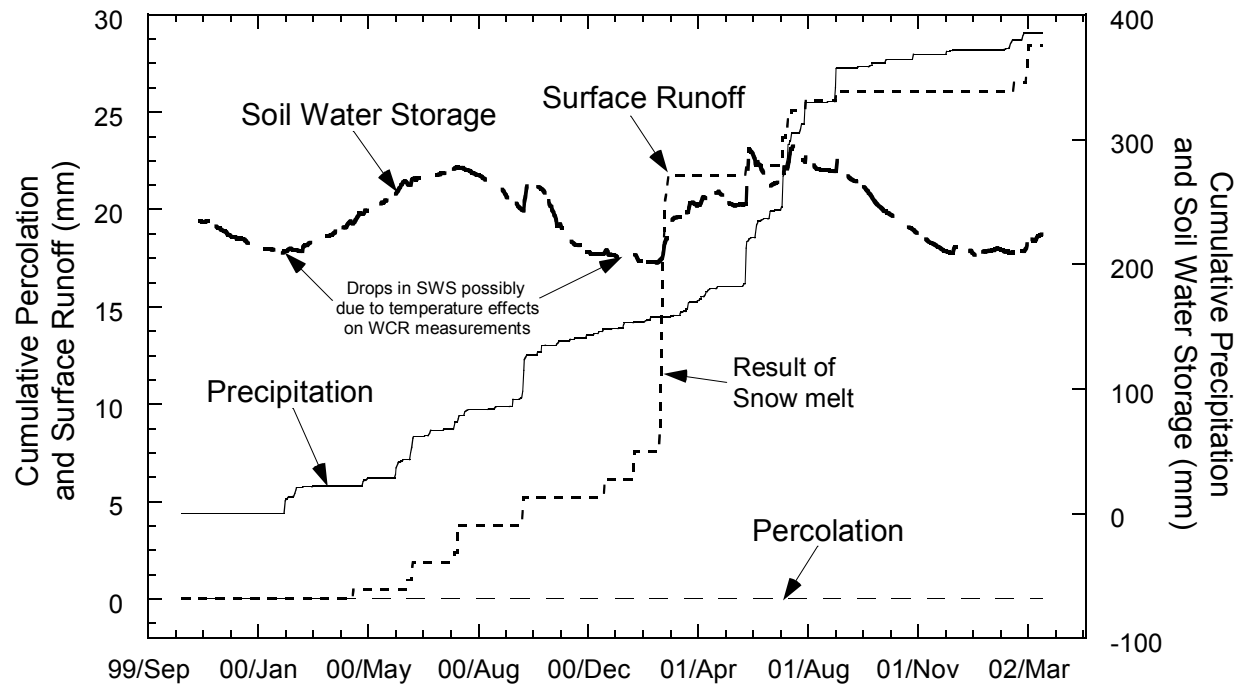


Fig. 4.7. Cumulative Water Balance at the Helena Site.

#### **4.3.1 Surface Runoff**

Surface runoff during the monitoring period is shown in Fig. 4.7. The total amount of surface runoff was 28.4 mm, or 7.4% of precipitation. The majority of surface runoff occurred during large rain events (9.5 mm) and snow melt events (18.9 mm), with the largest (14.2 mm) occurring in Spring 2001 as a result of a single snow melt event. The ground surface was frozen during both snowmelt events that occurred during the monitoring period (Fig. 4.8).

#### **4.3.2 Soil Water Storage**

The soil water storage capacity of the monolithic barrier (475 mm) was never close to being exceeded during the monitoring period (Fig. 4.7). The largest fluctuations of soil water storage occurred in the upper 460 mm (Fig. 4.9), whereas smaller fluctuations occurred in the lower soil layers. During the winter (November to February), the soil water storage appears to drop. However, this drop is the result of the WCR readings being affected by frozen ground. The WCRs record only the unfrozen water content, and thus do not reflect the actual volume of water in the soil during frozen conditions.

#### **4.3.3 Percolation**

No percolation was recorded during the monitoring period. Water reaches deeper depths of the cover profile, but is removed before percolation occurs.



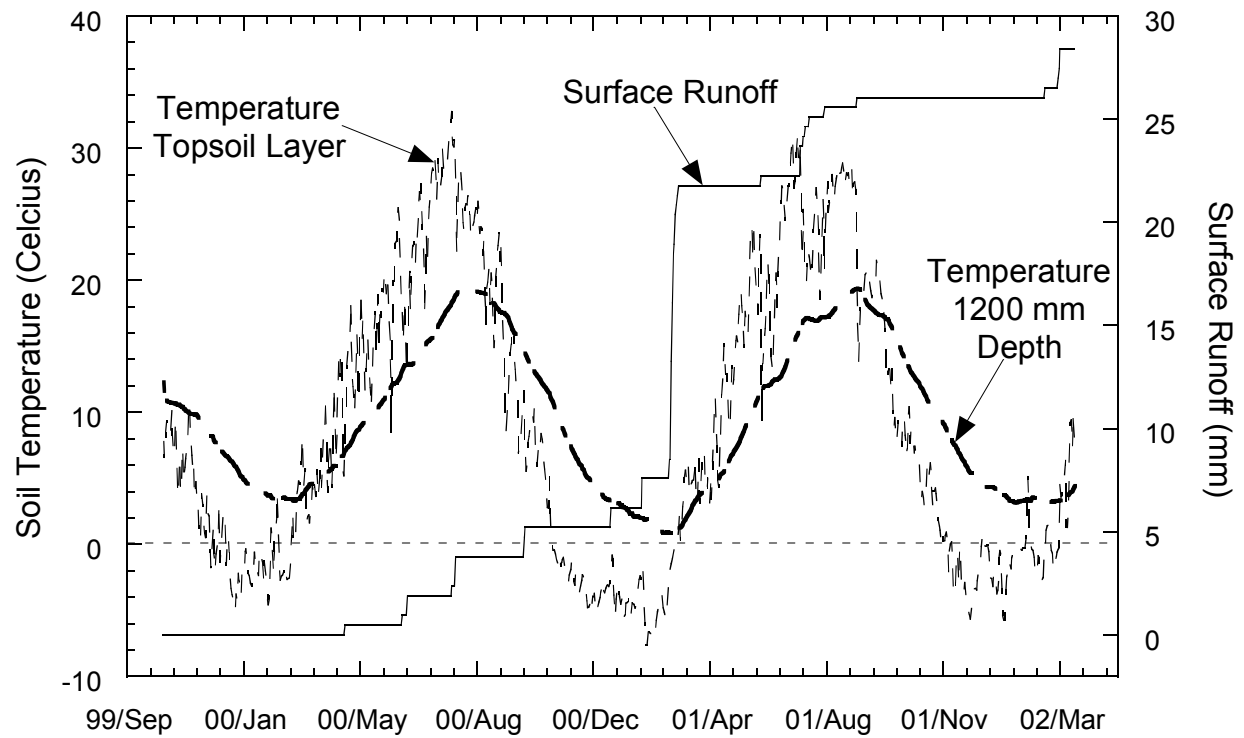


Fig. 4.8. Soil Temperatures and Surface Runoff for Alternative Cover at the Helena Site.

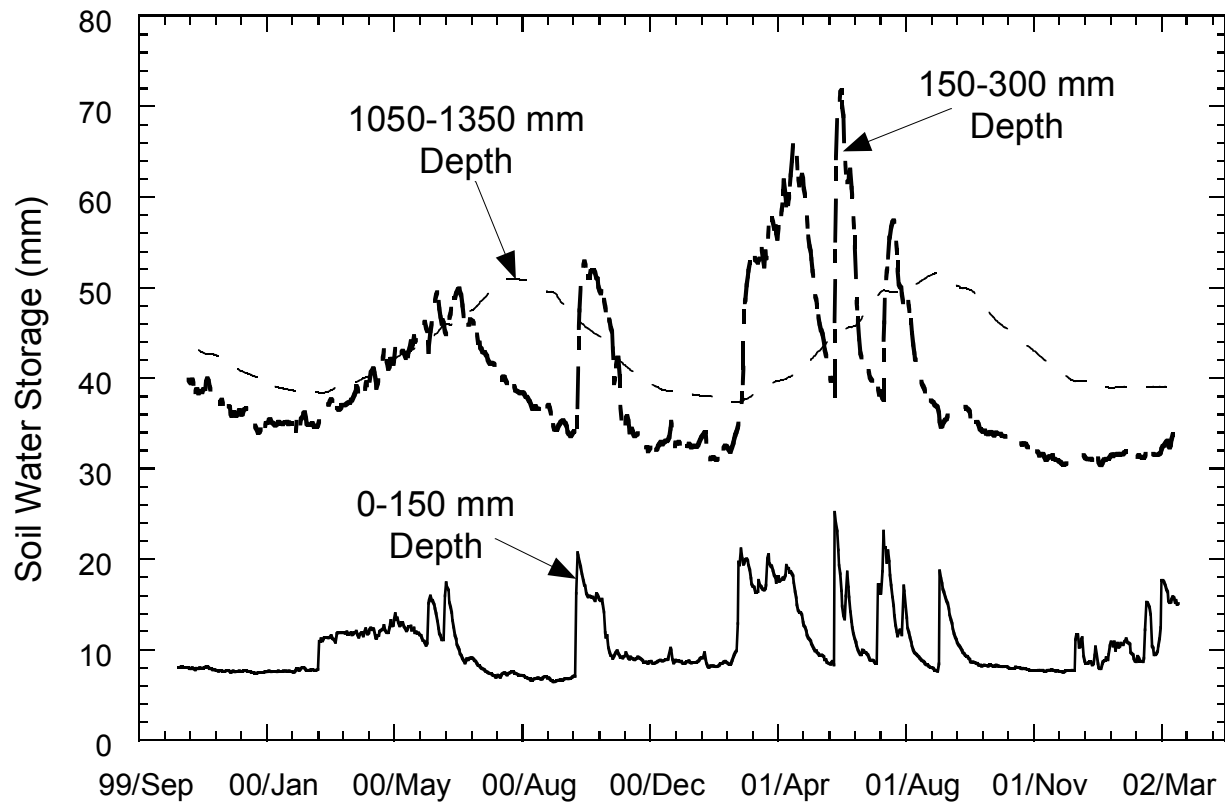


Fig. 4.9. Soil Water Storage for the Alternative Cover at the Helena Site.

#### **4.4 POLSON SITE**

Construction of two test sections at the Polson site was completed on October 19, 1999. Data collection also began on November 19, 1999. Total precipitation during the monitoring period was 744 mm, of which 27% was frozen. The water balance for each test section is shown in Fig. 4.10.

##### **4.4.1 Surface Runoff**

Surface runoff during the monitoring period is shown Fig. 4.10. Surface runoff from the alternative cover was 23.3 mm, and from the conventional cover it was 19.2 mm, which is 3.1% and 2.6% of precipitation. The small volume of surface runoff is attributed to the shallow slope (5%) of the test sections, the higher hydraulic conductivity ( $5 \times 10^{-5}$  cm/s) of the topsoil layer, and the well-established vegetation.

Most of the surface runoff occurred as a result of large snowmelt events at the end of winter and the beginning of spring. During this period, the ground is frozen, which enhances surface runoff. The snowmelt event during February 23-29, 2000 resulted in surface runoff (9.8 mm for the alternative cover and 9.3 mm for the conventional cover), more than double that occurring during snow melt events in subsequent years. For example, on March 6-14, 2001, surface runoff was 4.2 mm for the alternative cover and 2.8 mm for the conventional cover. During the next winter and spring (January 4, 2002 to March 4, 2002), 71.7 mm of melt water was generated, but no surface runoff occurred. During all of the snowmelt events, the ground surface was frozen. The decreasing trend of surface runoff is most likely because of dense vegetation, trapping the water.

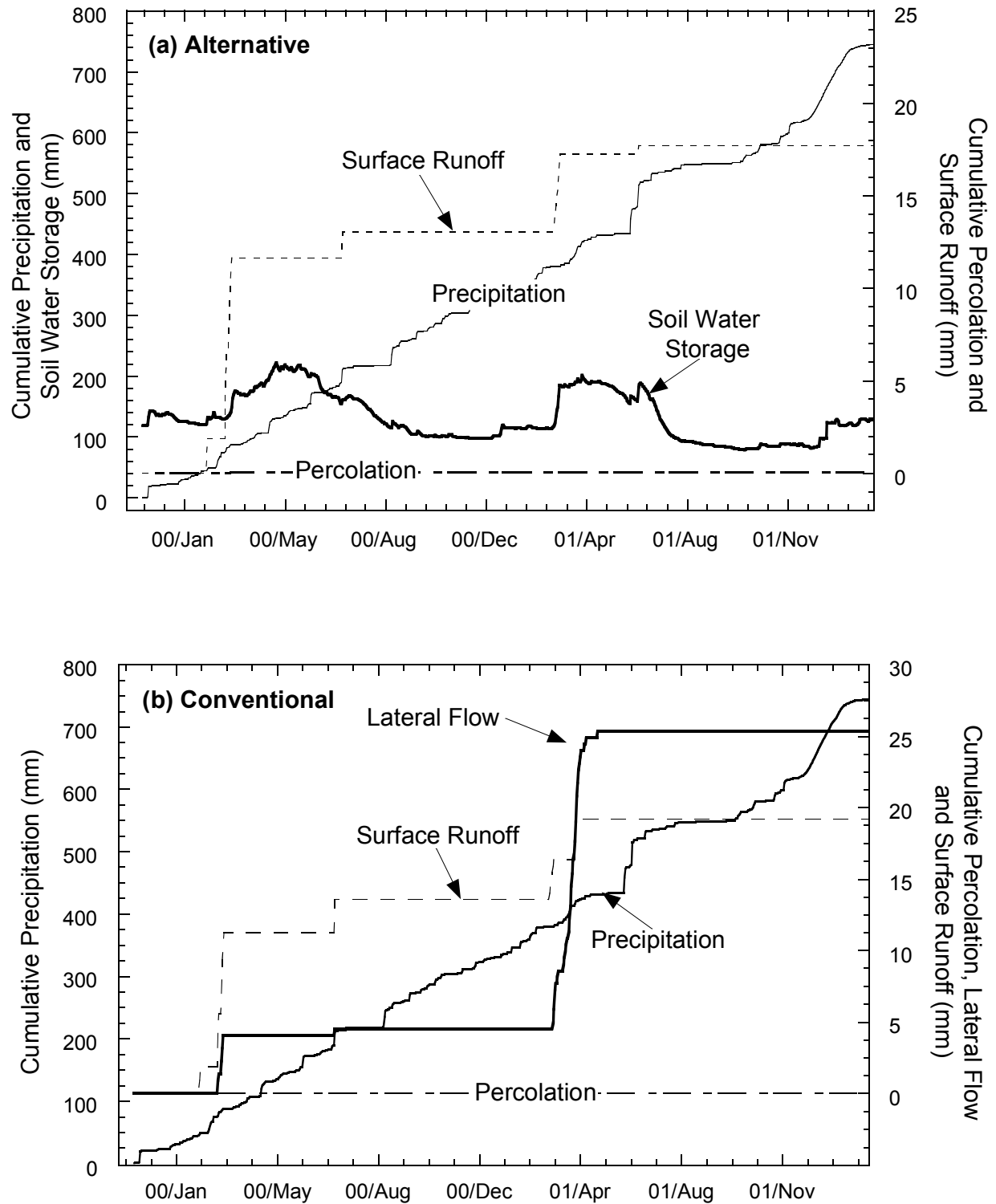


Fig. 4.10. Cumulative Water Balance at the Polson Site: (a) Alternative Cover and (b) Conventional Cover.

#### **4.4.2 Lateral Flow from Conventional Cover**

Lateral flow from the conventional cover was caused by the same events that yielded surface runoff. Typically, there was a delay of several hours to days after surface runoff was recorded before lateral flow would begin. During the snowmelt event in Spring 2001, the majority of the melt water infiltrated the cover, rather than running off. This event caused a large quantity of lateral flow (20.4 mm), as opposed to the snow melt event in Spring 2000, which resulted in 4.1 mm of lateral flow.

#### **4.4.3 Soil Water Storage**

Soil water storage typically increases during the winter and decreases in the spring and summer. Soil water storage peaks during the spring thaw and begins to decrease around May 1, which coincides with the start of the growing season. The soil water storage capacity was exceeded during Spring 2000 and 2001 for both the alternative cover and conventional covers (see Fig. 4.11).

For both covers, the soil water storage capacity of the upper layers (topsoil and storage layers for alternative cover, topsoil and vegetative layers for conventional cover) is greatly exceeded (see Fig. 4.12). However, the storage capacities that were computed did not account for the capillary barrier effect caused by the textural and hydraulic conductivity contrasts between the silt and fine sand layers in the alternative cover or the vegetative layer and drainage composite in the conventional cover. Nevertheless, for the conventional cover, the exceedance of the soil water storage capacity does correspond closely with a pulse of flow in the drainage layer, as shown in Fig. 4.10.

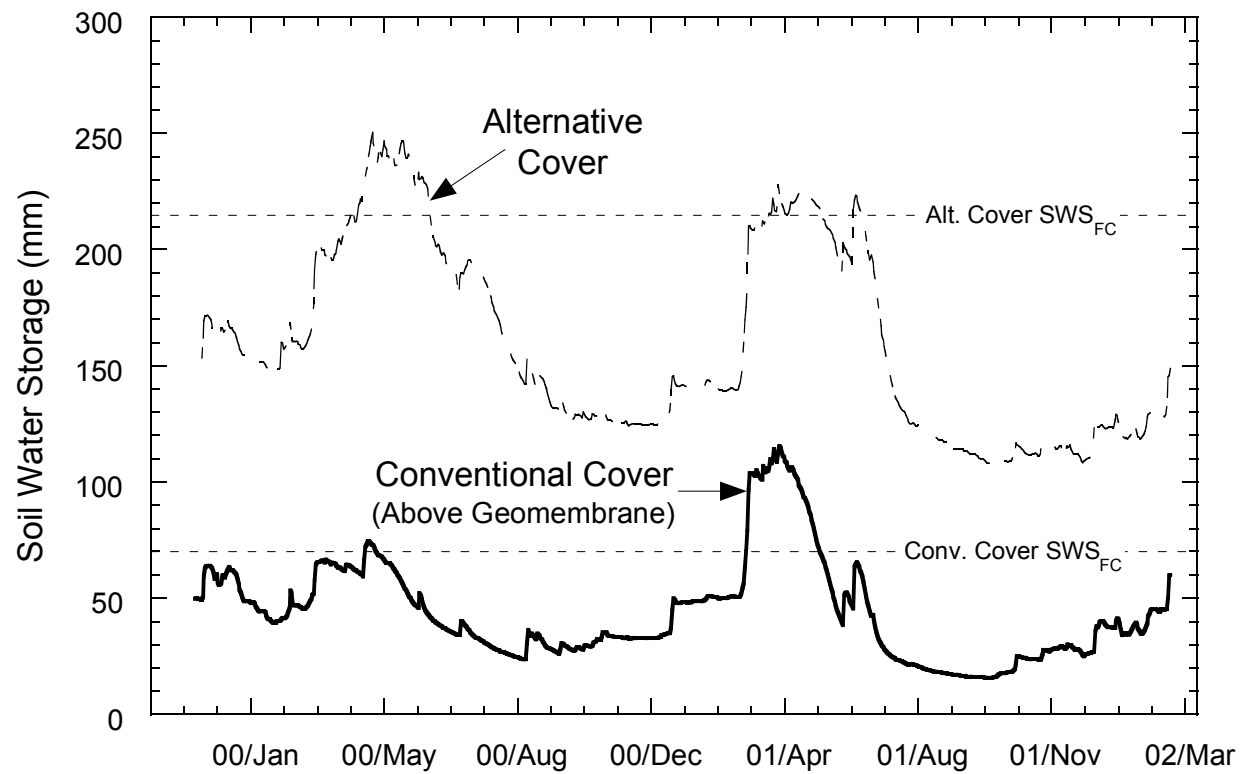


Fig. 4.11. Soil Water Storage for the Covers at the Polson Site.

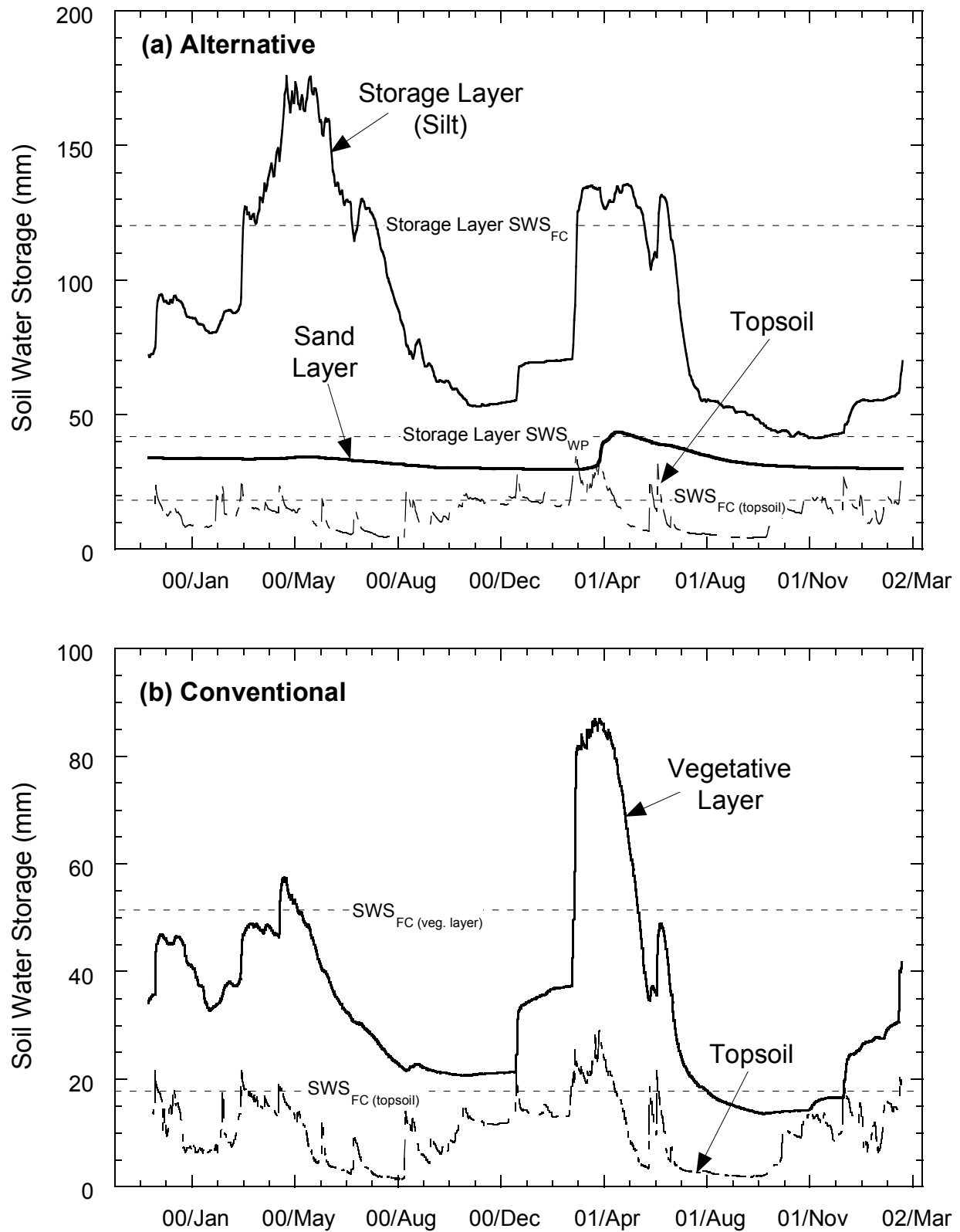


Fig. 4.12. Soil Water Storage in Each Layer at Polson Site: (a) Alternative Cover (b) Conventional Cover.

#### 4.4.4 Percolation

A detailed percolation record is shown in Fig. 4.13 for the Polson site. Percolation from the alternative cover is 0.43 mm, and from the conventional cover it is 0.48 mm. Field observations showed that the drainage pipes leading to the collection basins from both covers settled substantially. The settlement caused the drainage pipes to move inside the collection basins so that the outlet was no longer aligned with the tipping bucket. This problem was corrected on July 13, 2001, but the volume of water missed by the tipping buckets remains unknown. The percolation data presented in Fig. 4.13 were recorded by the tipping bucket, and thus this percolation volume may be underestimated. However, no flushes of the basin were recorded by the float switch during the monitoring period.

The first pulse of percolation recorded for each cover was the result of 30 mm of snowmelt in February 2000. Several more pulses were transmitted by both covers during the monitoring period due to rainfall. Percolation was transmitted when the soil water storage of the lower layers increased, but did not exceed the soil water storage capacity. At the end of the monitoring period (March 2002), snowmelt caused approximately 0.4 mm of percolation from the alternative cover.

Suctions on either side of the capillary break in the alternative cover are shown in Fig. 4.14. These suctions were estimated using water contents measured in the field with WCRs and the soil water characteristic curves measured in the laboratory. The suction in the silt layer increases during the summer, decreases during the winter, and approaches zero in the early spring due to infiltration from snowmelt events. Percolation typically is transmitted shortly after the suction in fine layer decreases below that in the coarser layer.



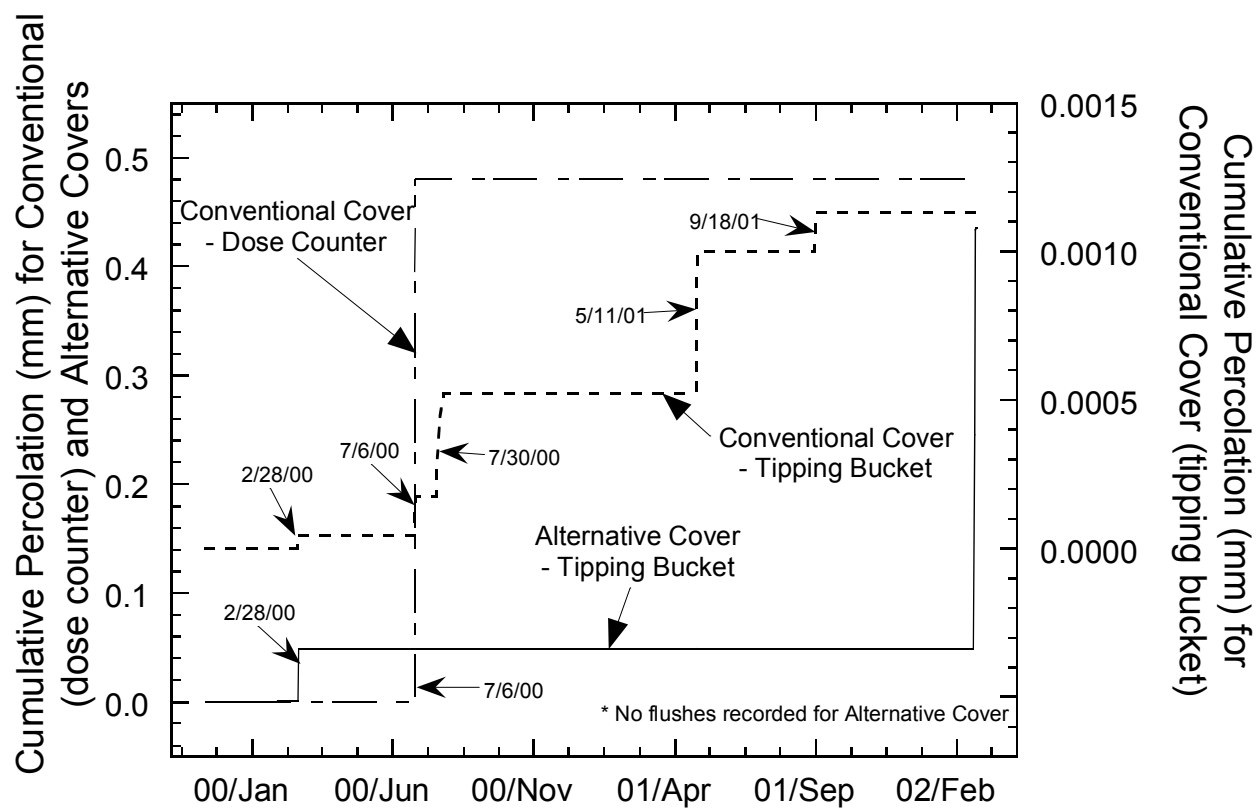


Fig. 4.13 Percolation for the Alternative Conventional Covers at the Polson Site.

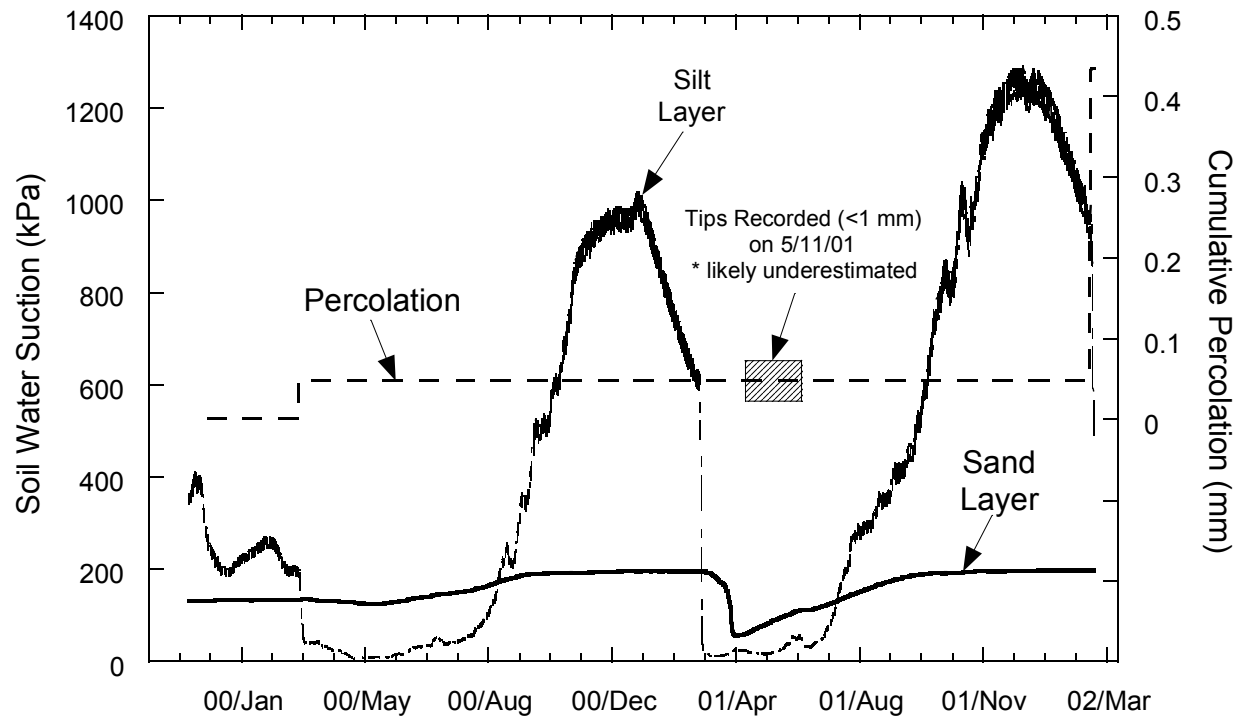


Fig. 4.14. Soil Water Suction Measurements Adjacent to Capillary Break in the Alternative Cover at the Polson Site.

During Spring 2001, breakthrough into the sand layer occurred. The capillary break prevented appreciable water flow into the sand during most of the monitoring period. Only small changes in suction occurred in the sand layer (Fig. 4.14) when the soil water storage of the silt layer increased dramatically (Fig. 4.12). During this period, water contents in the silt layer approached the porosity as a result of the spring thaw.

#### **4.5 BOARDMAN SITE**

Construction of the test sections (one conventional cover and two alternative covers) at the Boardman site was completed on November 2, 2000. Data collection began on December 9, 2000. The total precipitation during the monitoring period is 181 mm, of which 12.3% was frozen. The Boardman site has dry summers and wet winters. The water balance of each test section is shown in Fig. 4.15 and 4.16.

##### **4.5.1 Surface Runoff**

Virtually no surface runoff was recorded during the monitoring period, despite each test section having a 25% slope. This is likely due to a number of factors, such as absence of intense rain events that have typically produced surface runoff at the other sites, and the higher saturated hydraulic conductivity of the surface layer ( $2.0 \times 10^{-5}$  cm/s). Also, soil temperatures within each cover did not drop below 0°C during the monitoring period. Therefore, snowmelt during the spring thaw is not easily shed, as is the case at sites where the ground surface is frozen.

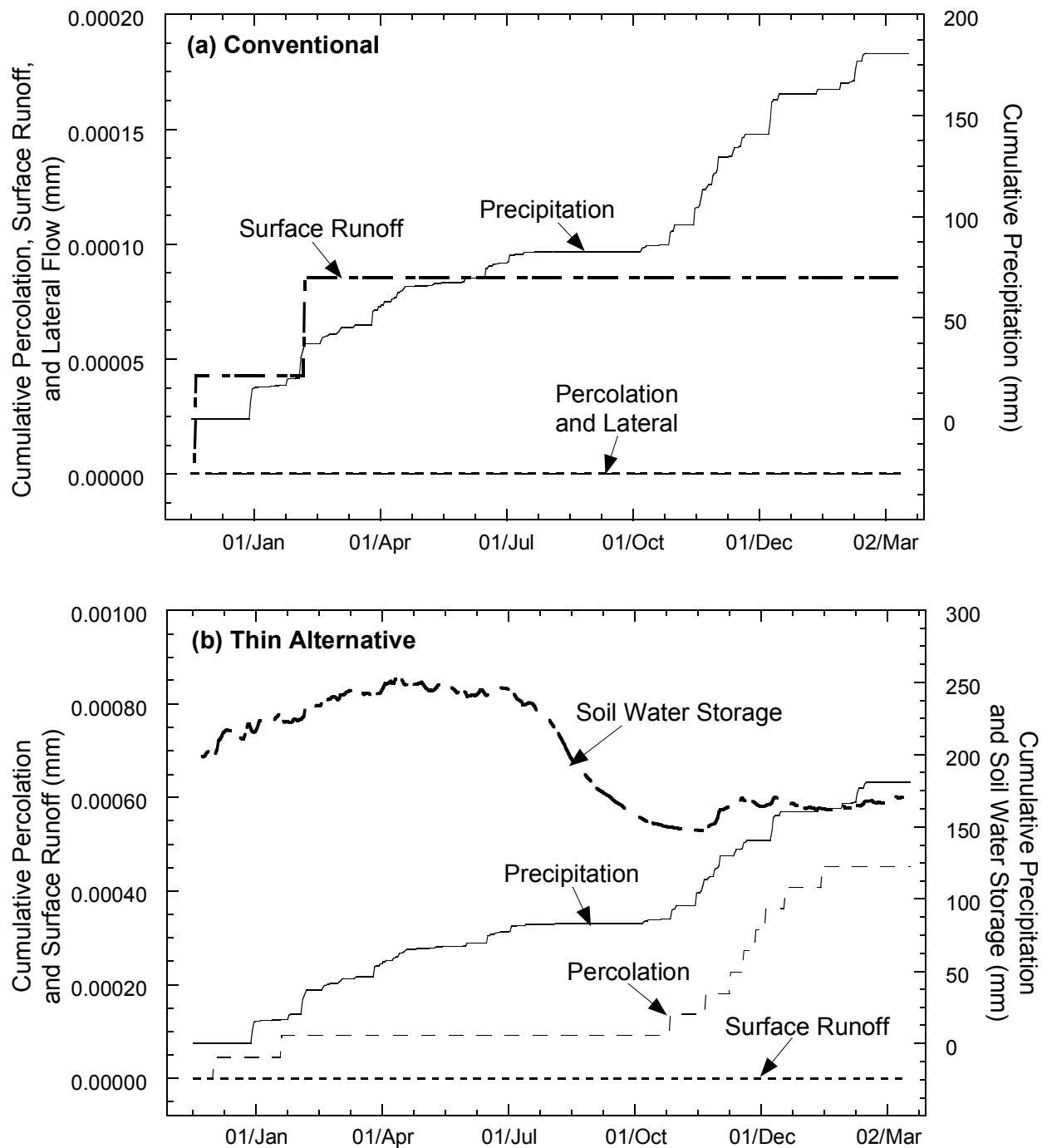


Fig. 4.15. Cumulative Water Balance at the Boardman Site: (a) Conventional Cover and (b) "Thin" Monolithic Barrier.

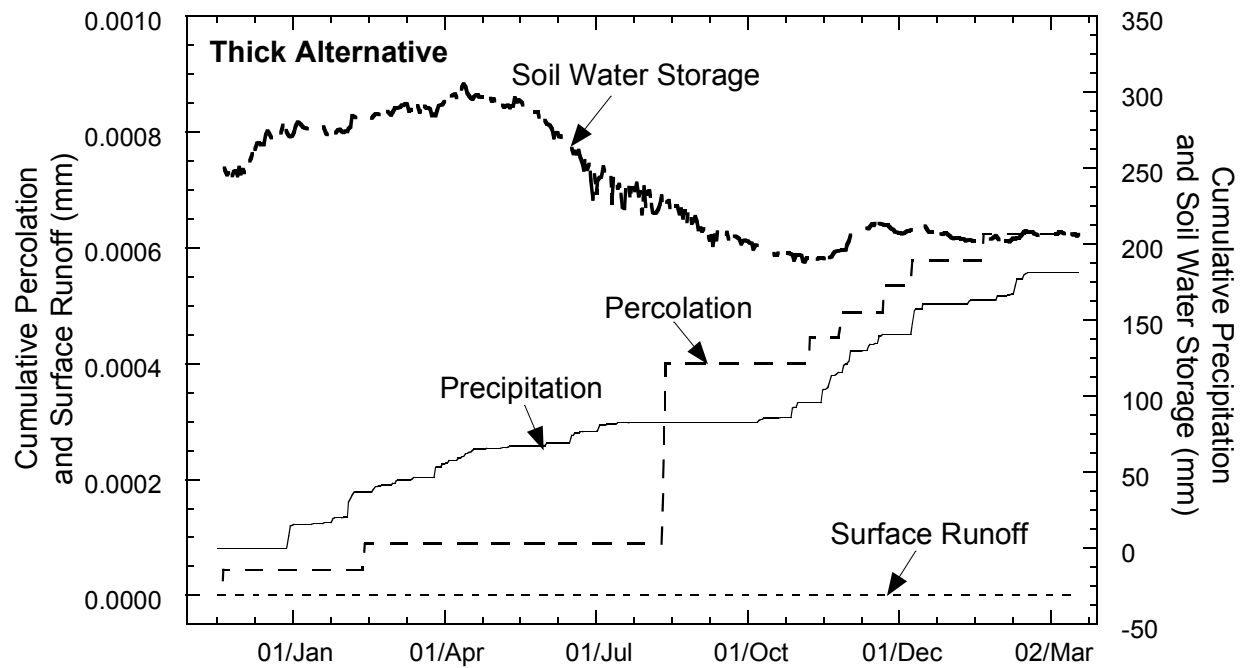


Fig. 4.16. Cumulative Water Balance at the Boardman Site: "Thick" Monolithic Barrier.

#### **4.5.2 Lateral Flow from Conventional Cover**

No lateral flow was collected from the conventional cover during the monitoring period.

#### **4.5.3 Soil Water Storage**

Soil water storage for each cover is shown in Fig. 4.17. Typically, soil water storage reaches a maximum during spring, as a result of the rainy season during the winter. At the end of April, the vegetation germinates and begins to extract water from the cover. The soil water storage gradually decreases during the summer and reaches a minimum prior to the onset of the rainy season in November.

In the alternative covers, peak volumetric water contents in each soil layer are reached at different times (Fig. 4.18). The time delay from the surface layer to the bottom layer is approximately 5 to 6 months. This indicates that water is reaching the lower soil zones, but is flowing downwards under unsaturated conditions at a slow rate.

The vegetation at the Boardman site appears to be capable of removing all of the available soil water. Water contents in the entire soil profile approach the wilting point by the end of each growing season (Fig. 4.18). For the “thick” monolithic barrier, the water content of the lowest soil zone fluctuates very little, lingering near the wilting point.

#### **4.5.4 Percolation**

Virtually no percolation was recorded in any of the test sections during the monitoring period. The cumulative percolation was less than 0.1 mm for each cover.

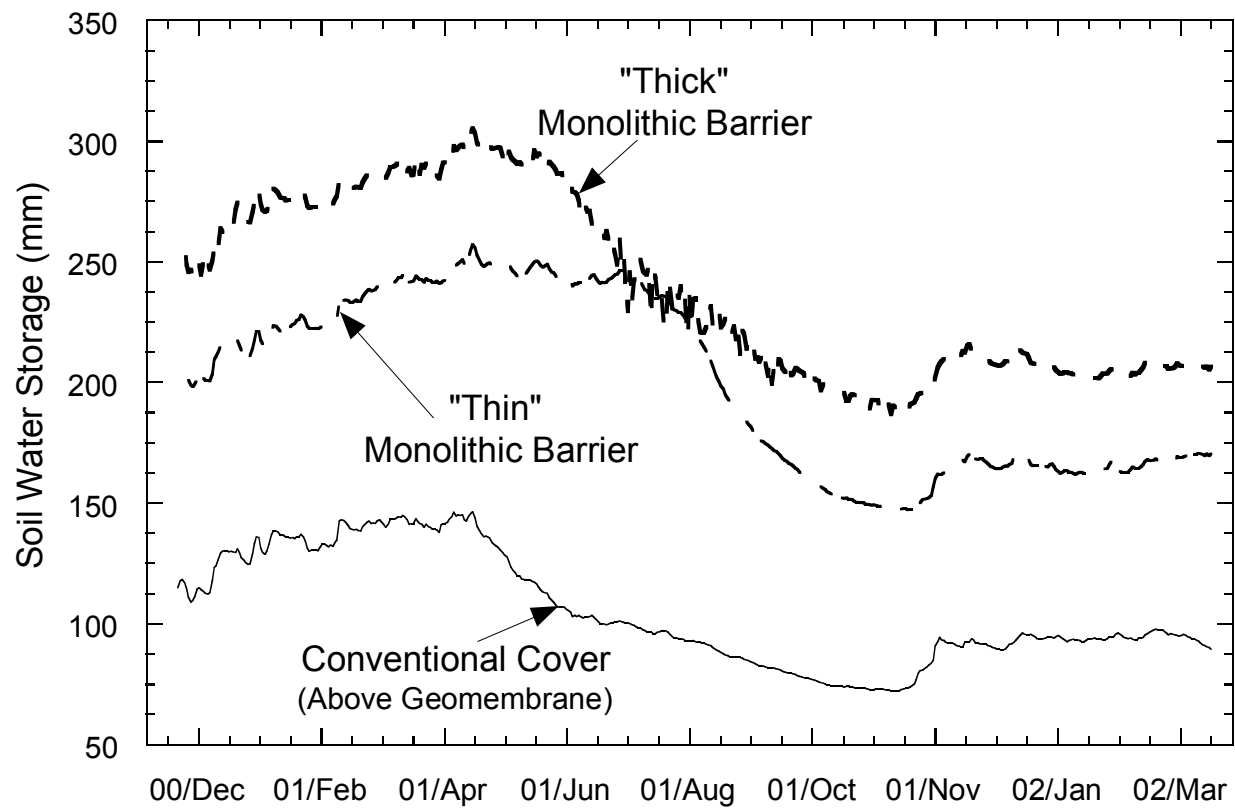


Fig. 4.17. Soil Water Storage for All Covers at the Boardman Site.

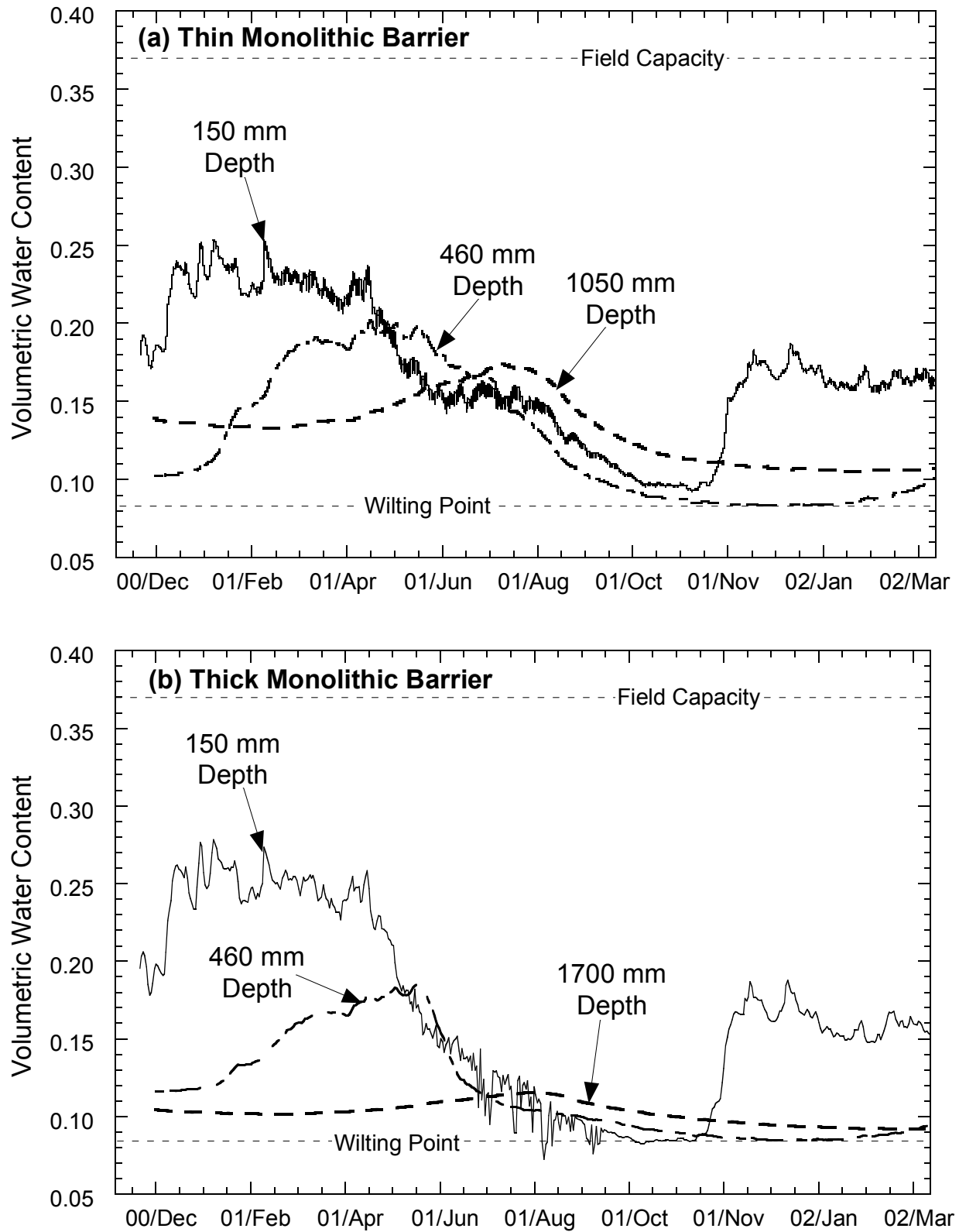


Fig. 4.18. Volumetric Water of Soil Layers at Boardman Site: (a) “Thin” Monolithic Barrier and (b) “Thick” Monolithic Barrier.



## **4.6 MARINA SITE**

Construction of the two test sections (one conventional cover and one alternative cover) at the Marina site was completed on May 25, 2000. Data collection began on May 27, 2000. Total precipitation during the monitoring period is 605 mm, with the majority of the precipitation (72%) occurring during the winter (November through February). The water balance for each test section is shown in Fig. 4.19.

### **4.6.1 Surface Runoff**

Surface runoff during the monitoring period is shown in Fig. 4.19. The surface runoff recorded from the conventional cover was 85.7 mm, which corresponds to 14.2% of precipitation. No surface runoff was recorded from the alternative cover, despite both covers being constructed with the same soil, seeded with the same vegetation, and at the same slope (25%). The difference in surface runoff is attributed to tilling of the surface layer of the alternative cover to improve vegetative growth.

### **4.6.2 Lateral Flow from Conventional Cover**

Lateral flow during the monitoring period is shown in Fig. 4.19. The lateral flow recorded from the conventional cover was 14.5 mm, and occurred nearly exclusively during Winter 2001. Lateral flow began approximately three months after the onset of winter precipitation, and gradually increased until the middle of February 2001. After this time, a malfunction may have occurred in the dosing siphon for the lateral flow collection basin. Surface runoff recorded after February was 38 mm, whereas the lateral flow was only 0.47 mm.

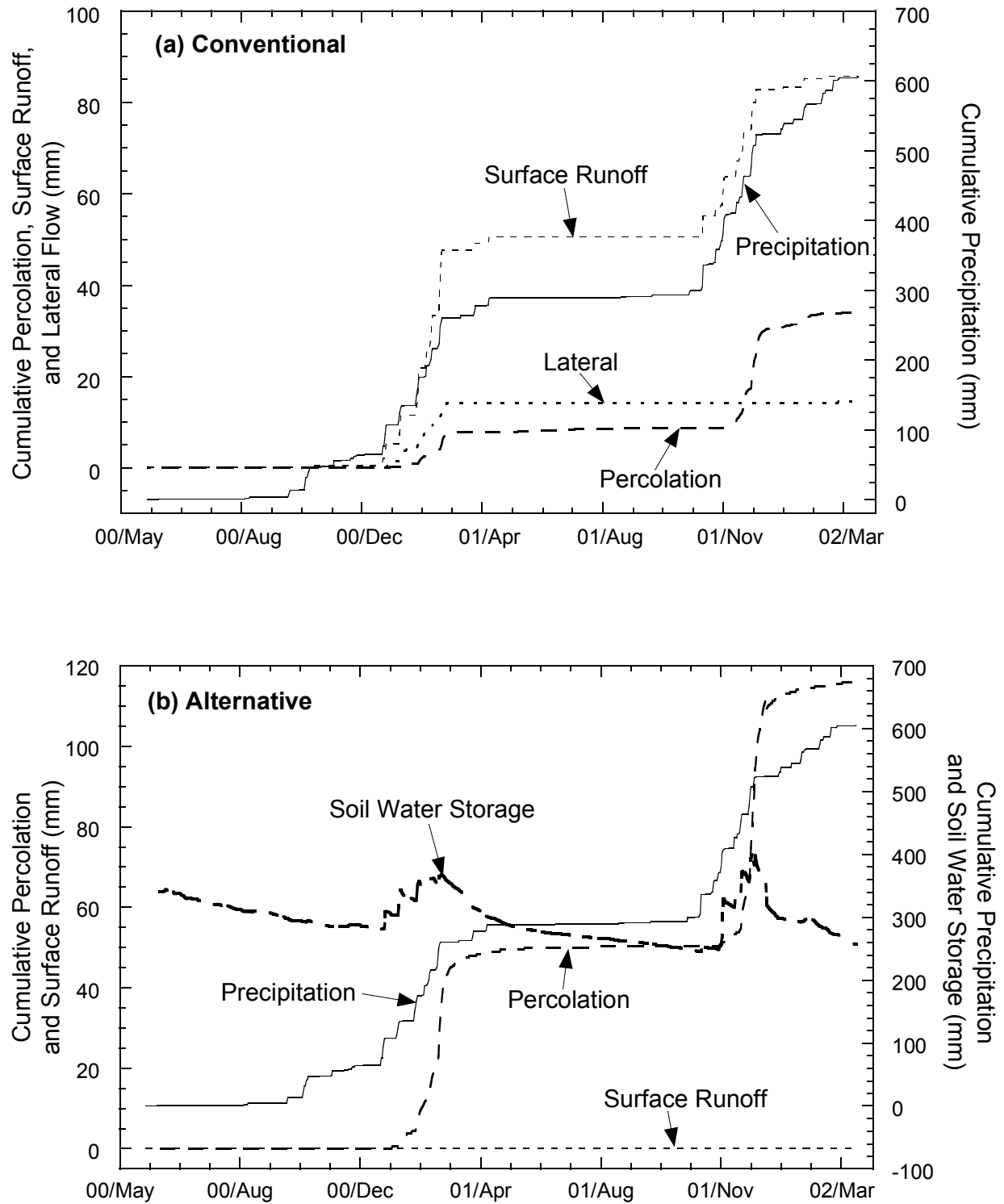


Fig. 4.19. Cumulative Water Balance at the Marina Site: (a) Conventional Cover and (b) Alternative Cover.

#### **4.6.3 Soil Water Storage**

Soil water storage records during the monitoring period are shown in Fig. 4.20. Soil water storage for both covers follows a similar trend, with increasing soil water storage during the rainy season (winter) followed by drying the following spring and summer.

For the alternative cover, the soil water storage capacity of the storage layer is never exceeded during the rainy season. However, a small amount of breakthrough into the sand layer (interim cover) occurred during the first year, whereas a large amount of breakthrough occurred during the second year (Fig. 4.21). During the dry summers, the vegetation is able to reduce the soil water storage, and the wilting point is not reached.

#### **4.6.4 Percolation**

Percolation for each cover during the monitoring period is shown in Figs. 4.19 and 4.20. The conventional cover transmitted 33.9 mm of percolation, whereas the alternative cover transmitted 115.9 mm of percolation. Most of the percolation occurred during the winter, when evapotranspiration was at its lowest and precipitation at its highest.

Percolation from the conventional cover may have been underestimated because the percolation data are based on measurements made with the tipping bucket rather than from the float switch. The tipping bucket data were used because the collection basin began leaking on approximately December 3, 2001.

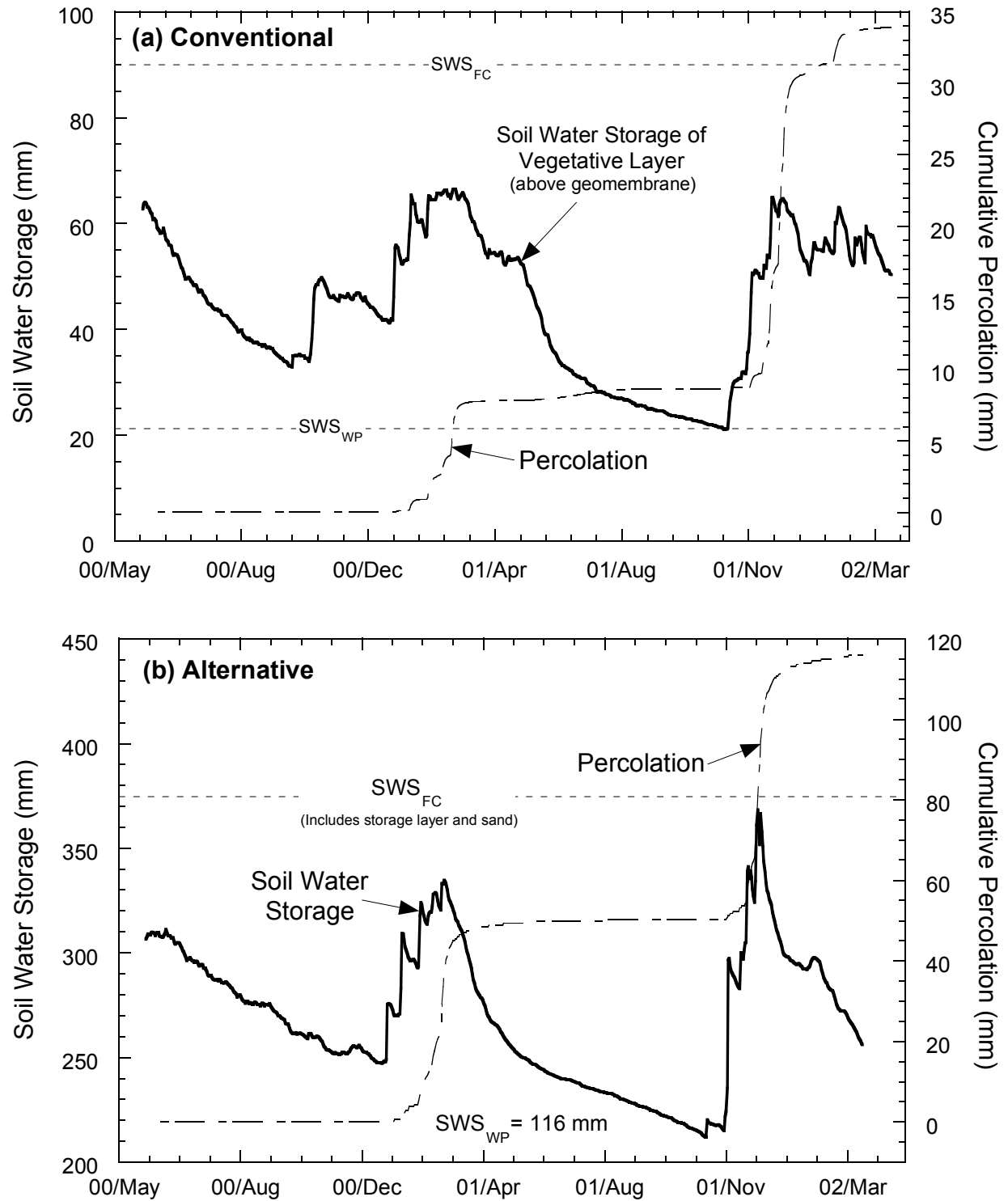


Fig. 4.20. Soil Water Storage at the Marina Site: (a) Conventional Cover and (b) Alternative Cover.

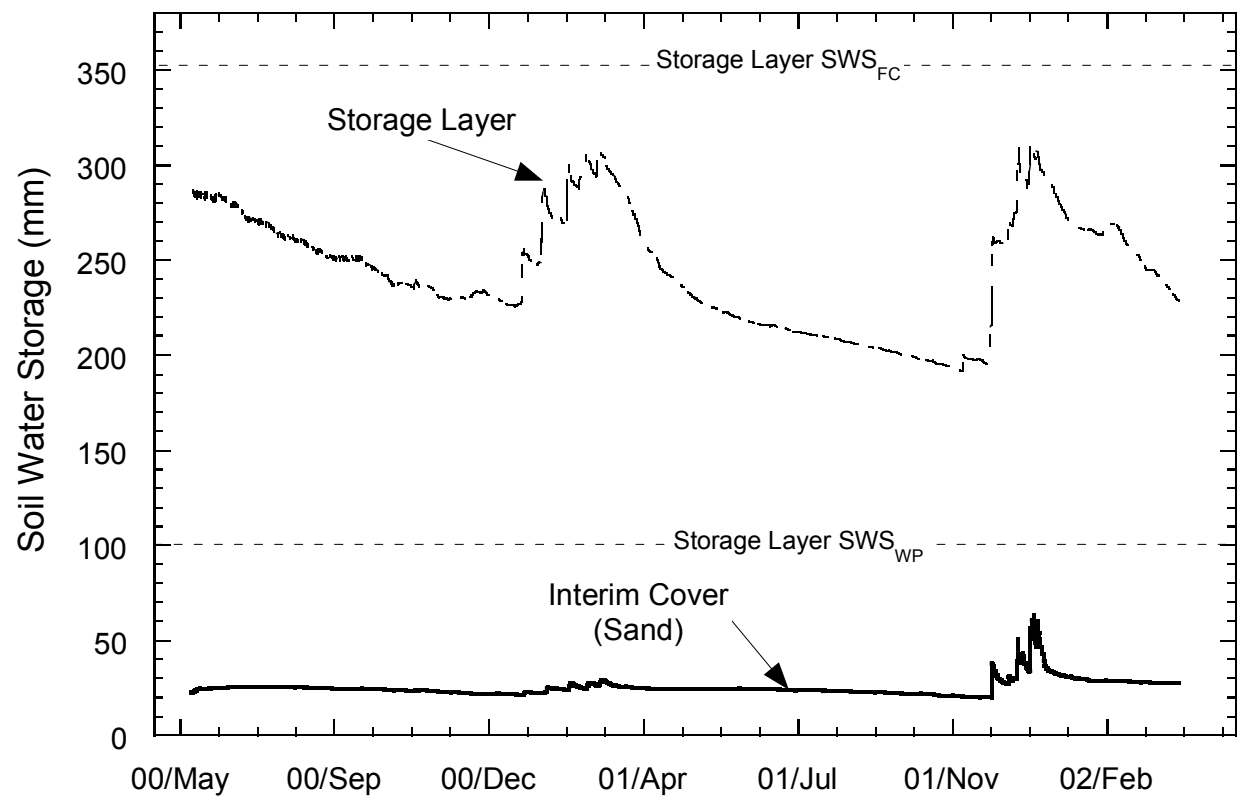


Fig. 4.21. Soil Water Storage of Individual Soil Layers for the Alternative Cover at the Marina Site.

Percolation from the conventional cover was transmitted during periods when the soil water storage of the vegetative layer (above the geomembrane) rose sharply (Fig. 4.21). Percolation was transmitted shortly thereafter because the compacted clay barrier beneath the geomembrane was placed wet of optimum water content. Percolation was still being transmitted by the conventional cover at the end of the monitoring period.

The relatively high percolation rate for this composite cover is probably due to punctures in the geomembrane. The vegetative cover was waste soil from nearby construction projects, and contained pieces of concrete and wire, which may have punctured the geomembrane. The waste soil was placed on top of the geomembrane without a protective layer (e.g., heavy geotextile) at the direction of the site owner even though a protection layer was recommended by the ACAP investigators.

Percolation from the alternative cover was transmitted during similar periods as the conventional cover, even though the soil water storage capacity was not exceeded. This may be due to preferential flow created by objects in the waste soil.

#### **4.7 ALBANY SITE**

Construction of the two test sections (conventional cover and alternative cover) at the Albany site was completed on March 18, 2000. Data collection began on April 19, 2000. Total precipitation during the monitoring period was 1615 mm. Irrigation was applied to the test sections to improve vegetative growth. During the monitoring period, 368 mm of irrigation was applied to the alternative cover and 46 mm to the conventional cover. The water balance for each cover is shown in Fig. 4.22.

#### **4.7.1 Surface Runoff**

Surface runoff during the monitoring period is shown in Fig. 4.22. Surface runoff recorded from the conventional cover was 168.5 mm and from the alternative cover it was 15.4 mm. No surface runoff was generated as a result of irrigation. Precipitation events that occur in this region tend to be very intense, generating large volumes of surface runoff. Surface runoff was 10.6% of the total precipitation (excluding irrigation) for the conventional cover, and 1% of the total precipitation for the alternative cover. Surface ponding was also observed during large storms.

The topsoil layer of the conventional cover eroded significantly because the vegetation was poor. To remedy the erosion problem, the topsoil layer was replaced in Fall 2001, and re-seeded with perennial rye grass on October 29, 2001. The erosion exposed desiccation cracks in the clay barrier approximately 10 to 25 mm wide and 100 to 150 mm deep. These cracks probably induced preferential flow, and may have reduced surface runoff.

Ninety-one percent of the surface runoff (14 mm) from the alternative cover occurred during the first growing season, when the vegetation was not fully established. Surface runoff was only 1% of precipitation due to (1) a loosely placed topsoil layer, (2) the hearty grass understory that was established early, and (3) tilling and trench work performed on the topsoil layer. The soil placed back into the trenches was loosely compacted, creating a sink for precipitation.

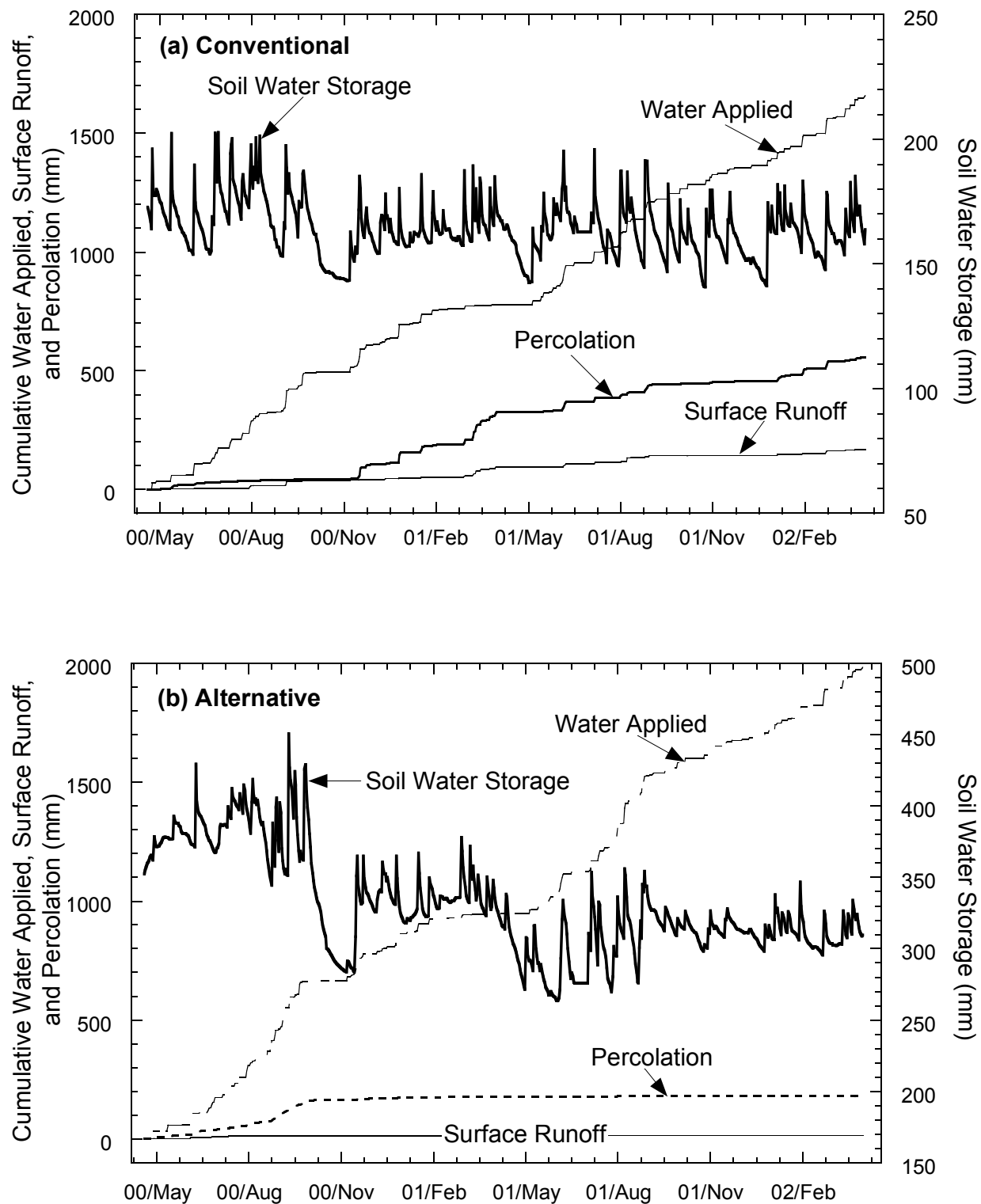


Fig. 4.22. Cumulative Water Balance at the Albany Site: (a) Conventional Cover and (b) Alternative Cover.



#### **4.7.2 Soil Water Storage**

The soil water storage record for the Albany site is shown in Fig. 4.23. Soil water storage for both covers fluctuated greatly throughout the entire monitoring period. The climate in Georgia can be characterized as hot and humid, with a lot of sunshine and intense rainstorms. This results in the entire soil profile becoming wet during rain events, followed by drying during subsequent days. The soil water storage capacity of both covers was never exceeded during the monitoring period, and never reached the wilting point.

For the alternative cover, the soil water storage dropped significantly in October 2000 due to the hybrid poplar trees becoming established (removing more available water) combined with a dry period (October 2000 thru mid-November 2000). Since then, soil water storage for the alternative cover has remained about 200 mm lower. In contrast, soil water storage for the conventional cover has remained approximately the same, on average, during the monitoring period.

#### **4.7.3 Percolation**

Percolation from both covers during the monitoring period is shown in Fig. 4.24. A large amount of percolation has been transmitted by both the conventional cover (468 mm) and alternative cover (180 mm).

The soil water storage capacity of the conventional cover was never exceeded during the monitoring period, even though significant percolation was recorded. Thus, flow most likely occurred through desiccation cracks. Preferential flow through the desiccation cracks became evident in November 2000, several months after

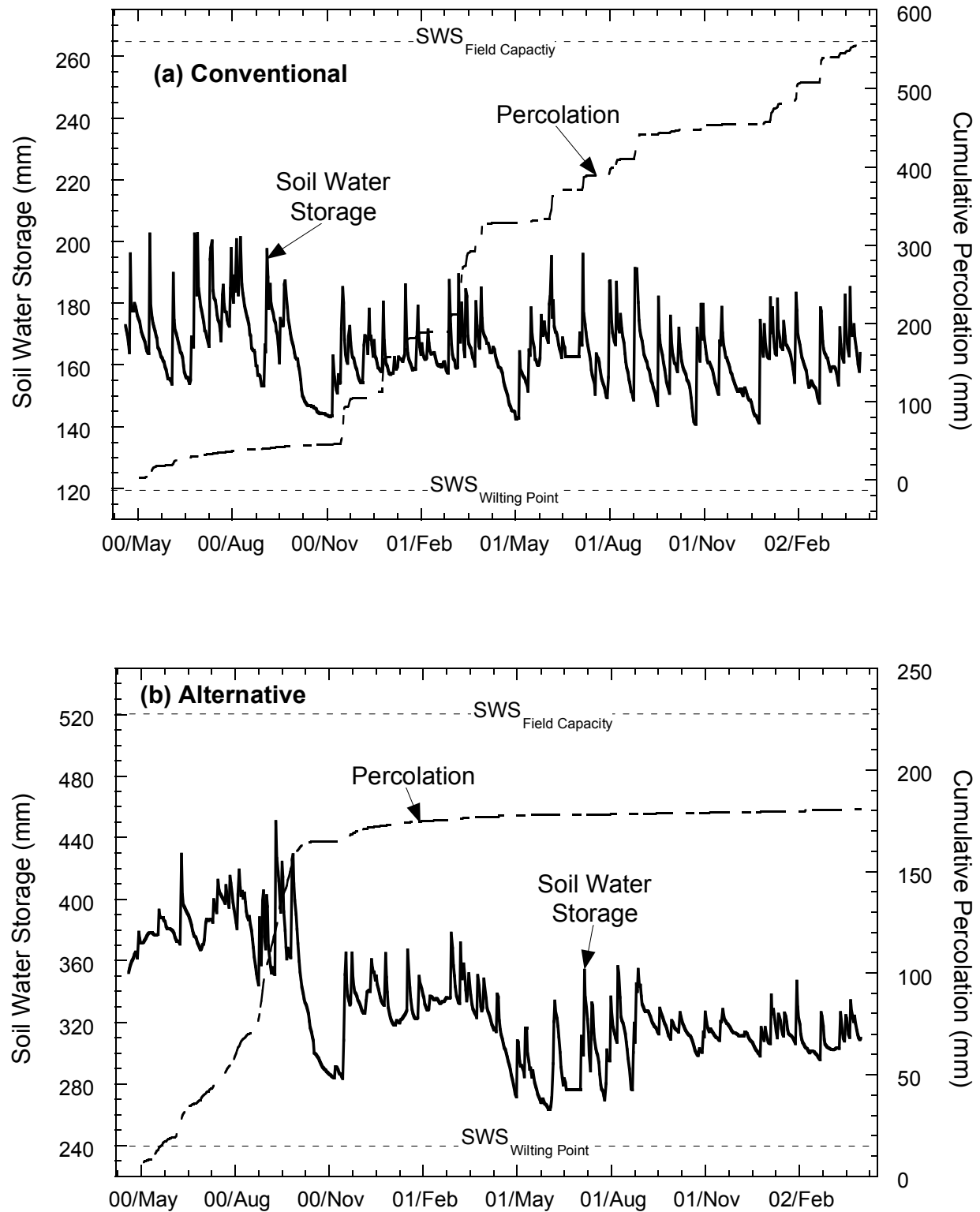


Fig. 4.23. Soil Water Storage Record at the Albany Site: (a) Conventional Cover and (b) Alternative Cover.

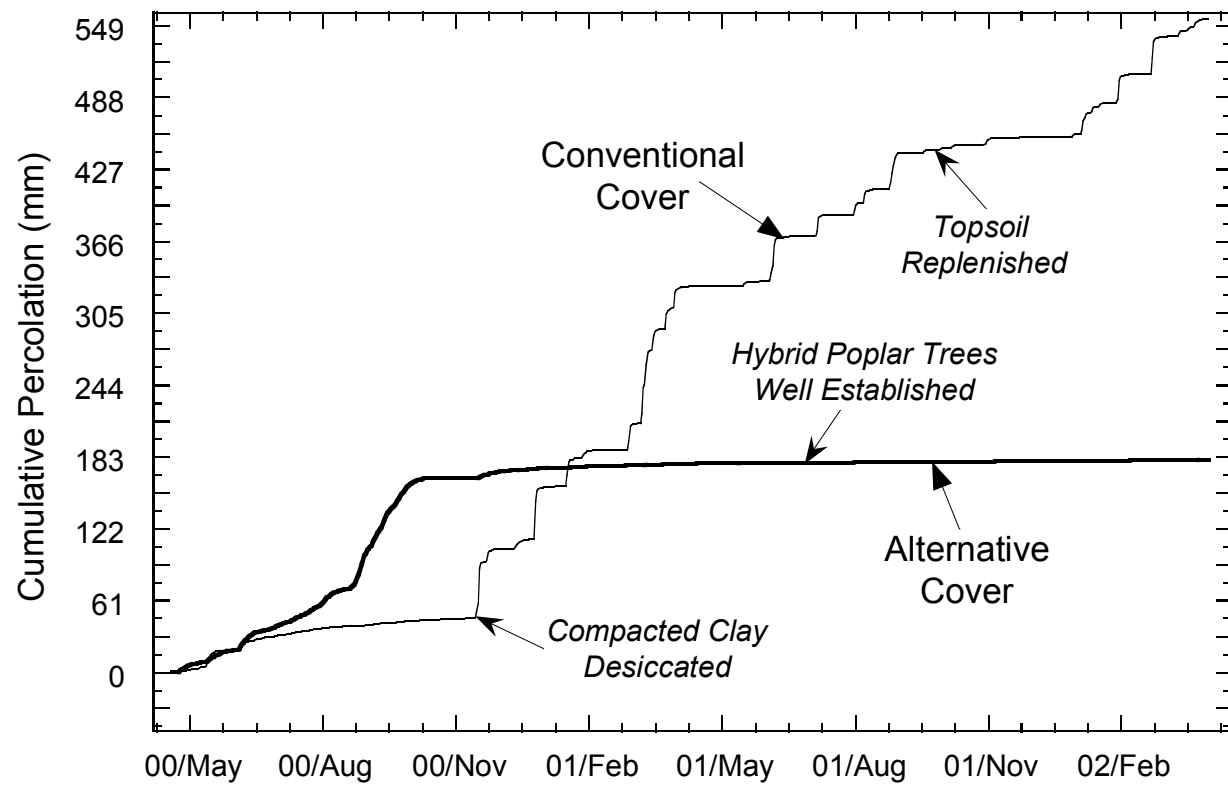


Fig. 4.24. Percolation at the Albany Site from the Conventional and Alternative Covers.

construction. Prior to mid November 2000, the percolation rate from the conventional cover was 83 mm/yr. After November, the percolation rate jumped to 385 mm/yr. In addition, the cumulative percolation increased smoothly prior to November 2000, but afterwards the percolation record was comprised predominately of pulses following precipitation events.

For the alternative cover, percolation was recorded immediately after construction, and sharply increased during the first growing season. In October 2000, the percolation rate diminished, after which only 10% (18 mm) of the total percolation was recorded. This drop in percolation rate can be attributed to transpiration by the hybrid poplar trees. Since January 2001, the percolation rate has been 6 mm/yr.

## **4.8 CEDAR RAPIDS SITE**

Construction of three test sections at the Cedar Rapids site (composite cover, compacted clay cover, and alternative cover) was completed on October 2, 2000. Data collection began on October 3, 2000. Total precipitation during the monitoring period was 772 mm, of which 12.7% was frozen. The water balance for each test section is shown in Figs. 4.25 and 4.26. Data are presented only through October 18, 2001 due to a malfunction of the datalogger. The datalogger was repaired on March 20, 2002.

### **4.8.1 Surface Runoff**

Surface runoff during the monitoring period is shown in Figs. 4.25 and 4.26. Surface runoff was 22.0 mm for the composite cover, 14.9 mm for the compacted clay cover, and 26.8 mm for the alternative cover. Surface runoff ranged between 1.9-3.5% of precipitation, with the alternative cover having the greatest fraction of runoff (3.5%).

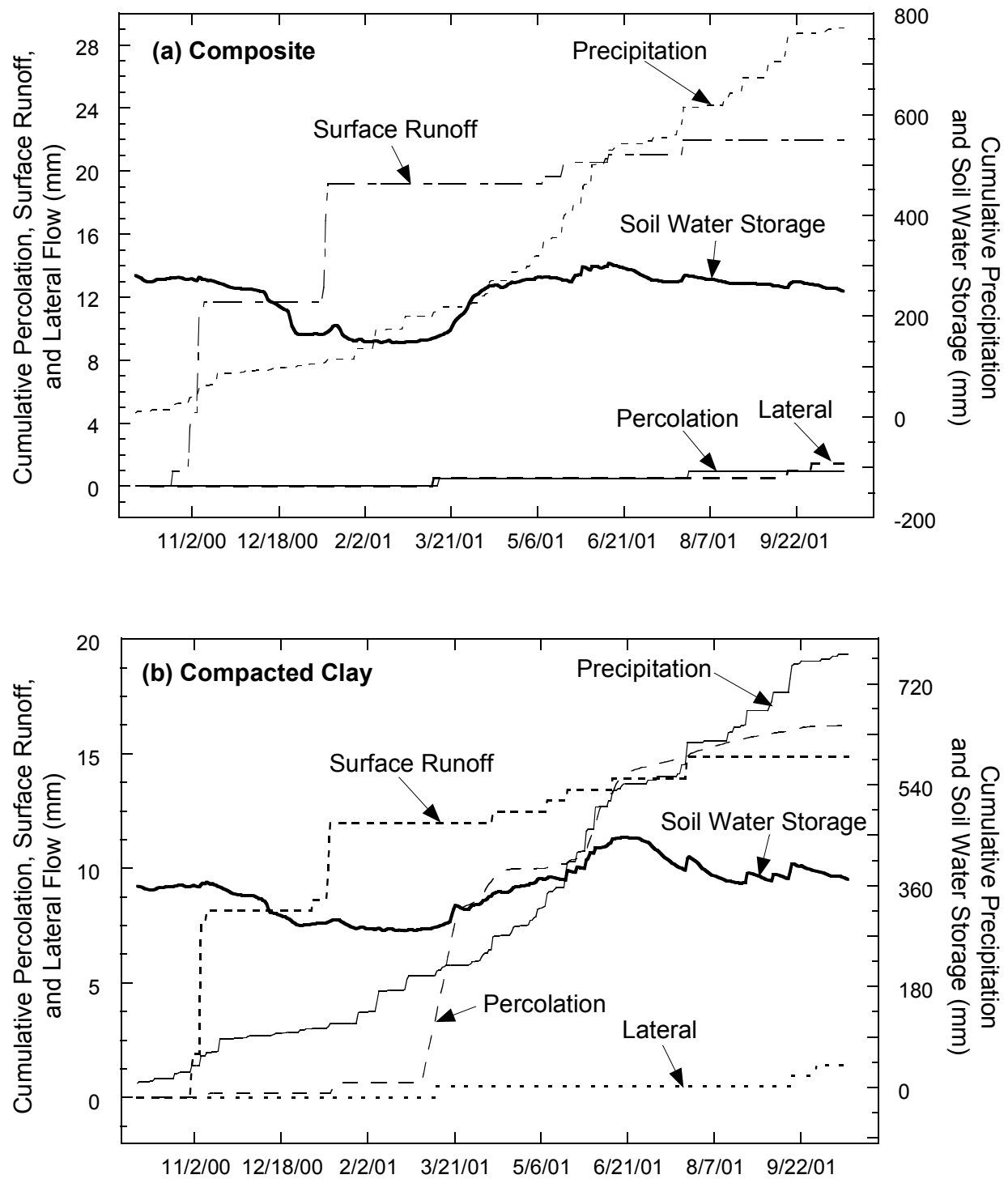


Fig. 4.25. Cumulative Water Balance at the Cedar Rapids Site: (a) Composite Cover and (b) Compacted Clay Cover.

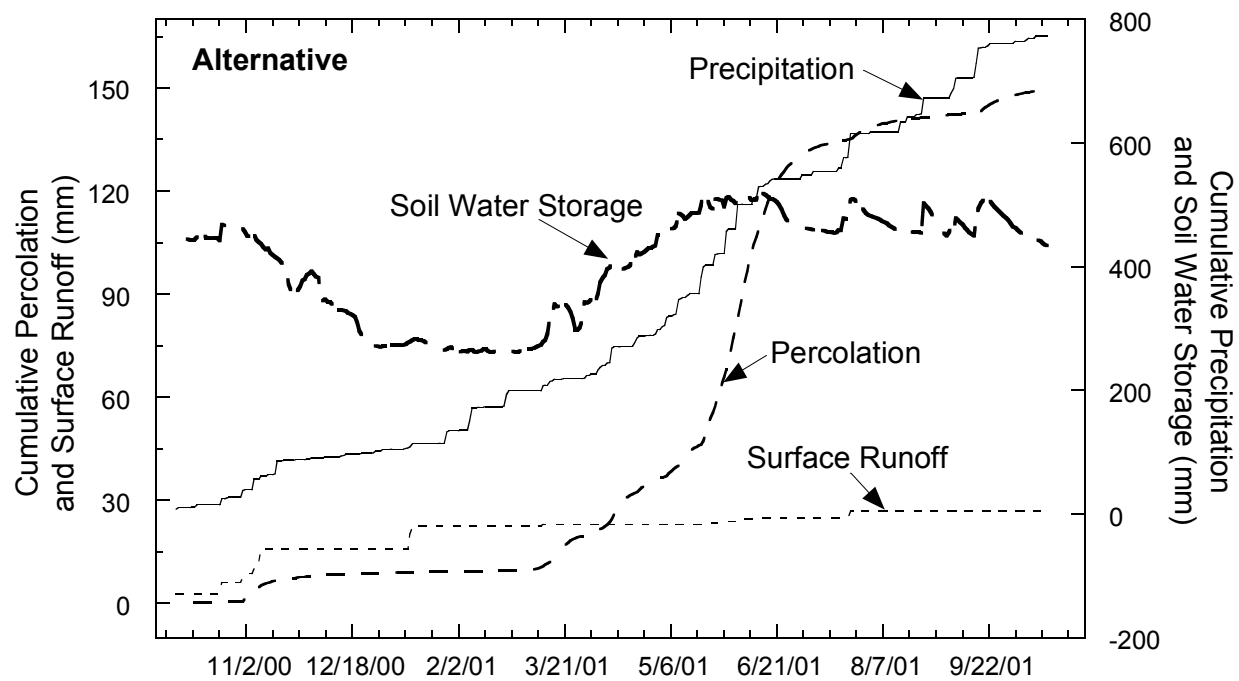


Fig. 4.26. Cumulative Water Balance at the Cedar Rapids Site: Alternative Cover.

The first major surface runoff event occurred on November 6, 2000 as a result of an intense rain event (17.5 mm). After this date, the air temperature dropped below 0°C, causing additional precipitation to be stored as snowpack. In the middle of January 2000, the air temperature rose above 0°C and rain was recorded, causing a large snowmelt event. Surface runoff was next recorded on the alternative cover on March 12, 2001 due to a snowmelt event from the on-set of the spring rains. This event did not produce any surface runoff from the conventional covers, even though the ground was still frozen for all covers (Fig. 4.27). Surface runoff was next recorded on April 11, 2001 for the compacted clay barrier as the result of an intense rain event (23 mm) and on May 10, 2001 for the composite barrier as the result of another intense rain event (23 mm).

#### **4.8.2 Lateral Flow**

Lateral flow records for the composite cover and compacted clay cover are shown in Fig. 4.25. Lateral flow was recorded for both the composite cover (1.44 mm) and compacted clay cover (1.44 mm) during the same time periods (March 12, September 12, and October 1, 2001).

#### **4.8.3 Soil Water Storage**

Soil water storage records are shown in Fig. 4.28. Hydraulic properties of each layer are presented in Tables 4.3 through 4.5. Soil water storage for each cover reaches a minimum during late summer, and reaches a maximum in late spring after the spring rains and snowmelt.

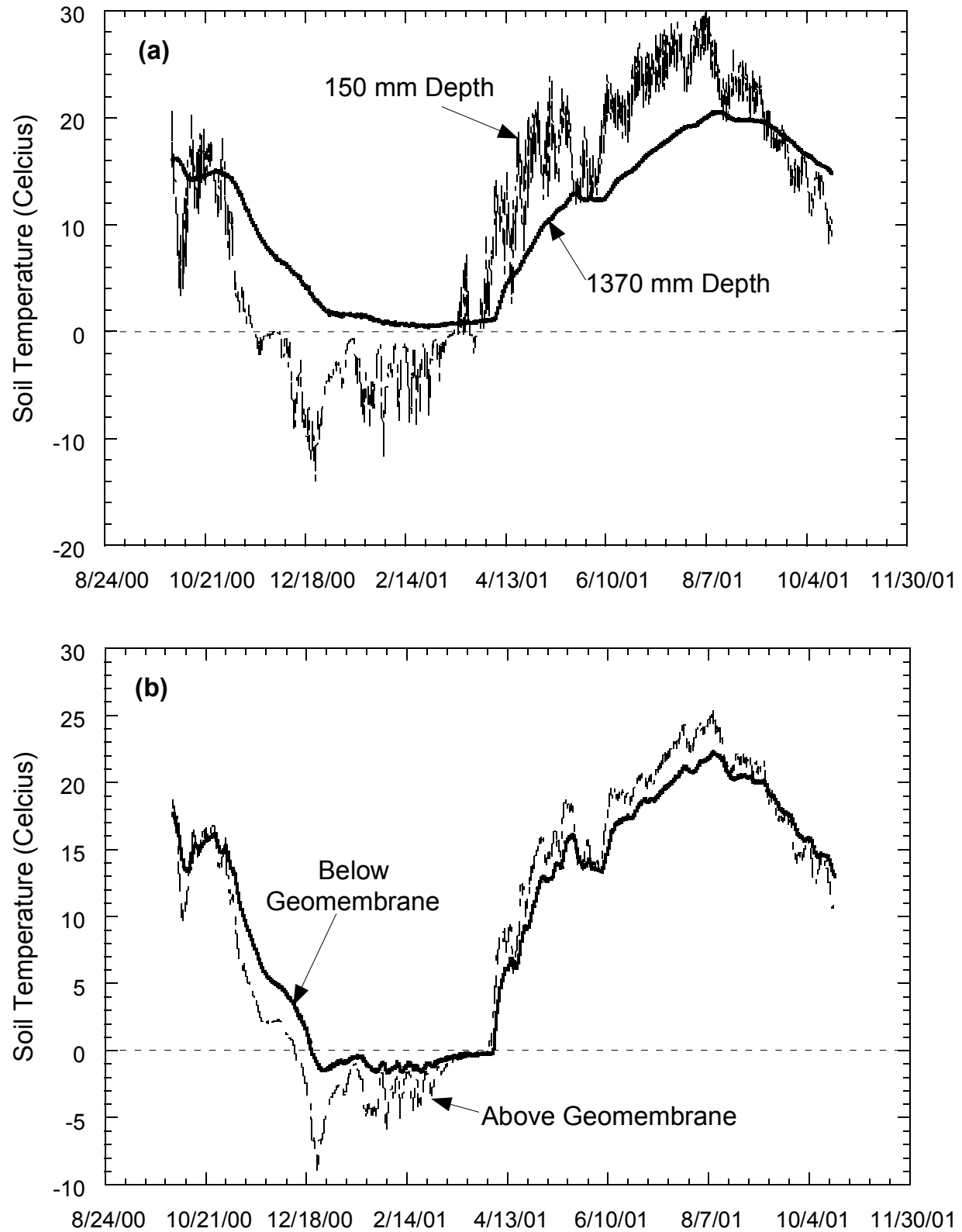


Fig. 4.27. Soil Temperatures in Test Sections: (a) Alternative Cover and (b) Composite Cover.



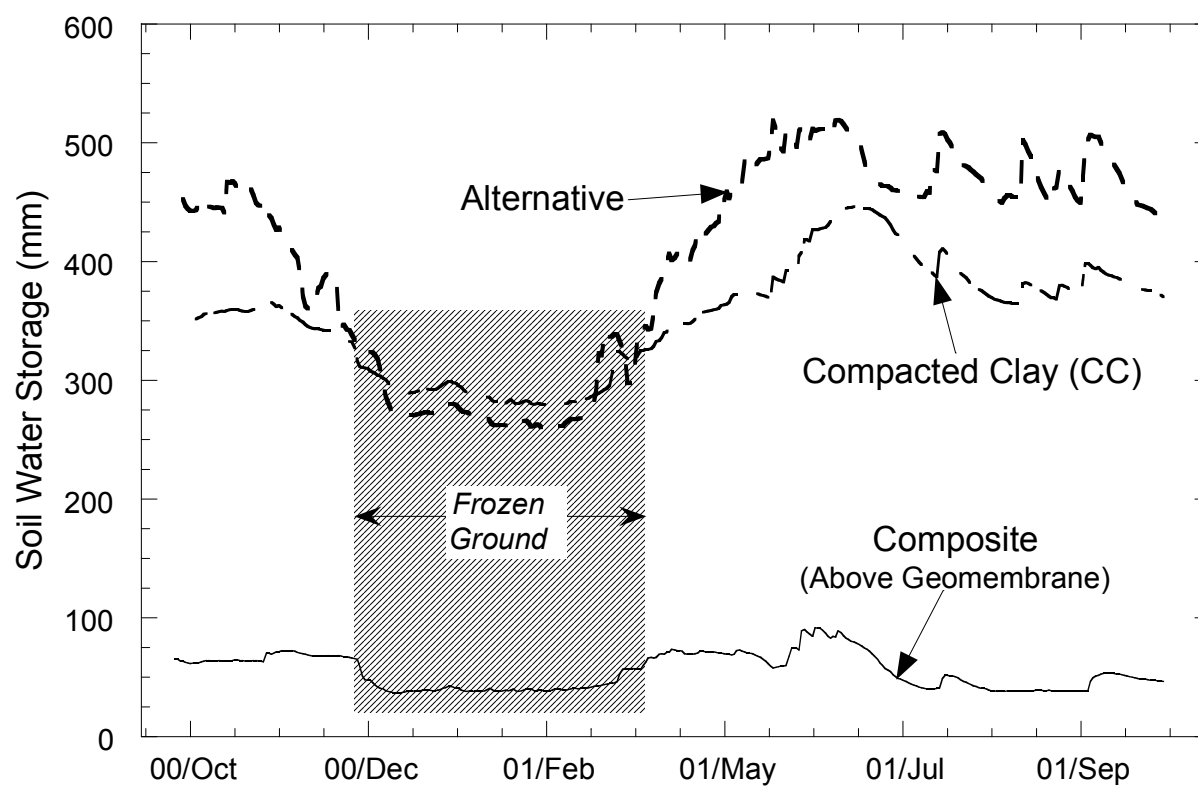


Fig. 4.28. Soil Water Storage at Cedar Rapids Site.

Table 4.3. Hydraulic Properties of the Alternative Cover at the Cedar Rapids Site.

Layer	$\theta_r$	$\theta_s$	$\alpha$ (cm <sup>-1</sup> )	n	Field Capacity	Wilting Point	$K_s$ (cm/s)
Storage	0.00	0.33	0.00017	1.55	0.33	0.18	$5.34 \times 10^{-6}$
Support	0.00	0.27	0.00028	1.40	0.27	0.15	$2.52 \times 10^{-7}$
Interim Cover	0.00	0.27	0.00038	1.46	0.27	0.12	$3.41 \times 10^{-6}$

Hydraulic properties from Gurdal (2002).

Table 4.4. Hydraulic Properties of the Compacted Clay Cover at the Cedar Rapids Site.

Layer	$\theta_r$	$\theta_s$	$\alpha$ (cm <sup>-1</sup> )	n	Field Capacity	Wilting Point	$K_s$ (cm/s)
Topsoil	0.00	0.57	0.00331	1.27	0.49	0.20	$2.0 \times 10^{-5}$
Barrier	0.00	0.29	0.00052	1.37	0.28	0.13	$2.2 \times 10^{-8}$
Interim Cover	0.00	0.32	0.00011	1.54	0.32	0.21	$2.5 \times 10^{-6}$

Hydraulic properties from Gurdal (2002). Laboratory testing not complete (parameters based on 5 of 20 samples collected during construction).

Table 4.5. Hydraulic Properties of the Composite Cover at the Cedar Rapids Site.

Layer	$\theta_r$	$\theta_s$	$\alpha$ (cm <sup>-1</sup> )	n	Field Capacity	Wilting Point	$K_s$ (cm/s)
Topsoil	0.00	0.53	0.00331	1.27	0.45	0.18	$5.8 \times 10^{-6}$
Barrier	0.00	0.29	0.00010	1.91	0.29	0.17	$1.7 \times 10^{-8}$
Interim Cover	0.00	0.31	0.00021	1.48	0.31	0.17	$7.2 \times 10^{-6}$

Hydraulic properties from Gurdal (2002). Laboratory testing not complete (parameters based on 6 of 16 samples collected during construction).

During the winter, the apparent drop in soil water storage is an artifact of frozen ground conditions (Fig. 4.27). The WCRs record only the unfrozen water content, and thus do not reflect the actual volume of water during frozen conditions. Temperatures below 0°C were measured throughout the entire cover profile in the composite cover, to a depth of 600 mm in the compacted clay cover (i.e., bottom of topsoil layer), and to a depth of 920 mm in the alternative cover (bottom of storage layer).

For the composite cover, soil water storage in the topsoil layer increases in early Spring 2001, after the spring thaw (see Fig. 4.29). The soil water storage decreases slightly in the late spring, likely due to evapotranspiration, and then increases after several large rain events. During Summer 2001, soil water storage in the topsoil layer decreases appreciably due to evapotranspiration. Soil water storage reaches the wilting point during the summer.

For the compacted clay cover, soil water storage in the topsoil and compacted clay layers increased significantly due to the spring thaw (see Fig. 4.30a). The capacity of the compacted clay layer was exceeded in late Spring 2001, despite the capacity of the topsoil layer not being exceeded. During the summer, soil water storage in the topsoil layer decreases rapidly to the wilting point, and fluctuates throughout the summer due to rain events. Soil water storage in the compacted clay layer is slowly reduced during the summer, most likely due to water draining through the cover, rather than by evapotranspiration.

For the alternative cover, soil water storage in the storage and support layers increased significantly due to spring thaw (see Fig. 4.30b). The capacity of the support layer was exceeded by late spring, despite the capacity of the storage layer not being

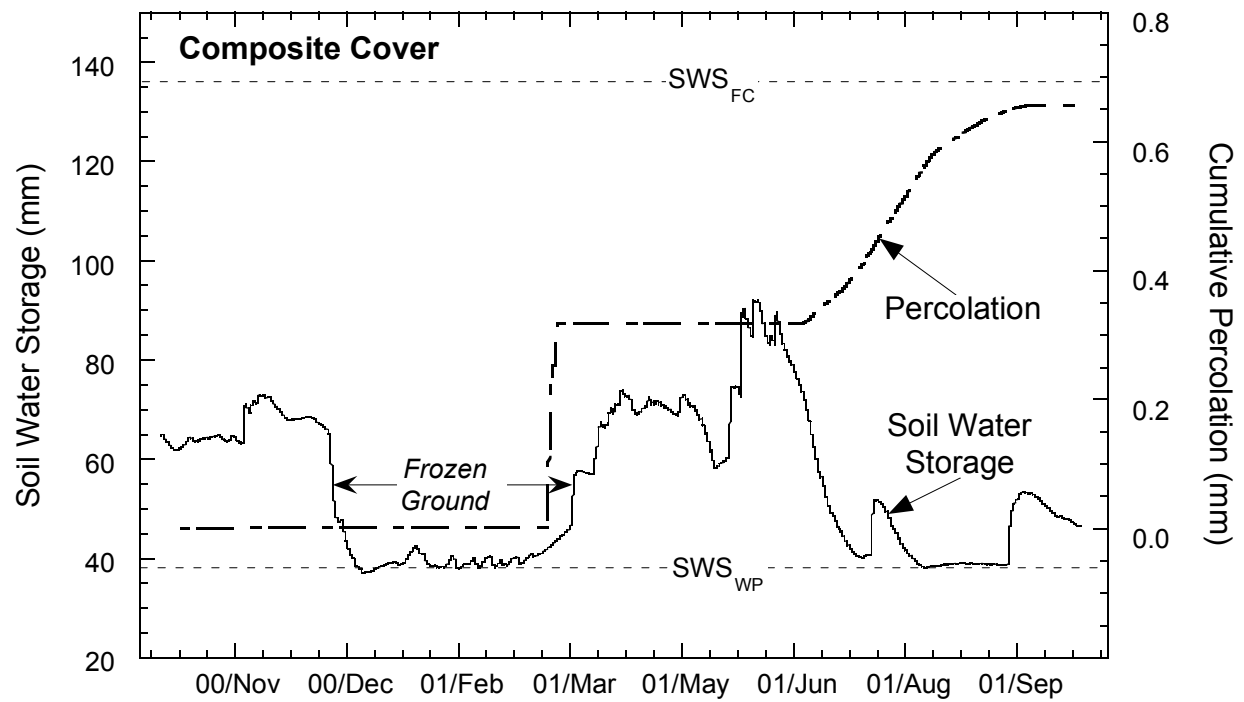


Fig. 4.29. Soil Water Storage of Topsoil Layer and Cumulative Percolation for the Composite Cover at the Cedar Rapids Site.

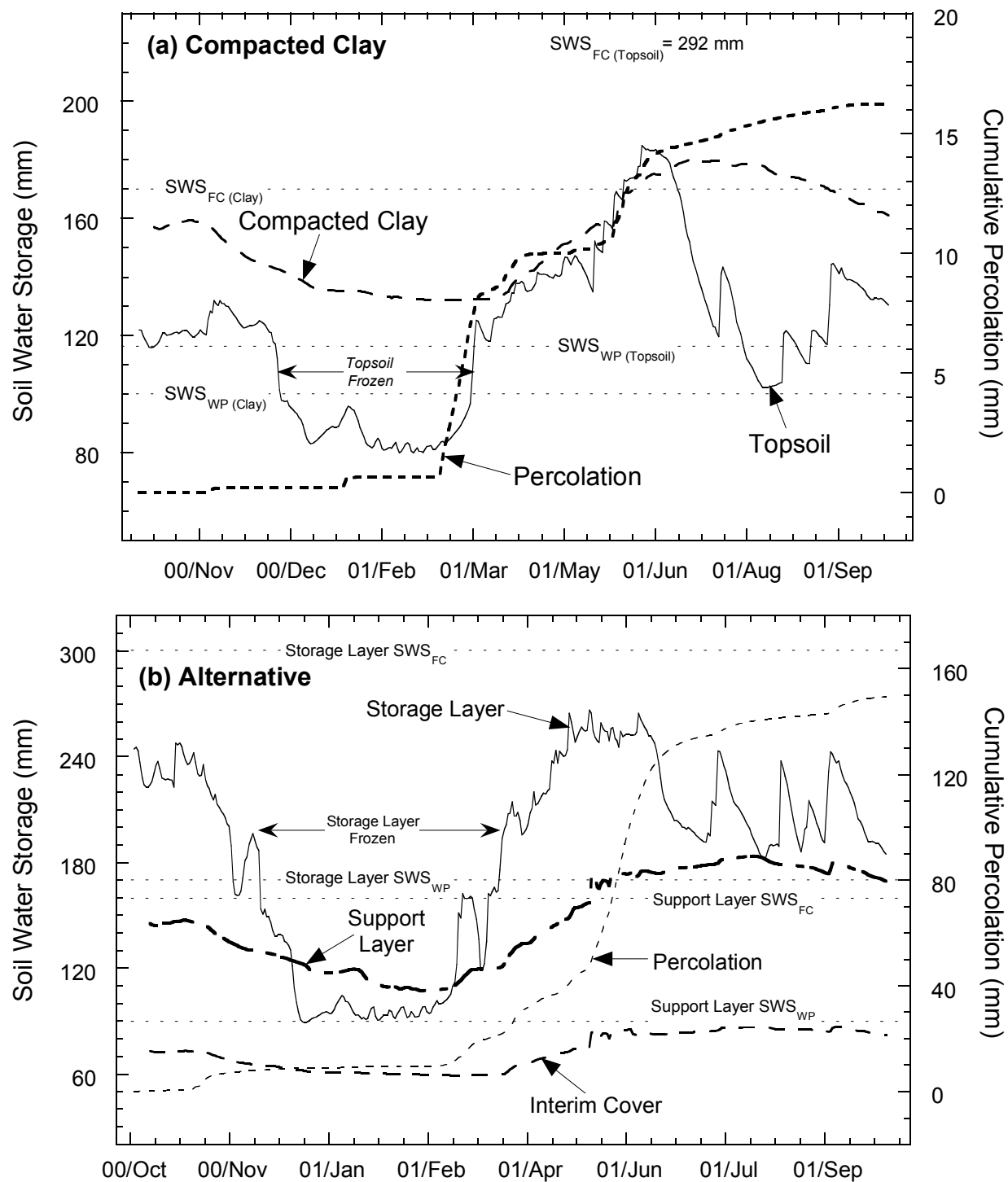


Fig. 4.30. Soil Water Storage of Individual Soil Layers at Cedar Rapids Site: (a) Compacted Clay Cover and (b) Alternative Cover

exceeded. Flow through the storage layer was likely through preferential flow paths, which were likely created by trenching during installation of the trees. During the summer, soil water storage in the storage layer first decreased rapidly, and then fluctuated throughout the summer due to rain events. The trees and the understory of grass are capable of maintaining the soil water storage of the storage layer well below the field capacity during the summer, but little water is removed from the support layer. Water is probably not being removed from the support layer as of yet because the roots have not yet penetrated to this depth.

#### **4.8.4 Percolation**

Percolation was recorded from each cover during the monitoring period (Fig. 4.31). The least percolation was from the composite cover (0.94 mm), then the compacted clay cover (16.2 mm), and the alternative cover (149.4 mm).

Percolation was first transmitted from each cover during the same time period (March 10-22, 2001), in response to a large snowmelt event accompanied by rain. All of the snowmelt infiltrated the cover profiles because the ground surface was no longer frozen. During this period, the composite cover transmitted a pulse of percolation (0.45 mm), whereas the compacted clay and alternative covers began to transmit significant percolation regularly throughout the remainder of the monitoring period. Prior to March 10, 10 mm of percolation was transmitted from the alternative cover.

A pulse of percolation was first transmitted from the composite cover in early Spring 2001, due to the spring thaw (Fig. 4.29). Percolation was transmitted again in Summer 2001 after heavy rains. The percolation rate increased as the soil water

storage of the topsoil layer decreased, and then tailed off towards the end of the monitoring period, when the topsoil layer reached the wilting point.

For the compacted clay cover, percolation initially was transmitted during warmer periods in the winter. This percolation is probably due to thaw consolidation and drainage. Percolation began again in the spring as field capacity was approached, and then tailed off towards the end of the monitoring period, as the soil water storage in the compacted clay layer decreased (Fig. 4.30a).

For the alternative cover, percolation was readily transmitted through the cover profile, most likely due to preferential flow paths. The percolation rate increased significantly when the soil water storage of the support layer was exceeded in late Spring 2001 (Fig. 4.30b).

## **4.9 OMAHA SITE**

Construction of three test sections (one conventional cover and two alternative covers) at the Omaha site was completed on August 11, 2000. Data collection began on October 5, 2000. Total precipitation recorded during the monitoring period was 719 mm, 8.7% of which was frozen. The water balance for each test section is shown in Figs. 4.32 and 4.33. Precipitation records have not been acquired since December 6, 2001 because the rain gauge malfunctioned.

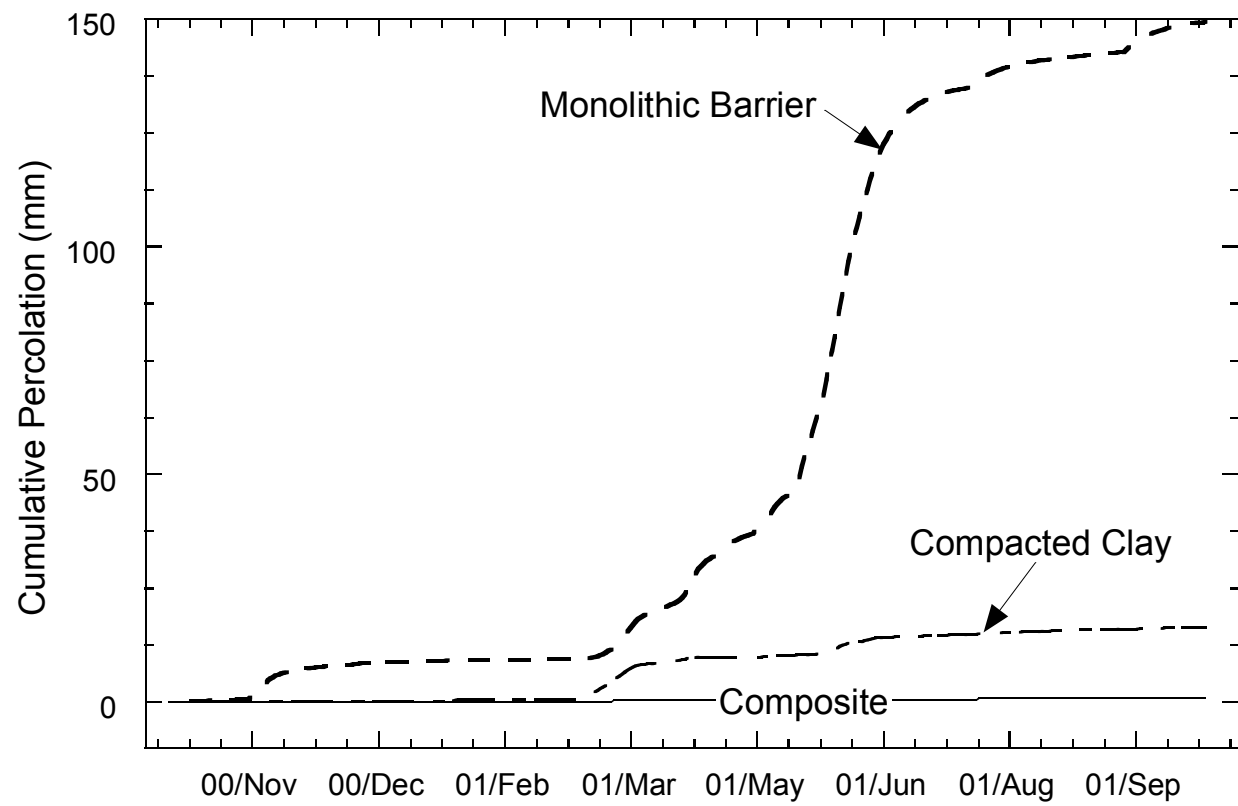


Fig. 4.31. Percolation from Test Sections at Cedar Rapids Site.



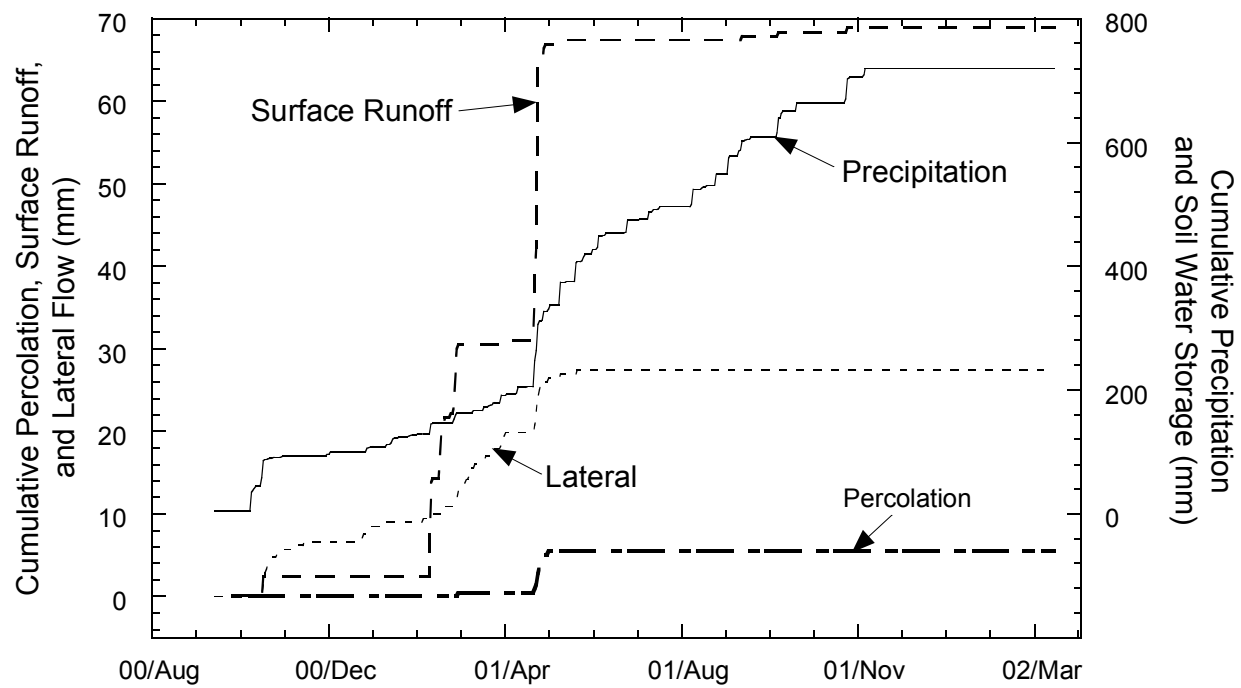


Fig. 4.32. Cumulative Water Balance at the Omaha Site: Conventional Cover.

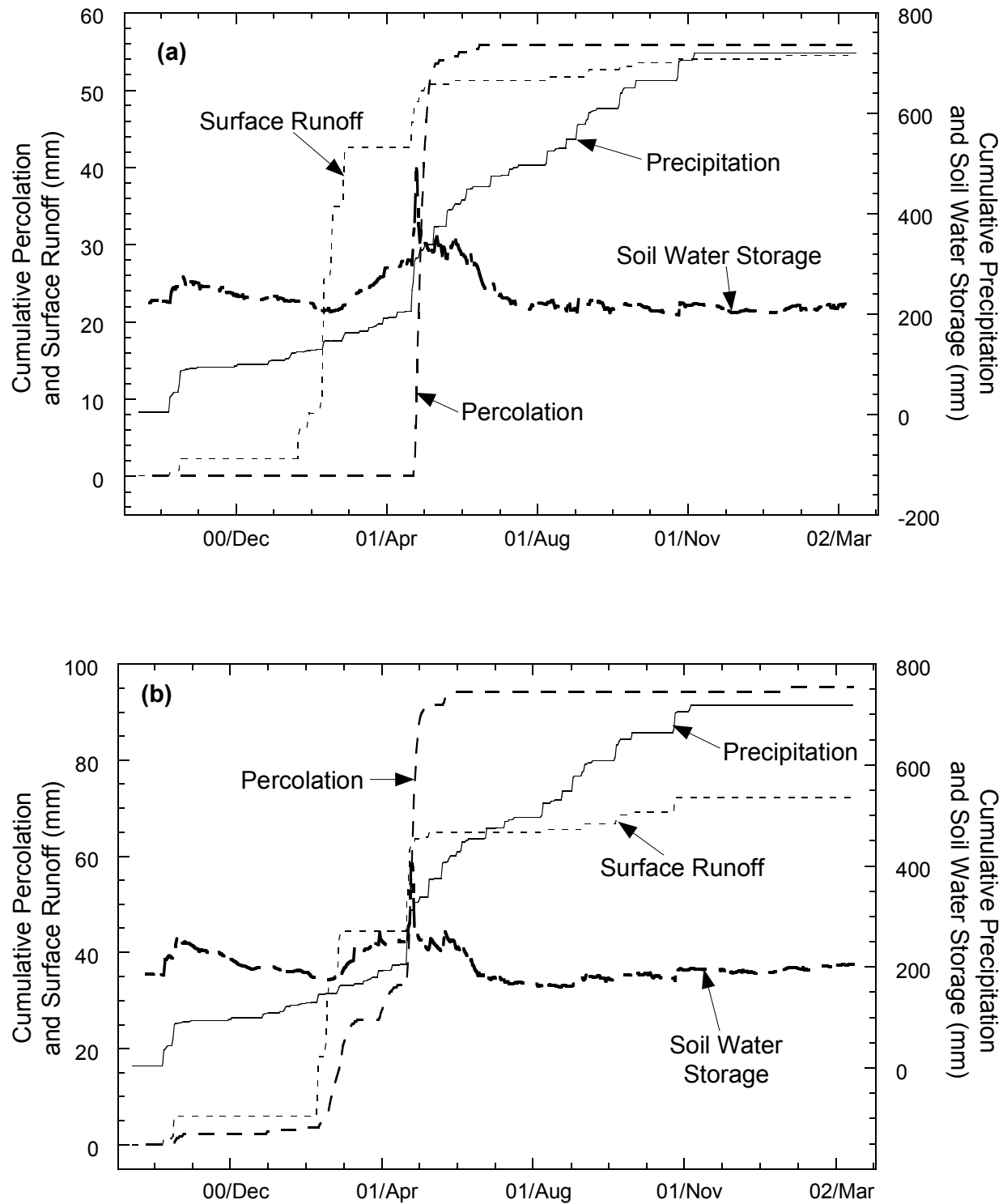


Fig. 4.33. Cumulative Water Balance at the Omaha Site: (a) Thin Capillary Barrier (760 mm) and (b) Thick Capillary Barrier (1060 mm).

#### **4.9.1 Surface Runoff**

Surface runoff is shown in Figs. 4.32 ad 4.33. Surface runoff was 68.8 mm from the composite barrier, 72.3 mm from the thin capillary barrier (760 mm), and 54.4 mm from the thick capillary barrier (1060 mm), corresponding to 7.5-10.1% of precipitation. The surface runoff from each cover is comparable because the covers have the same vegetation, slope, and topsoil.

Surface runoff was generated by intense rain and large snowmelt events, such as three large rain events during Spring and Fall 2001 that accounted for 36% of precipitation. Also, snow melt (approximately 39 mm) occurring at the end of February 2001 and the beginning of March 2001 caused considerable surface runoff (28 mm from the composite cover, 38 mm from the thin capillary barrier, and 38 mm from the thick capillary barrier). Between 72-97% of the snowmelt became surface runoff because of frozen ground conditions.

No surface runoff was recorded during Spring 2002. The absence of runoff is likely due to the vegetation being established, and the mild winter in 2002. The mild winter prevented the ground surface from freezing (Fig. 4.34), and therefore precipitation was not shed as easily as in 2001.

#### **4.9.2 Lateral Flow from Conventional Cover**

Lateral flow from the conventional cover is shown in Fig. 4.32. Lateral flow during the monitoring period was 27.4 mm, with the majority of flow being the result of snowmelt and intense rain events. Water that infiltrated during the intense rain events reached the geomembrane with very little delay.

### 4.9.3 Soil Water Storage

The soil water storage record for the Omaha site is shown in Fig. 4.35. Soil water storage for each cover typically begins to increase in late winter due to the spring thaw, and decreases during the summer. The large peaks in soil water storage (Fig. 4.36) are caused by a large and abrupt increase in water content in the sand layer, caused by an intense rain event (132.6 mm) on May 3-13, 2001.

Soil water storage for all covers reaches a peak after the spring thaw in 2001, and begins to decrease during the summer, as expected. Soil water storage in each cover also appears to drop during Winter 2000. However, this drop in soil water storage is an artifact of frozen ground conditions. During Winter 2001, soil water storage is not affected by frozen ground conditions because of the mild winter (Fig. 4.34).

For the alternative covers, the vegetation is capable of removing most of the available soil water during the summer.

### 4.9.4 Percolation

Percolation during the monitoring period is shown in Fig. 4.37. The conventional cover transmitted 5.5 mm of percolation, the thin (760 mm) capillary barrier transmitted 95.1 mm of percolation, and the thick (1060 mm) capillary barrier transmitted 55.7 mm of percolation. The majority of the percolation from each cover occurred during a single period (May - June 2001), during which a large amount of rainfall was recorded.

Percolation was transmitted from the “thin” capillary barrier on several occasions, with the first being on November 6, 2000 due to 43 mm of rain. Percolation was also transmitted between March 12-15, 2001 due to 23.5 mm of rain and snow melt, and

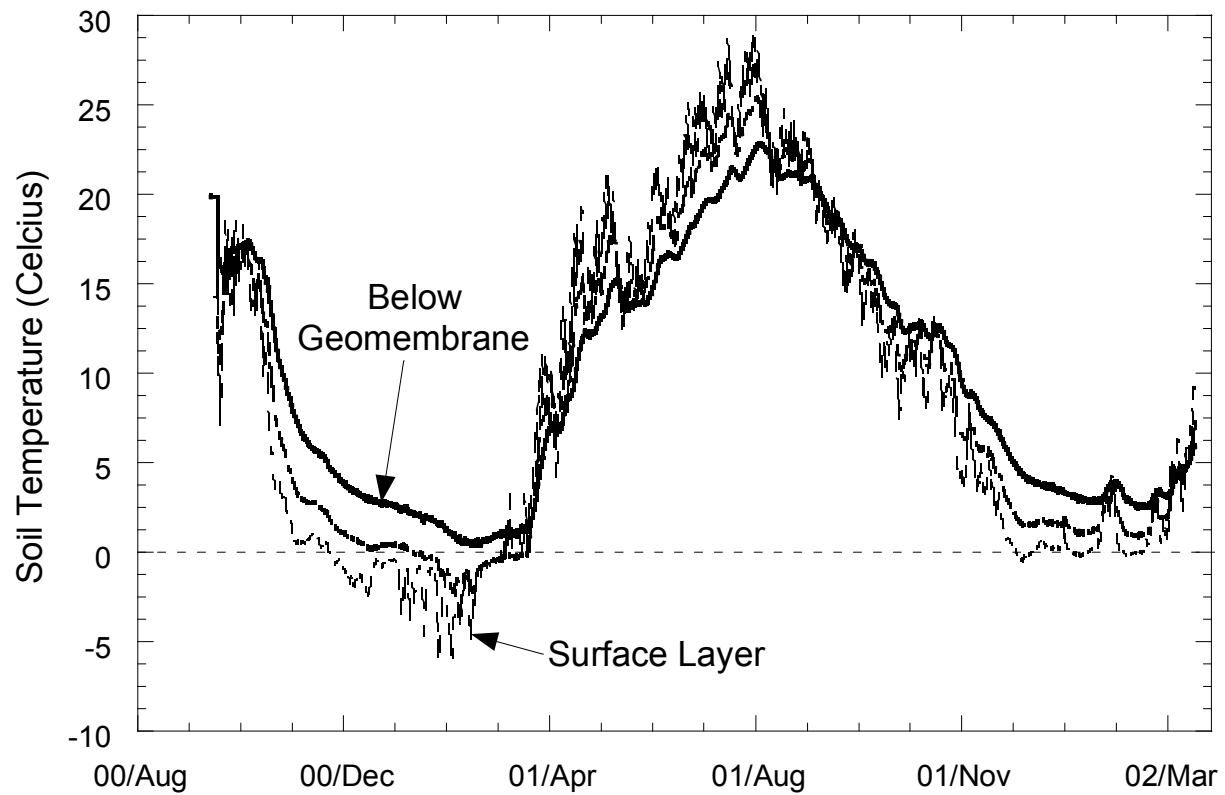


Fig. 4.34. Soil Temperatures in Conventional Cover at the Omaha Site.

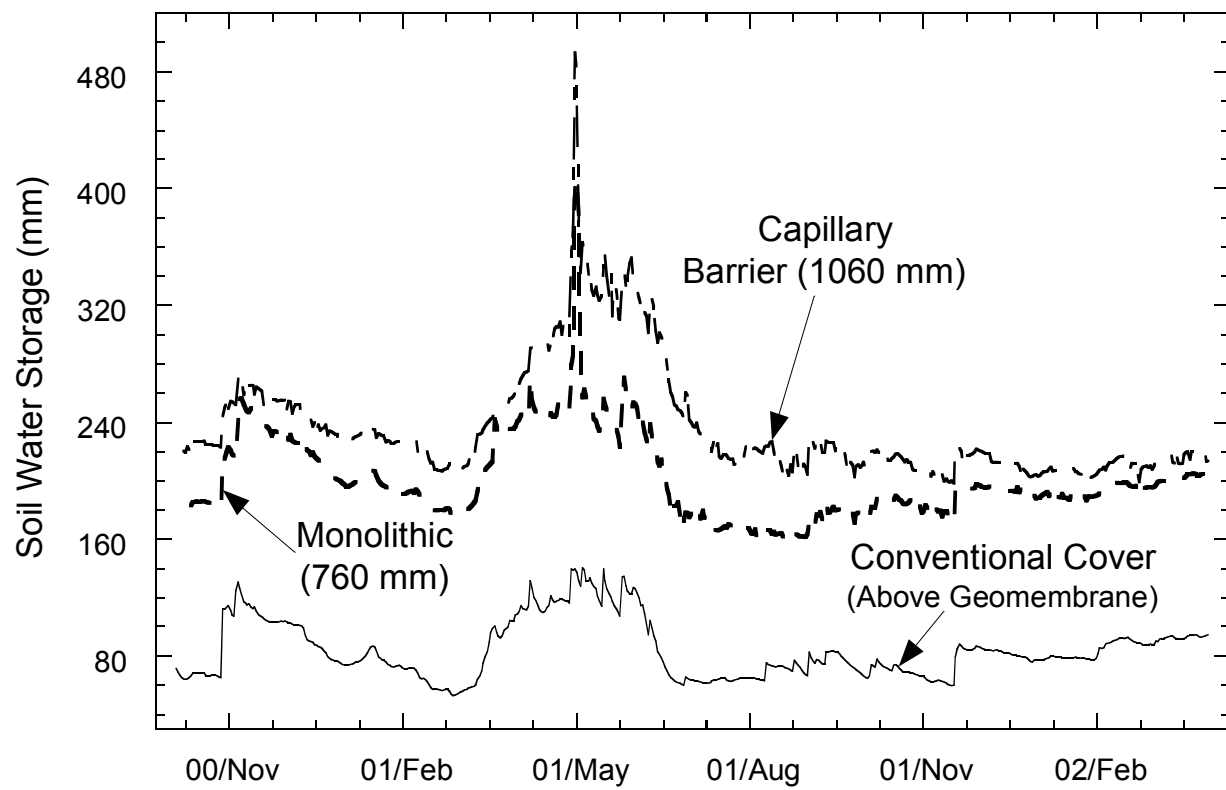


Fig. 4.35. Soil Water Storage at the Omaha Site.

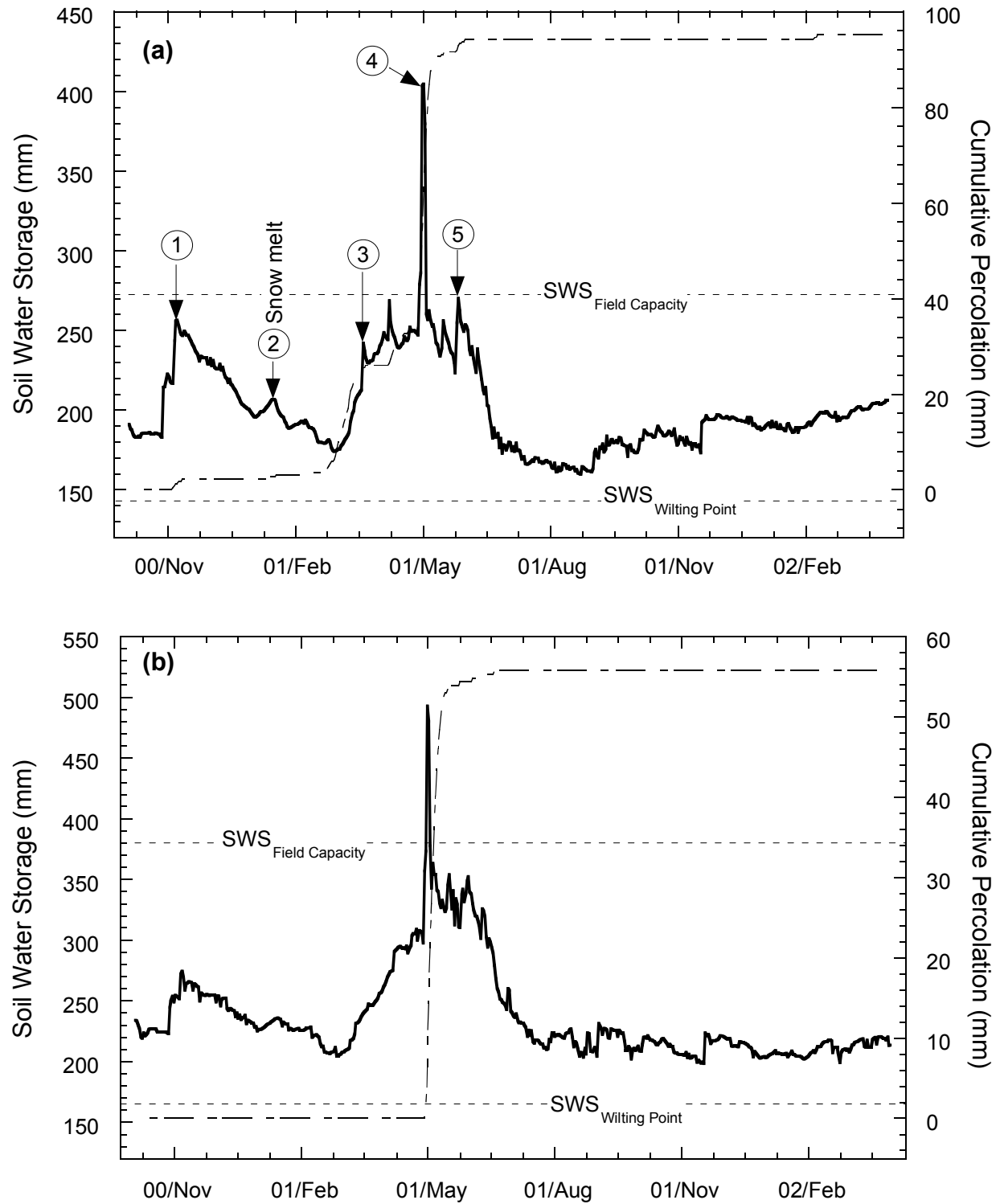


Fig. 4.36. Soil Water Storage and Percolation at Omaha Site: (a) Thin Capillary Barrier (760 mm) and (b) Thick Capillary Barrier (1060 mm).

between May 3-13, 2001 due to 122 mm of rain. The percolation events from the thin capillary barrier correspond to peaks in the soil water storage record, as shown in Fig. 4.36. The exception is the second event, but the storage reported for this event is artificially low due to the impact of frozen soil on water contents reported by the WCRs. The first peak (220 mm) corresponds to the lowest soil water storage that induced percolation. Thus, the soil water storage capacity of the thin capillary barrier appears to be approximately 220 mm.

The thick capillary barrier transmitted less percolation than the thin capillary barrier because the thicker barrier has greater soil water storage capacity. All of the percolation can be attributed to the heavy rain during early May. Percolation from the thick barrier ceased when the soil water storage dropped below 350 mm. Thus, the soil water storage capacity of the thick capillary barrier is at least 350 mm.

#### **4.10 MONTICELLO SITE**

Construction of the alternative cover at the Monticello site was completed on June 23, 2000. Data collection began on August 2, 2000. Total precipitation recorded during the monitoring period was 514 mm, 30.5% of which was frozen. The water balance for the test section is shown in Fig. 4.38.

##### **4.10.1 Surface Runoff**

Surface runoff during the monitoring period is shown in Fig. 4.38. The total surface runoff was 9.3 mm, or 1.8% of precipitation. Surface runoff was collected in a 20 m by 10 m test plot, within the 3.0 ha portion of the final cover being monitored. Surface



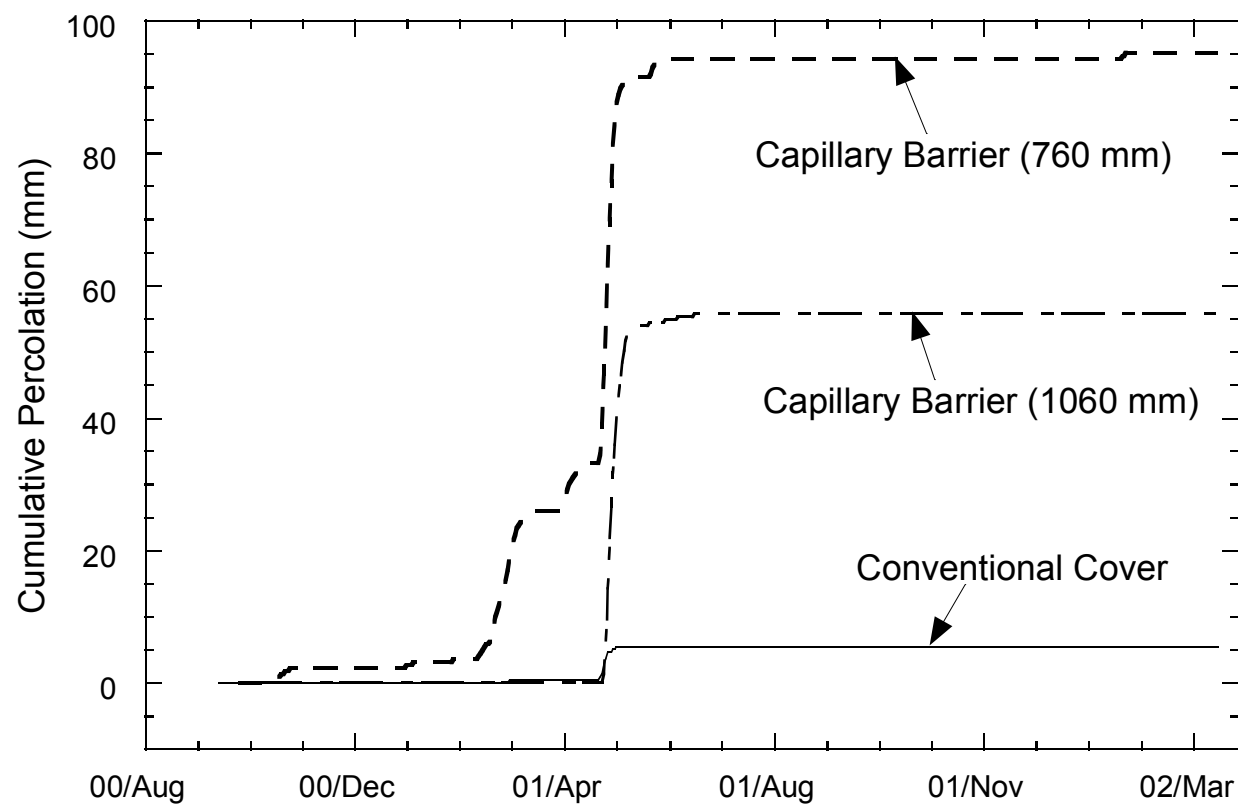


Fig. 4.37. Percolation at the Omaha Site.

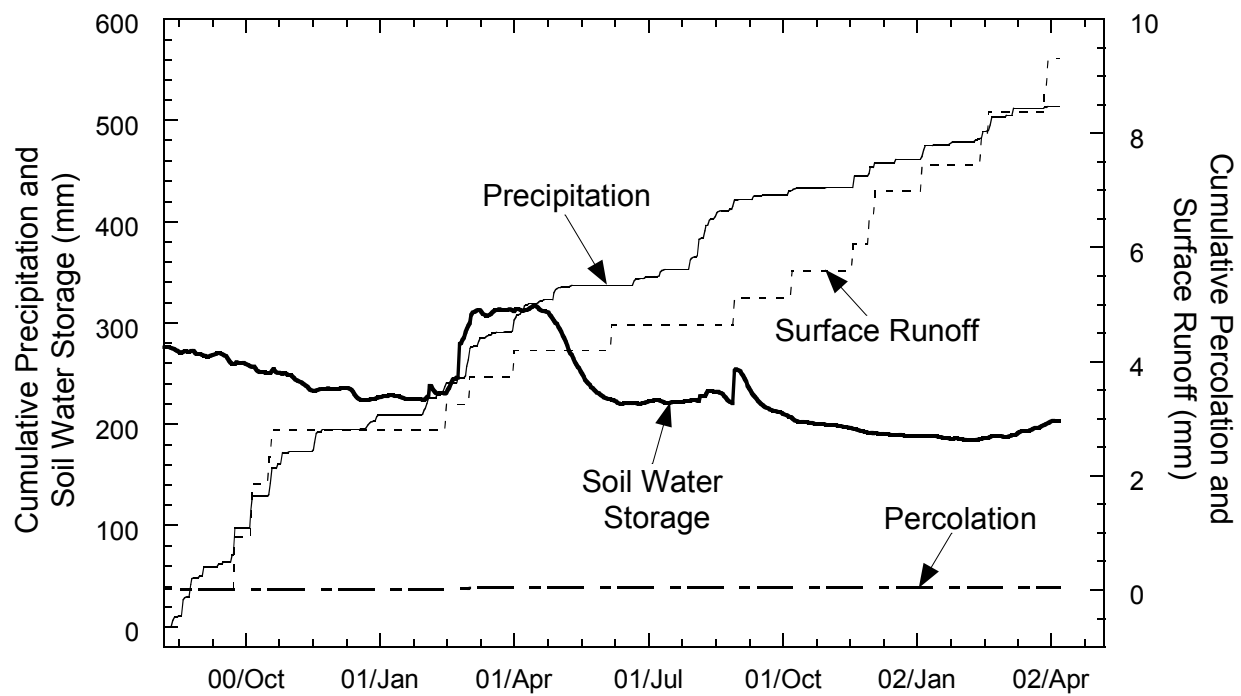


Fig. 4.38. Cumulative Water Balance for the Alternative Cover at the Monticello Site.

runoff is measured in a large area with sparse vegetation, whereas the remainder of the final cover has significantly less bare soil. The vegetative cover differed because the topsoil admixture was obtained from two separate borrow areas, which had different organic content.

Surface runoff occurred during large rainfall events (typically greater than 10 mm), or during large snow melt events. Almost one quarter of the surface runoff came from snowmelt, during which the surface layer was frozen. Soil temperatures below the 200 mm thick surface layer never went below 0°C, and sub-freezing temperatures in the surface layer would only be measured for short durations, typically in January and February.

#### **4.10.2 Soil Water Storage**

Soil water storage of entire cover profile for the alternative cover is shown in Fig. 4.39. Hydraulic properties of each layer are presented in Table 4.6.

Soil water storage increased in late winter and early spring, due to large snowmelt and rain events. During the summer, the soil water storage decreases significantly, but does not reach the wilting point. In August and September 2001, Monticello received 73 mm of rainfall, which briefly increased the soil water storage. Soil water storage remained at a minimum during Winter 2002, and began increasing again in early Spring 2002 due to the spring thaw.

The water content in topsoil increases significantly in February 2001, and then rapidly decreases due to water draining into the primary storage layer. During the following summer, the topsoil water content is further reduced by evapotranspiration,

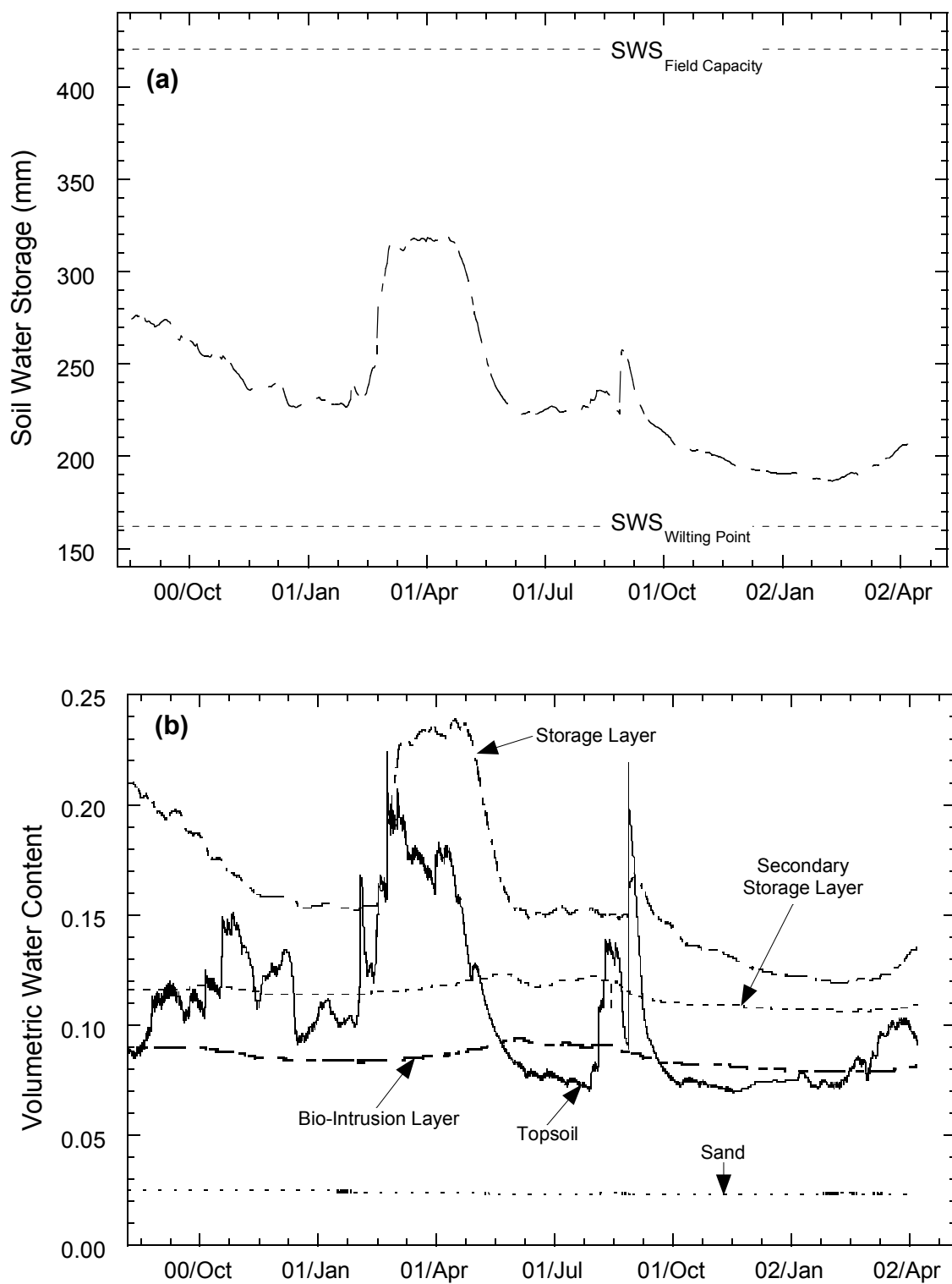


Fig. 4.39. Alternative Cover at the Monticello Site: (a) Soil Water Storage, and (b) Average Water Content in Each Layer

Table 4.6. Hydraulic Properties of the Alternative Cover at Monticello.

Layer	$\theta_r$	$\theta_s$	$\alpha$	n	Field Capacity	Wilting Point	$K_{sat}$ (cm/s)
Soil/Gravel Admixture <sup>a</sup>	0.00	0.46	0.0163	1.37	0.24	0.06	$8.4 \times 10^{-4}$
Storage <sup>b</sup>	0.00	0.30	0.000350	1.38	0.30	0.11 <sup>c</sup>	$3.4 \times 10^{-5}$
Bio-Intrusion <sup>a</sup>	0.03	0.29	8.10	1.78	0.03	0.03	$1.4 \times 10^{-2}$
Secondary Storage <sup>b</sup>	0.00	0.30	0.000350	1.38	0.30	0.11 <sup>c</sup>	$4.9 \times 10^{-5}$
Sand <sup>a</sup>	0.03	0.32	0.5380	1.68	0.04	0.03	$8.6 \times 10^{-5}$

<sup>a</sup> Hydraulic properties from Meyer and Serne (1999).

<sup>b</sup> Hydraulic properties from Gurdal (2002).

<sup>c</sup> Wilting point based on lowest water content measured in root zone during the monitoring period.

and approaches the wilting point ( $\theta_{WP}=0.06$ ). The water content of the storage layer does not begin decreasing until later Spring 2001, and does not reach the wilting point ( $\theta_{WP}=0.11$ ). Water contents (Fig. 4.39b) below the primary storage layer did not change significantly (less than  $\pm 0.01$ ) throughout the monitoring period.

#### **4.10.3 Percolation**

Cumulative percolation during the monitoring period was less than 0.04 mm. Percolation was transmitted through the cover in later Winter 2001 and early Spring 2001, at which time the soil water storage in the cover was at its minimum. Breakthrough into the sand layer during the monitoring period is not apparent in the water content data (Fig. 4.39). However, WCR probes were installed in only three nests, within the 3 ha area. Thus, isolated points of breakthrough would be difficult to capture.

## SECTION FIVE EVALUATION OF WATER BALANCE MODELS

Two models were used to simulate field conditions at eight of the ACAP sites described in Section 3.2. These models are the Hydrologic Evaluation of Landfill Performance (HELP) Model, Version 3 (Schroeder et al. 1994) and the Unsaturated Water and Heat Flow (UNSAT-H) Model, Version 2.04 (Fayer and Jones 1990). The models differ appreciably in formulation. HELP uses a water routing approach assuming unit gradient flow, whereas UNSAT-H solves a modified form of Richards' equation describing unsaturated flow, root water uptake, and evaporation from the soil surface. A detailed comparison of the formulations can be found in Khire et al. (1997).

### 5.1 WATER BALANCE COMPUTATIONS

The water balance of a landfill cover consists of water entering the system from precipitation ( $P$ ), and water leaving the system via evapotranspiration ( $ET$ ), lateral drainage ( $L_o$ ), surface runoff to adjacent areas ( $R_o$ ), and/or percolation ( $P_r$ ). The difference between the water entering and exiting the system is the change in soil water storage ( $\Delta S$ ). Mathematically, the water balance is written as (Tanner 1967):

$$P = ET + R_o + L_o + P_r + \Delta S \quad (1)$$

To apply Eq. 1 to the ACAP demonstration, the following assumptions were made: (1) interception of precipitation by the plant canopy is negligible, (2) all water movement is downward, except for lateral flow in drainage layers and (3) no water is

stored on the surface. Measurements of  $P_r$ ,  $R_o$ ,  $L_o$ ,  $P$ , and  $\Delta S$  are made continuously in each ACAP test section. ET is obtained by re-arranging Eq. 1:

$$ET = P - P_r - R_o - L_o - \Delta S \quad (2)$$

Because ET is computed as a residual quantity via Eq. 2, it includes the errors inherent in each of the water balance quantities being measured. In addition, Eq. 2 does not account for the dynamic effects in the system on a small time scale. For example, daily ET may be overestimated at times due to a delay in response between percolation and precipitation events. See Appendix 1 for an explanation of the ET computation and the methods used to correct errors in the ET calculation.

## 5.2 HELP MODEL FORMULATION

HELP is a quasi-two-dimensional hydrologic model used to predict the water balance of landfills, including the cover system (Schroeder et al. 1994). Input parameters include meteorological data (air temperature, solar radiation, and precipitation), soil properties (field capacity and the wilting point, initial water content, saturated hydraulic conductivity, and surface runoff curve number), plant characteristics (maximum LAI and growing season), and design attributes (layer types and thickness). The parameters are used in a series of algorithms to calculate the daily water balance. Schroeder et al. (1994) provide a detailed description of the algorithms.

HELP models water movement from the top of the profile to the bottom, beginning with input of precipitation. Precipitation is rainfall when the mean temperature



is above 0°C and no snow cover is present, or is stored as snow pack when the mean temperature is below 0°C. Rainfall is immediately applied to the system, whereas the snow pack must first be melted. HELP calculates snowmelt using the SNOW-17 algorithm when the mean temperature is above 0°C (Anderson 1973). The snowmelt calculation depends on whether rain is occurring when the air temperature is above 0°C. Rain-on-snowmelt is computed using an energy balance approach, whereas snow melt without rain is computed using air temperature as an index of energy exchange across the snow-air interface (Schroeder et al. 1994). The water applied to the system can become surface runoff, infiltration, and evapotranspiration. HELP also includes water as a result of daily soil thawing. The daily thaw is assumed to be 5 mm, and is assigned as infiltration.

Daily runoff is a function of daily rainfall and a surface retention parameter, which is related to soil properties (water content, field capacity, and wilting point) and a runoff curve number. The curve number can be specified based on an antecedent moisture condition or computed by HELP using an algorithm that accounts for slope length, slope angle, soil texture, and properties of the vegetation. Maximum surface retention occurs when the volumetric water content at the surface is midway between field capacity and the wilting point. When the ground surface is frozen, HELP increases the surface runoff curve number, thereby reducing the infiltration capacity of the soil. The calculated surface runoff approaches the net water applied when frozen ground conditions exist. HELP uses a modification of algorithms from the CREAMS model (Knisel et al. 1985) to predict freezing of the soil. The soil is assumed to be frozen when the average air

temperature during the previous 30 days is less than 0 °C. For all model simulations in this study, the curve number computed by HELP was used.

Daily infiltration into the cover is the daily rainfall and snowmelt less surface runoff. Infiltration in excess of the sum of the storage capacity of the cover and percolation is added to the runoff or held as surface water storage (Schroeder et al. 1994). Water that has infiltrated the profile can either flow downwards, leading to percolation, or be removed by evapotranspiration.

Evapotranspiration is assumed to remove water from an “evaporative depth” in the cover, which is defined by the user. Potential evapotranspiration (PET) is computed using the Penman equation (Penman 1963). PET is first applied to evaporation of water or snow on the surface. The remaining PET demand is applied to evaporation of water in the soil profile (PE) and transpiration by plants (PT). Evaporation or transpiration of water within the soil profile cannot exceed the available water, and when the soil is frozen, HELP assumes no soil water evaporation or transpiration takes place.

Actual plant transpiration (APT) is set equal to the potential plant transpiration unless the soil water evaporated (AET) plus the potential plant transpiration (PT) is greater than PET. PT is calculated based on the leaf area index (LAI), which varies throughout the year. The variation is computed using a vegetative growth model, which assumes the vegetation is perennial grass. The growth model computes the total vegetative biomass using maximum LAI (entered by the user), daily temperature and solar radiation, and mean monthly temperatures. Vegetative growth is assumed to begin at the germination date, and continues for three quarters of the growing season. The below ground biomass is assumed to be 20% of the total biomass.

Once the infiltration and evaporative demand is calculated, HELP routes water movement through the profile using Darcy's Law. The soil water storage of each layer is a function of the water content, and the flows into ( $Q_{in}$ ) and out ( $Q_{out}$ ) of the layer:

$$\Delta S = Q_{in} - Q_{out} - ET \quad (3)$$

Vertical flow can be unsaturated or saturated. Unsaturated flow only occurs in vertical percolation layers, and is assumed to occur under a unit gradient. Thus, the flux equals the unsaturated hydraulic conductivity, which is described using a Brooks-Corey function (Brooks and Corey 1964) as reported by Campbell (1974):

$$K_{\psi} = K_s \left[ \frac{\theta - \theta_r}{\theta_s - \theta_r} \right]^{3 + \left( \frac{2}{\lambda} \right)} \quad (4)$$

where  $K_{\psi}$  is the unsaturated hydraulic conductivity,  $K_s$  is the saturated hydraulic conductivity,  $\theta$  is the volumetric water content,  $\theta_r$  is the residual volumetric water content,  $\theta_s$  is the saturated volumetric water content, and  $\lambda$  is the pore-size distribution index. Residual volumetric water content is estimated based on the wilting point. The pore-size distribution index is estimated using the field capacity and wilting point entered by the user.

Soil barrier layers are assumed to be saturated at all times. Flow through barrier layers only occurs when head accumulates on the barrier layer. The rate of flow is calculated based on Darcy's law. Water flow through geomembranes is assumed to occur via vapor transport and leakage through holes. Vapor transport is modeled using

a “hydraulic conductivity” of the geomembrane. Leakage through holes is computed using Giroud’s equation (Giroud and Bonaparte 1989).

### 5.3 UNSAT-H FORMULATION

UNSAT-H is a one-dimensional finite-difference computer program for simulating water and heat flow through soil (Fayer et al. 1992). UNSAT-H predicts the water balance by solving a modified Richards’ partial differential equation for liquid and vapor water flow, Fick’s law for vapor diffusion, and Fourier’s equation for heat flow (Fayer and Jones 1990; Khire et al. 1999). The modified Richards’ equation solved by UNSAT-H is (Fayer and Jones 1990):

$$\frac{\partial \theta}{\partial \psi} \frac{\partial \psi}{\partial t} = - \frac{\partial}{\partial z} \left[ K_T \frac{\partial \psi}{\partial z} + K_{\psi} + q_{VT} \right] - S(z, t) \quad (5)$$

where  $\psi$  is matric suction,  $t$  is time,  $z$  is the vertical coordinate,  $K_{\psi}$  is unsaturated hydraulic conductivity,  $K_{V\psi}$  is the isothermal water vapor conductivity,  $K_T = K_{\psi} + K_{V\psi}$ ,  $q_{VT}$  is the thermal vapor flux density, and  $S(z, t)$  is the sink term representing water uptake by the vegetation. Because UNSAT-H is a one-dimensional model, it cannot compute lateral drainage or simulate flow through holes in geomembranes (Khire 1995). Therefore, UNSAT-H cannot be used to model covers that include lateral drainage layers or geomembranes.

For cover simulations, the upper boundary is treated as a flux boundary where water flow is either downward (infiltration) or upward (evaporation). Precipitation is partitioned into runoff or infiltration based on the infiltration capacity of the soil. UNSAT-

H does not consider absorption and interception of water by vegetation (Khire 1995). The lower boundary can be assigned as a unit gradient, constant head, a specified boundary flux, or as an impermeable boundary. For all simulations conducted during this study, the unit gradient boundary was used. The unit gradient option corresponds to gravity-induced drainage and is appropriate for profiles that extend below the root zone and in which drainage is not impeded. With the unit gradient condition, the calculated drainage flux depends on the liquid water conductivity of the lower boundary node. Because UNSAT-H is one-dimensional, the runoff computation does not consider slope angle or slope length.

Water that has infiltrated the surface of the profile flows downward in accordance with the modified Richards' equation, and can be removed from the profile by evaporation, transpiration, or percolation. Evaporation from the soil surface is computed using Fick's Law, with the gradient being calculated using the difference between the relative humidity of the atmosphere and the soil gas. Transpiration is assumed to occur at the potential transpiration (PT) rate unless water stress exists. PT is partitioned from PET using the Ritchie and Burnett (1971) formulation, which is a function of LAI. Water stress is computed using the limiting function in Feddes and Zaradny (1978), which requires the anaerobiosis point, limiting point, and wilting point as inputs.

The LAI is seasonally variable and is input as a LAI function. PT demand is applied to each node proportional to the root length density using a volumetric sink term in Richards' equation. After the PT demand is distributed to each node, actual transpiration is calculated by multiplying the potential sink term at each node by the transpiration limiting function, which is a function of water content. When the water

content exceeds the anaerobiosis point or is below the wilting point, the limiting function equals zero. When the water content is between the limiting and wilting points, the limiting function is computed by linear interpolation between 0-1. For water contents between the anaerobiosis and limiting points, the limiting function equals 1.0.

## 5.4 INPUT DATA

Properties obtained from laboratory testing conducted on soil and vegetative samples collected from each site were used to formulate the input parameters. When data were missing, estimates of the input parameters were made based on data from the literature or using data from other ACAP sites.

### 5.4.1 Meteorological Data

HELP and UNSAT-H require the following daily meteorological data: precipitation, air temperature, solar radiation, wind speed, relative humidity, cloud cover, dew point, surface albedo, and initial snow accumulation. The meteorological data were collected at each site using a weather station. Some of the meteorological inputs for HELP are shown in Table 5.1.

At sites that receive snow, snow was melted and added to the total daily precipitation. HELP has a snowmelt algorithm built into the program (Section 5.2). For UNSAT-H, the restricted degree-day radiation balance approach (Kustas et al. 1994) was used to calculate the daily snowmelt ( $M$ ):

$$M = a_r T_D + m_Q R_n \quad (6)$$

Table 5.1. Meteorological Inputs for HELP

Site	Number of Simulation Years	Day 1 Date	Avg. Wind Speed (km/hr)	Quarterly Relative Humidity (%)			
				1 <sup>st</sup>	2 <sup>nd</sup>	3 <sup>rd</sup>	4 <sup>th</sup>
Altamont	1	1-Jan-01	20.1	80.2	55.6	56.1	62.3
Omaha	1	1-Jan-01	11.1	80.5	71.9	71.3	65.7
Boardman	1	1-Jan-01	8.8	84.7	57.4	42.4	62.0
Sacramento	2	1-Jan-00	8.8	79.1	66.3	48.6	64.3
Polson	2	1-Jan-00	7.9	87.0	62.9	44.7	73.1
Helena	2	1-Jan-00	9.6	75.9	54.1	41.7	59.5
Albany	1	1-Jan-01	3.9	70.3	65.3	75.8	71.6
Marina	1	1-Jan-01	8.6	78.3	82.2	83.0	84.7

where  $T_D$  is the daily average air temperature,  $R_n$  is the net solar radiation,  $a_r$  is the restricted degree-day factor, and  $m_Q$  is the conversion factor for energy flux density to snow melt depth. The value for  $m_Q$  was 0.026 cm/d per  $W/m^2$  (each 1  $W/m^2$  of daily average energy results in 0.026 cm/d of snowmelt depth) and  $a_r$  was 0.23  $cm/^\circ C$  (Kustas et al. 1994). Snow was only melted when the air temperature was above 0  $^\circ C$ . The daily net solar radiation was calculated as the average of the hourly solar radiation measured on site multiplied by an albedo of 0.74 (Winkler 1999).

#### **5.4.2 Initial Conditions**

The initial condition for HELP consisted of assigning the initial water content of each layer, as measured by WCR probes in the test sections (Section 3.1.2). The initial conditions for UNSAT-H were specified by assigning the initial suction at each node. The suctions for each layer were calculated using the van Genuchten equation (see discussion in Section 5.3) and the average water content of the layer. All nodes within a layer were assigned the same suction. A summary of the initial water contents and suctions assigned to each layer is in Table 5.2 and 5.3.

#### **5.4.3 Hydraulic Properties**

HELP requires the saturated hydraulic conductivity, field capacity, wilting point, and saturated water content (porosity) as input. UNSAT-H requires the saturated hydraulic conductivity and the soil water characteristic curve. For this study, the soil



Table 5.2. Hydraulic Properties Input to UNSAT-H.

Site	Test Section	Component (Top to Bottom)	Thickness (mm)	Van Genuchten Parameters				$K_s$ (cm/s)	Calculated	Measured
				$\theta_r$	$\theta_s$	$\theta$ (cm <sup>3</sup> /cm <sup>3</sup> )	n		Soil Suction (kPa)	Initial Water Content (vol/vol)
Altamont	Monolithic	Vegetative Cover	460	0.00	0.36	0.00395	1.18	$2.8 \times 10^{-6}$	910	0.19
		Support Layer	600	0.00	0.37	0.00172	1.22	$2.8 \times 10^{-6}$	2461	0.16
		Interim Cover	300	0.00	0.39	0.00172	1.22	$4.3 \times 10^{-5}$	3317	0.16
Omaha	"Thin" Capillary	Topsoil	150	0.00	0.48	0.00015	1.61	$6.1 \times 10^{-6}$	4673	0.14
		Vegetative Cover	460	0.00	0.44	0.00039	1.97	$6.1 \times 10^{-6}$	543	0.19
		Sand	150	0.05	0.41	0.03500	7.22	$2.1 \times 10^{-2}$	5	0.06
		Interim Cover	300	0.00	0.40	0.00077	1.28	$6.1 \times 10^{-6}$	808	0.24
	"Thick" Capillary	Topsoil	150	0.00	0.44	0.00015	1.61	$4.5 \times 10^{-7}$	6565	0.11
		Vegetative Cover	760	0.00	0.42	0.00039	1.97	$1.4 \times 10^{-7}$	554	0.18
		Sand	150	0.05	0.41	0.03500	7.22	$2.0 \times 10^{-2}$	5	0.06
		Interim Cover	300	0.00	0.42	0.00077	1.28	$5.2 \times 10^{-7}$	709	0.26
Boardman	"Thin" Capillary	Vegetative Cover	1220	0.00	0.46	0.00176	1.29	$1.9 \times 10^{-5}$	4423	0.13
		Interim Cover	300	0.00	0.46	0.00356	1.34	$1.7 \times 10^{-5}$	566	0.17
	"Thick" Capillary	Vegetative Cover	1840	0.00	0.45	0.00176	1.29	$1.4 \times 10^{-5}$	4695	0.13
		Interim Cover	300	0.00	0.46	0.00356	1.34	$1.9 \times 10^{-5}$	831	0.15

Table 5.2. Hydraulic Properties Input to UNSAT-H (*continued*).

Site	Test Section	Component (Top to Bottom)	Thickness (mm)	Van Genuchten Parameters				$K_s$ (cm/s)	Calculated	Measured
				$\theta_r$	$\theta_s$	$\theta$ (cm <sup>-1</sup> )	n		Soil Suction (kPa)	Initial Water Content
Sacramento	"Thin" Monolithic	Topsoil	150	0.00	0.44	0.00670	1.38	$9.0 \times 10^{-7}$	173	0.17
		Vegetation Cover 1	920	0.00	0.37	0.00650	1.26	$4.0 \times 10^{-4}$	2354	0.10
		Interim Cover	460	0.00	0.37	0.00750	1.33	$1.3 \times 10^{-4}$	314	0.13
	"Thick" Monolithic	Topsoil	150	0.00	0.46	0.00670	1.38	$9.0 \times 10^{-7}$	96	0.22
		Vegetation Cover 2	1840	0.00	0.43	0.00300	1.30	$1.7 \times 10^{-7}$	1657	0.13
		Vegetation Cover 1	460	0.00	0.41	0.00650	1.26	$4.0 \times 10^{-4}$	4819	0.09
		Interim Cover	460	0.00	0.31	0.00750	1.33	$1.3 \times 10^{-4}$	181	0.13
Polson	Capillary	Topsoil	150	0.00	0.40	0.06761	1.40	$4.9 \times 10^{-5}$	38	0.11
		Sandy Silt	460	0.00	0.44	0.01951	1.27	$4.7 \times 10^{-7}$	246	0.16
		Silty Sand	600	0.00	0.40	0.07113	1.43	$9.8 \times 10^{-5}$	129	0.06
		Interim Cover	460	0.03	0.32	0.31060	3.00	$6.1 \times 10^{-3}$	5	0.03
Helena	Capillary	Topsoil	150	0.00	0.37	0.06070	1.36	$5.0 \times 10^{-7}$	393	0.05
		Vegetative Cover	1200	0.00	0.43	0.01292	1.19	$2.2 \times 10^{-7}$	3402	0.14
		Gravel	300	0.05	0.41	0.24630	3.00	$7.1 \times 10^{-1}$	1	0.10
		Interim Cover	150	0.00	0.43	0.01292	1.19	$2.2 \times 10^{-7}$	280	0.22
Albany	ECap	Vegetative Cover	600	0.00	0.44	0.00144	1.37	$1.9 \times 10^{-7}$	247	0.27
		Foundation Layer	700	0.00	0.35	0.00029	1.49	$6.0 \times 10^{-7}$	672	0.23
		Interim Cover	150	0.00	0.38	0.00020	1.52	$2.0 \times 10^{-6}$	914	0.25
	Compacted Clay	Topsoil	150	0.00	0.34	0.00017	1.22	$1.3 \times 10^{-4}$	6976	0.20
		Barrier Layer	460	0.00	0.35	0.00046	1.58	$7.3 \times 10^{-8}$	318	0.24
		Interim Cover	150	0.00	0.38	0.00015	1.79	$3.2 \times 10^{-7}$	1049	0.23
Marina	Monolithic	Vegetative Cover	1220	0.00	0.34	0.00235	1.39	$6.7 \times 10^{-8}$	615	0.23
		Interim Cover	300	0.07	0.39	0.05300	2.85	$3.6 \times 10^{-3}$	18	0.07

Table 5.3. Hydraulic Properties Input to HELP.

Site	Test Section	Layer	Thickness (mm)	Soil Texture Number	Total Porosity	Field Capacity	Wilting Point	K <sub>s</sub> (cm/s)	Initial Water Content
Altamont	Monolithic	Vertical Percolation	460	-	0.36	0.32	0.17	2.8x10 <sup>-6</sup>	0.19
		Vertical Percolation	600	-	0.37	0.34	0.18	2.8x10 <sup>-6</sup>	0.16
	Composite	Vertical Percolation	300	-	0.39	0.36	0.19	4.3x10 <sup>-5</sup>	0.16
		Vertical Percolation	300	-	0.36	0.32	0.17	2.0x10 <sup>-5</sup>	-
		Lateral Drainage	5	20	-	-	-	-	-
		Geomembrane	1.5	36	-	-	-	-	-
		Soil Barrier	300	-	0.31	0.29	0.15	2.2x10 <sup>-7</sup>	-
		Vertical Percolation	300	-	0.31	0.29	0.15	7.8x10 <sup>-5</sup>	-
		Vertical Percolation	300	-	0.35	0.33	0.17	2.2x10 <sup>-7</sup>	-
Helena	Capillary	Vertical Percolation	150	-	0.37	0.13	0.03	5.0x10 <sup>-7</sup>	0.05
		Vertical Percolation	1200	-	0.43	0.32	0.16	2.2x10 <sup>-7</sup>	0.14
		Vertical Percolation	300	-	0.41	0.05	0.05	7.1x10 <sup>-1</sup>	0.10
		Vertical Percolation	150	-	0.43	0.32	0.16	2.2x10 <sup>-7</sup>	0.22

Table 5.3. Hydraulic Properties Input to HELP (continued).

Site	Test Section	Layer	Thickness (mm)	Soil Texture Number	Total Porosity	Field Capacity	Wilting Point	K <sub>s</sub> (cm/s)	Initial Water Content
Omaha	"Thin" Capillary	Vertical Percolation	150	-	0.48	0.48	0.33	6.1x10 <sup>-6</sup>	0.14
		Vertical Percolation	460	-	0.44	0.43	0.2	6.1x10 <sup>-6</sup>	0.19
		Vertical Percolation	150	-	0.41	0.05	0.05	2.1x10 <sup>-2</sup>	0.06
		Vertical Percolation	300	-	0.4	0.39	0.22	6.1x10 <sup>-6</sup>	0.24
	"Thick" Capillary	Vertical Percolation	150	-	0.44	0.44	0.3	4.5x10 <sup>-7</sup>	0.11
		Vertical Percolation	760	-	0.42	0.41	0.19	1.4x10 <sup>-7</sup>	0.18
		Vertical Percolation	150	-	0.41	0.05	0.05	2.0x10 <sup>-2</sup>	0.06
		Vertical Percolation	300	-	0.42	0.40	0.23	5.6x10 <sup>-7</sup>	0.26
	Composite	Vertical Percolation	150	-	0.4	0.40	0.27	1.5x10 <sup>-6</sup>	0.12
		Vertical Percolation	300	-	0.44	0.43	0.2	6.9x10 <sup>-7</sup>	0.18
		Drainage Composite	5	20	-	-	-	-	-
		Geomembrane	1	35	-	-	-	-	-
		Soil Barrier	460	-	0.38	0.38	0.07	3.2x10 <sup>-6</sup>	0.21
		Vertical Percolation	300	-	0.44	0.42	0.24	1.3x10 <sup>-6</sup>	0.27
Boardman	"Thin" Capillary	Vertical Percolation	1220	-	0.46	0.42	0.18	1.9x10 <sup>-5</sup>	0.13
		Vertical Percolation	300	-	0.46	0.37	0.12	1.7x10 <sup>-5</sup>	0.17
	"Thick" Capillary	Vertical Percolation	1840	-	0.45	0.41	0.17	1.4x10 <sup>-5</sup>	0.13
		Vertical Percolation	300	-	0.46	0.37	0.12	1.9x10 <sup>-5</sup>	0.15
	Composite	Vertical Percolation	900	-	0.45	0.41	0.17	3.8x10 <sup>-5</sup>	0.13
		Lateral Drainage	5	20	-	-	-	-	-
		Geomembrane	1.5	36	-	-	-	-	-
		GCL	6	17	0.75	-	-	3.3x10 <sup>-9</sup>	-
		Vertical Percolation	300	-	0.46	0.37	0.12	7.2x10 <sup>-6</sup>	0.11
Sacramento	"Thin" Monolithic	Vertical Percolation	150	-	.44	0.30	.08	9.0x10 <sup>-7</sup>	0.17
		Vertical Percolation	920	-	.37	0.28	.11	4.0x10 <sup>-4</sup>	0.10
		Vertical Percolation	460	-	.37	0.26	.08	1.3x10 <sup>-4</sup>	0.13

Table 5.3. Hydraulic Properties Input to HELP (*continued*).

Site	Test Section	Layer	Thickness (mm)	Soil Texture Number	Porosity	Field Capacity	Wilting Point	K <sub>s</sub> (cm/s)	Initial Water Content
Sacramento	"Thick" Monolithic	Vertical Percolation	150	-	0.46	0.31	0.08	9.0x10 <sup>-7</sup>	0.22
		Vertical Percolation	1840	-	0.43	0.37	0.14	1.7x10 <sup>-7</sup>	0.133
		Vertical Percolation	460	-	0.41	0.31	0.12	4.0x10 <sup>-4</sup>	0.09
		Vertical Percolation	460	-	0.31	0.22	0.07	1.3x10 <sup>-4</sup>	0.13
Polson	Capillary	Vertical Percolation	150	-	0.4	0.11	0.02	4.9x10 <sup>-5</sup>	0.11
		Vertical Percolation	460	-	0.44	0.26	0.1	4.7x10 <sup>-7</sup>	0.157
		Vertical Percolation	600	-	0.4	0.10	0.02	9.8x10 <sup>-5</sup>	0.057
		Vertical Percolation	460	-	0.32	0.03	0.03	6.1x10 <sup>-3</sup>	0.03
	Composite	Vertical Percolation	150	-	0.41	0.12	0.03	4.9x10 <sup>-5</sup>	0.10
		Vertical Percolation	460	-	0.42	0.11	0.02	9.0x10 <sup>-5</sup>	0.07
		Lateral Drainage	5	20	-	-	-	-	-
		Geomembrane	1.5	36	-	-	-	-	-
		Soil Barrier	460	-	0.42	0.26	0.10	5.0x10 <sup>-7</sup>	0.13
		Vertical Percolation	460	-	0.32	0.05	0.05	6.1x10 <sup>-3</sup>	0.03
Albany	Compacted Clay	Vertical Percolation	150	-	0.34	0.34	0.26	1.3x10 <sup>-4</sup>	0.20
		Soil Barrier	460	-	0.35	0.34	0.11	7.3x10 <sup>-8</sup>	0.24
		Vertical Percolation	150	-	0.38	0.38	0.18	3.2x10 <sup>-7</sup>	0.23
	ECap	Vertical Percolation	600	-	0.44	0.41	0.14	1.9x10 <sup>-7</sup>	0.27
		Vertical Percolation	700	-	0.35	0.35	0.17	6.0x10 <sup>-7</sup>	0.23
		Vertical Percolation	150	-	0.38	0.38	0.20	2.0x10 <sup>-6</sup>	0.25
Marina	Monolithic	Vertical Percolation	1220	-	0.34	0.29	0.08	6.7x10 <sup>-8</sup>	0.23
		Vertical Percolation	300	-	0.39	0.07	0.06	3.6x10 <sup>-3</sup>	0.07
	Composite	Vegetative Cover	300	-	0.35	0.30	0.09	4.5x10 <sup>-6</sup>	0.21
		Geomembrane	1.5	36	-	-	-	-	-
		Soil Barrier	300	-	0.45	0.30	0.04	2.5x10 <sup>-8</sup>	0.41
		Vertical Percolation	600	-	0.35	0.07	0.06	3.6x10 <sup>-3</sup>	0.09

water characteristic curve used in UNSAT-H was defined using the van Genuchten equation:

$$\theta = \theta_r + (\theta_s - \theta_r) \left[ \frac{1}{1 + (\alpha\psi)^n} \right]^{1-1/n} \quad (7)$$

where  $\theta_r$  is the residual water content,  $\theta_s$  is the saturated water content, and  $\alpha$  and  $n$  are empirical parameters obtained by fitting Eq. 7 to soil water characteristic curves measured in the laboratory.

The unsaturated hydraulic conductivity ( $K_\psi$ ) was defined by the van Genuchten-Mualem equation, the parameters  $\theta_s$ ,  $\theta_r$ ,  $\alpha$ , and  $n$  in Eq. 7, and the saturated hydraulic conductivity:

$$K_\psi(\Theta) = K_s \Theta^{0.5} \left[ 1 - (1 - \Theta^{n/(n-1)})^{1-1/n} \right]^2 \quad (8)$$

In Eq. 8,  $\Theta$  is the relative saturation, which is defined as

$$\Theta = \frac{\theta - \theta_r}{\theta_s - \theta_r} \quad (9)$$

Saturated hydraulic conductivities and the parameters  $\theta_s$ ,  $\theta_r$ ,  $\alpha$ , and  $n$  were obtained from laboratory tests conducted on undisturbed specimens collected from each test section in thin-walled sampling tubes and as blocks. A summary of these measurements can be found in Gurdal (2002). For this study, the geometric mean saturated hydraulic conductivity and the geometric mean  $\alpha$  parameter were assigned to each layer. For the  $n$  parameter, the arithmetic mean was used. The geometric mean was used for the saturated hydraulic conductivity and  $\alpha$  because these parameters appear log-normally distributed. An arithmetic mean was used for  $n$  because it appears

to be normally distributed (Gurdal 2002). A summary of the saturated hydraulic conductivities, and the  $\alpha$  and  $n$  parameters that were used, is in Table 5.2. A tortuosity of 0.68 was used for vapor flow in the UNSAT-H simulations.

Field capacity was assumed to be the volumetric water content at a matric suction of 33 kPa, as defined using Eq. 7 and the parameters  $\theta_s$ ,  $\theta_r$ ,  $\alpha$ , and  $n$  in Table 5.2. For humid sites, the common 1500 kPa definition of the wilting point water content was used (Hillel 1998). In semi-arid and arid climates, however, the wilting point often corresponds to much higher suctions (Gee et al. 1999). For the semi-arid and arid sites, the wilting point was estimated as the lowest average water content measured in the lower portion of the root zone during the growing season. That is, the vegetation was assumed to remove all of the available water in the soil during the growing season. The topsoil layer was excluded from the wilting point determination because the topsoil is dried to a lower water content by transpiration as well as evaporation. The wilting, limiting, and anaerobiosis points input to UNSAT-H are shown in Table 5.4.

#### **5.4.4 Geosynthetic Properties**

HELP was the only model used to simulate covers with geomembranes. The geomembrane was assigned a hydraulic conductivity of  $2.0 \times 10^{-13}$  cm/s (HDPE) or  $4.0 \times 10^{-13}$  cm/s (LLDPE). Geosynthetic clay liners were assigned a saturated hydraulic conductivity of  $3.0 \times 10^{-9}$  cm/s, and geocomposite drainage layers were assigned a saturated hydraulic conductivity of 10 cm/s. Holes in the geomembrane were assigned to have an area of 1 cm<sup>2</sup> and a frequency of 50 holes/ha to replicate the condition in the

Table 5.4 Transpiration Parameters Input to UNSAT-H.

<b>Site</b>	<b>Wilting Point Suction (cm)</b>	<b>Limiting Point Suction (cm)</b>	<b>Anaerobiosis Suction (cm)</b>
Altamont	62,500	5018	330
Omaha	15,000	6832	330
Boardman	60,000	4126	330
Sacramento	62,500	2840	330
Polson	36,000	1488	330
Helena	36,000	2847	330
Albany	15,000	5651	330
Marina	45,000	2694	330



test section (i.e., a single 1 cm<sup>2</sup> hole was placed in the test sections with a geomembrane).

#### **5.4.5 Vegetation Data**

##### **5.4.5.1 Growing Season**

Dates for the growing season were obtained from historical data provided by the Western Regional Climate Center (RCC), Southeast RCC, Midwestern RCC, and High Plains RCC. For sites where freezing occurs, the growing season was assumed to begin after the final frost in the spring and no later than the first frost in the fall. In tropical climates, the growing season is defined by the rainy season. During the dry season, the vegetation goes dormant. The growing dates input to HELP and UNSAT-H are shown in Tables 5.5 and 5.6. The dates are entered in Julian day relative to the starting date of the data. For example, the start date for HELP is always January 1. However, the start date for UNSAT-H is based on the first day data collection began.

##### **5.4.5.2 Leaf Area Index (LAI)**

The LAI was measured on samples collected from the field for two of the ACAP sites (Sacramento and Albany). The samples were collected from 1 m x 1 m areas, sealed in plastic bags, and then analyzed in the laboratory. A Li-Cor LI-3100 area meter was used for the area measurements. For those sites where LAI was not measured, the LAI was estimated based on photographs and the type of vegetation.

For HELP, only the maximum LAI was entered. Algorithms in HELP were used to define the LAI function throughout the growing season. An LAI and Julian date are input

\

Table 5.5. Vegetation Input Parameters for HELP.

Site	Test Section	Evap. Zone Depth (mm)	Growing Season (Julian Day)		Maximum LAI	
			Germinate	Harvest	Year 1	Year 2
Altamont	Monolithic	1060	245	183	1.01	1.50
	Composite	300				
Sacramento	"Thin" Monolithic	1070	245	183	1.25	1.60
	"Thick" Monolithic	2450			1.95	2.50
Helena	Capillary	1350	135	263	0.77	1.50
Polson	Capillary	1210	130	271	0.82	2.50
	Composite	610				
Boardman	"Thin" Monolithic	1220	115	288	0.94	1.50
	"Thick" Monolithic	1840				
	Composite	900				
Marina	Monolithic	1220	275	153	0.88	1.50
	Composite	300				
Albany	ECap	1300	80	312	2.50	4.50
	Compacted Clay	600			0.11	0.20
Omaha	"Thin" Capillary	610	113	287	1.30	1.50
	"Thick" Capillary	910				
	Composite	460				

Table 5.6. Parameters for LAI Functions for UNSAT-H.

Site	Test Section	1st Year			2nd Year		
		Event	Julian Day	LAI	Event	Julian Day	LAI
Altamont	Monolithic	Day 1	1	0.0	Day 1	1	1.2
		Seed	20	0.0	Maximum	204	1.5
		Maximum	204	1.0	Harvest	234	0.0
		Harvest	234	0.0	Germinate	296	0.0
		Germinate	296	0.0	Maximum	326	1.5
		Maximum	326	0.5	End of Year	366	1.5
		End of Year	366	1.2			
Omaha	Capillary	Day 1	1	0.0	Day 1	1	0.4
		Harvest	8	0.0	Harvest	8	0.0
		Germinate	200	0.0	Germinate	200	0.0
		Maximum	344	1.3	Maximum	230	1.5
		End of Year	366	0.4	Maximum	344	1.5
					End of Year	366	0.4
Sacramento	"Thin" Monolithic	Day 1	1	0.0	Day 1	1	0.0
		Germinate	35	0.0	Germinate	35	0.0
		Seed	95	0.0	Maximum	65	1.6
		Maximum	309	1.3	Maximum	309	1.6
		Harvest	339	0.0	Harvest	339	0.0
		End of Year	366	0.0	End of Year	366	0.0
	"Thick" Monolithic	Day 1	1	0.0	Day 1	1	0.0
		Germinate	35	0.0	Germinate	35	0.0
		Seed	95	0.0	Maximum	65	2.5
		Maximum	309	2.0	Maximum	309	2.5
		Harvest	339	0.0	Harvest	339	0.0
		End of Year	366	0.0	End of Year	366	0.0

Table 5.6. Parameters for LAI Function for UNSAT-H (*continued*).

Site	Test Section	1st Year			2nd Year		
		Event	Julian Day	LAI	Event	Julian Day	LAI
Polson	Capillary	Day 1	1	0.0	Day 1	1	0.0
		Seed	144	0.0	Germinate	173	0.0
		Germinate	173	0.0	Maximum	203	2.5
		Maximum	284	0.8	Maximum	284	2.5
		Harvest	314	0.0	Harvest	314	0.0
		End of Year	366	0.0	End of Year	366	0.0
Helena	Capillary	Day 1	1	0.0	Day 1	1	0.0
		Seed	35	0.0	Germinate	209	0.0
		Germinate	209	0.0	Maximum	239	1.5
		Maximum	307	0.8	Maximum	307	1.5
		Harvest	337	0.0	Harvest	337	0.0
		End of Year	366	0.0	End of Year	366	0.0
Albany	ECap	Day 1	1	0.4	Day 1	1	4.5
		Maximum	172	2.5	Maximum	172	4.5
		Harvest	202	0.0	Harvest	202	0.0
		Germinate	336	0.0	Germinate	336	0.0
		End of Year	366	4.5	End of Year	366	4.5
	Compacted Clay	Day 1	1	0.02	Day 1	1	0.2
		Maximum	172	0.1	Maximum	172	0.2
		Harvest	202	0.0	Harvest	202	0.0
		Germinate	336	0.0	Germinate	336	0.0
		End of Year	366	0.2	End of Year	366	0.2
Marina	Monolithic	Day 1	1	0.0	Day 1	1	0.2
		Harvest	6	0.0	Harvest	6	0.0
		Seed-Germinate	127	0.0	Germinate	127	0.0
		Maximum	157	0.1	Maximum	157	1.5
		Maximum	341	0.9	Maximum	341	1.5
		End of Year	366	0.2	End of Year	366	0.2
Boardman	Monolithic	Day 1	1	0.0	Day 1	1	0.0
		Seed	63	0.0	Germinate	137	0.0
		Germinate	137	0.0	Maximum	167	1.5
		Maximum	167	0.2	Maximum	280	1.5
		Maximum	280	0.9	Harvest	310	0.0
		Harvest	310	0.0	End of Year	366	0.0
		End of Year	366	0.0			

to UNSAT-H. A typical LAI function that was used for UNSAT-H is shown in Fig. 5.1. For the first growing season, the LAI was assumed to increase linearly from the first day of the growing season or the seed date (whichever was later) to the point where the LAI would typically begin to decrease as it nears the dormant period. For the second season, the LAI was assumed to reach its maximum 30 days after the germination date, remain at the maximum throughout most of the growing season, and to decrease linearly 30 days prior to the harvest date. The LAI functions were input directly to UNSAT-H. UNSAT-H uses the germination and harvest dates, as well as the user-defined LAI function. The days entered do not correspond to the Julian day, but rather to the day relative to the start date.

A summary of the LAI parameters that were input is in Tables 5.5 and 5.6. Each of the LAI functions input to UNSAT-H is shown in Appendix 2. An albedo of 0.25 was assigned for every site. A bare soil surface fraction of 0.5 was used for the first year. For the second year, the bare surface fraction was assumed to be 0.25 to simulate establishment of the vegetation.

#### **5.4.5.3 Root Depth, Growth, and Density**

The maximum rooting depth for UNSAT-H and the evaporative depth for HELP was assumed to be the depth of the root barrier, or for test sections with composite barriers, the depth of the geomembrane. Root growth at each site was estimated using rates reported in the literature. Roots for crop plants typically elongate 10 mm or more per day (Russell 1977), whereas roots of plants in natural ecosystems may only

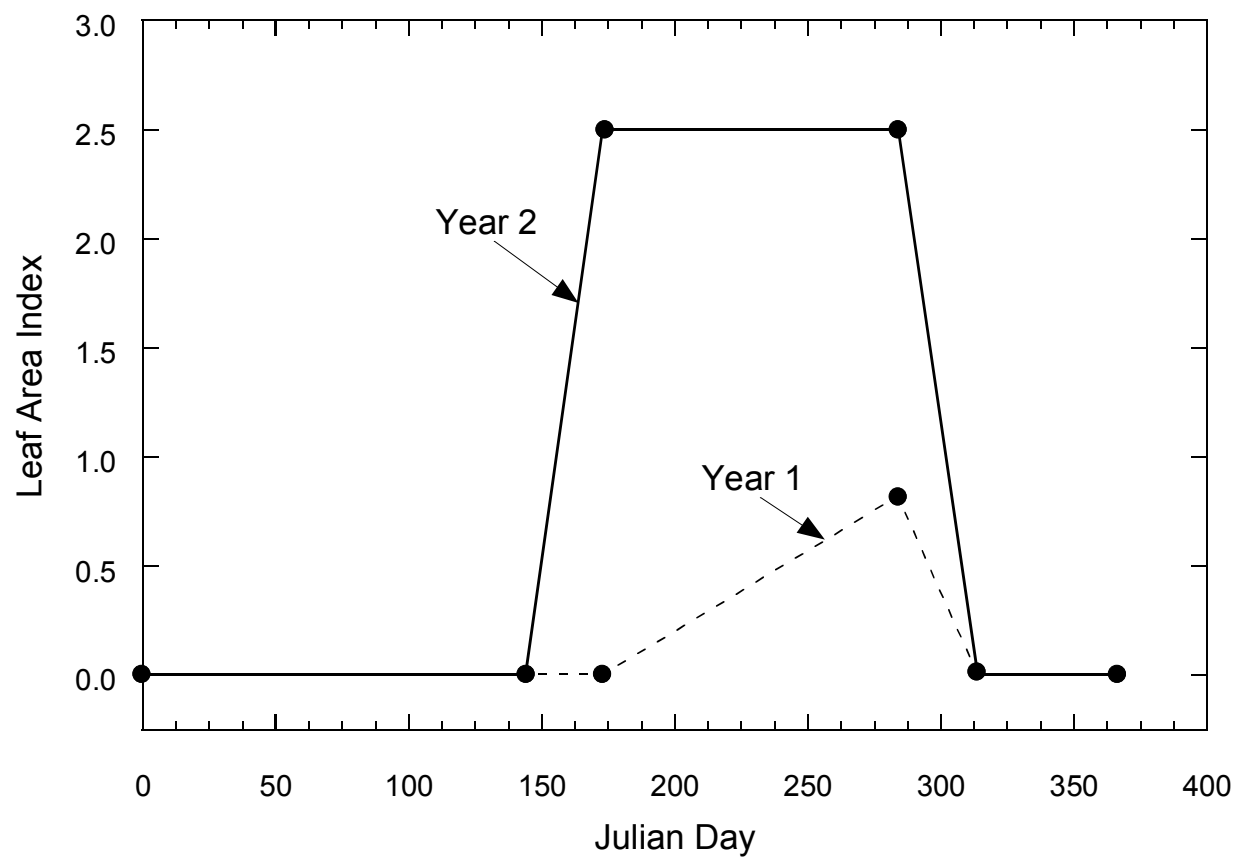


Fig. 5.1.. LAI Function Input to UNSAT-H for Polson Site.

elongate at 1 mm/d (Bundrett and Kendrick 1990). The maximum root growth is between 5 and 21 mm/d (Roche et al. 1994, Mahoney and Rood 1998).

Growth rates between 5 and 10 mm/day are more typical. Factors that affect the rate of elongation include the amount of nutrients available, degree of soil compaction, type of soil (granular or clayey), and climate (wet or dry). Root growth rates chosen for each test cover were selected based on a relative scale (between 0 and 10 mm/day) using the factors previously described, and are summarized in Table 5.7. For example, a test section was assigned a higher root growth rate if the cover profile was composed of soil that had sufficient nutrients and available water, and was lightly compacted. In contrast, a test section was assigned a lower growth rate if the cover profile had little nutrients and available water, and was compacted greater than 95% of maximum dry unit weight per standard Proctor.

The root length density function was estimated for each test cover, and is shown in Table 5.8. At several sites, measurements of the root length density function were made on undisturbed soil samples extending from the surface to a depth of approximately 900 mm. The Weaver-Darland box method described in Bohm (1979) was used to collect the samples. The density measurements were made in the laboratory using the method described in Liang et al. (1989). For the other sites, the root length density function was estimated based on data collected from the sites where samples were collected. Each root length density function was fit with the exponential model used in UNSAT-H:

$$R = a e^{-zb} + c \quad (8)$$

Table 5.7. Rates of Root Growth Input to UNSAT-H.

Site	Test Section	Root Growth Rate (mm/d)
Altamont	Monolithic Barrier	3.0
Sacramento	Monolithic Barriers	5.0
Helena	Capillary Barrier	5.0
Polson	Capillary Barrier	7.5
Boardman	Monolithic Barriers	7.5
Marina	Monolithic Barrier	7.5
Albany	ECap	10.0
	Compacted Clay Barrier	3.0
Omaha	Capillary Barriers	6.0



Table 5.8. RLD Function at ACAP Sites.

Site	Vegetation Type	Root Length Density Parameters		
		a	b (cm <sup>-1</sup> )	c
Altamont	Local Grasses	0.44	0.079	0.005
Boardman	Crested Wheat Grass	0.30	0.070	0.013
Sacramento	Grasses and shrubs	0.61	0.110	0.007
Marina <sup>a</sup>	Grasses	0.61	0.110	0.007
Omaha <sup>a</sup>	Grasses	0.61	0.110	0.007
Polson	Grasses, forbs, and shrubs	0.12	0.019	0.00
Helena	Grasses	0.38	0.029	0.00
Albany <sup>b</sup>	Grass + Poplar Trees	0.01	0.050	0.005
<b>Low (Winkler 1999)</b>		<b>0.06</b>	<b>0.061</b>	<b>0.012</b>
<b>High (Winkler 1999)</b>		<b>1.00</b>	<b>0.077</b>	<b>0.080</b>

<sup>a</sup> Based on RLD measured at Sacramento

<sup>b</sup> RLD function defined for Albany is for grass only.

where  $z$  is the depth, and  $a$ ,  $b$ , and  $c$  are empirical parameters. The root length density function curves for the ACAP sites are shown in Fig. 5.2, as well as upper and lower bounds based on a literature review by Winkler (1999). The root length density functions for the Cedar Rapids, Omaha, and Marina sites are based on the root length function of the Sacramento site. The Sacramento site was chosen because its root length density function is in middle of the range defined by the upper and lower boundaries provided by Winkler (1999).

#### **5.4.5.4 Runoff Curve Number**

A runoff curve number is input to HELP to estimate the rainfall-runoff relationship. The method for selecting a curve number considers the slope, slope length, texture of the surface layer, and level of vegetation. The level of vegetation is a range between 1 (bare ground) and 5 (excellent stand of grass). The input to HELP for each test section is shown in Table 5.9.

#### **5.4.6 Design Input**

Inputs required for HELP and UNSAT-H that are based on test section characteristics (area and slope) and site location (elevation and latitude) are summarized in Table 5.10.

#### **5.4.7 Simulation Control Parameters for UNSAT-H**

UNSAT-H requires the user to specify the nodal spacing throughout the entire profile of the soil cover (Fig. 5.3). A nodal spacing of 1 mm was used near the

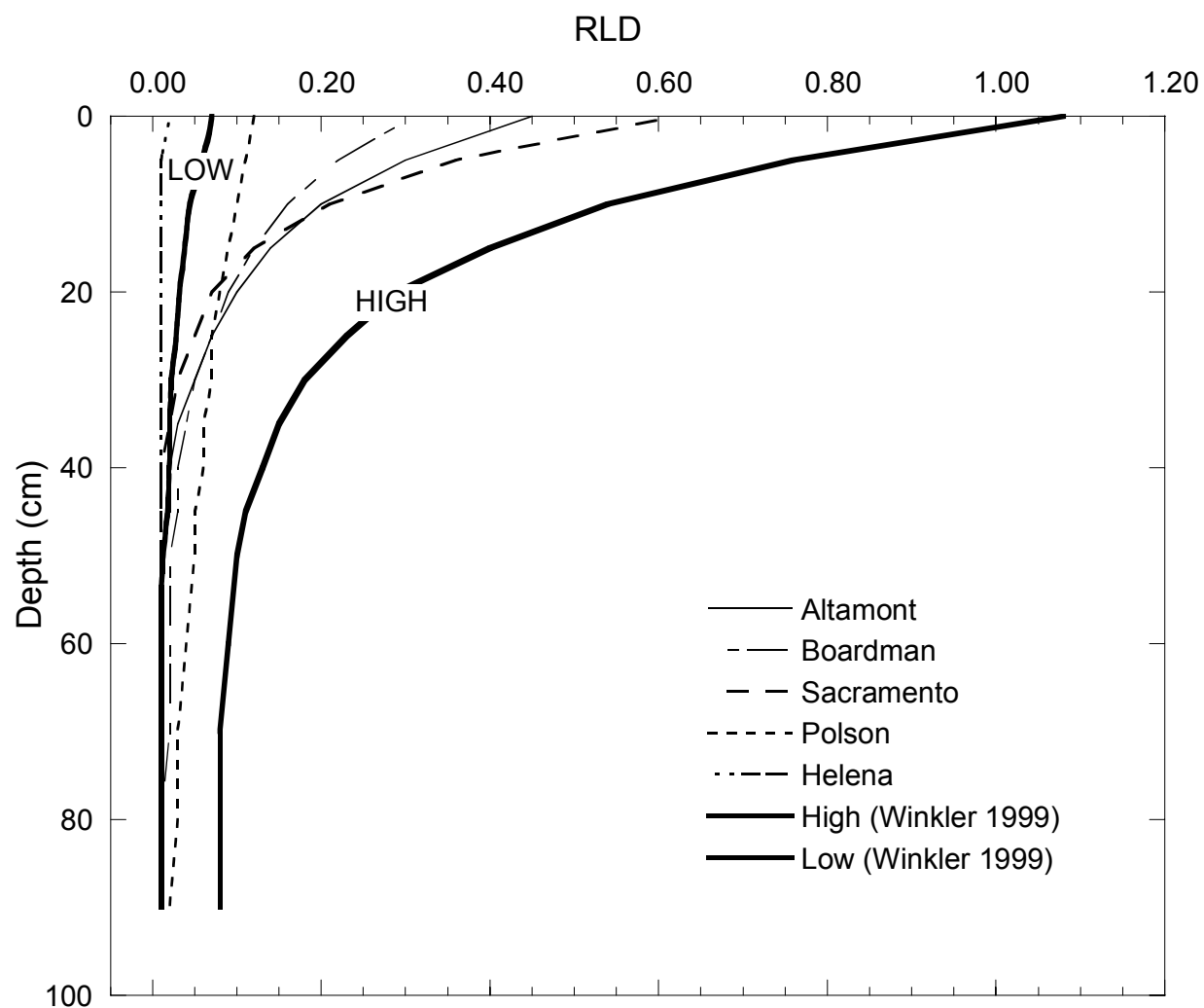


Fig. 5.2. Root Length Density Functions Measured at ACAP Sites with Upper and Lower Bounds Defined by Winkler (1999).

Table 5.9 Runoff Curve Numbers Computed by HELP.

Site	Test Section	Slope (%)	Slope Length (m)	Topsoil Texture Number	Vegetation (1-5)		Runoff Curve Number	
					2000	2001	2000	2001
Altamont	Monolithic	5	20	25	-	2	-	94.1
	Composite	5	20	25	-	2	-	94.1
Omaha	Capillary	25	20	25	-	3	-	91.4
	Composite	25	20	25	-	3	-	91.4
Boardman	Capillary	25	20	22	-	2	-	94.4
	Composite	25	20	22	-	2	-	94.4
Sacramento	Monolithic	5	20	27	2	3	91.1	91.1
Polson	Capillary	5	20	7	2	3	84.7	77.3
	Composite	5	20	7	2	3	84.7	77.3
Helena	Capillary	5	20	27	2	2	94.1	94.1
Albany	ECap	5	20	10	-	4	-	82.3
	Compacted Clay	5	20	10	-	2	-	90.9
Marina	Monolithic	25	20	10	-	4	-	83.1
	Composite	25	20	13	-	2	-	92.9

Table 5.10. Design Inputs for HELP and UNSAT-H.

<b>Site</b>	<b>Construction End Date</b>	<b>UNSAT-H Data Start Date</b>	<b>Test Section Area (ha)</b>	<b>Elevation (m)</b>	<b>Latitude (deg)</b>	<b>Slope (%)</b>
Altamont	8/30/00	11/10/00	0.1	457	37.7	5
Omaha	8/11/00	10/5/00	0.1	85	41.3	25
Boardman	11/2/00	12/9/00	0.1	178	45.7	5
Sacramento	7/25/99	7/29/99	0.1	61	38.5	5
Polson	10/19/99	11/19/99	0.1	893	48.3	5
Helena	10/18/99	10/19/99	0.1	1247	46.6	5
Albany	3/18/00	4/19/00	0.1	73	31.6	5
Marina	5/25/00	5/27/00	0.1	31	36.6	25

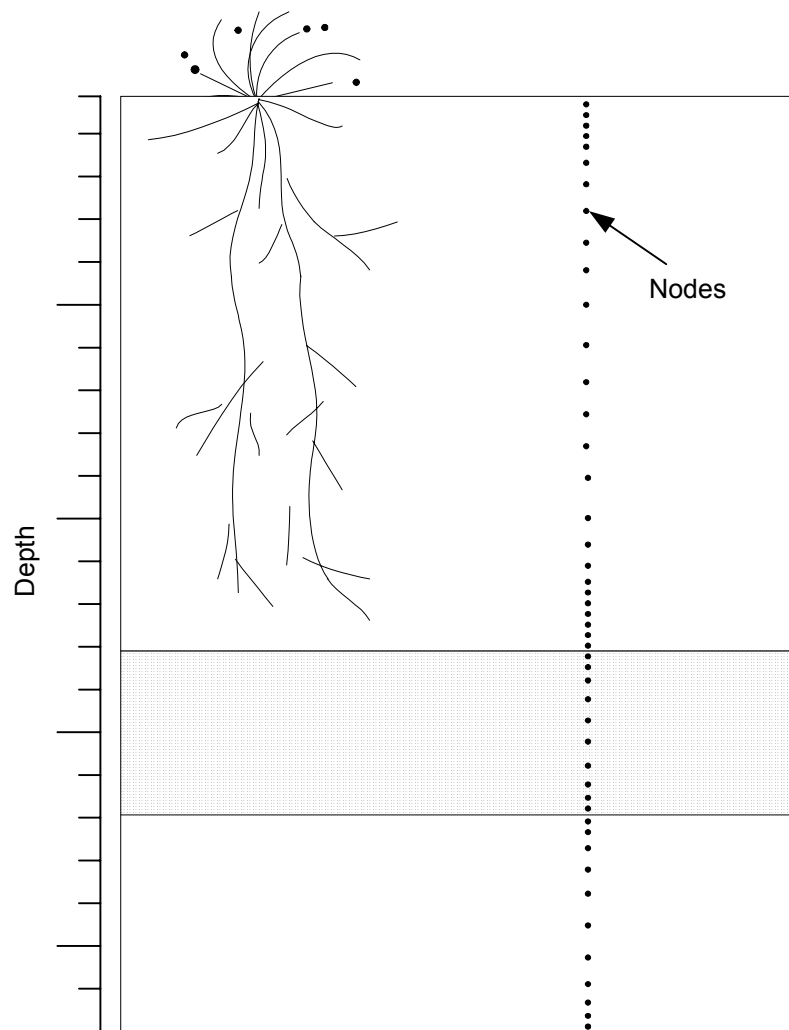


Fig. 5.3. Schematic of Typical Nodal Spacing Used in UNSAT-H.

boundaries, and at interfaces between layers. The spacing increased with depth or distance from a boundary or layer interface. A maximum nodal spacing of 50 mm was used.

Four iterations were allowed for solving the water flow equation. A time step control parameter of 0.001, a maximum allowable time step of 0.25 hr, and a minimum allowable time step of  $10^{-5}$  hr were used. Also, a maximum time step factor of 1, a rainfall initiation factor of 0.001, and a time step reduction factor of 0.1 were used.

## **5.5 COMPARISON BETWEEN ACTUAL AND SIMULATION RESULTS**

Water balance simulations with UNSAT-H and HELP were performed on each test section from ACAP, with the exception of the Cedar Rapids site and the Monticello site. Simulations were not run for these two sites because of large data gaps. The UNSAT-H and HELP simulations were run from the first day of data collection until April 2002. This section describes comparisons of measured and predicted surface runoff, lateral flow (if applicable), soil water storage, evapotranspiration, and percolation.

Initial simulations made with UNSAT-H and HELP using the measured hydraulic properties in Tables 5.11 and 5.12 greatly over-predicted surface runoff. The over predictions by UNSAT-H ranged from 0 to 85.6% of precipitation, and those by HELP ranged from 0.1 to 57.1% of precipitation. By greatly over-predicting surface runoff, the volume of water that infiltrates the cover is grossly underestimated. Therefore, all subsequent flow processes are incorrect. (Khire et al. 1997). This discrepancy is believed to be caused by the hydraulic conductivity of the surface layer (top soil) being too low. Hydraulic conductivity of the surface layer was measured on specimens collected immediately after construction that probably did not include macroscopic

Table 5.11. Surface Runoff Predictions From Original and Adjusted Simulations Using UNSAT.

Site	Test Section	Field Surface Runoff (mm)	Original Simulation			Decreased Surface Runoff	
			Surface Layer $K_s$ (cm/s)	SRO (mm)	Over-Prediction (%)	Surface Layer $K_s$ (cm/s)	SRO (mm)
Altamont	Monolithic	26	$2.8 \times 10^{-6}$	325	61.3%	$2.8 \times 10^{-4}$	2 <sup>a</sup>
Sacramento	Monolithic (1070 mm)	120	$9.0 \times 10^{-7}$	899	68.2%	$9.4 \times 10^{-5}$	51
	Monolithic (2450 mm)	68	$9.0 \times 10^{-7}$	899	72.7%	$2.8 \times 10^{-4}$	27 <sup>b</sup>
Helena	Capillary	28	$5.0 \times 10^{-7}$	359	85.6%	$2.8 \times 10^{-4}$	33
Polson	Capillary	23	$4.9 \times 10^{-5}$	288	35.6%	$2.8 \times 10^{-4}$	107
Boardman	Monolithic (1220 mm)	0	$1.9 \times 10^{-5}$	0	0.0%	- <sup>c</sup>	- <sup>c</sup>
	Monolithic (1840 mm)	0	$1.4 \times 10^{-5}$	0	0.0%	- <sup>c</sup>	- <sup>c</sup>
Marina	Monolithic	0	$6.7 \times 10^{-8}$	430	71.0%	$2.8 \times 10^{-4}$	122 <sup>a</sup>
Albany	ECap	15	$1.9 \times 10^{-7}$	1590	79.4%	$2.8 \times 10^{-4}$	0 <sup>d</sup>
	Compacted Clay	169	$1.3 \times 10^{-4}$	366	11.9%	$2.8 \times 10^{-4}$	357
Omaha	Capillary (760 mm)	72	$6.1 \times 10^{-6}$	0	-10.0%	- <sup>c</sup>	- <sup>c</sup>
	Capillary (1060 mm)	54	$4.5 \times 10^{-7}$	155	14.0%	$2.8 \times 10^{-4}$	43

<sup>a</sup> Split vegetative cover into two sub layers with a 150 mm surface layer.

<sup>b</sup> Increased  $K_s$  of vegetative cover underneath surface layer to decrease surface runoff appreciably. Made vegetative cover of thick barrier equal to vegetative cover of thin barrier ( $K^s = 3.98 \times 10^{-4}$  cm/s).

<sup>c</sup> Additional simulation not conducted because "original" simulation predicted less than or equal amount of surface runoff as measured in field.

<sup>d</sup> Increased  $K_s$  of entire surface layer, rather than creating a 150 mm sub-layer, to decrease surface runoff appreciably.



Table 5.12 Surface Runoff (SRO) Predictions From Original and Adjusted Simulations Using HELP.

Site	Test Section	Field SRO (mm)	Original Simulation				Decreased Surface Runoff		
			Surface Layer $K_s$ (cm/s)	Curve Number (CN)	SRO (mm)	Over-Prediction (%)	Surface Layer $K_s$ (cm/s)	Curve Number (CN)	SRO (mm)
Altamont	Composite	15	$2.0 \times 10^{-5}$	94.1	44	3.7%	$2.0 \times 10^{-5}$	88.1	16
	Monolithic	26	$2.8 \times 10^{-6}$	94.1	52	5.2%	$2.8 \times 10^{-4}$	94.1	20
Sacramento	Monolithic (1070 mm)	120	$9.0 \times 10^{-7}$	91.1	97	-2.0%	$9.4 \times 10^{-5}$	91.1	85
	Monolithic (2450 mm)	68	$9.0 \times 10^{-7}$	91.1	105	3.2%	$9.4 \times 10^{-5}$	91.1	80
Helena	Capillary	28	$5.0 \times 10^{-7}$	94.1	25	-0.8%	- <sup>a</sup>	- <sup>a</sup>	- <sup>a</sup>
Polson	Composite	19	$4.9 \times 10^{-5}$	84.7	49	3.4%	$4.9 \times 10^{-5}$	77.3	13
	Capillary	23	$4.9 \times 10^{-5}$	84.7	54	4.2%	$4.9 \times 10^{-5}$	77.3	9
Boardman	Composite	0	$3.8 \times 10^{-5}$	94.4	2	1.1%	- <sup>a</sup>	- <sup>a</sup>	- <sup>a</sup>
	Monolithic (1220 mm)	0	$1.9 \times 10^{-5}$	94.4	0.2	0.1%	- <sup>a</sup>	- <sup>a</sup>	- <sup>a</sup>
	Monolithic (1840 mm)	0	$1.4 \times 10^{-5}$	94.4	0.2	0.1%	- <sup>a</sup>	- <sup>a</sup>	- <sup>a</sup>
Marina	Composite	86	$4.5 \times 10^{-6}$	92.9	257	28.2%	$2.8 \times 10^{-4}$	92.9	164
	Monolithic	0	$6.7 \times 10^{-8}$	83.1	151	25.0%	$2.8 \times 10^{-4}$	83.1	6
Albany	ECap	15	$1.9 \times 10^{-7}$	90.9	459	22.4%	$2.8 \times 10^{-4}$	82.3	32
	Compacted Clay	166	$1.3 \times 10^{-4}$	90.9	697	31.9%	$1.3 \times 10^{-4}$	82.3	639
Omaha	Composite	67	$1.5 \times 10^{-6}$	92.0	479	57.1%	$2.8 \times 10^{-4}$	92.0	89
	Capillary (760 mm)	72	$6.1 \times 10^{-6}$	94.4	136	8.9%	$2.8 \times 10^{-4}$	94.4	119
	Capillary (1060 mm)	54	$4.5 \times 10^{-7}$	94.4	164	15.1%	$2.8 \times 10^{-4}$	94.4	123

<sup>a</sup> Additional simulation not conducted because "original" simulation predicted less than or equal amount of surface runoff as measured in field.

features (desiccation and freeze-thaw cracks, root holes, worm holes, etc.) that affect the saturated hydraulic conductivity at field scale. In addition, tilling was conducted at three sites (Albany, Cedar Rapids, and Marina) subsequent to construction to facilitate vegetative growth, and probably increased the saturated hydraulic conductivity above that measured immediately after construction.

To account for these post-construction changes in hydraulic conductivity, another set of simulations was conducted using different parameters for the surface layer. The saturated hydraulic conductivity of the upper most layer was adjusted until the runoff predicted by UNSAT-H and HELP was similar to that measured in the field. If a topsoil layer did not exist, the surface layer was divided into two layers, with the uppermost layer being 150 mm thick.

Graphs of the water balance predicted using UNSAT-H and HELP with the original parameters used as input are shown in Appendices 4 and 5. Simulations conducted with “original” parameters refer to simulations using the saturated hydraulic conductivity measured immediately after construction. Graphs illustrating the predicted water balance from UNSAT-H and HELP using adjusted parameters, as compared to field measurements, are shown in Section 5.5.1 and 5.5.2. Simulations conducted with “adjusted” parameters refer to simulations using adjusted saturated hydraulic conductivities and surface runoff curve numbers (HELP only)

UNSAT-H calculates surface runoff as the difference between precipitation and infiltration, the later being a function of the water content of the soil, and the hydraulic properties of the cover layers. The infiltration rate decreases as the wetted depth increases, and approaches the lowest saturated hydraulic conductivity of any layer within the wetted depth. For many cases, predictions of surface runoff made with

UNSAT-H came considerably closer to that measured in the field when the surface layer had a saturated hydraulic conductivity of  $2.8 \times 10^{-4}$  cm/s. For some cases, adjusting the saturated hydraulic conductivity of the surface layer was not necessary. For other cases, however, increasing the saturated hydraulic conductivity of the surface layer was not sufficient to match the predicted and measured runoff.

An example of the latter case is shown in Fig. 5.4, in which multiple simulations were conducted by varying the saturated hydraulic conductivity of topsoil layer in the thick monolithic barrier at Sacramento. UNSAT-H did not predict a surface runoff less than 267 mm (field surface runoff was 68 mm), even when the saturated hydraulic conductivity of the topsoil was increased to  $1.0 \times 10^{-3}$  cm/s. The only means of decreasing the predicted surface runoff sufficiently was to increase the saturated hydraulic conductivity of the storage layer below the topsoil layer from  $1.7 \times 10^{-7}$  cm/s (measured) to  $4.0 \times 10^{-4}$  cm/s (i.e., same hydraulic conductivity as was measured for the thin monolithic barrier).

As was obtained for the thick barrier at Sacramento, UNSAT-H over-predicted surface runoff for the alternative (Fig. 5.5) and conventional covers at Albany regardless of the saturated hydraulic conductivity that was used for the surface layer. For the alternative cover, the saturated hydraulic conductivity of the entire surface layer (600 mm) had to be increased to  $2.8 \times 10^{-4}$  cm/s to replicate the field runoff. For the conventional cover, accurately predicting the surface runoff was not possible without increasing the saturated hydraulic conductivity of the compacted clay barrier to  $7.3 \times 10^{-5}$  cm/s.

HELP fared considerably better than UNSAT-H at predicting the measured surface runoff, even though the same hydraulic properties were used for both models.

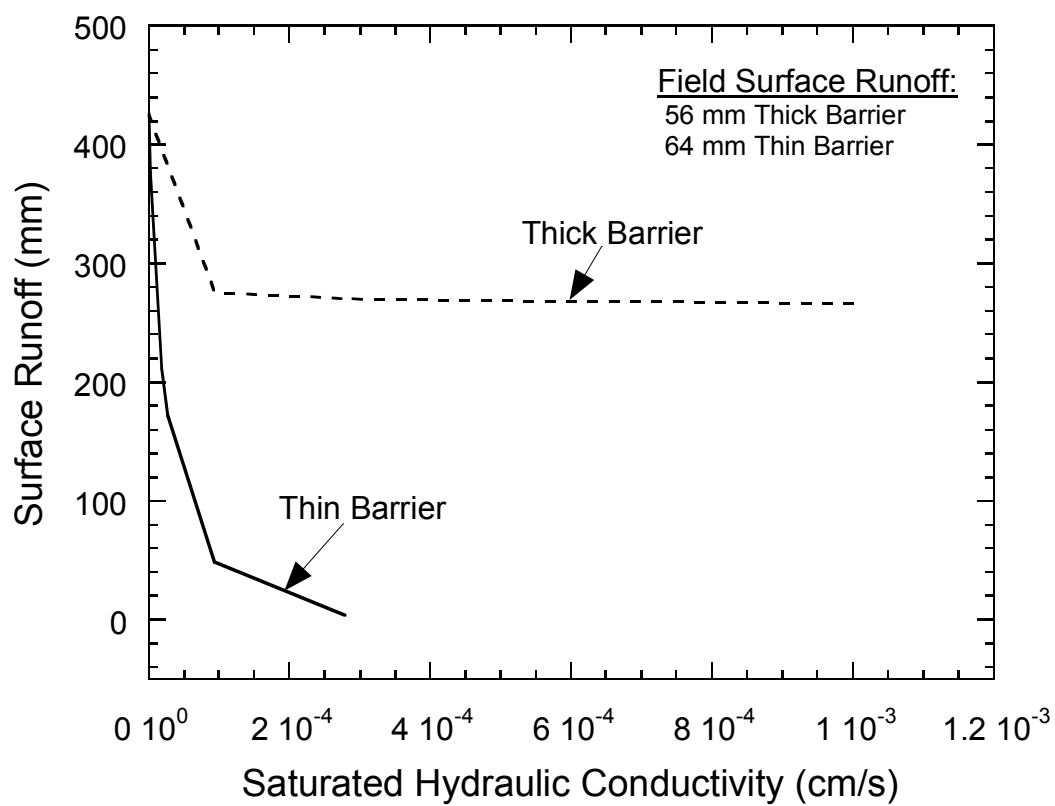


Fig. 5.4. Surface Layer Adjustment for Alternative Covers at Sacramento Site Using UNSAT-H.

HELP was more accurate because a surface runoff curve number (based on slope, vegetation cover, and soil texture) initially partitions rainfall into surface runoff and infiltration. The curve number is entered by the user, and is used to calculate a maximum retention parameter. The retention parameter is adjusted by HELP, depending on the water content of the vegetative zone, and frozen ground conditions. As the water content of the vegetative zone increases, the retention parameter decreases, and the amount of precipitation that becomes surface runoff increases. All of the precipitation will become surface runoff if the vegetative zone becomes saturated.

Surface runoff could be significant for covers that have little soil water storage capacity, lower saturated hydraulic conductivity, and receive intense rain events. The vegetative zone for the conventional cover at Albany only includes the 150 mm topsoil layer, because HELP assumes that the compacted clay barrier is saturated at all times. Therefore, the conventional cover has approximately 45 mm of storage (based on porosity), which is often approached during the intense rain events at Albany.

To more accurately predict surface runoff for the alternative cover at Albany using HELP, the surface runoff curve number and the saturated hydraulic conductivity of the entire storage layer had to be adjusted (Fig. 5.5). Surface runoff was accurately predicted when the curve number was 82.3 and the saturated hydraulic conductivity was  $2.8 \times 10^{-4}$  cm/s.

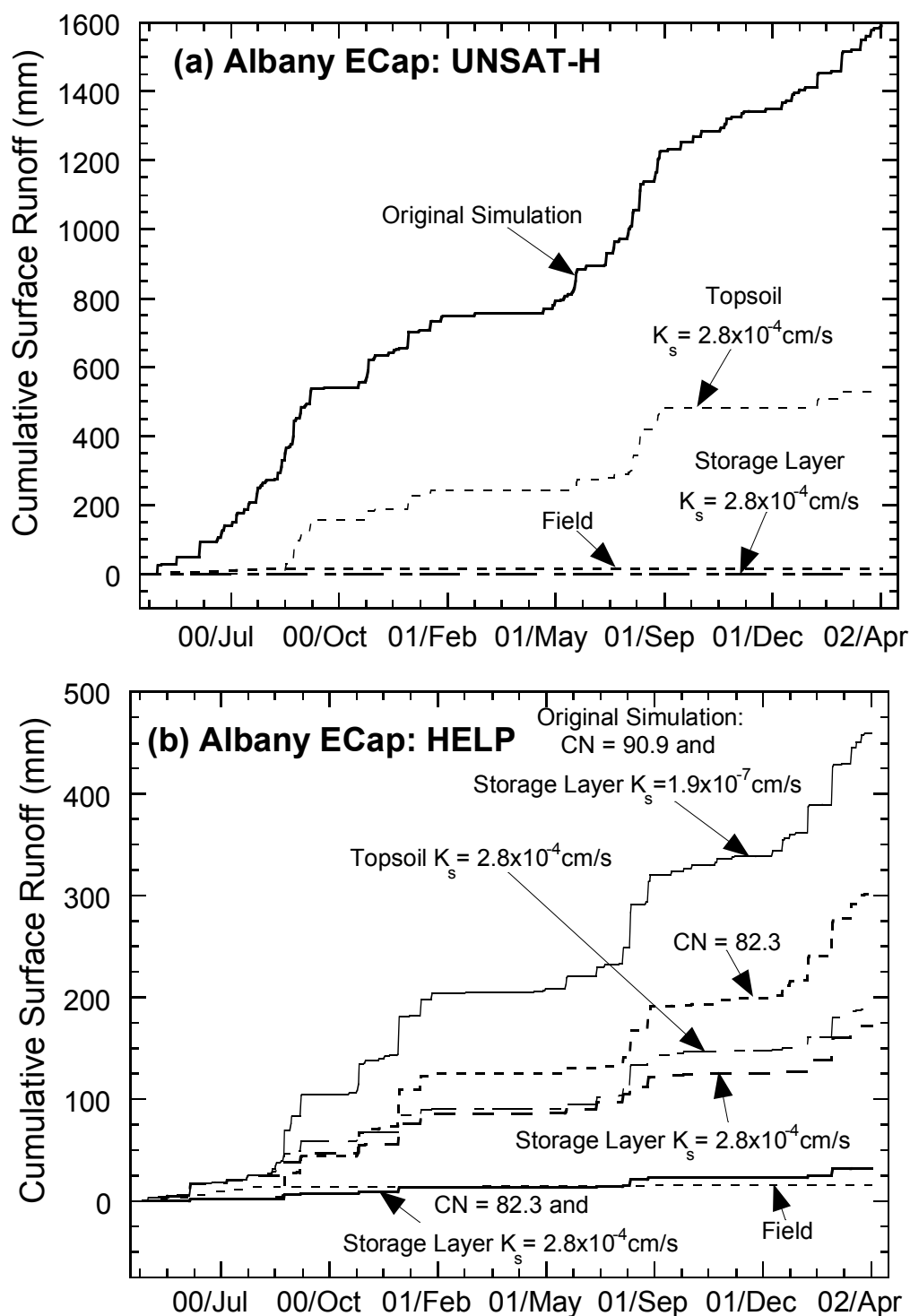


Fig. 5.5. Adjustment of Hydraulic Conductivity and Curve Number for Surface Layer for ECap Cover at Albany Site: (a) UNSAT-H and (b) HELP.

### 5.5.1 Alternative Covers

The following sections provide a comparison of the water balance measured at each site and predictions made with HELP and UNSAT-H using the measured hydraulic properties, and hydraulic properties that were adjusted so that the surface runoff predicted by the models was comparable to that measured in the field.

#### 5.5.1.1 Altamont Site

Water balance measurements and predictions by HELP and UNSAT-H are shown in Fig. 5.6. The saturated hydraulic conductivity of the surface layer (150 mm) was set at  $2.8 \times 10^{-4}$  cm/s in UNSAT-H, and the runoff curve number was reduced to 88.1 in HELP, so that the predicted runoff would be comparable to that occurring in the field.

HELP under-predicted surface runoff by 6.6 mm during the entire monitoring period. HELP was able to predict the occurrence of surface runoff for the majority of runoff events measured in the field. However, between December 15, 2001 and January 2, 2002, approximately 100 mm of rain fell at Altamont, which caused 20.6 mm of surface runoff in the field. HELP greatly under-predicted surface runoff for this period (only 6.8 mm of surface runoff was predicted).

HELP under-predicted soil water storage during the winter months (rainy season), and during the dry season. After the winter rains cease, the soil water storage in the field gradually decreases, reaching a minimum at the end of the dry season. In contrast, HELP removes all of the available water from the cover profile immediately after the winter rains cease, causing the soil to reach the wilting point at the end of April. After the wilting point is reached, HELP no longer predicts evapotranspiration until the winter rains occur again.

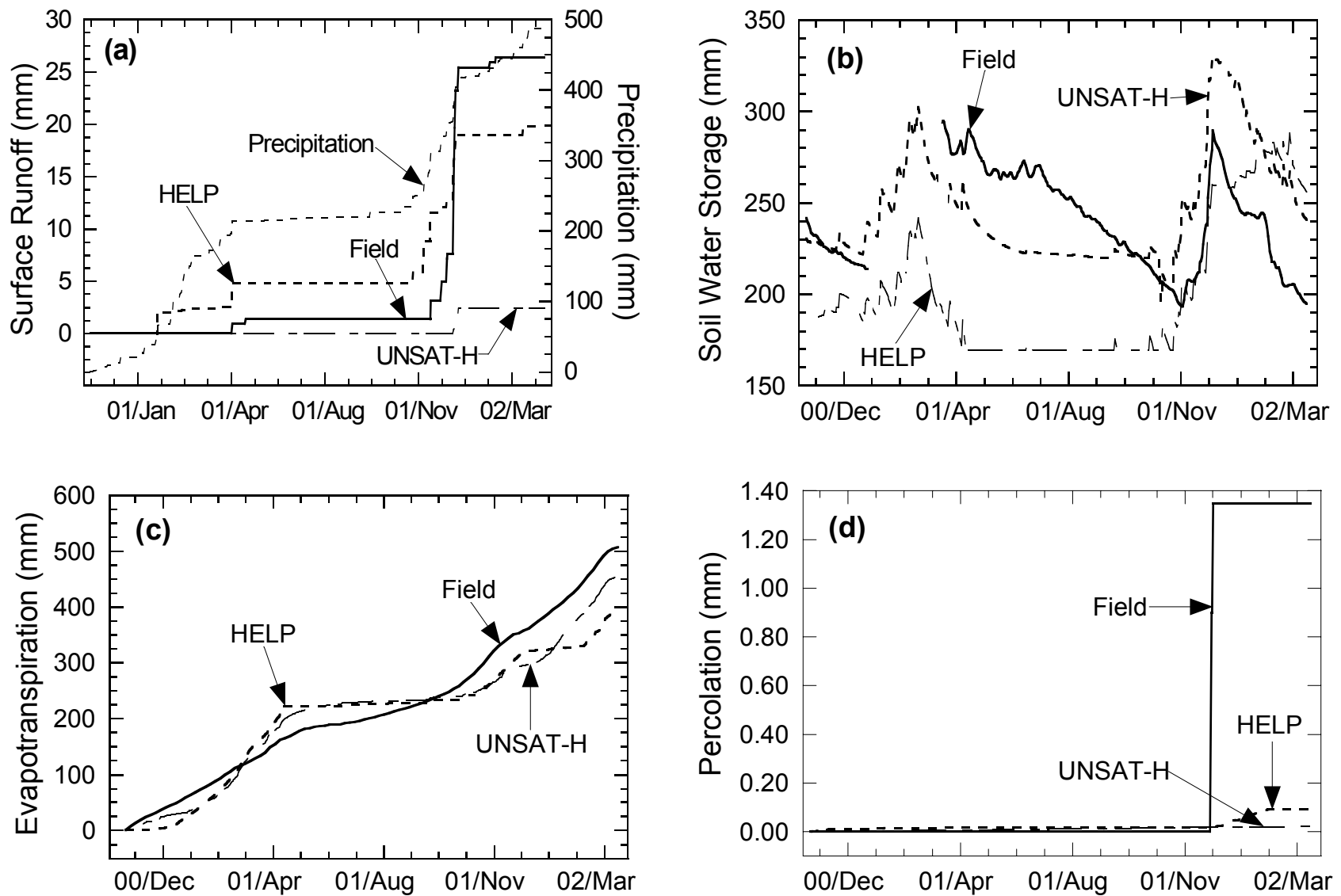


Fig. 5.6. Comparison of Water Balance Data for the Altamont Site to Predictions Made with UNSAT-H and HELP: (a) Surface Runoff, (b) Soil Water Storage, (c) Evapotranspiration, and (d) Percolation.



Even though the soil water storage capacity of the alternative cover at Altamont (460 mm based on field capacity) was never reached, 1.3 mm of percolation was measured at the end of December 2001. HELP under-predicted percolation, predicting only 0.1 mm. HELP began predicting percolation during the same time as occurred in the field, but HELP predicted that the percolation extended over two months, rather than the sudden pulse of percolation observed in the field.

UNSAT-H under-predicted surface runoff measured in the field by 18.2 mm when the adjusted hydraulic conductivity of the surface layer was used as input. The original hydraulic conductivity of the surface layer (measured immediately after construction) was  $2.8 \times 10^{-6}$  cm/s. The saturated hydraulic conductivity used for these simulations was  $2.8 \times 10^{-4}$  cm/s, and was not refined specifically for the Altamont site. The predicted surface runoff probably would have been closer if a more accurate hydraulic conductivity was assigned to the surface layer. Samples are being collected at each site during 2002-03 to better characterize the saturated hydraulic conductivity operative in the field.

UNSAT-H was able to follow the soil water storage trend observed in the field during the first year of the monitoring period, but was not able to reach the minimum soil water storage observed in the field by the end of the dry season. UNSAT-H, similar to HELP, did not predict evapotranspiration during the dry season, resulting in no change in soil water storage during this period. During the second winter, UNSAT-H predicted higher soil water storage than occurred in the field. This over-estimate is most likely due to the over-estimation of soil water storage during the dry season, the under-estimation of surface runoff at the end of December 2001, and the under-estimation of evapotranspiration.

#### 5.5.1.2 Sacramento Site

The measured water balance and predictions by HELP and UNSAT-H for the thin and thick barriers in Sacramento are shown in Figs. 5.7 and 5.8. To predict runoff better, the saturated hydraulic conductivity assigned to the surface layer (uppermost 150 mm) for the thin barrier was set at  $9.4 \times 10^{-5}$  cm/s in HELP and UNSAT-H. For the thick barrier, the hydraulic conductivity of the surface layer was assigned  $9.4 \times 10^{-5}$  cm/s in HELP, and  $2.8 \times 10^{-4}$  cm/s in UNSAT-H. Also, the saturated hydraulic conductivity of the storage layer in the thick barrier had to be increased to  $4.0 \times 10^{-4}$  cm/s (similar to that in the thin barrier) for UNSAT-H. When the saturated hydraulic conductivity of the storage layer for the thick barrier was not increased, surface runoff was greatly over-estimated (see Appendix 2).

HELP was able to predict the occurrence of surface runoff during the entire monitoring period, but under-predicted surface runoff by 35 mm for the thin barrier, and by 12 mm for the thick barrier. The largest discrepancy was in February 2001 and December 2001. During these two periods, the measured surface runoff was approximately 25% of precipitation for the thin barrier. In contrast, surface runoff was only 10.5% of precipitation over the entire monitoring period. Surface runoff may have been greater during these two periods because of intense rain events. In both February and December 2001, 90 mm of rainfall was measured.

HELP was able to predict the trend in soil water storage fairly closely prior to Winter 2001. After Winter 2001, HELP grossly under-predicted soil water storage for both covers. This discrepancy is due to (1) the prediction of percolation during the first two winters, when no percolation actually occurred, and (2) predicting greater evapotranspiration during Spring 2001 than occurred in the field.

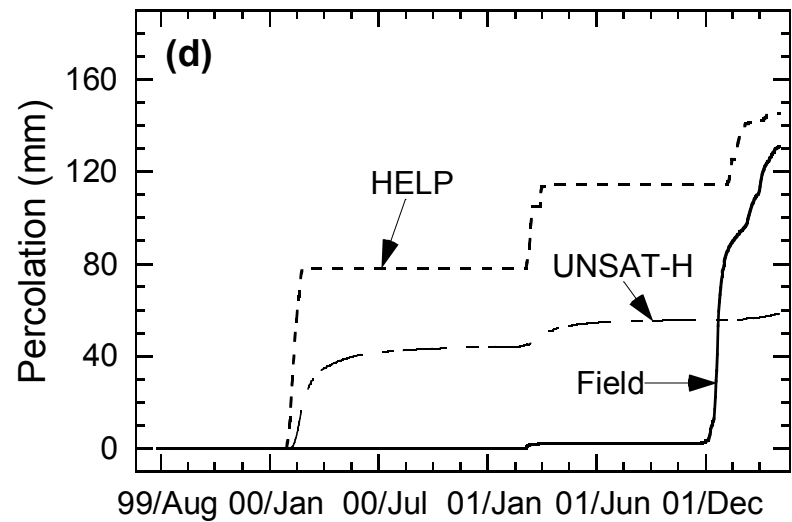
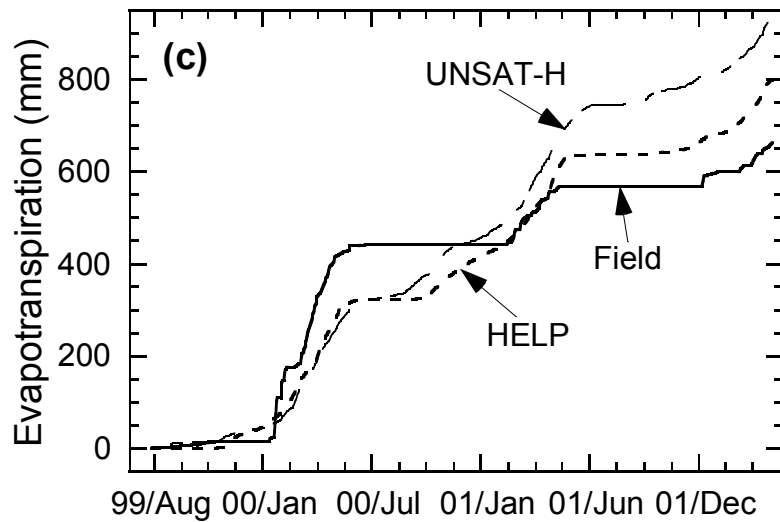
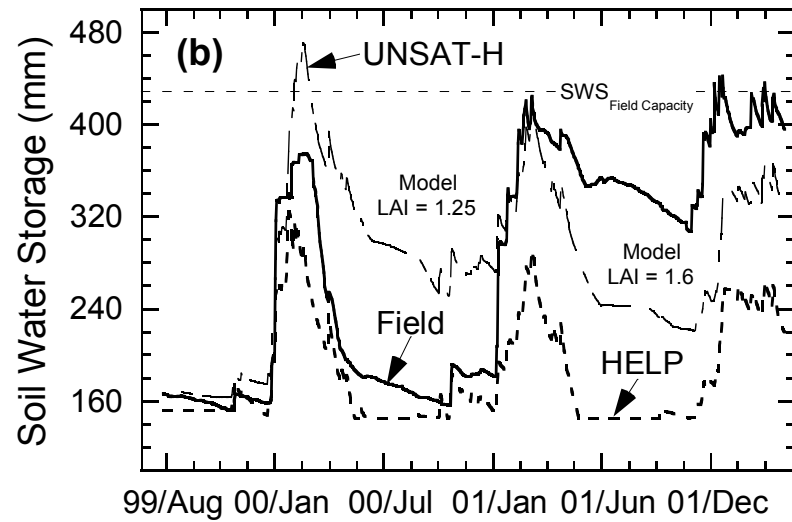
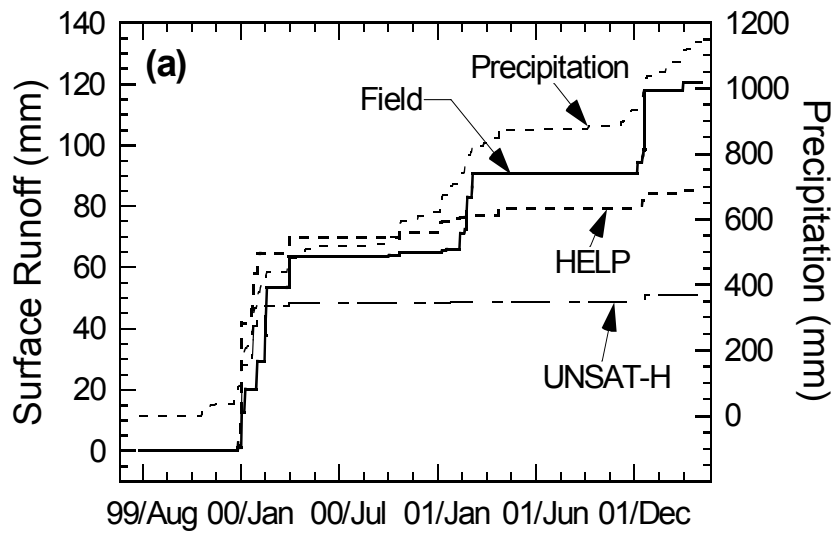


Fig. 5.7. Comparison of Water Balance Data for the Sacramento Site (Thin Monolithic Barrier) to Predictions Made with UNSAT-H and HELP: (a) Surface Runoff, (b) Soil Water Storage, (c) Evapotranspiration, and (d) Percolation.

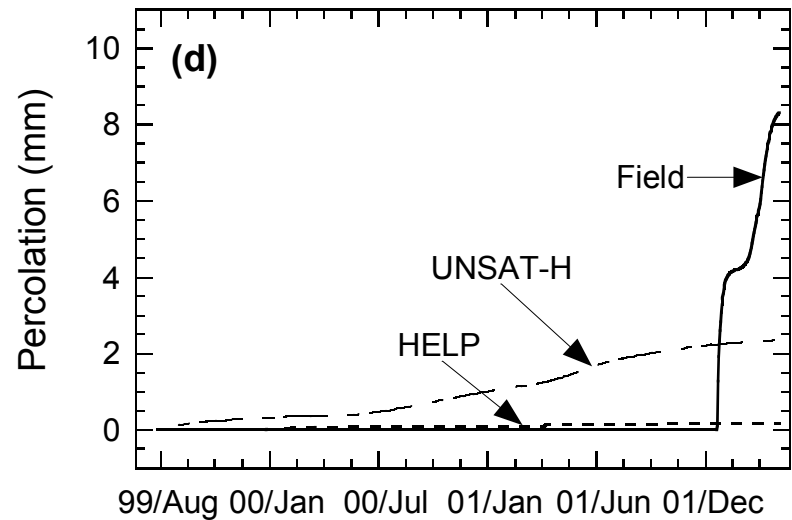
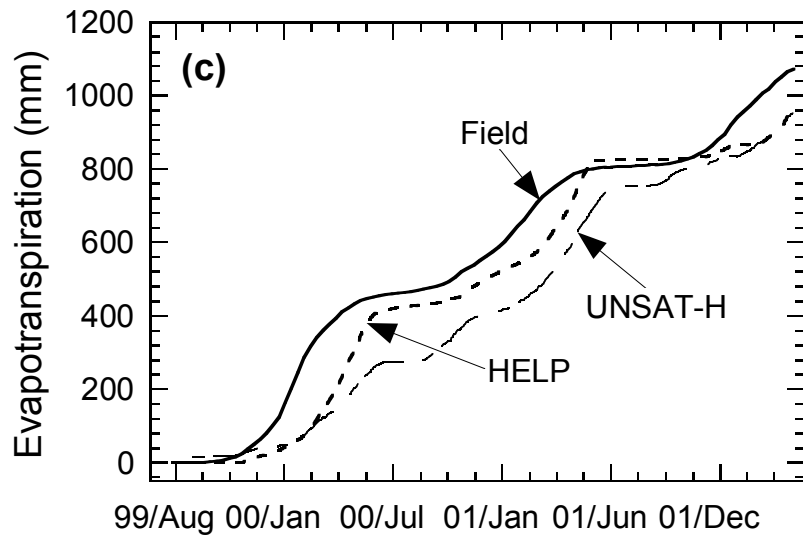
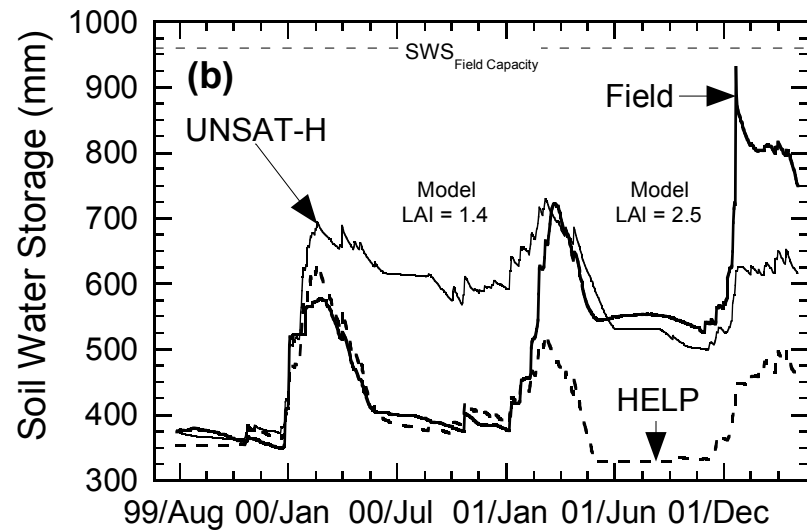
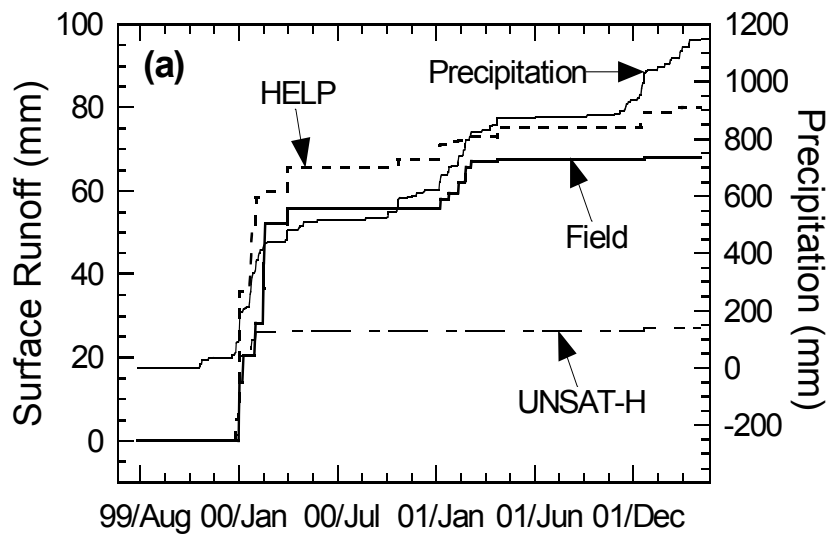


Fig. 5.8. Comparison of Water Balance Data for the Sacramento Site (Thick Monolithic Barrier) to Predictions Made with UNSAT-H and HELP: (a) Surface Runoff, (b) Soil Water Storage, (c) Evapotranspiration, and (d) Percolation.

Another likely cause of the under-prediction is due to the method by which HELP outputs soil water storage. HELP outputs a weighted average of the volumetric water content of the evaporative zone, rather than the soil water storage of the entire cover profile (such as from UNSAT-H). To compare the soil water storage calculated from HELP with the soil water storage from UNSAT-H and that calculated by the WCRs in each test section, the soil water storage of the evaporative zone from HELP was added to the initial soil water storage of the other layers measured in the field. The flaw in this approach is that any water that is routed by HELP to the layers below the evaporative zone will not be captured. For example, HELP under-predicted the maximum soil water storage for the thin barrier at Sacramento by 70 mm (March 2001) when the interim cover was not included in the calculation of soil water storage measured in the field (see Fig. 5.9). However, HELP over-predicted soil water storage by 133 mm when the interim cover was included in the soil water storage calculation.

During Spring 2001, HELP removed all of the available soil water in the evaporative zone by evapotranspiration and percolation (thin barrier only), whereas significantly less evapotranspiration and percolation actually occurred in the field. The vegetation at the Sacramento site most likely went dormant several months earlier than expected, but a typical growing season was used in the HELP simulations.

HELP grossly over-predicted percolation from the thin barrier during most of the monitoring period, but under-predicted percolation that occurred at the end of the monitoring period for both covers. At no time during the monitoring period did HELP predict that the soil water storage was exceeded. The large amount of percolation transmitted through the thin barrier can be attributed to the high saturated hydraulic

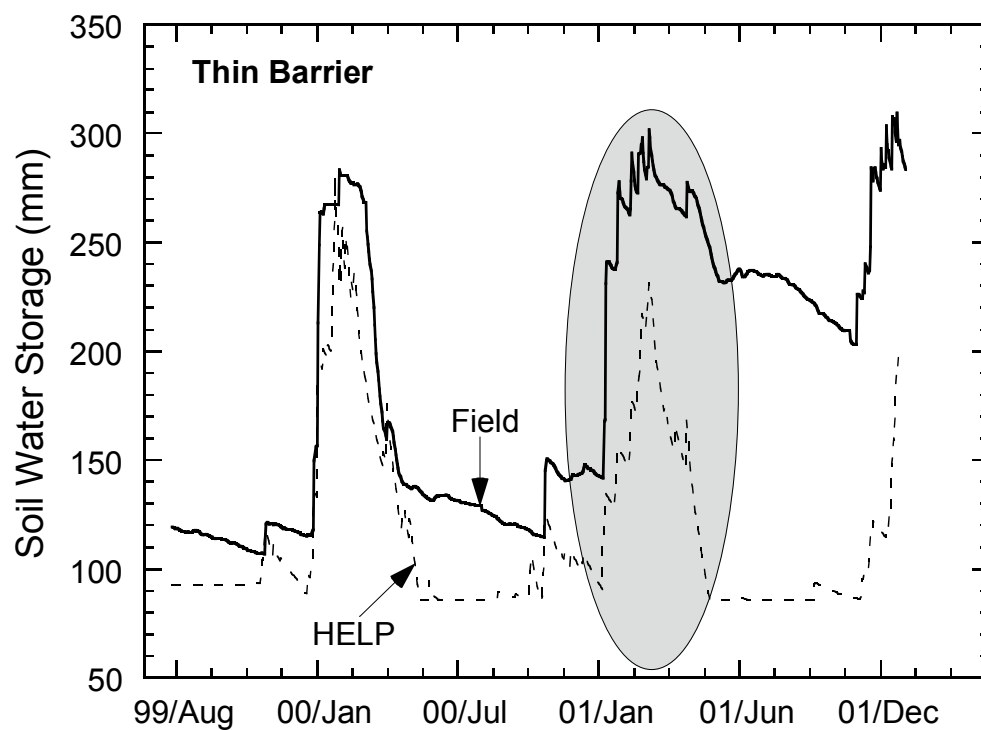


Fig. 5.9. Soil Water Storage Predicted by HELP and Measured in Field for the Thin Monolithic Barrier at the Sacramento Site.

conductivity of the storage layer ( $4.0 \times 10^{-4}$  cm/s). For the thick barrier, the combination of additional thickness and the lower saturated hydraulic conductivity of the storage cover ( $1.7 \times 10^{-7}$  cm/s) limited percolation to less than 1 mm during the monitoring period.

UNSAT-H did not perform as well HELP in predicting occurrences of surface runoff during the monitoring period. UNSAT-H under-predicted surface runoff by 69.2 mm for the thin barrier, and by 40.9 mm for the thick barrier. The majority of surface runoff predicted by UNSAT-H occurred from mid-January to mid-February 2000. During this period, UNSAT-H only slightly under-predicted surface runoff from the thin barrier (6 mm), but grossly under-predicted surface runoff from the thick barrier by (26 mm). The inaccuracy for the thick barrier is likely due to the surface layer being assigned a saturated hydraulic conductivity that is too high.

The trend in soil water storage was predicted by UNSAT-H. However, UNSAT-H did not predict the minimum and maximum soil water storage measured in the field. UNSAT-H under-predicted evapotranspiration prior to Winter 2001, which caused an over-prediction in peak soil water storage in Winter 2000. Also, UNSAT-H did not extract water to the wilting point (151 mm thin barrier, 351 mm thick barrier) in Summer 2000, as occurred in the field. Evapotranspiration may have been under-predicted due to an under-estimate of maximum LAI. The LAI was measured at Sacramento, but the vegetation samples were not collected during the peak of the growing season, when LAI is at a maximum.

Percolation was only transmitted from the two covers at the end of the monitoring period (131 mm for the thin barrier and 8.3 mm for the thick barrier). During Winter 2000 and 2001, UNSAT-H predicted that the soil water storage would exceed the capacity of

the thin barrier, which caused 58 mm of percolation. For the thick barrier, 2.4 mm of percolation was predicted to occur throughout the entire monitoring period.

#### **5.5.1.3 Helena Site**

The measured water balance and predictions made with HELP and UNSAT-H are shown in Fig. 5.10. For UNSAT-H, the saturated hydraulic conductivity assigned to the surface layer (150 mm) was  $2.8 \times 10^{-4}$  cm/s to improve the runoff prediction.

HELP under-predicted surface runoff by only 3 mm during the monitoring period, despite missing a snowmelt event in March 2001, and over-predicting surface runoff during Spring 2001. The field data show that 14 mm of surface runoff occurred during a snowmelt in March 2001, even though only 4 mm of water was applied using the snowmelt algorithm (described in Section 5.4.1). This discrepancy may be due to snow being melted prior to March 2001 by the snowmelt algorithms used in HELP and UNSAT-H, or that snowfall was not accurately measured during Winter 2001.

During two rain events in June 2001 (28.7 mm) and July 2001 (24.9 mm), HELP predicted that surface runoff was approximately 25% of precipitation, whereas less than 1 mm of surface runoff was measured. The high percentage of surface runoff during those two events may be due to the intense precipitation that occurred in June and July 2001, which is atypical for Helena. The saturated hydraulic conductivity of the surface layer may also have been too low to allow the water to infiltrate sufficiently.

The field data show that soil water storage increases during the spring (snowmelt) and summer (rainy season), and decreases in the fall and winter. HELP greatly under-predicts soil water storage during nearly the entire monitoring period.



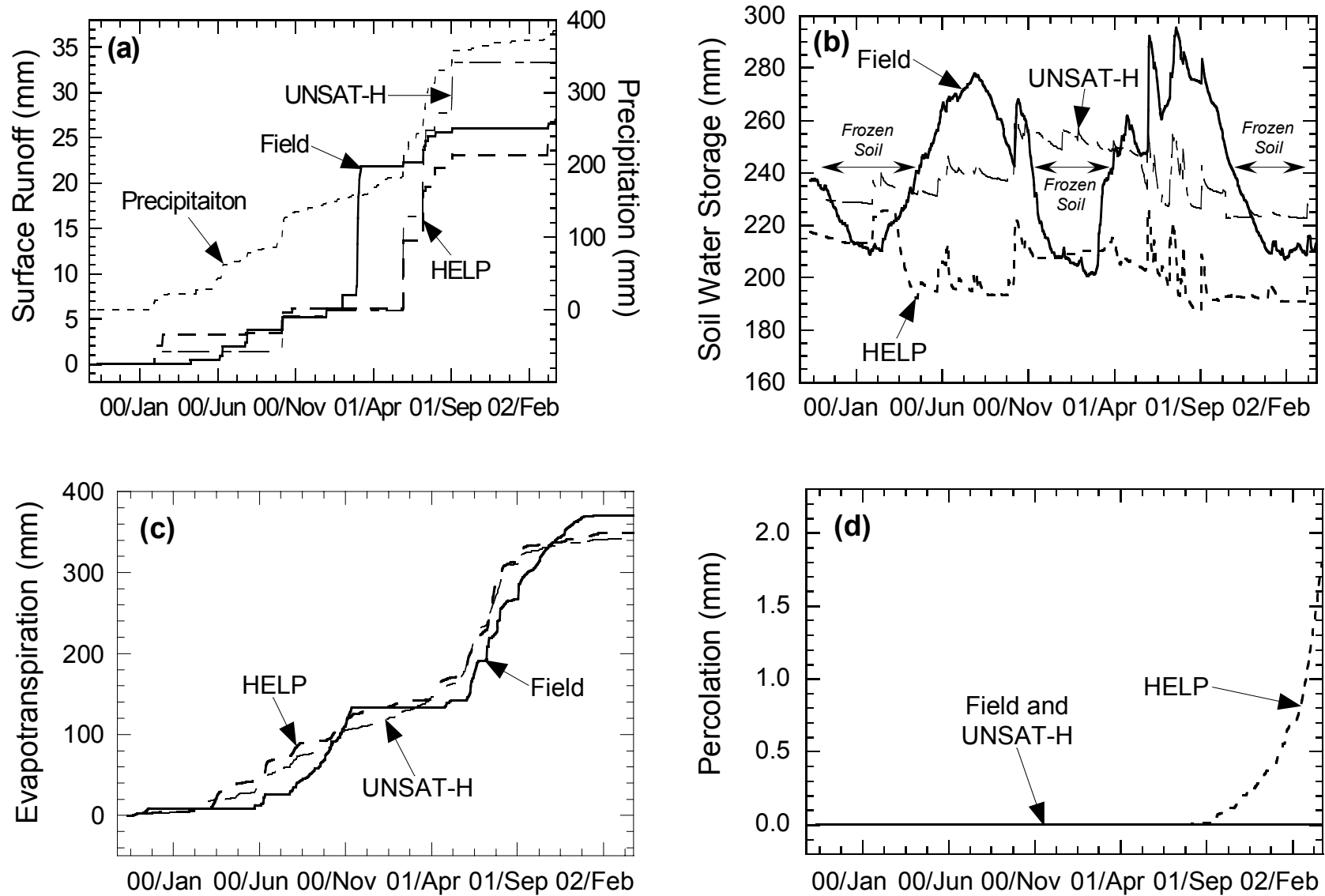


Fig. 5.10. Comparison of Water Balance Data for the Helena Site to Predictions Made with UNSAT-H and HELP: (a) Surface Runoff, (b) Soil Water Storage, (c) Evapotranspiration, and (d) Percolation.

During the spring, HELP under-predicts soil water storage by approximately 70 mm. The field data show a large increase in soil water storage in the spring, whereas HELP only shows small peaks in soil water storage that diminish rapidly. This may be due to HELP over-predicting evapotranspiration during these periods, or draining water to lower layers (below the evaporative zone). HELP predicted 2.3 mm of percolation from the cover, beginning in September 2001, despite no percolation being measured during the monitoring period.

UNSAT-H over-predicted surface runoff by only 5 mm during the monitoring period. However, like HELP, UNSAT-H missed the snowmelt event in March 2001, and over-predicted surface runoff.

UNSAT-H was able to follow the trend in soil water storage measured in the field better than HELP, but still under-predicted soil water storage in the summer by 30 mm, and over-predicted soil water storage in the winter by approximately 20 mm. During Winter 2001, UNSAT-H over-predicted soil water storage by almost 55 mm. The large apparent drop in soil water storage measured in the field is a result of frozen soil (see Section 4.3.2), in which case both HELP and UNSAT-H predictions would more closely follow the soil water storage trend.

UNSAT-H closely predicts the trend in evapotranspiration calculated from the field data, except during the winter. The potential artificial drop in soil water storage during the winter causes an artificial increase in evapotranspiration, whereas UNSAT-H predicts very little evapotranspiration.

UNSAT-H does not predict any percolation during the monitoring period, which is consistent with the field data.

#### 5.5.1.4 Polson Site

The measured water balance and predictions made with HELP and UNSAT-H are shown in Fig. 5.11. To predict surface runoff better, the saturated hydraulic conductivity assigned to the surface layer (150 mm) for UNSAT-H was  $2.8 \times 10^{-4}$  cm/s. For HELP, the runoff curve number was reduced to 77.3.

HELP under-predicted surface runoff by 11.3 mm for the entire monitoring period, but most of the under-prediction occurred February 2000. During this time period, 11.7 mm of surface runoff was measured, most of which was caused by snowmelt. HELP predicted only 2 mm of surface runoff during the same time period, despite predicting frozen ground conditions.

Surface runoff predicted by HELP using the original parameters is shown in Fig. 5.12, along with predictions using a higher saturated hydraulic conductivity and a lower runoff curve number. During Winter 2000, the HELP simulations using the original parameters and an elevated saturated hydraulic conductivity accurately predict surface runoff, but greatly over-predict runoff during the following winters. In contrast, lowering the curve number results in a poor prediction during Winter 2000, but a close prediction in subsequent winters. This may suggest that the saturated hydraulic conductivity needs to be increased, and the curve number reduced over-time.

The field data show that soil water storage increases in the spring, and decreases dramatically in the summer. A similar trend is evident in soil water storage predicted by HELP. However, HELP under-predicted soil water storage in Spring 2000 by 70 mm, and in Spring 2001 by 35 mm, because percolation was over-predicted. HELP allowed water to drain from the profile, rather than being retained in soil water storage.

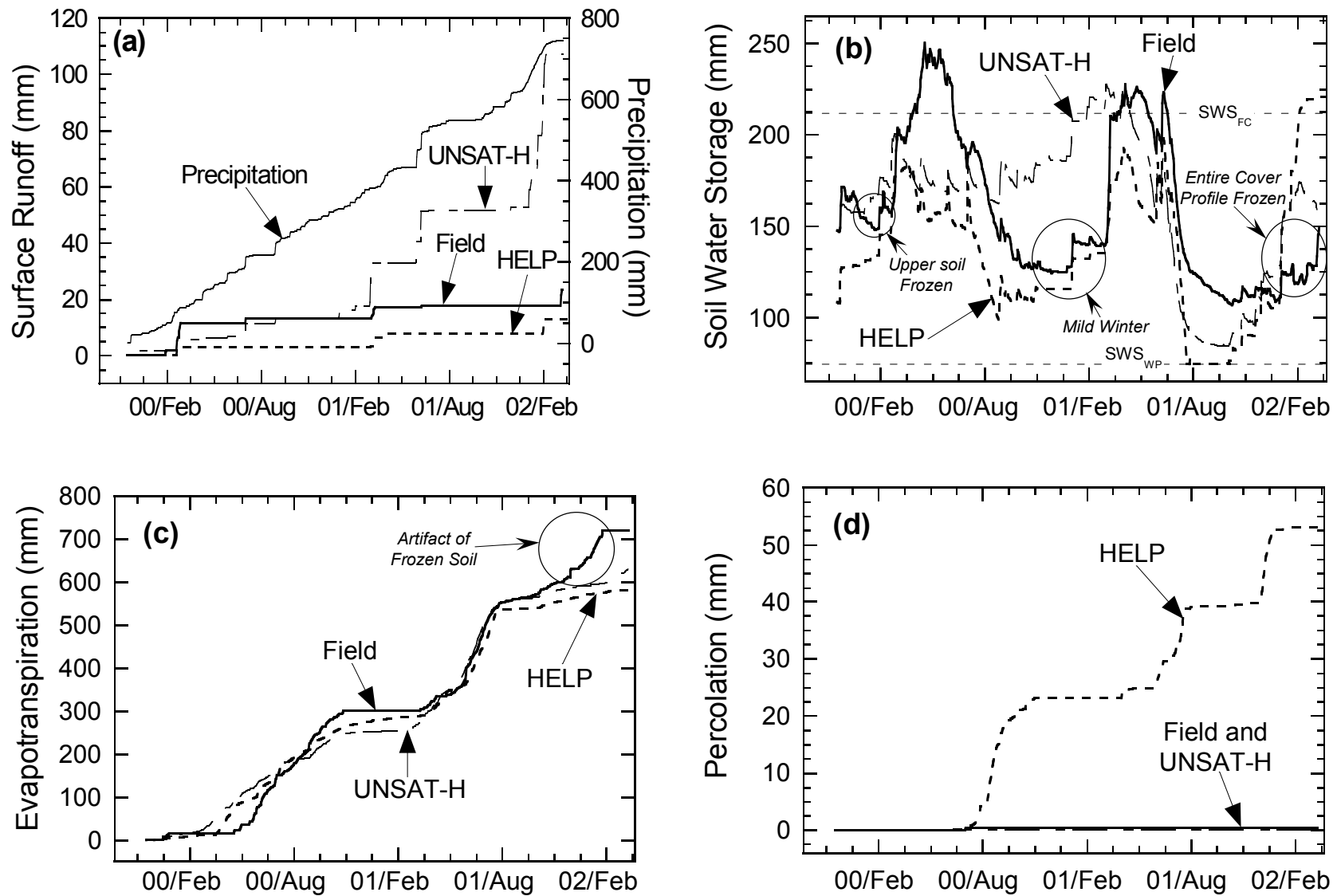


Fig. 5.11. Comparison of Water Balance Data for the Polson Site to Predictions Made with UNSAT-H and HELP: (a) Surface Runoff, (b) Soil Water Storage, (c) Evapotranspiration, and (d) Percolation.

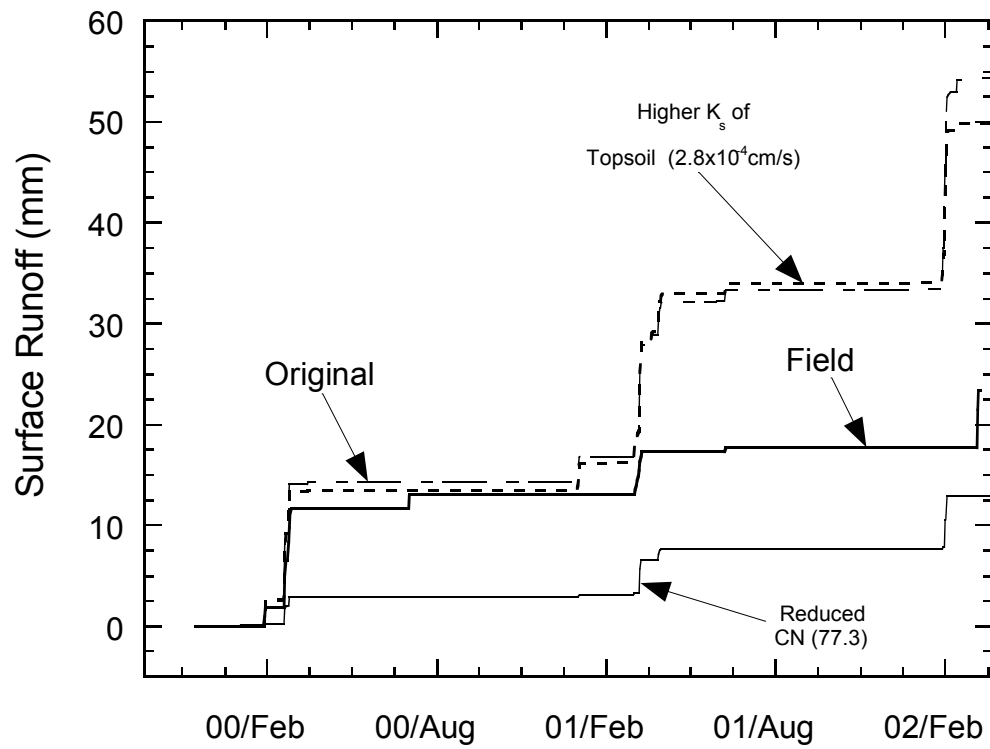


Fig. 5.12. Measured Surface Runoff and Predictions by HELP for the Alternative Cover at Polson Using Original and Adjusted Parameters for the Surface Layer.

During Winter 2002, HELP and UNSAT-H predicted soil water storage to increase significantly earlier than occurred in the field. This is likely due to frozen ground conditions that occurred in the field. Soil temperatures below 0°C were measured in the entire cover profile between December 22, 2001 and March 14, 2002, and any precipitation that infiltrated the cover probably was not detected by the WCR probes. This is also realized in the evapotranspiration data, which was calculated to increase during Winter 2002, whereas little or no evapotranspiration was anticipated.

HELP predicted percolation in Summer 2000 and 2001, as a result of snowmelt during the spring, because the influence of the capillary break between the finer and coarser layers is not simulated. HELP continued to drain water downwards until it finally became percolation. The percolation predicted in Winter 2002 is likely due to the large increase in soil water storage that was predicted, which should have been either stored as snowpack or as added to soil water storage.

UNSAT-H over-predicted surface runoff by 83.7 mm, despite using an increased saturated hydraulic conductivity for the surface layer. The low saturated hydraulic conductivity of the underlying layer controls the infiltration rate for the cover, and causes the surface layer to saturate quickly during intense rain events and large snowmelt events. Once the surface layer approaches saturation, additional precipitation is shed as runoff. More than half of the predicted surface runoff (54 mm) occurred after January 2002, caused by 71 mm of snowmelt and 53 mm of rainfall.

Soil water storage predicted by UNSAT-H did not follow the measured trend until Summer 2001. UNSAT-H under-predicted soil water storage by 50 mm in Winter 2000, and over-predicted soil water storage by 63 mm in Summer 2000. Soil water storage predicted by UNSAT-H peaked prior to that measured in the field during each winter, as

was found for HELP. During Summer 2000, UNSAT-H did not predict the minimum soil water storage that occurred in the field. The maximum LAI assigned for 2000 was probably too low (0.82). The following summer, a maximum LAI of 2.5 was assigned, and UNSAT-H predicted the drop in soil water storage more accurately. However, UNSAT-H did under-predict the minimum soil water storage reached in Summer 2001 by 31 mm.

UNSAT-H did not predict any percolation during the monitoring because the capillary barrier effect is simulated by the model. As a result, the soil water storage can exceed the storage capacity based on field capacity, without appreciable drainage into the underlying coarser layer.

#### **5.5.1.5 Boardman Site**

The measured water balance and predictions made with HELP and UNSAT-H are shown in Figs. 5.13 and 5.14 for the Boardman site. The saturated hydraulic conductivity assigned to the surface layer and the surface runoff curve number did not have to be adjusted for either HELP or UNSAT-H, because both models predicted less than 1 mm of surface runoff and percolation during the monitoring period for both alternative covers. No surface runoff or percolation was measured from either cover. Therefore, graphs of surface runoff and percolation are not presented in this section.

HELP and UNSAT-H under-predicted soil water storage in Winter and Spring 2001, and over-predicted soil water storage in Summer and Fall 2001. The trend in soil water storage predicted by both models during Winter 2002 appears to match that observed in the field, but the magnitude is biased by the over-prediction of soil water storage during the previous year.

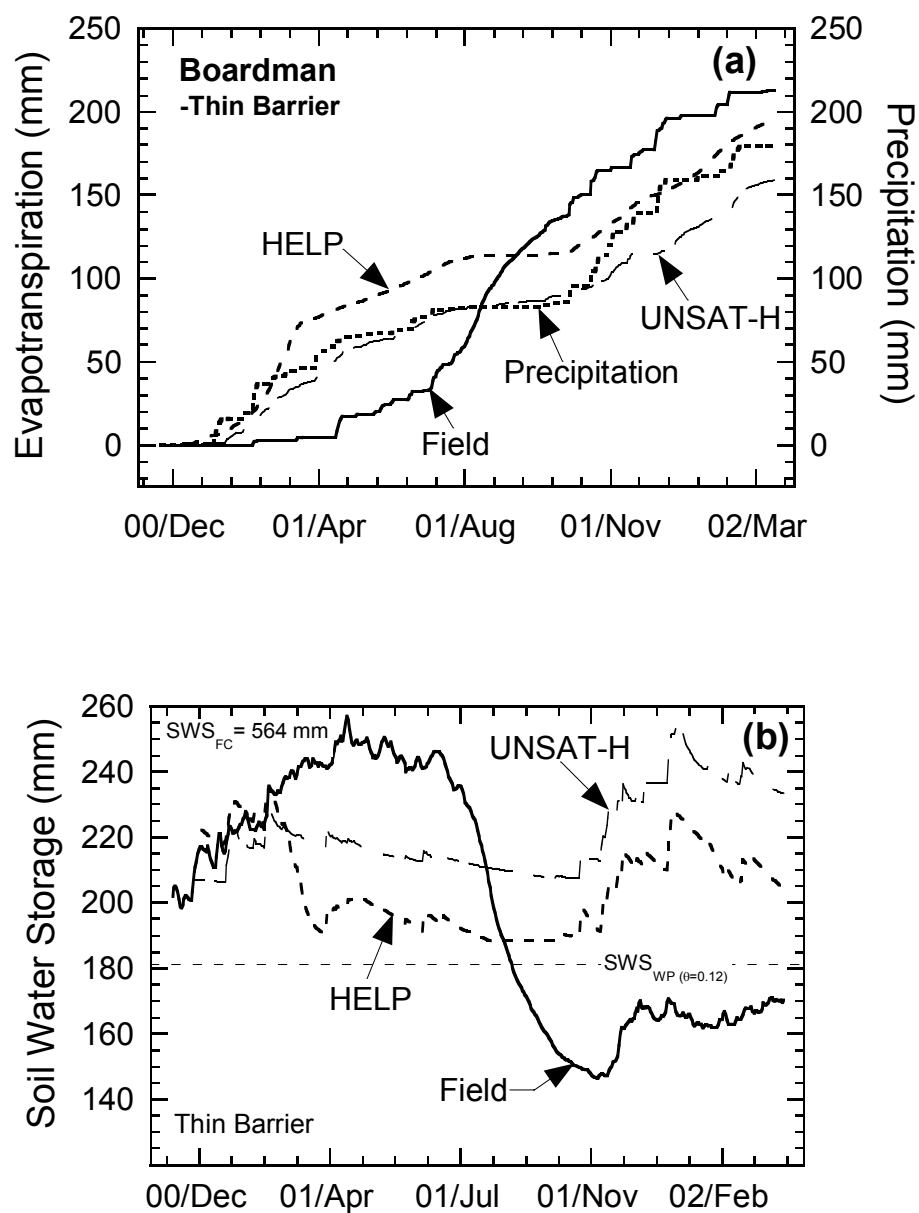


Fig. 5.13. Field Data and Predictions from HELP and UNSAT-H for the Thin Monolithic Barrier at the Boardman Site: (a) Evapotranspiration and (b) Soil Water Storage.



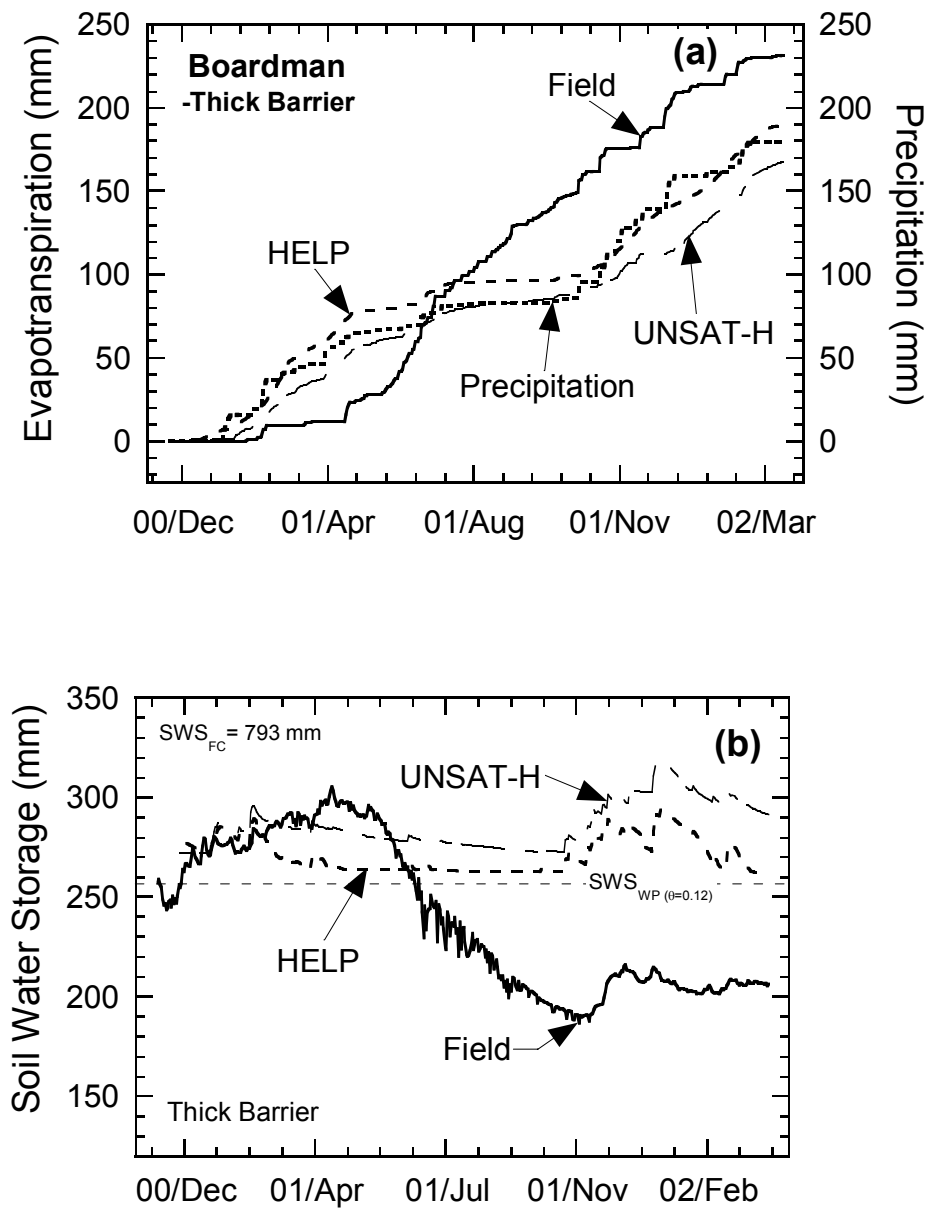


Fig. 5.14. Field Data and Predictions from HELP and UNSAT-H for the Thick Monolithic Barrier at the Boardman Site: (a) Evapotranspiration and (b) Soil Water Storage.

During Spring 2001, both models over-predicted evapotranspiration, which was followed by an under-prediction in Summer 2001. These errors in evapotranspiration mimic the errors in soil water storage, and suggest that properties of the vegetation may not have been chosen properly. To evaluate if the wilting point used in HELP (based on a suction of 1500 kPa) was responsible for the under-prediction of evapotranspiration in Summer 2001 (Fig. 5.15), additional simulations were conducted, where the wilting point for HELP was assigned the lowest water content ( $\theta = 0.06$ ) measured in the thick barrier during the monitoring period (excluding the WCR probe closest to the surface). Additional simulations of this type were not conducted for UNSAT-H, because the wilting point assigned to UNSAT-H was based on a suction of 6000 kPa ( $\theta = 0.07$ ).

For the simulation with a lower wilting point, HELP under-predicted soil water storage by rapidly removing soil water until the wilting point was reached during Summer 2001. Therefore, an addition simulation was conducted, with a lower wilting point and a reduced LAI (from 1.5 to 0.5). For this simulation, HELP accurately predicts the soil water storage reduction during Summer 2001.

#### **5.5.1.6 Marina Site**

The measured water balance and predictions made with HELP and UNSAT-H are shown in Fig. 5.16-5.18. The saturated hydraulic conductivity assigned to the surface layer (150 mm) for HELP and UNSAT-H was  $2.8 \times 10^{-4}$  cm/s. When the study was initiated, van Genuchten parameters were available for only a limited number of tests (storage layer:  $\alpha = 0.00035 \text{ cm}^{-1}$ ,  $n = 1.4$ ; interim cover:  $\alpha = 0.053 \text{ cm}^{-1}$ ,  $n = 2.85$ ). Further laboratory testing yielded different van Genuchten parameters (storage

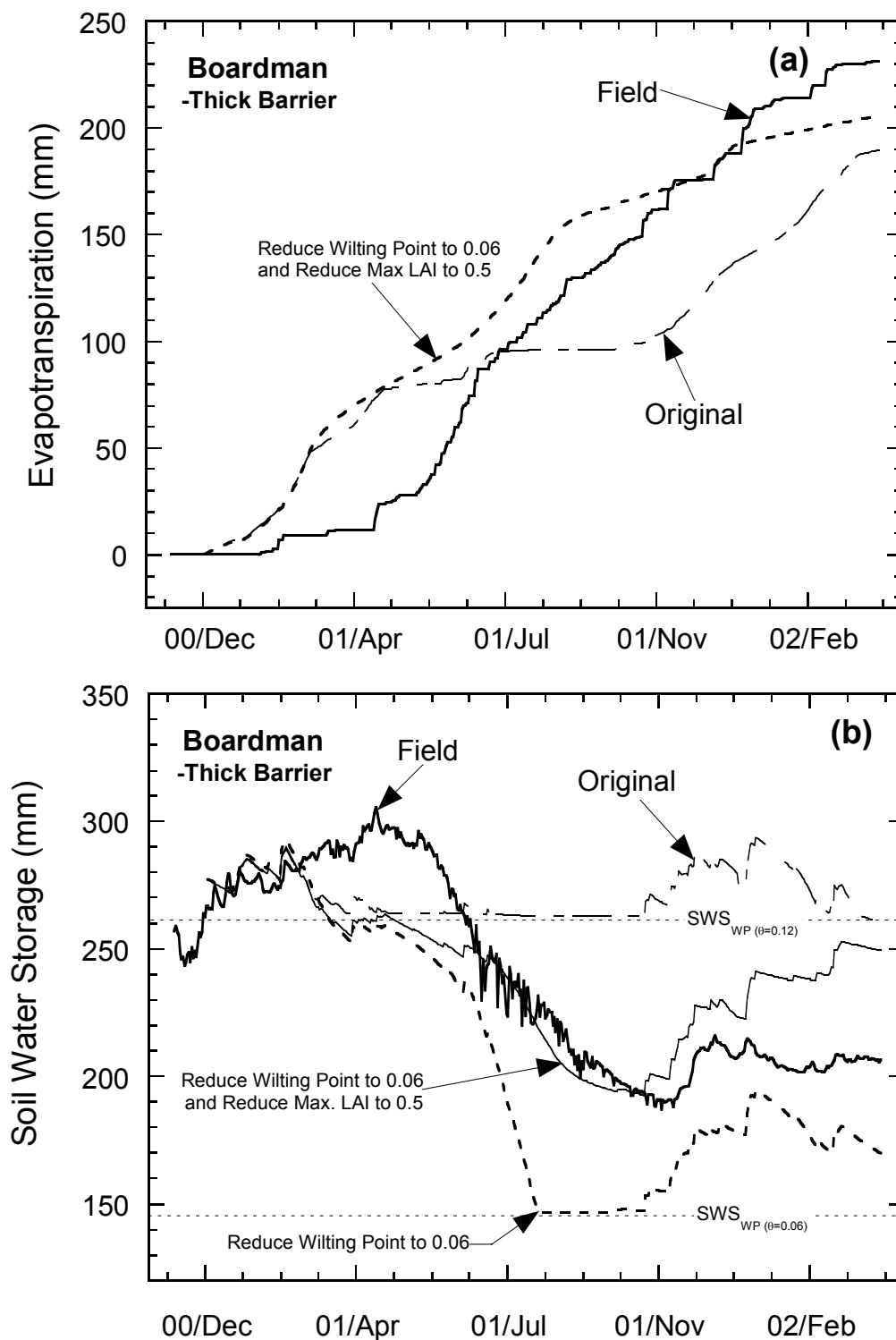


Fig. 5.15. Field Data and Predictions by HELP for the Thick Monolithic Barrier at the Boardman Site Using Adjusted Wilting Point and LAI Parameters: (a) Evapotranspiration and (b) Soil Water Storage.

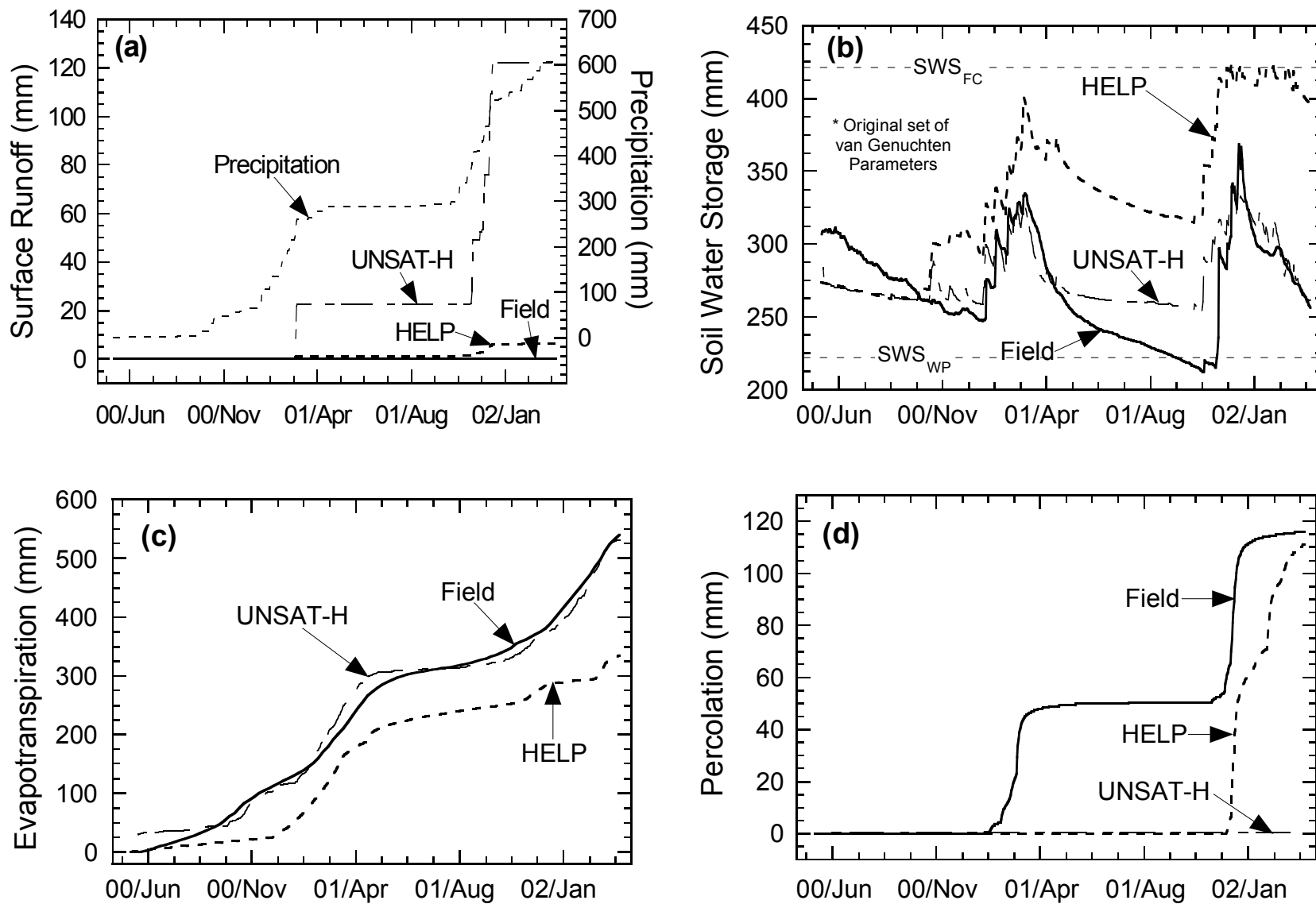


Fig. 5.16. Comparison of Water Balance Data for the Marina Site to Predictions Made with UNSAT-H and HELP Using First Parameter Set: (a) Surface Runoff, (b) Soil Water Storage, (c) Evapotranspiration, and (d) Percolation.

layer:  $\alpha = 0.00235 \text{ cm}^{-1}$ ,  $n = 1.4$ ; interim cover:  $\alpha = 0.0492 \text{ cm}^{-1}$ ,  $n = 3.46$ ). The second parameter set reduced the soil water storage capacity of the cover ( $\theta_{FC}$  reduced from 0.33 to 0.29), and the wilting point ( $\theta_{WP}$  reduced from 0.17 to 0.08). Simulations were conducted using both parameter sets to assess how uncertainty in the hydraulic properties could affect the predictions.

Surface runoff was not measured in the field due to the surface layer being tilled. The absence of surface runoff was not expected, because of the 25% slope. HELP slightly over-predicted surface runoff, despite an increased saturated hydraulic conductivity of the surface layer, and a low runoff curve number (83.1). HELP predicted surface runoff during rainfall events greater than 15 mm, and on days following these large rainfall events.

The field data show that soil water storage increases in the winter, and decreases in the spring and summer. A similar trend is evident in soil water storage predicted by HELP. However, HELP over-predicted soil water storage in Winter 2001 (by 70 mm) and in Winter 2002 (by 30 mm). The over-prediction of soil water storage during the winter (rainy season) is due to the under-prediction of evapotranspiration during the previous summer. The rapid drop in soil water storage measured in the field is also due to percolation transmitting through the cover. In Summer 2001, HELP under-predicted percolation by 50 mm.

HELP closely matched the total amount of percolation that was transmitted through the cover during the entire monitoring period, but significantly under-predicted percolation in Winter 2001, and over-predicted percolation in Winter 2002 (i.e., the errors compensated). The field data show that the soil water storage capacity had never

been exceeded. Therefore, percolation was likely transmitted through preferential flow paths, which HELP cannot simulate.

Use of the second set of van Genuchten parameters resulted in small changes in the predictions of evapotranspiration, surface runoff, and soil water storage. Therefore, these graphs are not shown. However, percolation predicted by HELP increased substantially when the second parameter set (see Figs. 5.17) was used as input.

To better understand the reason for the reduction in soil water storage during Summer 2001, an additional HELP simulation was conducted using a higher maximum LAI of 2.5 for 2001 (Fig. 5.17). The second set of van Genuchten parameters was used as input for this simulation. HELP over-predicted soil water storage by 103 mm using an LAI of 1.5 during Summer 2001, but only over-predicted soil water storage by 24 mm using an LAI of 2.5 (Fig. 5.17). When the rainy season began in Fall 2001 and Winter 2002, the HELP simulation with LAI = 2.5 provided more available soil water storage because of a large reduction in soil water storage predicted during the previous summer. As a result, HELP more closely predicted percolation during Winter 2002. Percolation was slightly over-predicted by only 8 mm.

UNSAT-H (using the first set of van Genuchten and LAI parameters) did not accurately predict surface runoff, when the saturated hydraulic conductivity of the surface layer was increased (Fig. 5.18). UNSAT-H over-predicted surface runoff by 122 mm, corresponding to events in the beginning of March 2001 (22 mm) and December 2001 (100 mm). Infiltration into the cover during these periods is controlled by the low

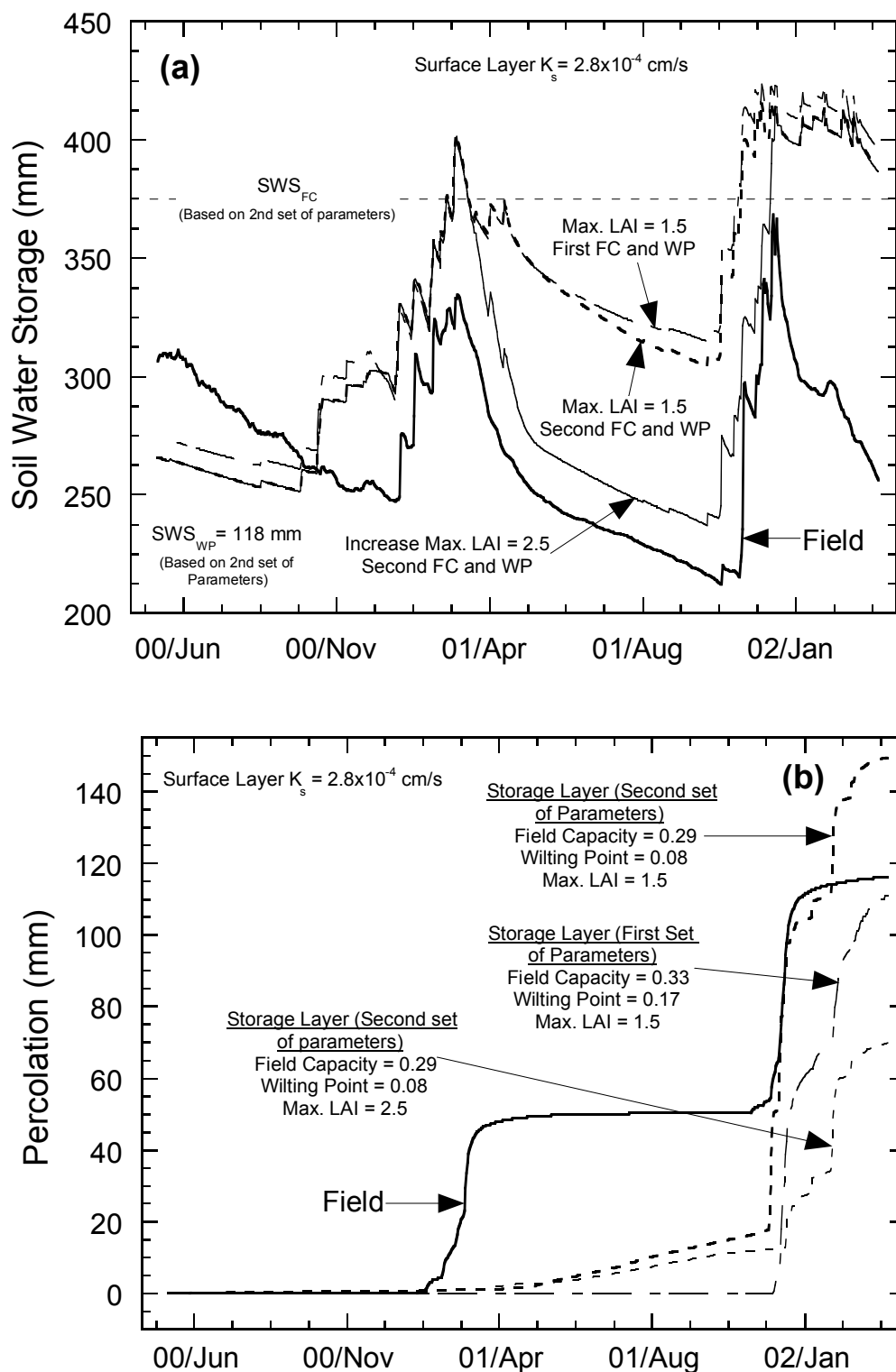


Fig. 5.17. Comparison of Water Balance Data for the Alternative Cover at the Marina Site to Predictions Made with HELP Using Adjusted van Genuchten and LAI Parameters: (a) Soil Water Storage and (b) Percolation.

saturated hydraulic conductivity of the storage layer below the surface layer. During large rain events, the surface layer becomes saturated, and precipitation is shed as surface runoff because water cannot penetrate quickly into the storage layer.

UNSAT-H was able to predict the trend in soil water storage more closely than HELP (Fig. 5.18). However, UNSAT-H predicted the soil water storage would immediately drop at the start of the monitoring period (May 2000). This is likely due to an inappropriate LAI. A maximum LAI of 0.8 was assigned for the first growing season (harvest date in June), even though the test section was not seeded to the test section until November 2000. During Summer 2001, UNSAT-H over-predicted soil water storage, as was found for HELP.

UNSAT-H grossly under-predicted percolation by 115 mm. This may be due to the over-predictions of surface runoff during times when percolation was transmitted through the cover.

An additional UNSAT-H simulation was conducted using adjusted parameters, as was done for HELP, to determine if the predictions by UNSAT-H would change. For this simulation, the second set of van Genuchten parameters was used with a maximum LAI of 2.5 for 2001 (see Fig. 5.18).

When the adjusted parameters were used, UNSAT-H predicted substantially more surface runoff than occurred in the field and was predicted using the first set of parameters (Fig. 5.18). This may have been due to a reduction in the field capacity of the storage layer, which caused the uppermost surface layer to become saturated quicker during periods of high rainfall. Precipitation was more easily shed as runoff during these periods.



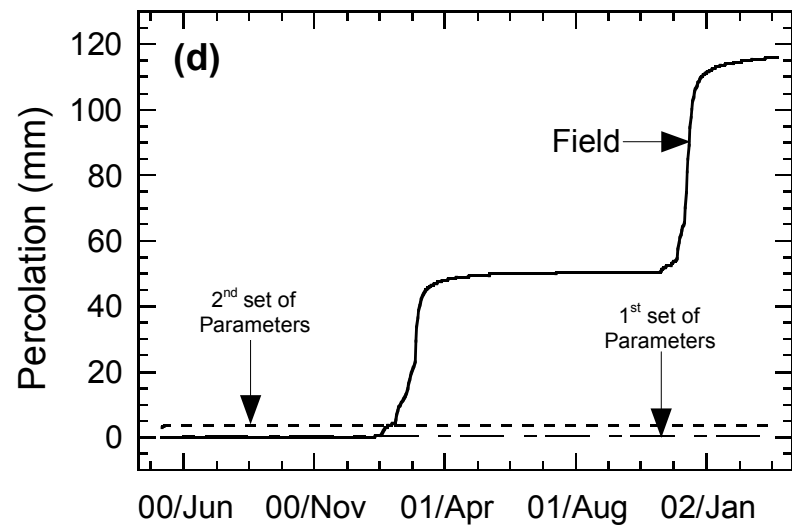
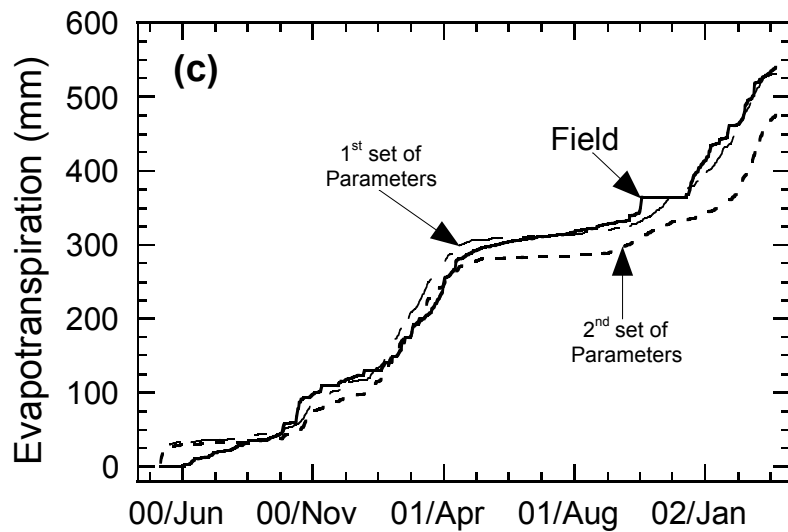
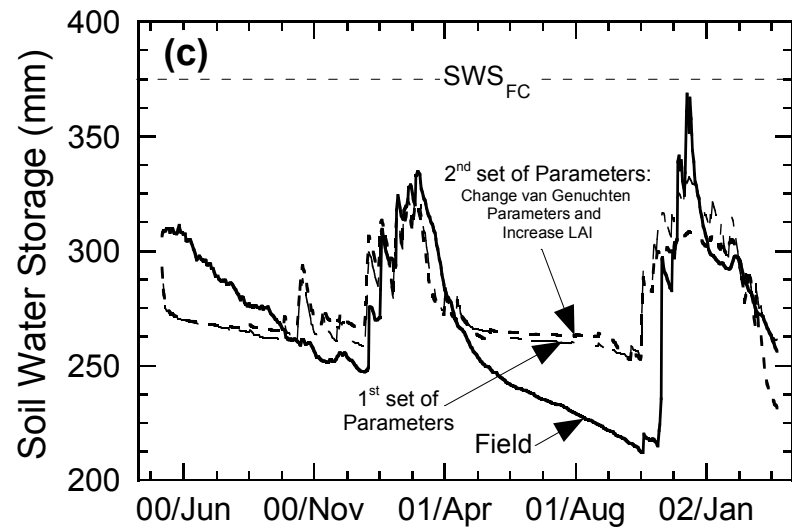
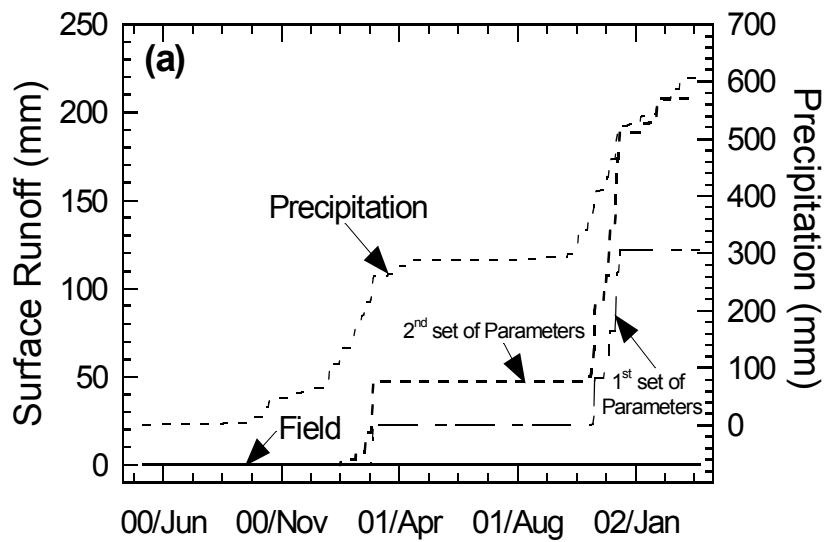


Fig. 5.18. Comparison of Water Balance Data at the Marina Site and Predictions Made with UNSAT-H Using Adjusted Parameters: (a) Surface Runoff, (b) Soil Water Storage, (c) Evapotranspiration, and (d) Percolation.

The trend in soil water storage predicted by UNSAT-H did not change significantly from the first set of parameters to the second, which is opposite of what occurred for HELP.

The only difference was approximately 3 mm of percolation being predicted at the start of the monitoring period. The percolation was caused by drainage of water from the 300-mm-thick sand layer, which had an initial water content of 0.07.

#### **5.5.1.7 Albany Site**

The measured water balance and predictions made by HELP and UNSAT-H are shown in Fig. 5.19. The saturated hydraulic conductivity assigned to the storage layer (600 mm) for HELP and UNSAT-H was set at  $2.8 \times 10^{-4}$  cm/s, and the runoff curve number for HELP was reduced to 82.3.

HELP over-predicted surface runoff by 16.4 mm, and was not able to match the occurrences of surface runoff, with the exception of two runoff events. The majority of the surface runoff (14 mm) measured in the field occurred within the first four months of the monitoring period, of which, HELP only predicted 16% of that measured in the field. After this period, surface runoff became negligible due to well-established vegetation. HELP could not accurately predict precipitation being trapped by the grass and trees even with a maximum LAI of 4.5, and a reduced runoff curve number.

Irrigation was applied to the alternative cover at Albany during times of plant stress. Surface runoff was never measured in the field during irrigation, because the irrigation was applied using a water drip line. In contrast, HELP predicted surface runoff on days that irrigation was applied.

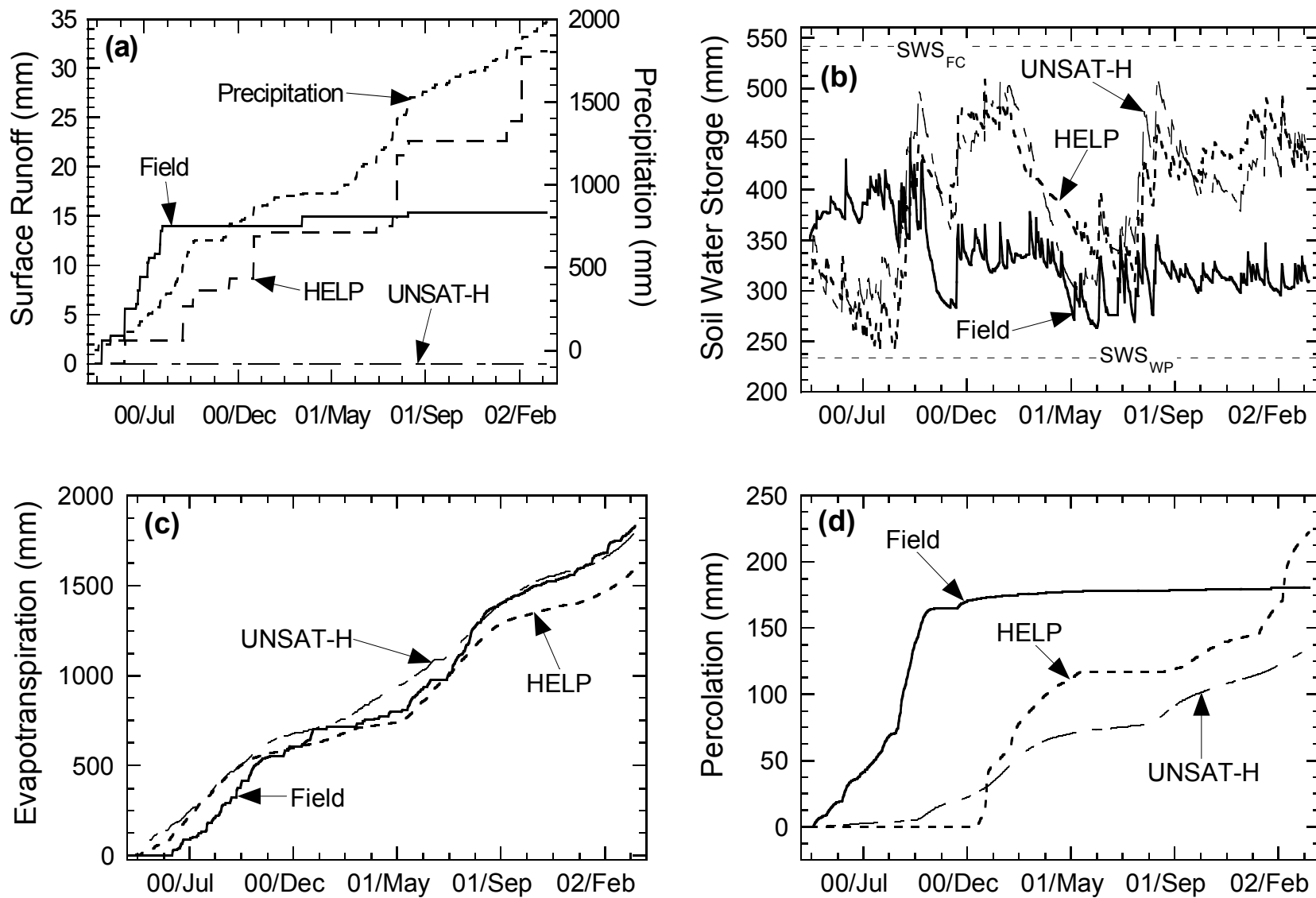


Fig. 5.19. Comparison of Water Balance Data for the Albany Site to Predictions Made with UNSAT-H and HELP: (a) Surface Runoff, (b) Soil Water Storage, (c) Evapotranspiration, and (d) Percolation.

The field data show rapid fluctuations in soil water storage over a short period, without exceeding the storage capacity of the cover. There also is a distinguishable drop in storage at the beginning of October 2000, after which the soil water storage fluctuates at a lower level. This drop in storage corresponded to a large decrease in the percolation rate, and was maintained by the maturing trees.

HELP and UNSAT-H initially under-predicted soil water storage by approximately 200 mm, which is likely due to an over-prediction of evapotranspiration. A maximum LAI of 2.5 was used for both models during the first growing season. However, the vegetation likely had not been established prior to October 2000.

HELP and UNSAT-H grossly over-predicted soil water storage during the remainder of the monitoring period, with the exception of Summer 2001. Both models predicted a large drop in soil water storage during Winter and Spring 2001, which corresponded to a prediction of a large amount of percolation. During this period, HELP predicted 116 mm of percolation, whereas UNSAT-H predicted 70 mm of percolation. In contrast, only 13 mm of percolation occurred in the field during this period.

At the end of Summer 2001, HELP and UNSAT-H predicted an increase in soil water that was significantly greater than measured. The storage increased because the models under-predicted evapotranspiration during June-August 2001. Even with a maximum LAI of 4.5, neither model could predict the large amount of soil water removal by the hybrid poplar trees.

Prior to January 1, 2001, almost 95% of the percolation had been transmitted through the alternative cover at Albany. After this time, the percolation rate significantly decreased to a rate of 6 mm/yr. In contrast, percolation predicted by the models prior to January 1, 2001 was less than 23% of the total percolation. After

January 1 2001, HELP predicted a percolation rate of 143 mm/yr, and UNSAT-H predicted a percolation rate of 82 mm/yr.

#### **5.5.1.8 Omaha Site**

The measured water balance and predictions by HELP and UNSAT-H for the two monolithic barriers at the Omaha site are shown in Fig. 5.20 and Fig. 5.21. The saturated hydraulic conductivity assigned to the surface layer (150 mm) for both covers was set at  $2.8 \times 10^{-4}$  cm/s for HELP and UNSAT-H (thick barrier only). The UNSAT-H simulations for both barriers were conducted using only the top portion of the covers (above the sand layer), because large numerical errors were encountered when the capillary break was included. Despite refinements to the spatial and temporal discretization, the error could not be eliminated. HELP simulations were conducted using the entire cover profile.

HELP over-predicted surface runoff by 46 mm for the thin barrier, and by 69 mm for the thick barrier. Even though HELP was able to predict the occurrences of surface runoff throughout the monitoring period, each event was over-predicted. The largest over-prediction for both covers occurred during May 2001, when the site received 200 mm of rainfall. In May 2001, HELP over-predicted surface runoff by 15.3% of precipitation for the thin barrier, and by 23.3% of precipitation for the thick barrier. The discrepancy is likely due to the storage layer being assigned a saturated hydraulic conductivity (which controls the infiltration rate) that was too low, or a malfunction with the surface runoff collection system (surface runoff may have been under reported).

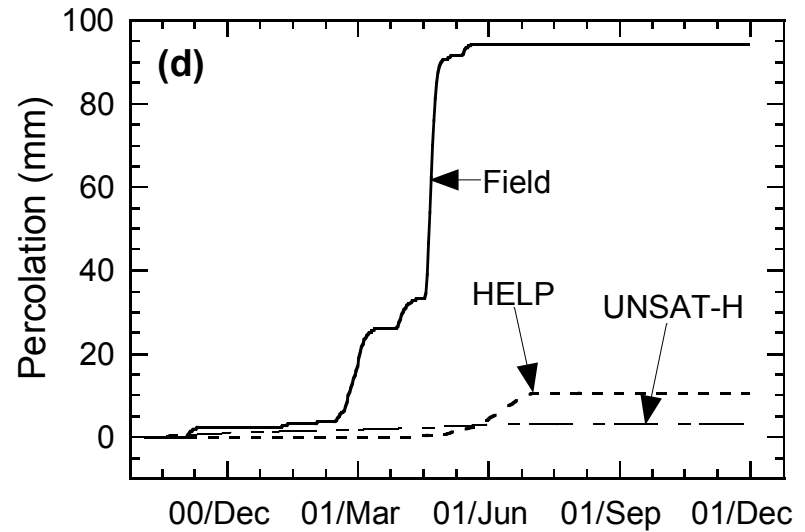
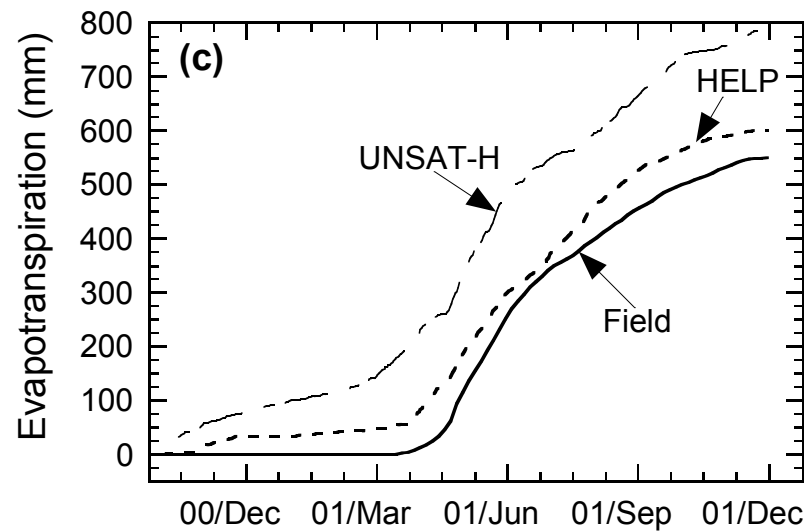
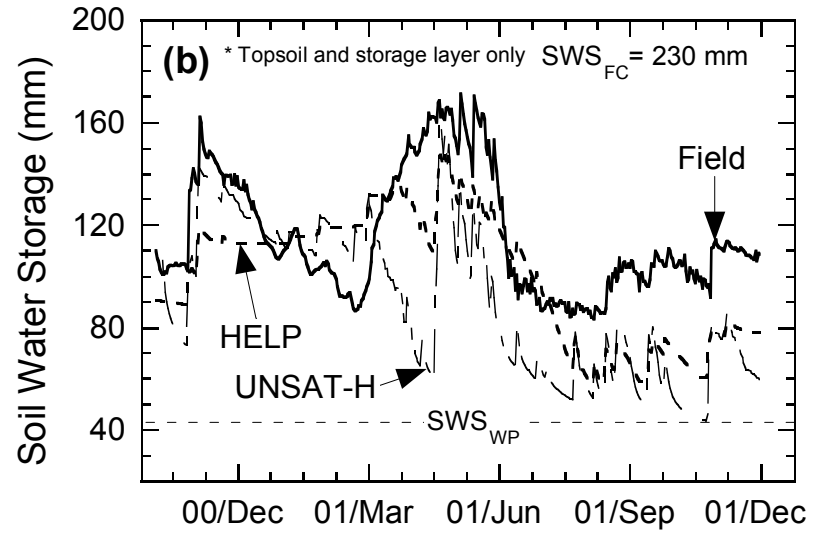
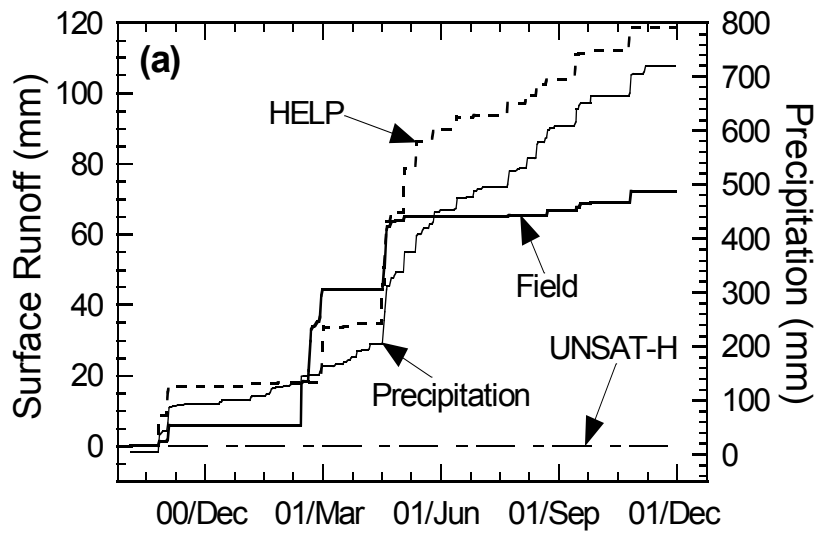


Fig. 5.20. Comparison of Water Balance Data for the Omaha Site (Thin Monolithic Barrier) to Predictions Made with UNSAT-H and HELP: (a) Surface Runoff, (b) Soil Water Storage, (c) Evapotranspiration, and (d) Percolation.

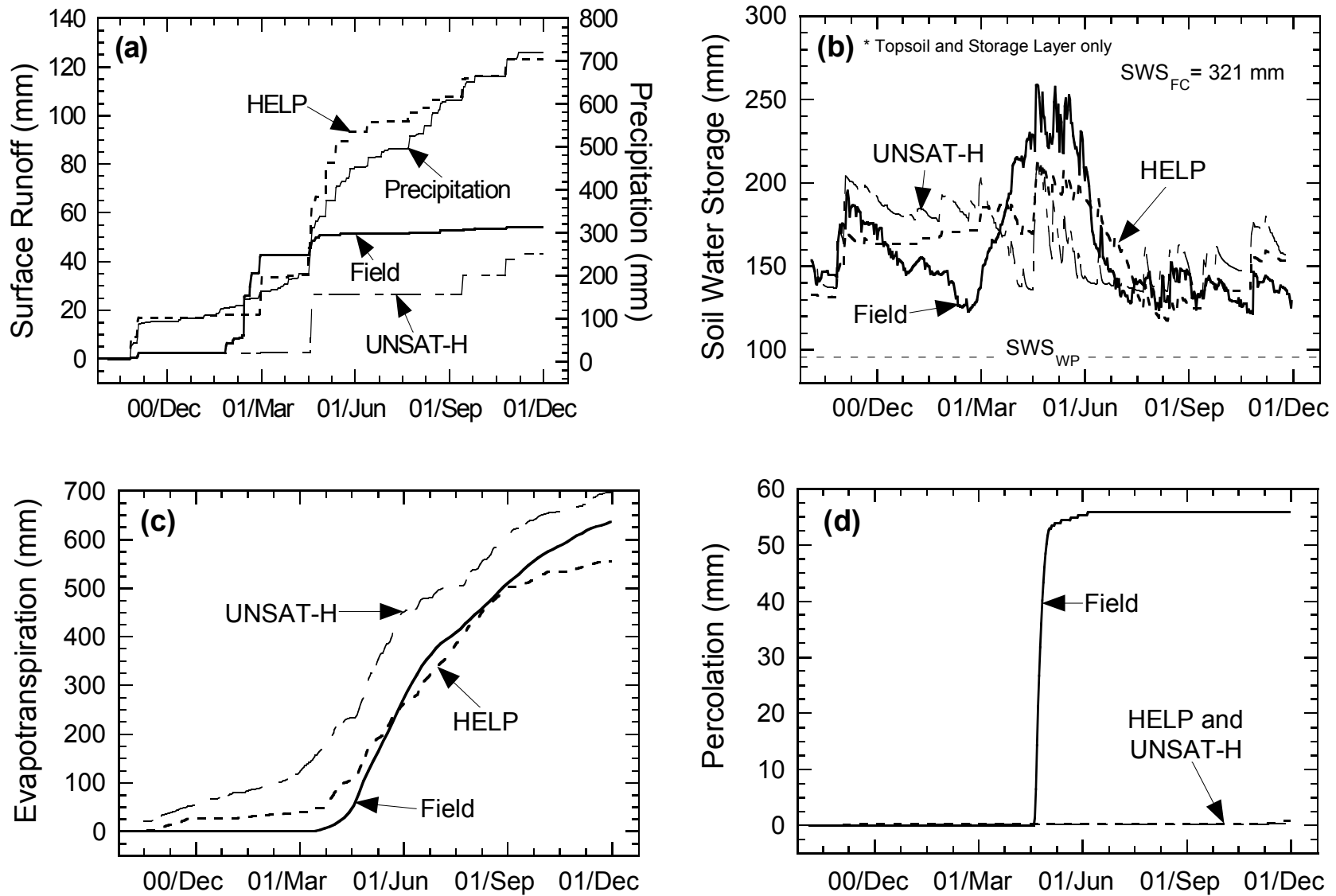


Fig. 5.21. Comparison of Water Balance Data for the Omaha Site (Thick Monolithic Barrier) to Predictions Made with UNSAT-H and HELP: (a) Surface Runoff, (b) Soil Water Storage, (c) Evapotranspiration, and (d) Percolation.

UNSAT-H over-predicted surface runoff by 72 mm for the thick barrier, and under-predicted surface runoff by 11 mm for the thin barrier. UNSAT-H did not predict surface runoff for the thin barrier during the entire monitoring period when the hydraulic properties of the topsoil were used as input. The saturated hydraulic conductivity of the topsoil and storage layers for the thin barrier is higher than that for the thick barrier. Additional simulations using higher saturated hydraulic conductivity for the surface layer were not necessary and were not conducted.

For the thick barrier, UNSAT-H was not able to predict the occurrence of surface runoff in late Winter and early Spring 2001, but over-predicted surface runoff events throughout the remainder of the monitoring period. Surface runoff measured in the field during Winter/Spring 2001 was caused by frozen ground conditions (February 5 – March 27, 2001). UNSAT-H does not account for frozen ground and, therefore, allowed the precipitation to infiltrate the cover. The over-prediction of surface runoff during the rest of the monitoring period is likely due to the saturated hydraulic conductivity assigned to the surface layer of the thick barrier being too low.

HELP was able to follow a similar soil water storage trend as measured in the field. HELP under-predicted soil water storage during most of the monitoring period, but over-predicted soil water storage during Winter and early Spring 2001 (Fig. 5.21b). The field data show the soil water storage dropped significantly during the winter. This drop in soil water storage may be artificial, because the WCR probes used to measure water content are affected by soil temperature, and by phase change (liquid to solid) in the soil water when the ground becomes frozen (See Section 4.9). When the ground temperature rises in late March to April, the measured soil water storage rises.



UNSAT-H predicted soil water storage more accurately than HELP, especially during late Fall 2000. However, both models predicted a reduction in soil water storage in Spring 2001, which was not observed in the field. Higher evapotranspiration was likely predicted due to an over-estimate of the maximum LAI.

Because evapotranspiration was over-predicted in Spring 2001, UNSAT-H predicted that both covers would have sufficient storage capacity to prevent percolation during Spring 2001. As a result, percolation from the thin barrier (Fig. 5.20D) and the thick barrier (Fig. 5.21d) was grossly under-predicted.

### **5.5.2 Conventional Covers**

The following sections provide a comparison of the water balance measured for conventional covers at six sites and predictions made with HELP using the measured hydraulic properties, and hydraulic properties that were adjusted so that the surface runoff predicted by the models were comparable to that measured in the field. All of the covers are composite covers, except for the compacted clay cover constructed at Albany. UNSAT-H simulations were not conducted for composite covers, but were conducted for the compacted clay cover at Albany. UNSAT-H simulations were not conducted for the composite covers, because UNSAT-H cannot simulate lateral flow or flow through defects in geomembranes. Soil water storage presented in this section includes only the water stored in soil layers above the geomembrane.

#### **5.5.2.1 Altamont Site**

The measured water balance and predictions made by HELP for the composite cover at the Altamont site are shown in Fig. 5.22. A datalogger error resulted in a large

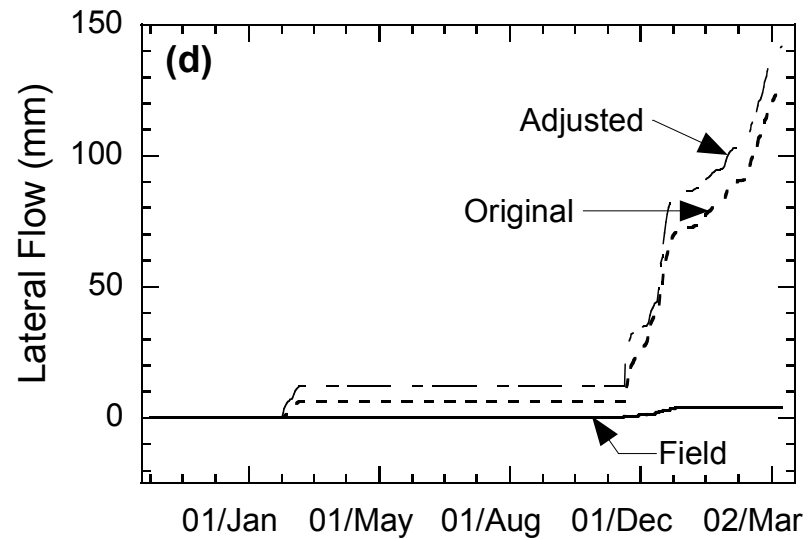
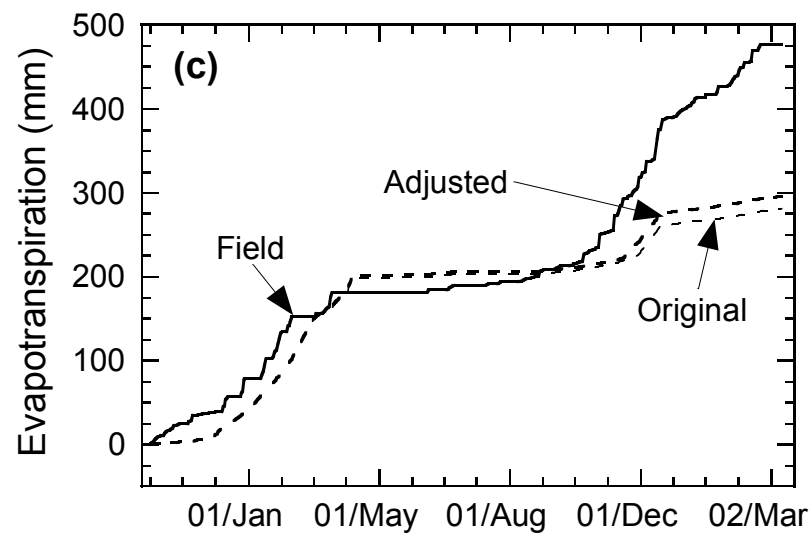
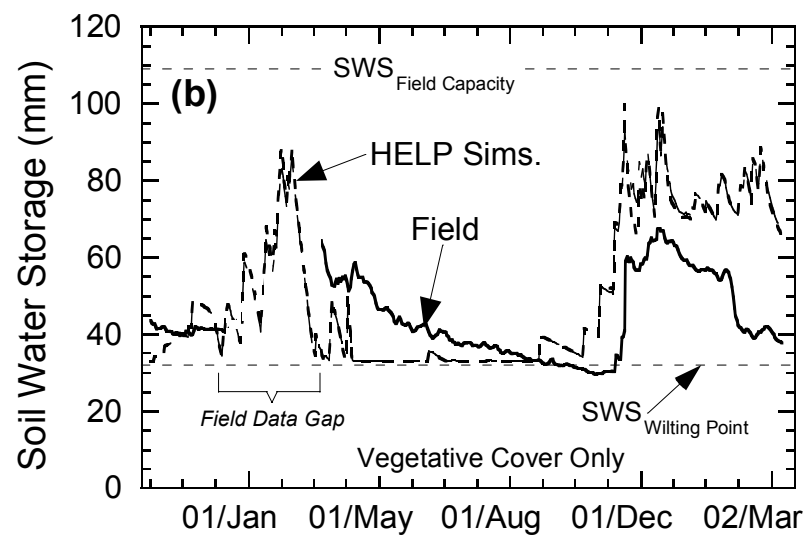
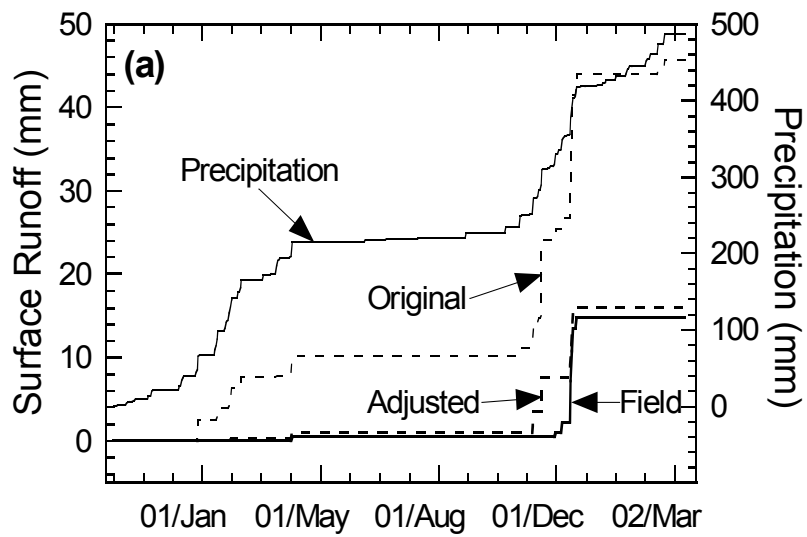


Fig. 5.22. Comparison of Water Balance Data for the Altamont Site (Composite Cover) to Predictions Made with HELP: (a) Surface Runoff, (b) Soil Water Storage, (c) Evapotranspiration, and (d) Lateral Flow.

data gap between January 10, 2001 and March 29, 2001. However, meteorological input for HELP were obtained from a nearby weather station. To predict surface runoff better, the runoff curve number assigned to the surface layer (300 mm) was reduced from 94.1 to 88.1.

When the adjusted runoff curve number was used, HELP over-predicted surface runoff by 1.2 mm. However, HELP had difficulty predicting small runoff events on the same day as occurred on the cover.

HELP predicted 141.6 mm of lateral flow during the monitoring period, despite only 3.8 mm of lateral flow being measured. HELP predicted a large amount of lateral flow, primarily because evapotranspiration was under-predicted. In the beginning of March 2001, HELP predicted 11.8 mm of lateral flow. However, because of a datalogger error, this prediction of lateral flow cannot be checked. HELP did not predict lateral flow again until December 2001, after which HELP predicted lateral flow at a rate of approximately 1 mm/day.

Measured and predicted soil water storage of the vegetative layer (above cover geomembrane) are shown in Fig. 5.22b. The field data show that soil water storage increases in the fall and winter, and decreases during the spring. Soil water storage reaches the wilting point by the end of the summer. A similar trend is evident in soil water storage predicted by HELP. However, HELP over-predicted the peak soil water storage by 24 mm during Winter 2001, and by 31 mm during Winter 2002.

During Spring 2001, HELP predicted that soil water storage would reach the wilting point earlier than measured. This is may be due to the maximum LAI used in HELP being too high. During early Fall 2001, HELP predicted an increase in soil water storage more than two months prior to the measure soil water storage, and significantly

over-predicted soil water storage for the remainder of the monitoring period. HELP likely over-predicted soil water storage and lateral flow after December 2001, because of a gross under-prediction of evapotranspiration.

HELP did not predict any percolation during the monitoring period, which is consistent with the field data.

#### **5.5.2.2 Polson Site**

The measured water balance and predictions made by HELP for the composite cover at the Polson site are shown in Fig. 5.23. To predict surface runoff better, the runoff curve number assigned to the surface layer (150 mm) was reduced from 84.7 to 77.3.

When the curve number was reduced, HELP under-predicted surface runoff by 6.8 mm, of which 93% of the error occurred during a single runoff event at the end of February 2000. For the same runoff event, the original HELP simulation (CN= 84.7) slightly over-predicted surface runoff by 2 mm. However, HELP over-predicted surface runoff by 35.1 mm for the entire monitoring period in the original simulation. Measured surface runoff in February 2000 was 78% of precipitation, due to frozen ground conditions. HELP accurately predicted frozen ground conditions, and increased the curve number for each simulation to improve the prediction of surface runoff. However, the curve number for the adjusted HELP simulation was only increased to 95 (for initial  $CN \leq 80$ ), whereas the curve number for the original HELP simulation was increased to 98 (for initial  $CN \geq 80$ ). This suggests that the runoff curve number should be adjusted over time, rather than from the start of the monitoring period.

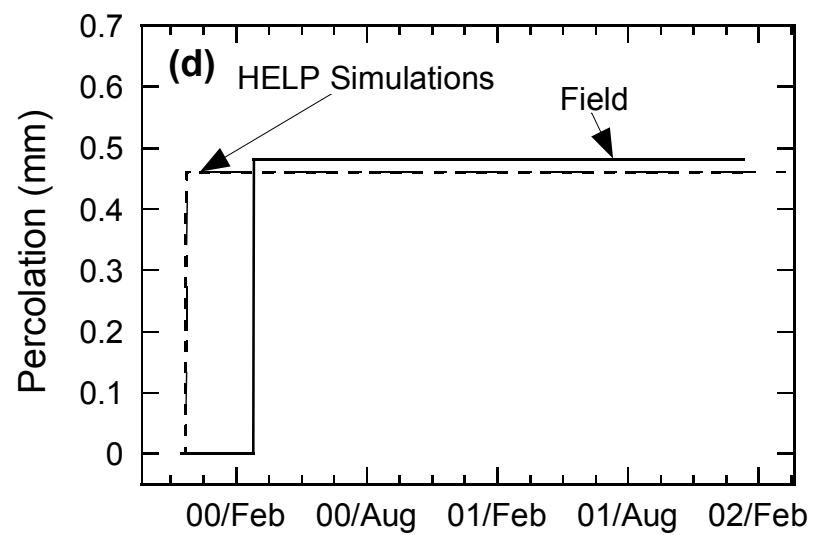
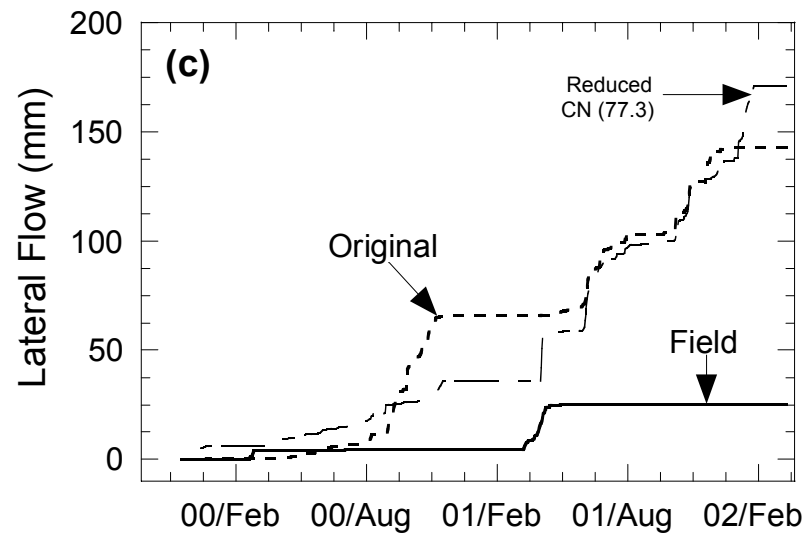
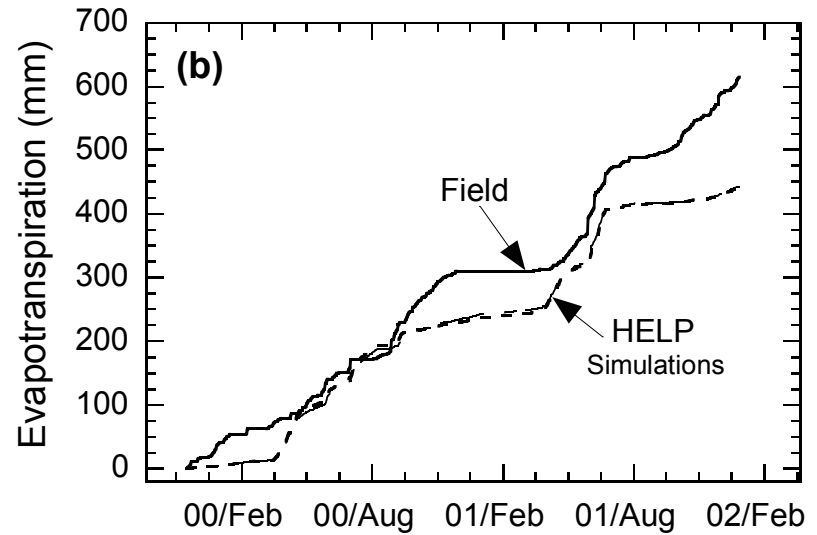
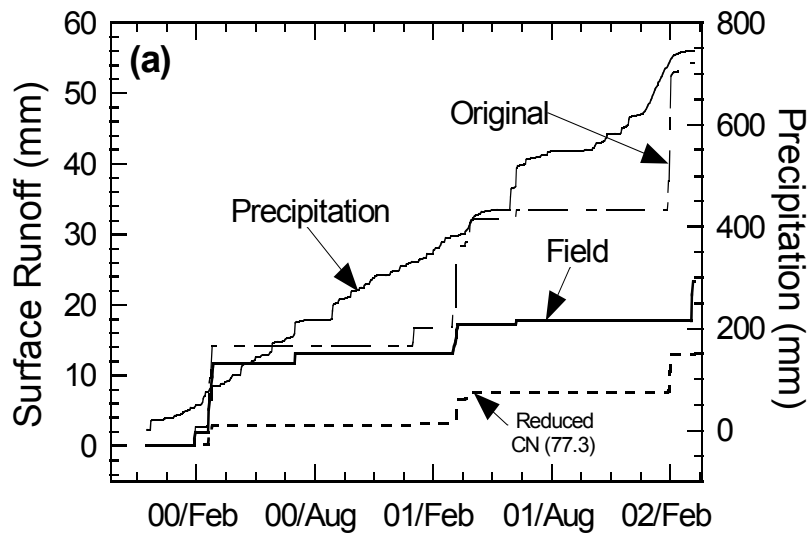


Fig. 5.23. Comparison of Water Balance Data for the Polson Site (Composite Cover) to Predictions Made with HELP: (a) Surface Runoff, (b) Evapotranspiration, (c) Lateral Flow, and (d) Percolation.

HELP grossly over-predicted lateral flow by 145.6 mm over the entire monitoring period. HELP predicted lateral flow would occur due to the spring melt, and steadily increase during the summer. HELP predicted that lateral flow would cease at the on-set of winter, and frozen ground conditions.

Measured and predicted soil water storage for the topsoil and vegetative layers are shown in Fig. 5.24. The field data show that soil water storage begins to increase in the fall, and reaches a peak during the spring, as a result of the spring thaw. The soil water storage decreases during the summer, and approaches the wilting point. A similar trend is evident in soil water storage predicted by HELP. However, HELP typically under-predicts soil water storage.

HELP initially under-predicts soil water storage by 30 mm, because HELP artificially removed water from the topsoil and vegetative layers via evaporation prior to the date that data collection began. HELP must begin the simulation on January 1 of each year, and therefore requires the user to input data between January 1 and the date that data collection began. For this study, a value of zero was entered for precipitation, solar radiation, and temperature.

During Spring 2000, HELP slightly over-predicts the peak soil water storage measured by 5 mm, but predicts the peak to occur one month earlier than actually occurred. HELP also predicted a rapid reduction of soil water storage beginning approximately one month too early in Spring 2000, and in Spring 2001. This may be due to the germination date (May 1) that was assigned being too early or due to the unit gradient assumption of vertical flow used in HELP.

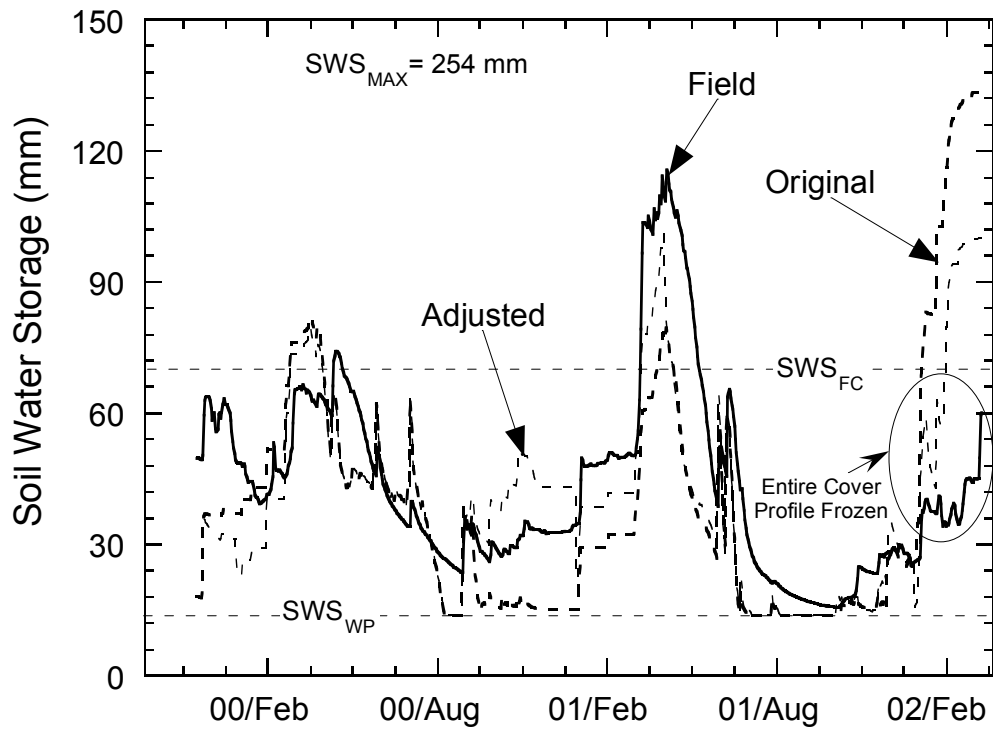


Fig. 5.24. Comparison of Soil Water Storage Measured at Polson Site (Composite Cover) and Predictions Made with HELP.

In Fall 2001, the measured and predicted soil water storage reach the wilting point. During Winter 2002, HELP predicted the soil water storage to increase significantly almost 1.5 months prior to that measured in the field. During this period, soil temperatures measured in the entire cover profile were below 0°C. Thus, the soil water storage computed from the WCR measurements is too low. Also, HELP may not have accurately predicted snowpack, and allowed precipitation to infiltrate the cover.

The measured and predicted soil water storage exceeded the capacity of the upper portion of the composite cover each spring, but did not result in any percolation. HELP accurately predicted the amount of percolation, and even predicted that the percolation would be a pulse, rather than a gradual increase. However, HELP predicted the pulse would occur approximately three months prior to the actual occurrence. The pulse of percolation predicted by HELP was caused by the 460-mm-thick interim cover layer draining to the wilting point ( $\theta_{WP} = 0.029$ ), from a water content of 0.030 [i.e.,  $(0.030 - 0.029) 460 \text{ mm} = 0.46 \text{ mm percolation}$ ].

### **5.5.2.3 Boardman Site**

The measured water balance and predictions by HELP for the composite cover at the Boardman site are shown in Fig. 5.25. Two simulations were conducted for the composite cover, with the only difference being the wilting point that was input. For the original simulation, a wilting point of 0.12 was used, which is based on a suction of 1500 kPa. For the adjusted simulation, a wilting point of 0.07 was used, which is based on the lowest water content measurement in the root zone of the vegetative layer (excluding the top most WCR probe) during the monitoring period.



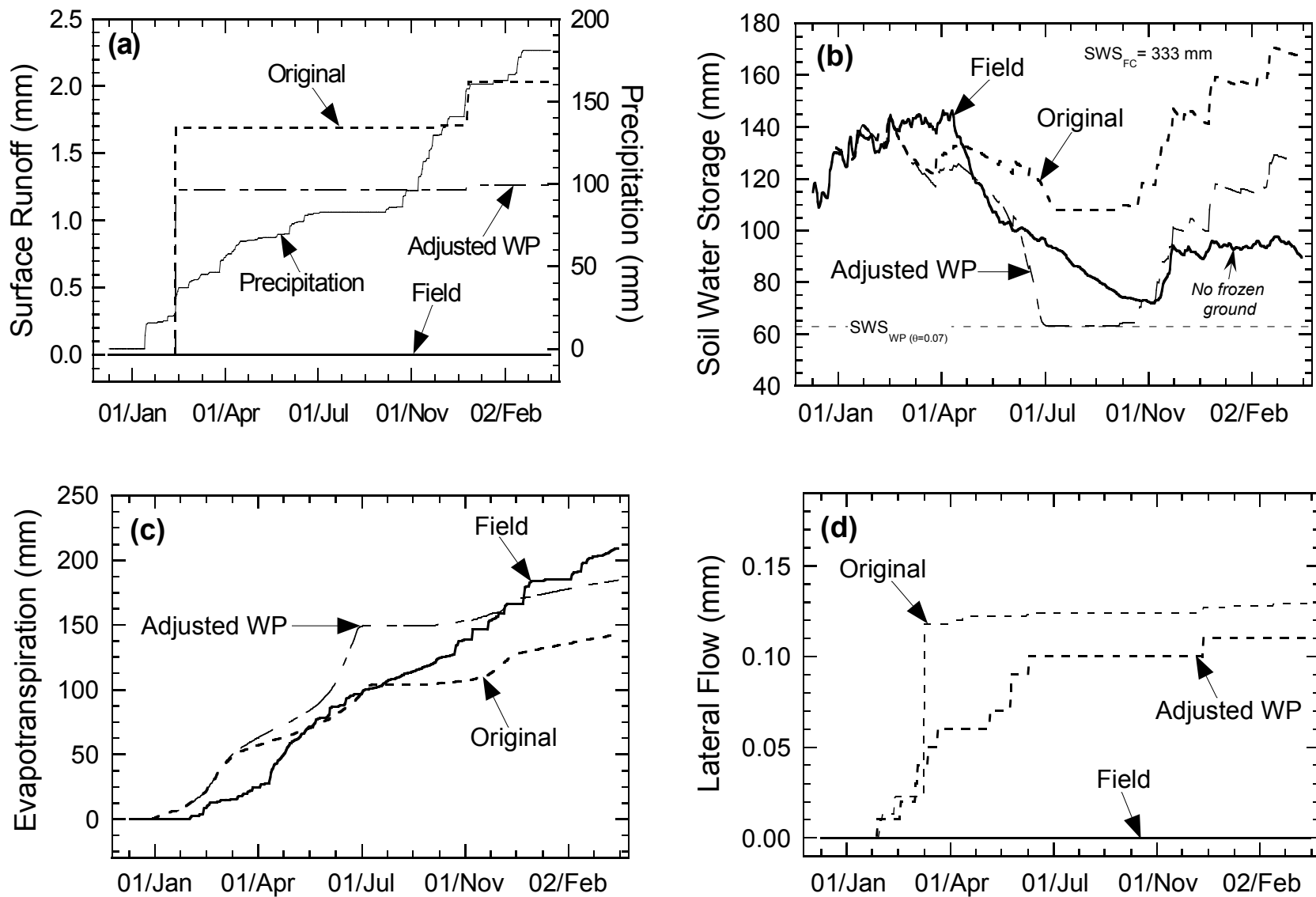


Fig. 5.25. Comparison of Water Balance Data for the Boardman Site (Composite Cover) to Predictions Made with HELP: (a) Surface Runoff, (b) Soil Water Storage, (c) Evapotranspiration, and (d) Lateral Flow.

Both HELP simulations predicted 1.3 mm of surface runoff, even though no surface runoff was measured. HELP predicted 98% of the surface runoff at the end of February 2000, which was caused by the largest rain event (10.2 mm) recorded at Boardman during the monitoring period. The second runoff event (0.03 mm) was predicted during the second largest rain event (8.6 mm). HELP most likely predicted surface runoff due to a slight over-estimate of the surface runoff curve number (94.4).

The field data show that soil water storage increases during the winter to a maximum during the spring, and then decreases at the start of the growing season to approximately the wilting point in the fall. A similar trend is evident in soil water storage predicted by HELP. However, HELP predicted the on-set of decreasing soil water storage two months early, and the minimum soil water storage three months early. HELP also over-predicted soil water storage during Winter 2002.

During Winter 2001, HELP began removing water from the vegetative layer, even though the vegetation had not yet germinated. This may have been caused by (1) incorrect predictions of snow cover (the evaporation rate increased significantly after HELP predicted rain, rather than snow, at the end of February 2001), (2) over-estimating the maximum evaporation depth (HELP computed a maximum depth of 920 mm, which is based on the saturated hydraulic conductivity of the vegetative layer), and/or (3) over-estimating the evaporation rate. Once the vegetation germinated, HELP predicted the removal of all available soil water in the 900 mm thick vegetative within three months. This may have been due to an over-estimate of the maximum LAI (0.94). LAI measurements were not made at Boardman.

During Winter 2002, HELP over-predicted soil water storage because evapotranspiration was under-predicted, which is the opposite trend as seen in the previous year. The measured soil water storage began to increase at the on-set of the winter, but did not increase to the same storage measured during the previous year.

HELP predicted 0.1 mm of lateral flow, and no percolation, which is consistent with the field data.

#### **5.5.2.4 Marina Site**

The measured water balance and prediction by HELP for the composite cover at the Marina site are shown in Fig. 5.26. To predict surface runoff better, the saturated hydraulic conductivity of the surface layer (150 mm) was set at  $2.8 \times 10^{-4}$  cm/s, and the curve number was reduced from 92.9 to 86.0.

HELP over-predicted surface runoff by 72 mm during the monitoring period. However, the greatest over-prediction occurred in December 2001, when HELP predicted surface runoff to be 42% of precipitation (measured surface runoff was 11%). During this period, HELP predicted the vegetative layer to be near saturation, which resulted in a greater percentage of the precipitation being shed as runoff.

HELP over-predicted lateral flow by 76.9 mm, but this over-prediction may be artificially inflated due to a malfunction in the lateral flow collection system (See Section 4.6.2). Measured and predicted lateral flow first occurred in January 2001 due to heavy rains, and ceased towards the end of the rainy season in March 2001. HELP predicted lateral flow to occur again in December 2001, and steadily increase at a rate of approximately 0.5 mm/day to the end of the monitoring period. During this period, the

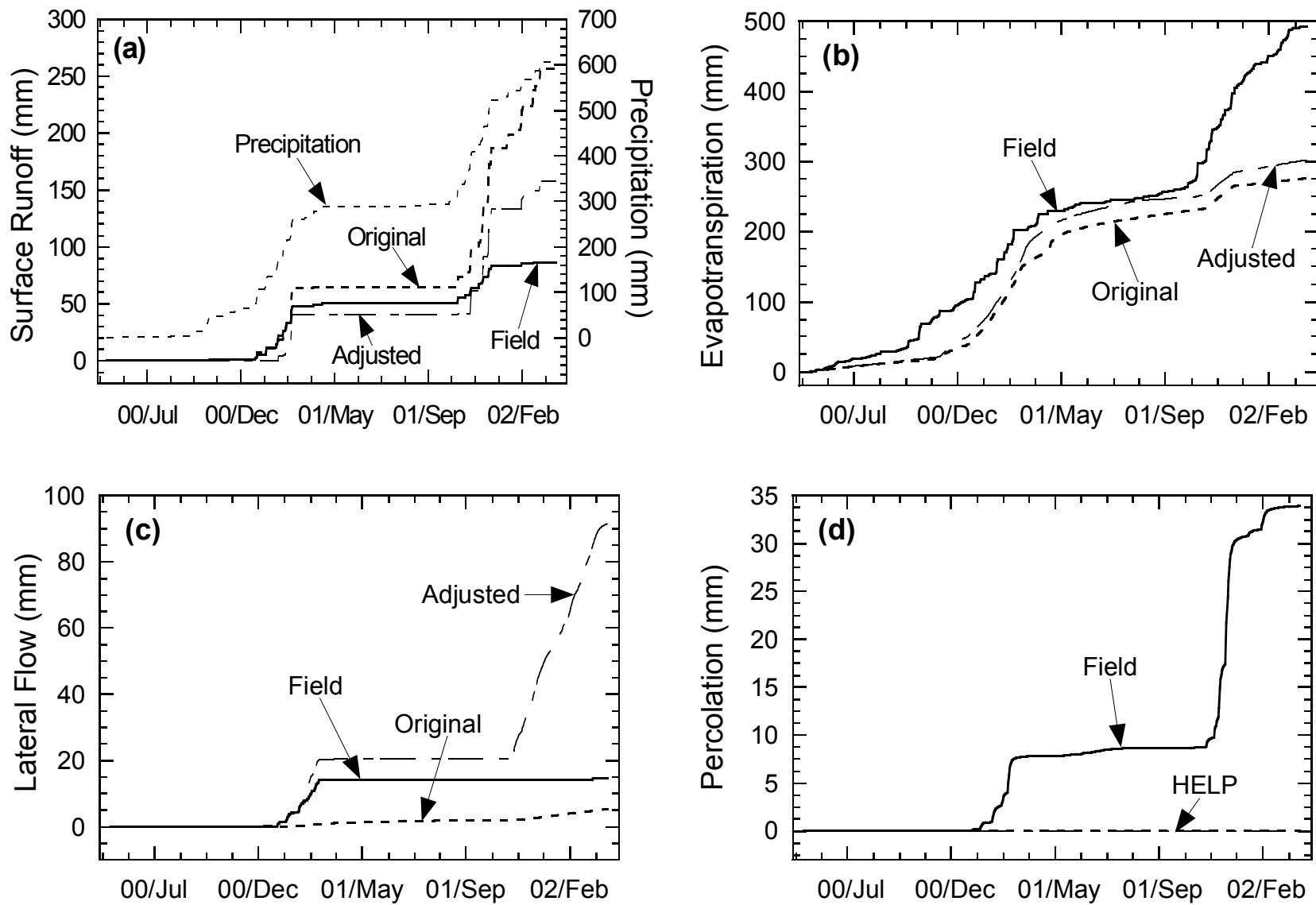


Fig. 5.26. Comparison of Water Balance Data for the Marina Site (Composite Cover) to Predictions Made with HELP: (a) Surface Runoff, (b) Evapotranspiration, (c) Lateral Flow, and (d) Percolation.

soil water storage capacity of the vegetative layer was exceeded. The saturated hydraulic conductivity of lower portion of vegetative layer is  $4.5 \times 10^{-6}$  cm/s, which corresponds to 0.4 mm/day under unit-gradient conditions.

The field data show that soil water storage increases during the fall, reaching a maximum in the winter, and decreasing to the wilting point in the summer (Fig. 5.27). A similar trend is evident in soil water storage predicted by HELP. However, HELP over-predicts soil water storage by 40 mm each winter, and predicts an increase in soil water storage slightly earlier than measured.

During each winter, HELP predicted the soil water storage to reach saturation (Fig. 5.27). During the same periods, HELP under-predicted soil water removal by evapotranspiration (Fig. 5.26b), especially in Winter 2002. The under-prediction of evapotranspiration is likely due to an under-estimate of the maximum LAI [a maximum LAI of 1.5 was used], and the absence of lateral flow in the field. The latter makes more water available for evapotranspiration.

Percolation was measured from the composite cover during each winter, of which 78% occurred during Winter 2002. HELP did not predict any percolation during the entire monitoring period, despite predicting an average head of 236 mm on the geomembrane. The initial simulation was conducted with a hole frequency of 50 holes/ha. An additional simulation was conducted with an increased hole frequency (150 holes/ha). However, even with a greater number of defects, HELP still did not yield any percolation.

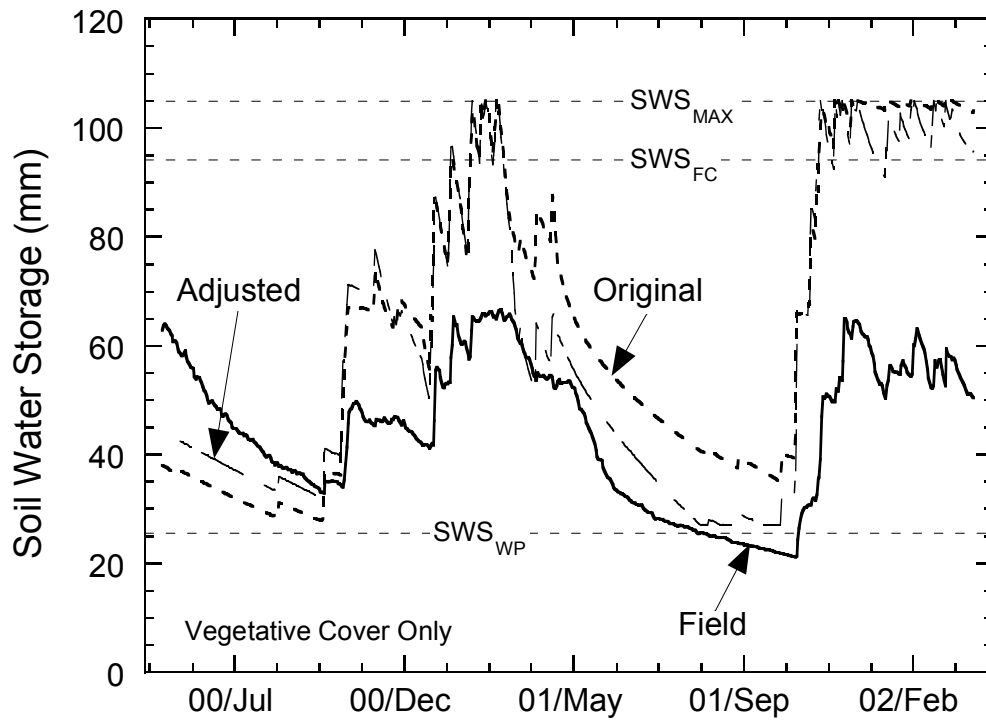


Fig. 5.27. Comparison of Soil Water Storage at the Marina Site (Composite Cover) and Predictions Made with HELP.

#### 5.5.2.5 Albany Site

The measured water balance and predictions made with HELP and UNSAT-H for the compacted clay cover at the Albany site are shown in Figs. 5.28 and 5.29. To predict surface runoff better, the saturated hydraulic conductivity of the topsoil layer (150 mm) was set at  $2.8 \times 10^{-4}$  cm/s, and the runoff curve number was reduced from 90.9 to 82.3.

Both models grossly over-predicted surface runoff, despite an attempt to increase infiltration (see Section 5.5). HELP over-predicted surface runoff by 470.5 mm, and UNSAT-H over-predicted surface runoff by 188.2 mm. HELP and UNSAT-H were able to predict the occurrences of surface runoff well, but over-predicted the amount of surface runoff.

The field data show that the soil water storage rapidly fluctuates during the entire monitoring period, which is caused by intense rain events that are typical at Albany, and high evaporation rates. HELP and UNSAT-H predicted a similar trend as measured in the field (Fig. 5.29), but under-predicted the peak soil water storage during the summer. HELP typically over-predicted the soil water storage of the topsoil layer by 15 mm, and frequently predicted that the topsoil layer was saturated. UNSAT-H typically under-predicted the soil water storage of the entire cover profile by 20 mm. For the topsoil layer, HELP predicted the soil water storage would approach the wilting point shortly after each rain event.

The over-predictions of soil water storage are due to the inability of the models to account for preferential flow, which is also evident in under-predictions of percolation (approximately 543 mm) by HELP and UNSAT-H. Preferential flow paths in the

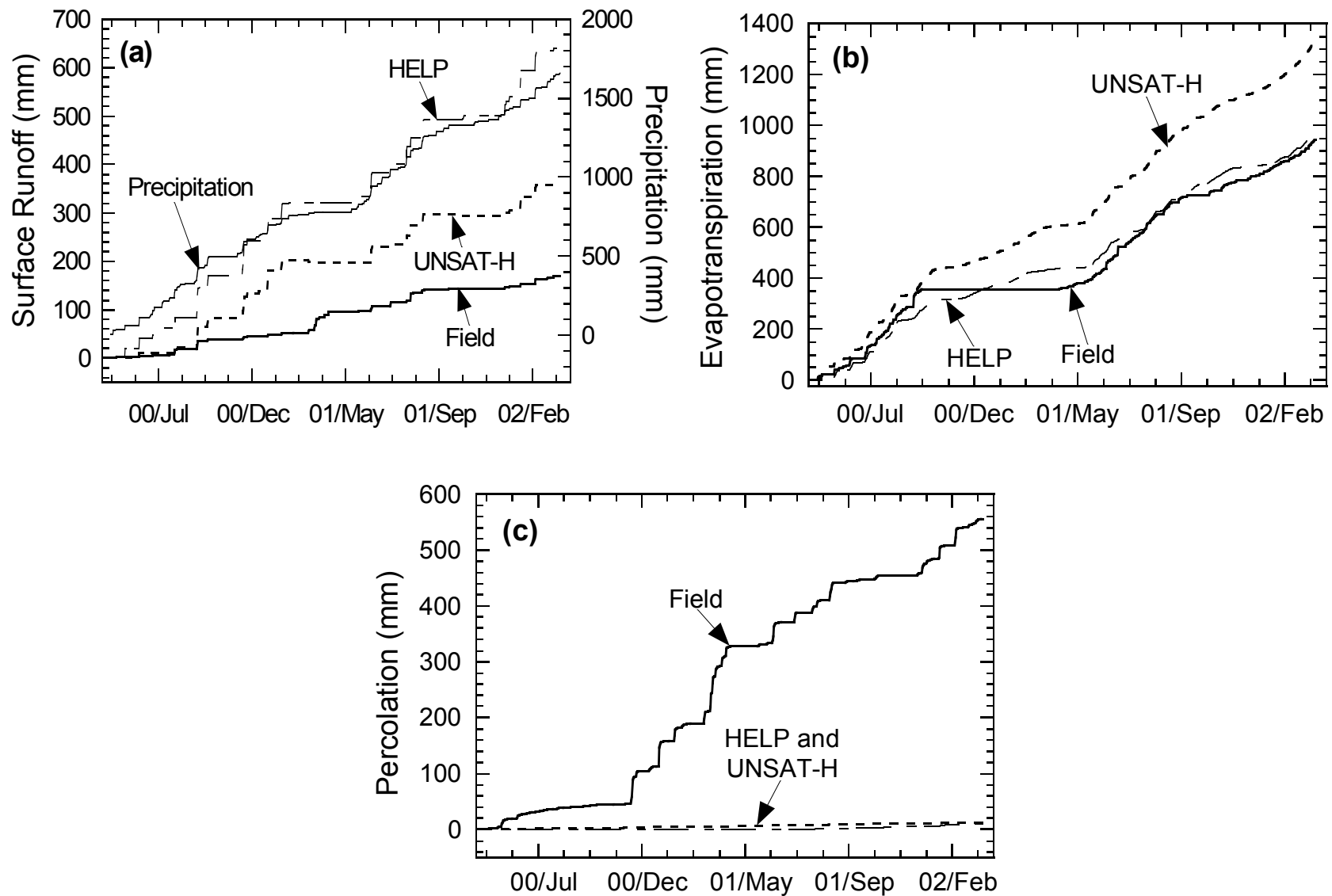


Fig. 5.28. Comparison of Water Balance for the Albany Site (Compacted Clay Cover) to Predictions Made with UNSAT-H and HELP: (a) Surface Runoff, (b) Evapotranspiration, and (c) Percolation.



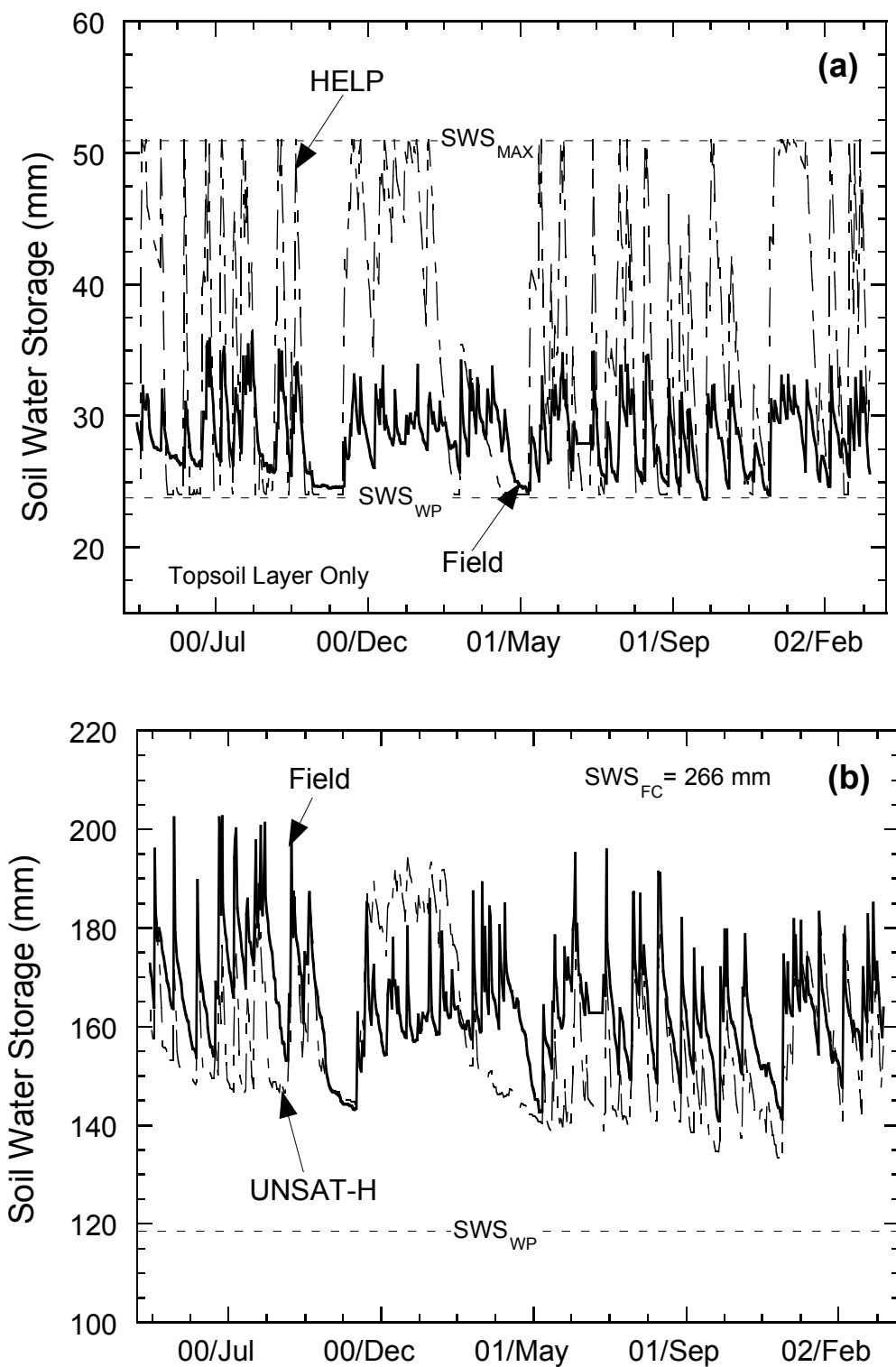


Fig. 5.29. Comparison of Soil Water Storage for the at Albany Site (Compacted Clay Cover) to Predictions Made with (a) HELP and (b) UNSAT-H.

compacted clay barrier (see Section 4.7.3) led to the high percolation rate in the field

#### **5.5.2.6 Omaha Site**

The measured water balance and predictions by HELP for the composite cover at the Omaha site are shown in Fig. 5.30. To predict surface runoff better, the saturated hydraulic conductivity of the surface layer (150 mm) was set at  $2.8 \times 10^{-4}$  cm/s.

HELP over-predicted surface runoff by 20 mm, but predicted occurrences of surface runoff accurately. The majority of the over-prediction occurred after May 2001, when HELP over-predicted surface runoff by 14 mm. Closer agreement might have been obtained if the runoff curve number was decreased over time, to reflect establishment of the vegetative cover.

HELP under-predicted lateral flow by 27 mm, most likely due to a low saturated hydraulic conductivity assigned for the vegetative layer ( $6.9 \times 10^{-7}$  cm/s). HELP predicted slow progression of the wetting front through the vegetative layer, which caused the soil water storage to increase more than occurred in the field (Fig. 5.31). During two weeks in May 2001, HELP predicted the soil water storage of the vegetative layer to be exceeded, but did not predict lateral drainage. HELP either predicted water to be quickly removed by evapotranspiration, or to flow through the geomembrane. No drainage composite was installed above the geomembrane at Omaha. Instead the vegetative cover was designated as the lateral drainage layer. Thus, lateral drainage to the collection sump was likely delayed by the low saturated hydraulic conductivity of the vegetative layer.

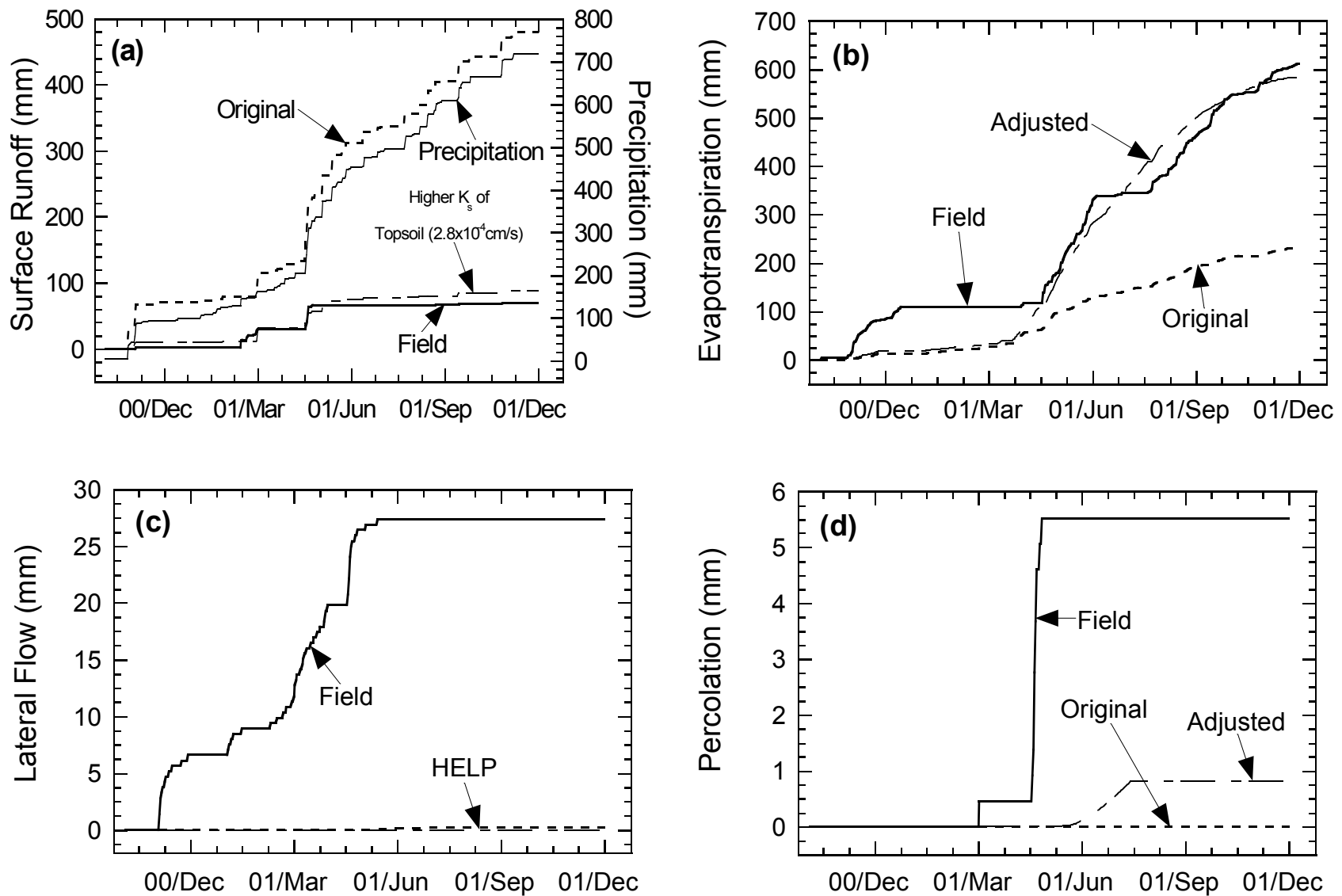


Fig. 5.30. Comparison of Water Balance Data for the Omaha Site (Composite Cover) to Predictions Made with HELP: (a) Surface Runoff, (b) Evapotranspiration, (c) Lateral Flow, and (d) Percolation.

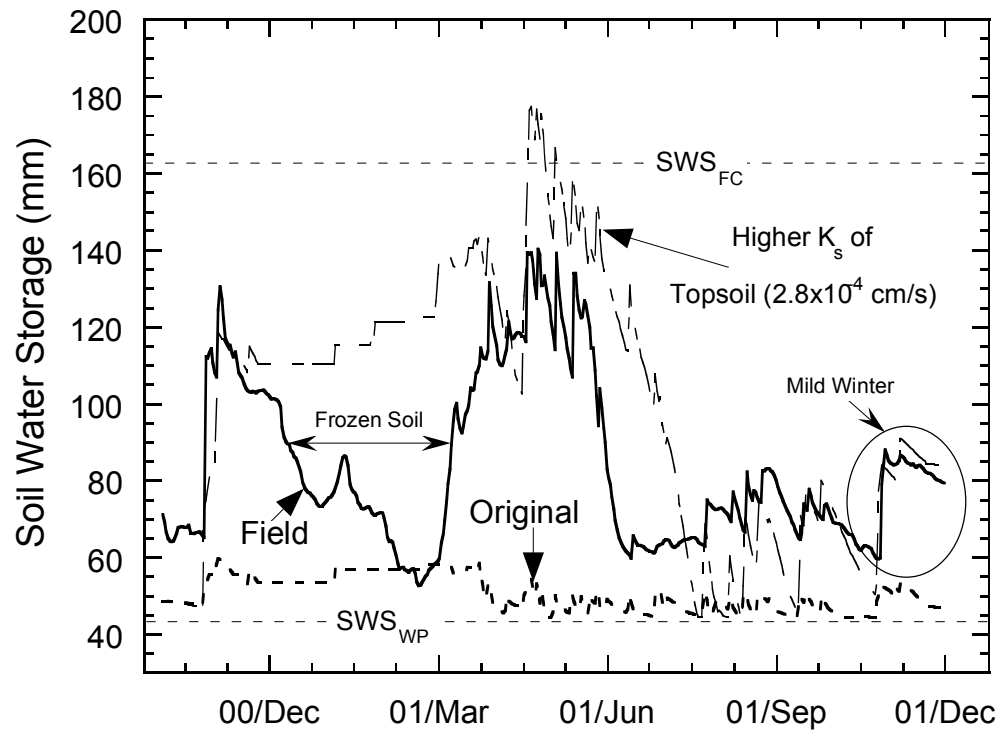


Fig. 5.31. Comparison of Soil Water Storage at the Omaha Site (Composite Cover) and Predictions Made with HELP.

The field data show that soil water storage increased significantly during times of intense rain in November 2000, and May 2001 (Fig. 5.31). The reduction in soil water storage during Winter 2001 is likely an artifact of soil freezing, which is reported as decrease in water content by the WCR probes installed in the cover. During Summer 2001, soil water storage decreases rapidly due to high evapotranspiration and percolation. HELP predicted a similar trend in soil water storage, but over-predicted soil water storage during Winter and Spring 2001, and slightly under-predicted soil water storage in Fall 2001.

During Spring 2001, HELP over-predicted soil water storage by 33 mm, and predicted the capacity of the vegetative layer to be exceeded. In June 2001, HELP predicted soil water storage to rapidly decrease, but under-predicted the minimum soil water storage by approximately 20 mm. HELP predicted that the soil water storage to reach the wilting point in the Summer 2001. During Fall 2001, HELP closely predicted the trend in soil water storage, but slightly under-predicted the storage during breaks in precipitation events. This may be due to an over-estimate of the maximum LAI.

HELP under-predicted percolation by 4.7 mm. Percolation was transmitted through the composite cover during two separate events in March and May 2001. In contrast, HELP did not predict percolation to begin until the beginning of June 2001.

## **5.6 PARAMETRIC STUDY**

A parametric study was conducted using HELP and UNSAT-H to gain a better understanding of how varying the model inputs would affect the model predictions. One parameter was varied at a time, while all other parameters remained constant.

The parametric study was performed using only one year of data rather than the entire monitoring period.

#### **5.6.1 Surface Runoff Curve Number in HELP**

The surface runoff curve number was adjusted for three test sections. Two are located in a humid climate (Albany), and one in an arid climate (Helena). Water balance predictions for these simulations are in Tables 5.13-5.15.

Surface runoff was insensitive to the curve number for the conventional cover at Albany (Table 5.13) and the alternative cover at Helena (Table 5.15). Helena does not receive the intense rain events like Albany, and therefore little surface runoff is generated unless a surface runoff curve number close to 100 (impermeable) is used.

For the conventional cover at Albany, the hydraulic conductivity of the barrier layer below the topsoil layer controls the infiltration rate. Decreasing the surface curve number increases the amount of infiltration into the topsoil layer. However, the conventional cover does not have enough storage capacity above the barrier layer, and water is not able to drain through the barrier faster than water is being applied. Therefore, additional water is routed to surface runoff. For the alternative cover at Albany, surface runoff is more sensitive to the curve number, because the more permeable storage layers can accept and retain more water (Table 5.14).

#### **5.6.2 Saturated Hydraulic Conductivity of Barrier Layer in HELP**

The saturated hydraulic conductivity of the barrier layer for the conventional cover at Albany was varied between  $7.3 \times 10^{-5}$  cm/s and  $1.0 \times 10^{-8}$  cm/s (Table 5.16). The water balance quantities were insensitive to the saturated hydraulic conductivity of the barrier layer until the saturated hydraulic conductivity was increased to  $1.0 \times 10^{-6}$  cm/s

Table 5.13. Water Balance Quantities Predicted by HELP for Compacted Clay Cover at Albany Site<sup>a</sup> for Various Surface Runoff Curve Numbers (CN). Percentage of Precipitation in Parentheses.

Curve Number	Evapotranspiration (mm)	Surface Runoff (mm)	Percolation (mm)	Change in Storage (mm)
80.6	472 (57.0%)	191 (23.2%)	0	7
82.3	477 (58.0%)	186 (22.6%)	0	7
90.9	469 (57.0%)	193 (23.5%)	0	8
94.4	441 (53.6%)	220 (26.7%)	0	9

<sup>a</sup> Simulation Period is from January 1 to December 31, 2001. Precipitation was 670 mm during this period. Surface Layer  $K_s = 1.3 \times 10^{-4}$  cm/s.

Table 5.14. Water Balance Quantities Predicted by HELP for ECap Cover at Albany Site<sup>b</sup> for Various Surface Runoff Curve Numbers (CN). Percentage of Precipitation in Parentheses.

Curve Number	Evapotranspiration (mm)	Surface Runoff (mm)	Percolation (mm)	Change in Storage (mm)
80.6	664 (80.1%)	38 (4.6%)	0.23 (0.03%)	121
82.3	664 (80.1%)	45 (5.5%)	0.22 (0.03%)	114
90.9	655 (79.6%)	109 (13.2%)	0.34 (0.04%)	59

<sup>b</sup> Simulation Period is from January 1 to December 31, 2001. Precipitation was 823 mm during this period. Surface Layer  $K_s = 1.9 \times 10^{-7}$  cm/s.

Table 5.15. Water Balance Quantities Predicted by HELP for Alternative Cover at Helena Site<sup>a</sup> for Various Surface Runoff Curve Numbers (CN). Percentage of Precipitation in Parentheses.

Curve Number	Evapotranspiration (mm)	Surface Runoff (mm)	Percolation (mm)	Change in Storage (mm)
70.7	134.6 (92.5%)	4.3 (3.0%)	0.0	6.6
80.6	134.6 (92.5%)	4.3 (3.0%)	0.0	6.6
90.9	132.7 (91.2%)	4.2 (2.9%)	0.0	8.6
91.1	133.2 (91.6%)	4.7 (3.2%)	0.0	7.6
94.1	133.7 (91.9%)	5.8 (4.0%)	0.0	6.0
97.1	133.6 (91.8%)	12.6 (8.7%)	0.0	-0.7

<sup>a</sup> Simulation Period is from January 1 to December 31, 2000. Precipitation was 145.5 mm during this period. Surface Layer  $K_s = 5.0 \times 10^{-7}$  cm/s

Table 5.16. Water Balance Quantities Predicted by HELP for Compacted Clay Cover at Albany Site<sup>a</sup> for Various Saturated Hydraulic Conductivities of the Barrier Layer. Percentage of Precipitation in Parentheses.

Saturated Hydraulic Conductivity (cm/s)	Evapotranspiration (mm)	Surface Runoff (mm)	Percolation (mm)	Change in Storage (mm)
$7.3 \times 10^{-5}$	350 (42.5%)	45 (5.5%)	288 (35.0%)	-13
$1.0 \times 10^{-6}$	442 (54.7%)	184 (22.4%)	58 (7.0%)	-14
$1.0 \times 10^{-7}$	444 (54.0%)	233 (28.3%)	7 (0.9%)	-14
$7.3 \times 10^{-8}$ (Measured in Laboratory)	455 (55.3%)	226 (27.5%)	3 (0.4%)	-14
$1.0 \times 10^{-8}$	461 (56.0%)	230 (28.0%)	0 (0.0%)	-21

<sup>a</sup>Simulation Period is from January 1, 2001 to December 31, 2001. Precipitation was 670 mm during this period.



(nearly two orders of magnitude higher than saturated hydraulic conductivity at time of construction). When the saturated hydraulic conductivity was increased from  $7.3 \times 10^{-8}$  cm/s (measured immediately after construction) to  $7.3 \times 10^{-5}$  cm/s, surface runoff decreased from 27.5% to 5.5% of precipitation, evapotranspiration decreased slightly from 55.3% to 42.5% of precipitation, and percolation increased from 0% to 35% of precipitation

Using a low saturated hydraulic conductivity resulted in large predictions of surface runoff. The infiltration rate into the cover is based on the hydraulic properties (e.g., saturated hydraulic conductivity, soil water storage capacity, initial water content) of the topsoil layer, and the hydraulic properties of the underlying layers. As the water content of the topsoil layer approached saturation, the infiltration rate decreased to the saturated hydraulic conductivity of the underlying barrier layer.

Flow through the barrier layer in the field was dominated by preferential flow caused by desiccation cracking, rather than conventional porous media flow. To match the percolation transmitted from the compacted clay cover at Albany (298 mm), the saturated hydraulic conductivity of the barrier layer had to be increased significantly to  $7.3 \times 10^{-5}$  cm/s, which is 1000 times higher than the saturated hydraulic conductivity at time of construction. This hydraulic conductivity is comparable to hydraulic conductivities for desiccated moderate to highly plastic compacted clays reported by Albrecht and Benson (2001).

### **5.6.3 Geomembrane Properties in HELP**

The number of defects and the placement condition for the geomembrane were varied for the composite covers at Omaha (Table 5.17) and Marina (Table 5.18). Two

Table 5.17. Effect of Placement Condition and Hole Frequency for Geomembrane on Predictions Made with HELP<sup>a</sup> for Composite Covers at Omaha.

Surface Layer $K_s$	Parameter		Lateral Flow (mm)	Leakage Thu Barrier Layer (mm)	Percolation (mm)
	Placement Condition	Hole Frequency (holes/ha)			
<b>As-Built</b>	1	(50)	0.00	0.00	0.00
	2	(50)	0.00	0.00	0.00
	3	(50)	0.00	0.00	0.00
	4	(50)	0.00	0.00	0.00
	5	(50)	0.00	0.00	0.00
	(2)	1	0.00	0.00	0.00
	(2)	50	0.00	0.00	0.00
	(2)	100	0.00	0.00	0.00
<b>Increased</b>	1 <sup>b</sup>	(50)	6.58	0.00	1.5
	2 <sup>b</sup>	(50)	7.53	0.19	1.35
	3 <sup>b</sup>	(50)	7.14	0.69	0.95
	4 <sup>b</sup>	(50)	6.70	3.53	0.16
	5 <sup>b</sup>	(50)	0.25	21.6	0.57
	(2)	1 <sup>b</sup>	7.92	0.02	1.49
	(2)	50 <sup>b</sup>	7.14	0.69	0.95
	(2)	100 <sup>b</sup>	6.6	0.02	0.59

<sup>a</sup>Simulation period is from January 1, 2001 to December 31, 2001.

<sup>b</sup>Increased  $K_s$  of topsoil layer to  $1.5 \times 10^{-4}$  cm/s, and  $K_s$  of the vegetative layer to  $7.0 \times 10^{-5}$  cm/s. Reduced runoff curve number to 84.3.

Table 5.18. Effect of Placement Condition and Hole Frequency for Geomembrane on Predictions Made with HELP<sup>a</sup> for Composite Cover at Marina.

Parameter		Lateral Flow (mm)	Leakage Thru Geomembrane (mm)	Percolation (mm)
Placement Condition	Hole Frequency (holes/ha)			
1	(50)	2.60	0.55	0.00
2	(50)	2.60	0.55	0.00
3	(50)	2.60	0.55	0.00
4	(50)	2.60	0.55	0.00
5	(50)	2.10	6.10	0.00
(3)	1	2.60	0.01	0.00
(3)	50	2.60	0.10	0.00
(3)	100	2.60	0.20	0.00

<sup>a</sup>Simulation period is from January 1, 2001 to December 31, 2001.

sets of simulations were conducted for Omaha. One set simulated the profile as it was constructed. The other set simulated the composite barrier with an increased saturated hydraulic conductivity of the topsoil and vegetative layers (above geomembrane), and a reduced runoff curve number to increase the head on the geomembrane. A drainage layer was not included in the composite covers at Omaha and Marina. Thus, the vegetative layer was designated as a lateral drainage layer. According to Schroeder et al. (1994), a lateral drainage layer is modeled in the same manner as a vertical percolation layer, except saturated lateral drainage is allowed.

There was no change in percolation when the placement condition and defect frequency was varied for the composite barrier at Omaha. Each simulation yielded 0 mm of percolation, because no water reached the geomembrane due to the low saturated hydraulic conductivity of the soil layer ( $7.0 \times 10^{-7}$  cm/s) above the geomembrane. Therefore, to increase the potential for HELP to predict percolation, an additional simulation was conducted with increased saturated hydraulic conductivities of the topsoil and vegetative layers, and a reduced runoff curve number. In contrast to what was expected, percolation decreased as the quality of placement was reduced, and as the defect frequency was increased. For several of the simulations, the predicted leakage through the barrier layer was less than the predicted percolation, which is not logical.

For the composite barrier at Marina, HELP predicted 0 mm of percolation for each simulation using the as-constructed hydraulic properties as input. Leakage through the geomembrane did increase slightly when placement condition 5 (worse case: bad contact) was simulated, and also when the hole frequency was increased.

#### **5.6.4 Maximum Leaf Area Index (LAI)**

The maximum LAI was adjusted for HELP and UNSAT-H to evaluate its effect on the water balance. Simulations were conducted at a humid site (ECap at Albany), a semi-arid site (thick monolithic barrier at Sacramento), and an arid site (alternative cover at Helena).

For HELP, increasing the maximum LAI caused an increase in evapotranspiration, a decrease in surface runoff and percolation, and a reduction in soil water storage (see Tables 5.19-5.21). However, the magnitude of these changes depended on the climate.

Evapotranspiration increased only 2% of precipitation at Helena (arid site) when the LAI was increased from 0.5 to 5.0, as opposed to 23.5% at Albany (humid site) and 34.1% at Kiefer (semi-arid). Helena was least sensitive because potential evapotranspiration is lower at Helena than at Sacramento, and Helena does not have the available water that exists at Albany.

LAI had a greater effect on surface runoff for Albany than the other sites. HELP predicted surface runoff would decrease approximately 22% of precipitation at Albany (Table 5.19), 2% of precipitation at Sacramento (Table 5.20), and less than 1% of precipitation at Helena (Table 5.21). As described in Section 5.5, HELP sheds more precipitation as surface runoff at Albany because the soil water storage capacity of the surface layer is quickly exceeded during intense rain events. When the LAI was increased at Albany, the vegetation was more capable of removing water, providing more void space for water retention in the surface layer.

Table 5.19. Water Balance Quantities Predicted by HELP for ECap Cover at Albany Site<sup>a</sup> (Humid) for Various Maximum LAI. Percentage of Precipitation in Parentheses.

<b>LAI</b>	<b>Evapotranspiration (mm)</b>	<b>Surface Runoff (mm)</b>	<b>Percolation (mm)</b>	<b>Change in Storage (mm)</b>
0.5	515 (62.6%)	307 (37.3%)	0.0 (0.0%)	0.4
1.0	585 (69.2%)	260 (31.5%)	0.0 (0.0%)	-21.9
2.0	695 (80.0%)	174 (21.1%)	0.0 (0.0%)	-46.4
3.0	738 (82.8%)	152 (18.5%)	0.0 (0.0%)	-67.8
4.0	766 (85.1%)	134 (16.3%)	0.0 (0.0%)	-77.4
5.0	778 (86.1%)	125 (15.2%)	0.0 (0.0%)	-80.7

<sup>a</sup> Simulation Period is from January 1 to December 31, 2001. Precipitation was 823 mm during this period.

Table 5.20. Water Balance Quantities Predicted by HELP for Thick Monolithic Barrier Cover at Sacramento Site<sup>a</sup> (Semi-Arid) for Various Maximum LAI. Percentage of Precipitation in Parentheses.

<b>LAI</b>	<b>Evapotranspiration (mm)</b>	<b>Surface Runoff (mm)</b>	<b>Percolation (mm)</b>	<b>Change in Storage (mm)</b>
0.5	290 (49.5%)	96 (16.4%)	0.76 (0.13%)	201 (34.4%)
1.0	367 (62.5%)	90 (15.3%)	0.57 (0.10%)	129 (22.0%)
2.0	472 (80.4%)	86 (14.7%)	0.51 (0.09%)	29 (4.9%)
3.0	496 (84.5%)	84 (14.3%)	0.45 (0.08%)	6 (1.0%)
4.0	489 (83.3%)	87 (14.8%)	0.25 (0.04%)	10 (1.7%)
5.0	491 (83.6%)	86 (14.7%)	0.22 (0.04%)	10 (1.7%)

<sup>a</sup> Simulation Period is from January 1 to December 31, 2000. Precipitation was 587 mm during this period.

Table 5.21. Water Balance Quantities Predicted by HELP for Alternative Cover at Helena Site<sup>a</sup> (Arid) for Various Maximum LAI. Percentage of Precipitation in Parentheses.

<b>LAI</b>	<b>Evapotranspiration (mm)</b>	<b>Surface Runoff (mm)</b>	<b>Percolation (mm)</b>	<b>Change in Storage (mm)</b>
0.1	128.0 (88.9%)	6.2 (4.3%)	0.0 (0.0%)	5.9 (4.1%)
0.5	134.7 (93.1%)	6.2 (4.3%)	0.0 (0.0%)	3.3 (2.3%)
5.0	136.7 (95.1%)	5.2 (3.6%)	0.0 (0.0%)	2.3 (1.6%)

<sup>a</sup> Simulation Period is from January 1 to December 31, 2000. Precipitation was 144 mm during this period.

Soil water storage in all three covers decreased as the LAI increased. At Albany, HELP was able to remove more water from the soil profile than was added by precipitation (Table 5.19). At Sacramento, soil water storage decreased significantly (nearly 33%) when the LAI was increased from 0.5 to 5.0 (Table 5.20). However, even when the LAI was large, HELP predicted that the vegetation on the thick monolithic barrier at Sacramento would not remove more soil water than added by precipitation, despite using an LAI of 5.0. At Helena, soil water storage decreased slightly (2.5%) when the LAI was increased from 0.5 to 5.0.

HELP only predicted percolation for the Sacramento site. The percolation rate decreased approximately 0.5 mm/yr (0.1% of precipitation) when the LAI was increased from 0.5 to 5.0. Even with an LAI of 5.0, HELP still predicted percolation would occur, because soil water at deeper depths could not be extracted from the thick (2450 mm) cover.

For UNSAT-H, varying the maximum LAI from 0.5 to 4.5 resulted in a trend similar to that found with HELP for the Sacramento site, but not for the Helena site (Tables 5.22 and 5.23). UNSAT-H predicted evapotranspiration at Helena to decrease slightly as the LAI increased (Table 5.23), despite more soil water being removed from the cover. The reduction in evapotranspiration is apparently due to a slight increase in the predicted surface runoff. Increasing the LAI increased the potential transpiration demand, but less water was available for evapotranspiration.

At Sacramento, UNSAT-H predicted evapotranspiration to increase by nearly 86 mm (4% of precipitation) when the LAI was increased from 0.5 to 4.5. By increasing the LAI, UNSAT-H predicted significantly more soil water removal, which resulted in less percolation. Surface runoff was not affected by an increase in LAI.



Table 5.22. Water Balance Quantities Predicted by UNSAT-H for Thin Monolithic Barrier Cover at Sacramento Site<sup>a</sup> for Various Maximum LAI. Percentage of Precipitation in Parentheses.

<b>LAI</b>	<b>Evapotranspiration (mm)</b>	<b>Surface Runoff (mm)</b>	<b>Percolation (mm)</b>	<b>Change in Storage (mm)</b>
0.5	342.6 (93.6%)	0.4 (0.1%)	22.6 (6.3%)	-8.7
1.6	395.1 (97.0%)	0.3 (0.1%)	12.8 (3.6%)	-50.9
2.5	415.6 (97.2%)	0.2 (0.1%)	9.7 (2.7%)	-68.7
4.5	428.8 (97.6%)	0.2 (0.1%)	8.1 (2.3%)	-80.2

<sup>a</sup> Simulation Period is from July 29, 2000 to July 28, 2001. Precipitation was 356.6 mm during this period.

Table 5.23. Water Balance Quantities Predicted by UNSAT-H for Alternative Cover at Helena Site<sup>a</sup> (Arid) for Various Maximum LAI. Percentage of Precipitation in Parentheses.

<b>LAI</b>	<b>Evapotranspiration (mm)</b>	<b>Surface Runoff (mm)</b>	<b>Percolation (mm)</b>	<b>Change Storage (mm)</b>
0.5	227.5 (88.9%)	23.5 (10.1%)	0.0	-17.5
1.5	231.4 (88.0%)	28.0 (12.0%)	0.0	-25.7
4.5	231.3 (87.3%)	29.7 (12.7%)	0.0	-27.3

<sup>a</sup> Simulation Period is from October 19, 2000 to October 18, 2001. Precipitation was 233.7 mm during this period.

### 5.6.5 Growing Season in HELP

The growing season dates chosen for HELP were adjusted for the Sacramento (Table 5.24) and Helena (Table 5.25) sites. Adjusting the germination and harvest dates changes the number of days during which transpiration occurs. This may become critical at some sites based on the timing of the rainy season and the spring thaw.

At Sacramento, evapotranspiration decreased slightly as the number of growing days was reduced. For example, evapotranspiration decreased 2% of precipitation when the number of growing days was reduced by 30 days (from a germination date of 275 to 245). Significant evapotranspiration did not occur during this period because only 6 mm of precipitation was received at the site. However, evapotranspiration was reduced by 38% when the harvest date was under-estimated, which reduced the number of growing days by 133 days.

At Helena, evapotranspiration was significantly less sensitive to varying the germination and harvest dates. There was negligible change in evapotranspiration when the growing season was reduced by 50 days (from a germination date of 158 to 108). During this period, only 19 mm of precipitation fell, which was easily removed from the soil once the vegetation germinated.

Surface runoff was not sensitive to varying the growing season dates at either site.

Percolation was only predicted for the Sacramento site, and the amount of percolation at Sacramento was insensitive to the germination dates. When the harvest date was under-estimated, percolation increased by only approximately 3.6 mm. However, the soil water storage increased substantially. Therefore, large percolation rates may have been predicted had additional years been simulated. This scenario

Table 5.24. Water Balance Quantities Predicted by HELP for Thick Monolithic Barrier Cover at Sacramento Site<sup>a</sup> (Semi-Arid) for Various Growing Season Dates Percentage of Precipitation in Parentheses.

Germination Julian Date (Date)	Number of Growing Days	Evapotranspiration (mm)	Surface Runoff (mm)	Percolation (mm)	Change in Storage (mm)
275 (10/2)	273	466.9 (79.5%)	84.5 (14.4%)	0.08 (0.01%)	35.4 (6.0%)
265 (9/22)	283	461.9 (78.7%)	87.9 (15.0%)	0.05 (0.01%)	37.1 (6.3%)
255 (9/12)	293	469.8 (80.0%)	87.3 (14.9%)	0.13 (0.02%)	29.7 (5.1%)
245 (9/2)	303	478.0 (81.4%)	86.0 (14.7%)	0.09 (0.02%)	22.4 (3.8%)
235 (8/23)	313	492.9 (84.0%)	85.6 (14.6%)	0.11 (0.02%)	8.3 (1.4%)
225 (8/13)	323	517.7 (85.8%)	85.5 (14.6%)	0.18 (0.03%)	-16.4
Germinate = 245 Harvest = 50 (2/19)	170	269.0 (45.8%)	90.5 (15.4%)	3.7 (0.63%)	223.7 (38.1%)

<sup>a</sup> Simulation Period is from January 1, 2000 to December 31, 2000. Precipitation was 587 mm during this period. Typical growing season for Kiefer site is 245 to 183 (Julian Day).

Table 5.25. Water Balance Quantities Predicted by HELP for Alternative Cover at Helena Site<sup>a</sup> (Arid) for Various Growing Season Dates. Percentage of Precipitation in Parentheses.

Germination Julian Day (Date)	Number of Growing Days	Evapotranspiration (mm)	Surface Runoff (mm)	Percolation (mm)	Change in Storage (mm)
105 (4/15)	158	134.6 (93.5%)	5.7 (4.0%)	0.0 (0.0%)	3.9 (2.7%)
115 (4/25)	148	130.6 (90.7%)	5.9 (4.1%)	0.0 (0.0%)	7.9 (5.5%)
125 (5/5)	138	133.3 (92.6%)	6.0 (4.2%)	0.0 (0.0%)	4.9 (3.4%)
135 (5/15)	128	133.7 (92.9%)	5.8 (4.0%)	0.0 (0.0%)	4.7 (3.3%)
145 (5/25)	118	135.8 (94.3%)	6.2 (4.3%)	0.0 (0.0%)	2.2 (1.5%)
155 (6/4)	108	135.0 (93.8%)	6.2 (4.3%)	0.0 (0.0%)	2.8 (1.9%)
Germinate = 135 Harvest = 291 (10/18)	156	135.9 (94.4%)	5.8 (4.0%)	0.0 (0.0%)	2.5 (1.7%)

<sup>a</sup> Simulation Period is from January 1, 2000 to December 31, 2000. Precipitation was 144 mm during this period. Typical growing season for Helena site is 135 to 263 (Julian Day).

occurred in the field. Vegetation at the Sacramento site ceased transpiring prior to the expected harvest date, resulting in more water remaining in the cover at the end of the summer than had been anticipated. During the following year, the soil water storage capacity of the cover was exceeded following the on-set of the rainy season, and the percolation rate increased.

Soil water storage decreased more at the Sacramento site than at the Helena site as the number of growing days was increased. Increasing the growing season at the Sacramento site by 40 d caused the soil water storage to decrease 27.1 mm (4.6% of precipitation). In contrast, the same change caused a decrease in soil water storage of only 0.7 mm at Helena (1.2% of precipitation).

In general, the water balance is not affected significantly by varying the growing season, as long as reasonable germination and harvest dates are chosen. For arid and semi-arid sites in warm climates (that are characterized as having hot summers and wet winters), the growing season should at least include the rainy season during which transpiration will occur at its maximum rate. Transpiration will also occur for a period after the rainy season as the plants scavenge for water, but during this period transpiration may be a smaller fraction of evapotranspiration. For sites in cooler climates, the spring thaw and first killing frost are adequate estimates for the start and end of the growing season.

## **SECTION SIX SUMMARY AND CONCLUSIONS**

This report describes the measured and predicted hydrology of twenty-one large-scale test sections simulating landfill final covers. The test sections are being monitored as part of the USEPA's Alternative Cover Assessment Program (ACAP). Data collected through April 2002 are included in this report. The predictions were made with two common models (HELP and UNSAT-H) using on-site meteorological and hydrological data for input. Comparisons between the predictions and the field data were made to assess the accuracy of the models. The following sections describe the salient aspects of the field data, and key findings of the comparison between the field data and model predictions.

### **6.1 SUMMARY OF FIELD PERCOLATION RATES**

#### **6.1.1 Percolation from Alternative Covers**

A summary of percolation rates from the alternative covers is in Table 6.1. The alternative covers in arid and semi-arid climates transmitted significantly less percolation than the alternative covers in humid climates, with the exception of the thin monolithic barrier at Sacramento. At the arid and semi-arid sites, the percolation rate was generally less than 1 mm/yr (except for the test sections in Sacramento). In contrast, percolation rates exceeding 30 mm/yr were measured at the humid sites. The relatively high percolation rates at the humid sites may diminish over time as the vegetation at these sites matures, and more effectively removes water stored in the cover.

Table 6.1. Summary of Percolation Data: Alternative Covers.

Climate	Site	Annual Precipitation (mm)	Cover Type	Percolation (mm/yr)
Arid and Semi-Arid	Altamont, CA	358	Monolithic Barrier	1.0
	Sacramento, CA	434	"Thin" Monolithic Barrier (1070 mm)	48.4
			"Thick" Monolithic Barrier (2450 mm)	3.1
	Helena, MT	289	Capillary Barrier	0.0
	Polson, MT	380	Capillary Barrier	0.4
	Boardman, OR	225	"Thin" Monolithic Barrier (1220 mm)	0.0
			"Thick" Monolithic Barrier (1840 mm)	0.0
Humid	Marina, CA	466	Monolithic Barrier	61.8
	Albany, GA	1263	Monolithic Barrier (ECap)	91.3
	Cedar Rapids, IA	915	Monolithic Barrier (ECap)	143.1
	Omaha, NE	760	"Thin" Capillary Barrier (760 mm)	62.9
			"Thick" Capillary Barrier (1060 mm)	36.8

At sites where snow occurred, there was a delayed response in runoff and infiltration because the snow was stored on the surface. When the snow cover melted, a significant amount of water infiltrated the cover. Much of this infiltration became percolation, because removal of soil water by evapotranspiration was minimal during and soon after the snowmelt. Thus, accounting for storage of snowmelt is a key factor that must be considered when designing alternative covers in seasonal climates.

The data from Sacramento illustrate the importance of long-term records when evaluating the efficacy of final covers. During the first growing season, the vegetation at Sacramento was very effective at removing stored water from the cover, leaving an empty reservoir for soil water storage the following winter. In contrast, the vegetation was ineffective at removing water during the second growing season, resulting in limited capacity to retain water during the subsequent winter. As a result, the storage capacity of both covers was exceeding during the winter, and appreciable amounts of percolation were transmitted. Future monitoring will show whether this behavior persists.

### **6.1.2 Percolation from Conventional Covers**

A summary of percolation rates from the conventional covers is in Table 6.2. Percolation rates less than 1 mm/yr were transmitted from the conventional covers at arid and semi-arid sites. At humid sites, the percolation rates ranged between 0.9 to 18.1 mm/yr for the composite cover and 15.5 to 280 mm/yr for compacted clay covers.

Table 6.2. Summary of Percolation Rates: Conventional Covers.

Climate	Site	Annual Precipitation (mm)	Cover Type	Percolation (mm/yr)
Arid and Semi-Arid	Altamont, CA	358	Composite Barrier	0.0
	Polson, MT	380	Composite Barrier	0.2
	Boardman, OR	225	Composite Barrier	0.0
Humid	Marina, CA	466	Composite Barrier	18.1
	Albany, GA	1263	Compacted Clay Barrier	280.4
	Cedar Rapids, IA	915	Compacted Clay Barrier	15.5
			Composite Barrier	0.9
	Omaha, NE	760	Composite Barrier	3.7



The percolation rate for the composite barrier at Marina, CA (18.1 mm/yr) was higher than anticipated during design. The composite barrier at Marina, CA was constructed without a drainage layer above the geomembrane, and without adequate protection of the geomembrane against puncture. The vegetative layer, which was placed directly above the geomembrane, was constructed with waste soil from nearby construction projects that contained concrete rubble and wire. Despite the potential for puncturing of the geomembrane by debris in the waste soil, no protection layer was provided on top of the geomembrane at the direction of the site owner. If a drainage composite had been used and a protection layer had been provided (both of which are typical in practice and were recommended by the ACAP investigators), percolation transmitted from the cover would have been significantly lower.

The data from the conventional cover at Albany, GA show that percolation from compacted clay covers is particularly sensitive to desiccation cracking of the clay. The cover with a compacted clay barrier transmitted over 550 mm of percolation during the two-year monitoring period, even though the storage capacity of the cover was never exceeded.

## **6.2 MODEL PREDICTIONS**

The modeling effort was not intended to calibrate HELP and UNSAT-H using the field data collected by ACAP, but rather to determine the accuracy of the models when well-defined parameters were used as input. Nevertheless, certain input parameters were adjusted in an attempt to match the field conditions after the outcomes of initial simulations were determined to be unsatisfactory.

### **6.2.1 Surface Runoff**

Surface runoff was found to be very sensitive to the hydraulic properties of the surface layer. Gross over-predictions of runoff were obtained when the hydraulic properties measured in the laboratory immediately after construction were used as input. Therefore, another set of simulations was conducted where the surface layer of was assigned higher saturated hydraulic conductivity. The purpose of these simulations was to account for pedogenesis that likely occurred after construction due to factors such as desiccation, freeze-thaw cycling, and biota intrusion. Increasing the saturated hydraulic conductivity resulted in more reasonable predictions of runoff for both models. After this change was made, HELP predicted runoff more accurately than UNSAT-H, even though the same hydraulic properties were used for both models.

Both models had difficulty accurately predicting surface runoff at sites that received intense rainfall (e.g., Albany, GA; Sacramento, CA) and have a soil layer with low saturated hydraulic conductivity beneath the surface layer. For these covers, the only way to match the surface runoff measured in the field was to increase the saturated hydraulic conductivity of the underlying soil layer.

### **6.2.2 Percolation in Alternative Covers**

Neither HELP of UNSAT-H predicted percolation from the alternative covers accurately, and no general bias in the models (i.e., over-prediction or under-prediction of percolation) was apparent. Both models captured the seasonal changes in percolation. The seasonal changes in soil water storage and evapotranspiration, both of which strongly influence percolation, were also captured. However, nuances in the

field data (e.g., elevated soil water storage or lower than expected evapotranspiration) were not captured by the models, and these nuances typically controlled the percolation rate. Preferential flow also appears to affect the percolation rate at some sites. Currently, preferential flow cannot be predicted reliably with conventional models.

Accurate predictions of percolation rate are tied to the predictions of soil water storage and evapotranspiration. Both of these water balance components are strongly influenced by the hydraulic properties of the covers soils and the properties of the vegetation. Thus, properties representative of the field condition are necessary to predict the water balance of alternative covers accurately. Additional characterization of soil and vegetation properties will be emphasized in future efforts by the ACAP investigators.

### **6.2.3 Lateral Flow and Percolation from Conventional Covers**

HELP was used to model the composite barriers, whereas both HELP and UNSAT-H were used to model the compacted clay barrier at Albany, GA. HELP predicted percolation record for composite covers constructed in arid and semi-arid climates accurately, but under-predicted percolation rates for composite covers in humid climates. For most of the composite covers, HELP over-predicted lateral flow.

HELP and UNSAT-H significantly over-predicted surface runoff from the compacted clay barrier at Albany, GA despite efforts to increase infiltration into the cover by increasing the saturated hydraulic conductivity of the topsoil layer, and decreasing the runoff curve number. Also, HELP and UNSAT-H did not predict

percolation from the compacted clay barrier at Albany accurately, because neither model accounts for preferential flow.

### **6.3 PRACTICAL IMPLICATIONS**

Analysis of the field data collected to date indicates that alternative covers generally are effective in limiting percolation to small amounts ( $< 1$  mm/yr) in semi-arid and arid areas provided the cover is designed for adequate storage capacity and is seeded with vegetation that can effectively remove stored water. The effectiveness of alternative covers in humid climates is not yet clear. Higher than anticipated percolation rates have been recorded to date, but lower rates are anticipated in the future as the vegetation matures.

The data from test sections simulating conventional covers indicate that composite barriers are very effective in limiting percolation in all climates ( $< 1$  mm/yr in semi-arid and arid climates, and  $< 5$  mm/yr in humid climates) provided that the cover is designed and constructed properly. Protecting the geomembrane is a key factor. Methods or materials that damage the geomembrane during construction will lead to higher than anticipated percolation rates. The data also show that covers relying on a compacted clay barrier (i.e., no geomembrane) as the primary impedance to flow may become ineffective even after a short service life. Cracking of the clay must be prevented for covers relying on a clay barrier to be effective.

Predicting the hydrology of covers (conventional and alternative) is challenging, even with an abundance of data describing the properties of the cover materials. Predictions made with current models represent seasonal trends well, but have limited

accuracy. At present, predictions made with current models can only be considered estimates of field performance. Field performance testing, using methods such as those employed by ACAP, is the best technique currently available to characterize the hydrology of covers

These inferences are predicated on the relatively short data record that has been collected. The unexpected conditions observed at some sites (e.g., Sacramento) are indicative of the need for a long-term record if a reliable understanding of the hydrology of final covers is to be attained.

## SECTION SEVEN REFERENCES

- Albrecht, B. and Benson, C. (2001). Effect of Desiccation on Compacted Natural Clays, J. of Geotech. and Geoenvironmental Eng., ASCE, 127(1), 67-76.
- Anderson, J., Shumar, M., Toft, N., and Nowak, R. (1987). Control of the Soil Water Balance By Sagebrush and Three Perennial Grasses in a Cold-Desert Environment. Arid Soil Research and Rehabilitation, 1, 229-224.
- Anderson, J. (1973). National Weather Service River Forecast System – Snow Accumulation and Ablation Model, Hydrologic Research Laboratory, National Oceanic and Atmospheric Administration, Silver Spring, MD.
- Benson, C., Abichou, T., Albright, W., Gee, G., and Roesler, A. (2001). Field Evaluation of Alternative Earthen Final Covers, International Journal of Phytoremediation, 3 (1), 105-127.
- Benson, C., Abichou, T., Wang, X., Gee, G., and Albright, W. (1999). Test Section Installation Instructions – Alternative Cover Assessment Program, Environmental Geotechnics Report 99-3, Dept. of Civil & Environmental Engineering, University of Wisconsin-Madison.
- Bohm, W. (1979). Methods of Studying Root Systems, Springer-Verlag, New York, NY.
- Bolen, M., Roesler, A., Benson, C., and Albright, W. (2001). Alternative Cover Assessment Program: Phase II Report, Geo-Engineering Report No. 01-10, University of Wisconsin, Madison, WI.
- Brooks, R. and Corey, A. (1964). Hydraulic Properties of Porous Media, Hydrology Papers (3), Colorado State University, Fort Collins, CO.
- Bundrett, M. and Kendrick, W. (1990). The Roots and Mycorrhizae of Herbaceous Woodland Plants, Quantitative Aspects of Morphology, New Phytologist, 114, 457-468.
- Burton, F., Skiens, W., Cline, F., Cataldo, D. and van Voris, P. (1986). A Controlled-Release Herbicide Device for Multiple-Year Control of Roots at Waste Burial Sites, J. of Controlled Release, 3(1), 47-54.
- Campbell, G. (1974). A Simple Method for Determining Unsaturated Hydraulic Conductivity from Moisture Retention Data, Soil Science, 117(6), 311-314.
- Campbell, G. and Anderson, R. (1998). Evaluation of Simple Transmission Line Oscillators for Soil Moisture Measurement, Comput. Electron. Agric., 20, 31-44.

- Fayer, M. and Jones, T. (1990). Unsaturated Soil-water and Heat Flow Model, Version 2.0, Pacific Northwest Laboratory, Richland, WA.
- Fayer, M., Rockhold, M., and Campbell, M. (1992). Hydrologic Modeling of Protective Barriers: Comparison of Field Data and Simulation Results, Soil Science Society of America Journal, 56, 690-700.
- Feddes, R. and Zaradny, H. (1978). Model for Simulating Soil Water Content Considering Evapotranspiration-comments, J. of Hydrology, 37, 393-397.
- Gee, G., Ward, A., and Meyer, P. (1999). Discussion of "Method to Estimate Water Storage Capacity of Capillary Barriers," by J. Stormont and C. Morris, J. of Geotechnical and Geoenvironmental Engineering, pp. 918-920.
- Giroud, J. and Bonaparte, R. (1989). Leakage Through Liners Constructed with Geomembrane Liners – Parts I and II, Geotextiles and Geomembranes, 8(1), pp. 27-67, 8(2), 71-111.
- Gurdal, T. (2002). Unsaturated and Saturated Hydrologic Properties of Alternative Cover Soils, MS Thesis, University of Wisconsin-Madison, Madison, WI.
- Hauser, V., Shaw, M., and Weand, B. (1994). Effectiveness of Soil-Vegetative Covers for Waste Sites, Proceedings Superfund XV, Superfund XV, Rockville, MD.
- Hillel, D. (1998). Environmental Soil Physics, Academic Press, New York.
- Khire, M. (1995). Field Hydrology and Water Balance Modeling of Earthen Final Covers for Waste Containment, PhD Dissertation, University of Wisconsin. Madison, WI.
- Khire, M., Benson, C., and Bosscher, P. (1997). Water Balance Modeling of Earthen Final Covers. J. of Geotechnical and Geoenvironmental Engineering, 123 (8), 744-754.
- Khire, M., Benson, C., and Bosscher, P. (1999). Field Data from a Capillary Barrier and Model Predictions with UNSAT-H. J. of Geotechnical and Geoenvironmental Engineering, 125 (6), 518-527.
- Khire, M., Benson, C., and Bosscher, P. (2000). Capillary Barriers: Design Variables and Water Balance, J. of Geotechnical and Geoenvironmental Engineering, 126 (8), 695-708
- Kim, K. (2002). Water Content Reflectometer Calibrations for Final Cover Soils, MS Thesis, University of Wisconsin-Madison, Madison, WI.

- Knisel, W., Moffitt, D., and Dumper, T. (1985). Representing Seasonally Frozen Soil with the CREAMS Model, J. American Society of Agricultural Engineering, 28, 1487-1492.
- Kustas, W., Rango, A., and Uijlenhoet, R. (1994). A Simple Energy Budget Algorithm for the Snow Melt Runoff Model, Water Resources Research, 30 (5), 1515-1527.
- Liang, Y., Hazlett, D., and Lauenroth, W. (1989). Biomass Dynamics and Water Use Efficiencies of Five Plant Communities in the Shortgrass Steppe, Oecologia, 80, 143-153.
- Mahoney, J. and Rood, S. (1998). Streamflow Requirements for Cottonwood Seedling Recruitment Integrative Model, Wetlands 18 (4), 634-645.
- Meyer, P. and Serne, R. (1999). Near-Field Hydrology Data Package for the Immobilized Low-Activity Waste – 2001 Performance Assessment, Report Prepared for U.S. Department of Energy by Pacific Northwest National Laboratories, Richland, WA.
- Penman, H. (1963). Vegetation and Hydrology, Technical Comment No. 53, Commonwealth Bureau of Soils, Harpenden, England.
- Phene, C, Hoffman, G., and Rawlins, S. (1971). Measuring Soil Matric Potential In-situ by Sensing Heat Dissipation within a Porous Body: Theory and Sensor Construction, Soil Science Society of America Proceedings, 35, 225-229.
- Roche, B., Roche, C., and Chapman, R. (1994). Impacts of Grassland Habitat on Yellow Starthistle Invasion, Northwest Science, 68, 86-96.
- Russell, R. (1977). Plant Root Systems: Their Function and Interaction with the Soil, McGraw-Hill Book Co. Ltd., London.
- Schroeder, P., Dozier, T., Zappi, P., McEnroe, B., Sjostrom, J., and Peyton, R. (1994). The Hydrologic Evaluation of Landfill Performance (HELP) Model: Engineering Documentation for Version 3, EPA/600/R-94/168b, US Environmental Protection Agency, National Risk Reduction Engineering Laboratory, Cincinnati, OH.
- Tanner, C. (1967). Measurement of Evapotranspiration, in Irrigation of Agricultural Lands, American Society of Agronomy, Madison, WI, 534-574.
- United States Environmental Protection Agency (1992). Subtitle D Clarification, Federal Register, Vol. 57 (124), 28626-28632.
- Winkler, W. (1999). Thickness of Monolithic Covers in Arid and Semi-Arid Climates, MS Thesis, University of Wisconsin-Madison, Madison, WI.



**APPENDIX 1**  
**CORRECTIONS TO ET CALCULATIONS**

Evapotranspiration (ET) was calculated on a daily basis by using Eq. 2 (Section 5), where  $P$  is precipitation,  $P_r$  is percolation,  $R_o$  is runoff,  $L_o$  is lateral flow, and  $\Delta S$  is change in soil water storage. Because ET is computed as a residual quantity, it includes the errors inherent in each of the water balance quantities being measured. In addition, the ET equation does not account for the dynamic effects in the system on a small time scale. For example, daily ET may be over-estimated at times due to a delay in response between percolation and precipitation events (See Fig. A1a).

Also, ET may be over-estimated at times when there is an artificial decrease in soil water storage, which is caused by temperature effects on the WCR probes (see Fig. A1b). Kim (2002) indicates that there can be a 6% error in volumetric water content due to temperature effects alone. Campbell Scientific, Inc. (CSI), manufacturer of WCR probes (CS615), recommends applying a correction for temperature to the soil specific calibration equation (that relates volumetric water content and CS615 output). When frozen ground conditions exist, the WCR measurements only reflect the unfrozen water content rather than the true volume of water in the soil.

To remove the artificial increase in ET (followed by a decrease), cumulative ET was re-calculated on a daily basis by assigning the “minimum” value of ET between the existing day and the last day of data. An example of this computation is shown in Fig. A2.

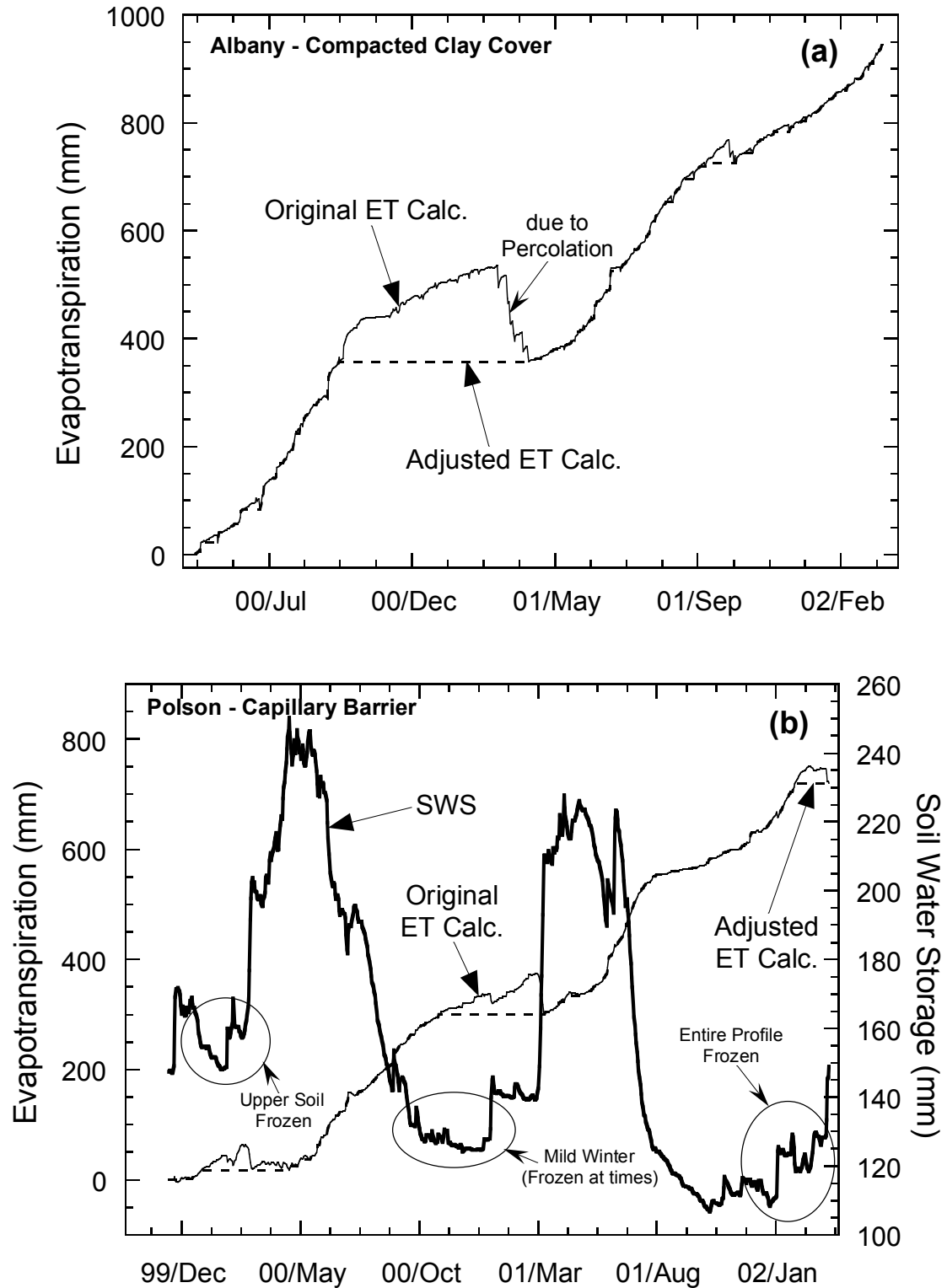


Fig. A1. Effects on Daily Evapotranspiration Calculation Due to (a) Delay in Percolation and (b) WCR Sensitivity to Temperature.

Daily						Cum. ET (mm) "adjusted"
Date	Cum. Precip. (mm)	SWS (mm)	Perc Cum. Flush (mm)	SRO Cum. Flush (mm)	Cum. ET (mm)	
11/19/1999	0	147.24	0	0	0.00	0.00
11/20/1999	0.254	147.69	0	0	0.00	0.00
11/21/1999	0.254	147.45	0	0	0.05	0.00
11/22/1999	0.254	146.99	0	0	0.51	0.00
11/23/1999	0.254	146.83	0	0	0.67	0.00
11/24/1999	0.254	147.29	0	0	0.21	0.00
11/25/1999	1.524	148.98	0	0	0.00	0.00
11/26/1999	18.542	160.85	0	0	4.93	0.00
11/27/1999	19.304	168.93	0	0	0.00	0.00
11/28/1999	19.812	171.34	0	0	0.00	0.00
11/29/1999	19.812	171.34	0	0	0.00	0.00
11/30/1999	20.066	171.62	0	0	0.00	0.00
12/1/1999	20.066	171.00	0	0	0.00	0.00
12/2/1999	20.066	170.52	0	0	0.00	0.00
12/3/1999	20.066	169.63	0	0	0.00	0.00
12/4/1999	20.066	166.61	0	0	0.70	0.70
12/5/1999	20.066	164.13	0	0	3.18	0.99
12/6/1999	20.066	165.77	0	0	1.54	0.99
12/7/1999	20.066	166.32	0	0	0.99	0.99
12/8/1999	20.066	164.59	0	0	2.72	1.04
12/9/1999	20.066	163.62	0	0	3.69	1.04
12/10/1999	20.32	163.66	0	0	3.91	1.04
12/11/1999	20.32	163.83	0	0	3.73	1.04
12/12/1999	20.32	166.07	0	0	1.50	1.04
12/13/1999	20.32	166.02	0	0	1.55	1.04
12/14/1999	20.32	164.58	0	0	2.99	1.04
12/15/1999	20.828	165.11	0	0	2.96	1.04
12/16/1999	21.844	168.05	0	0	1.04	1.04
12/17/1999	22.098	167.71	0	0	1.63	1.46
12/18/1999	23.114	168.90	0	0	1.46	1.46

Fig. A2. Example of Water Balance Computation for the Alternative Cover at the Polson Site.

**APPENDIX 2**  
**LAI GRAPHS FOR ACAP SITES**

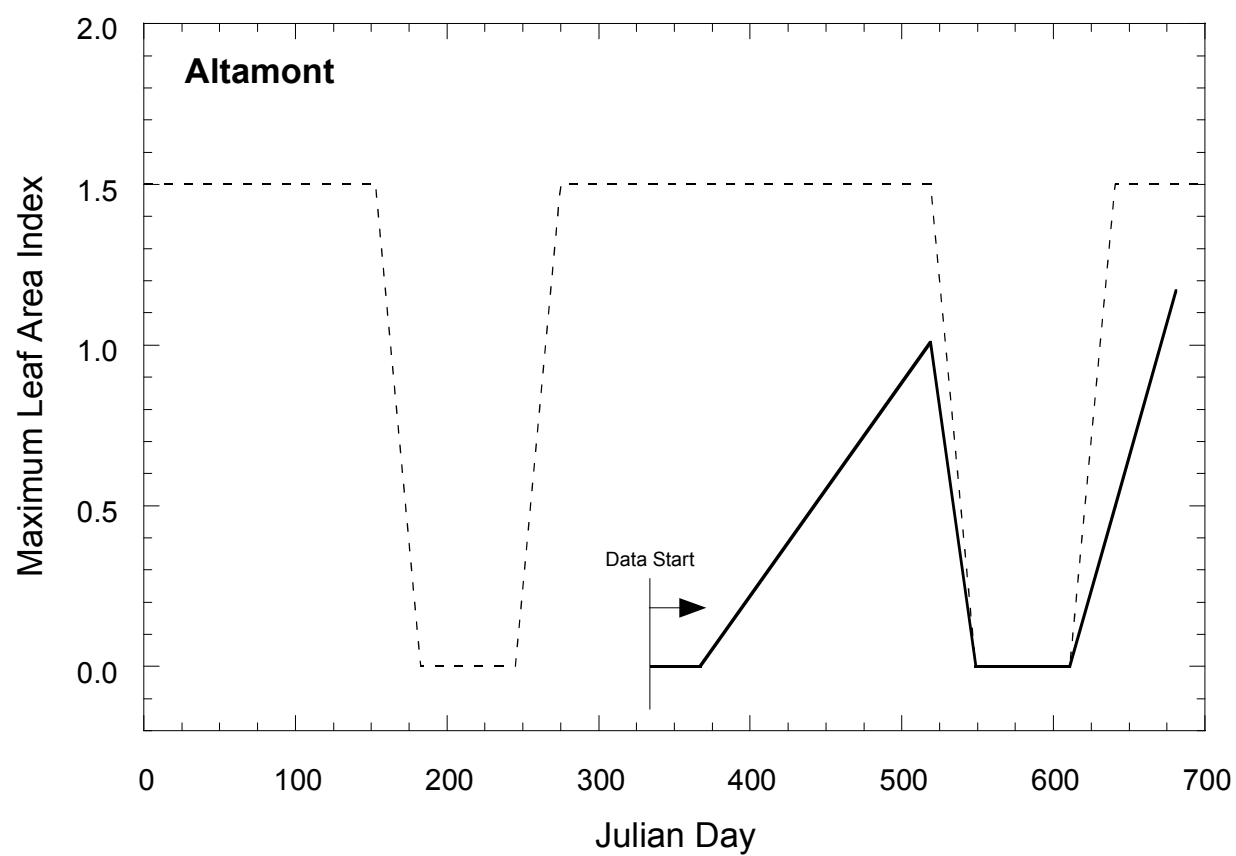


Fig. A3. LAI Plot for Altamont Site.

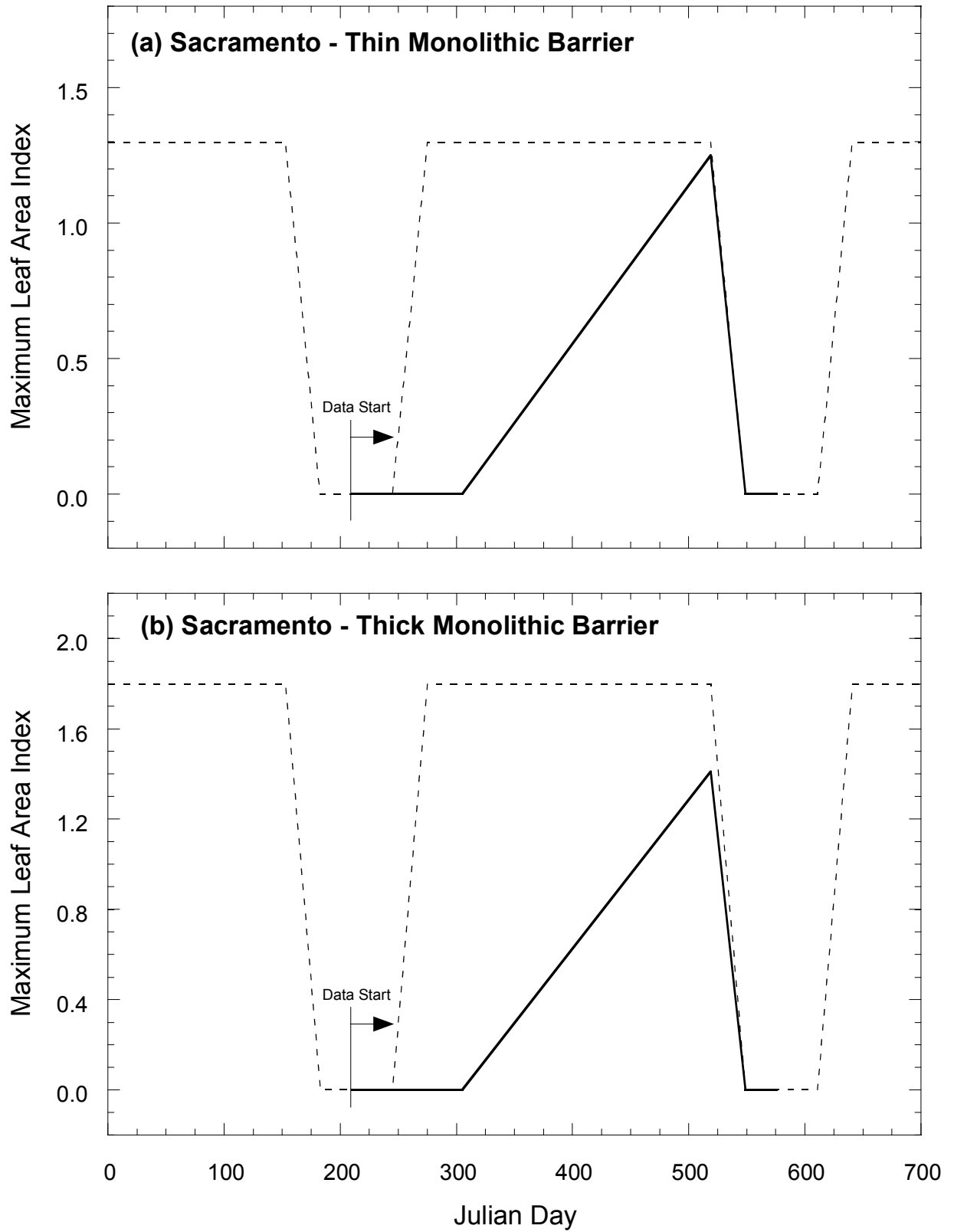


Fig. A4. LAI Plot for Sacramento Site: (a) Thin Barrier and (b) Thick Barrier.

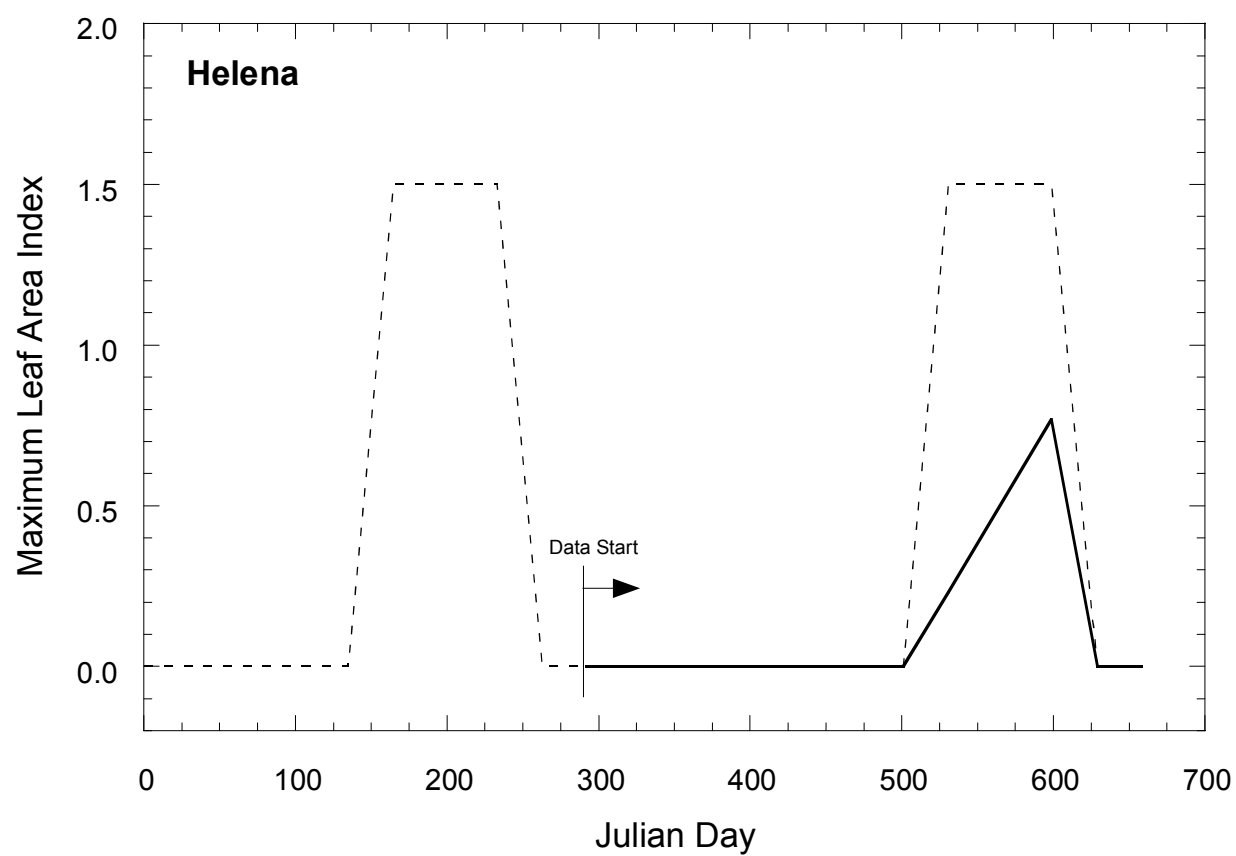


Fig. A5. LAI Plot for Helena Site.



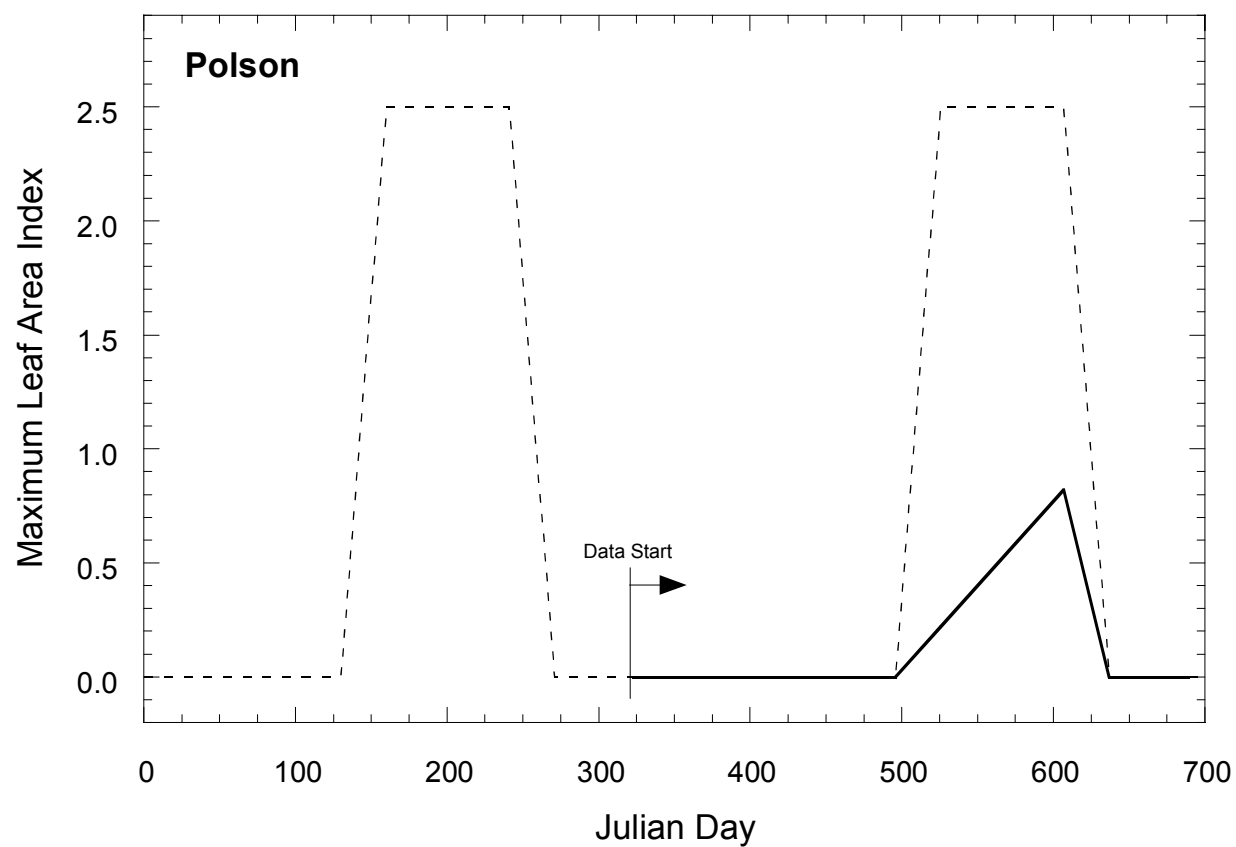


Fig. A6. LAI Plot for Polson Site.

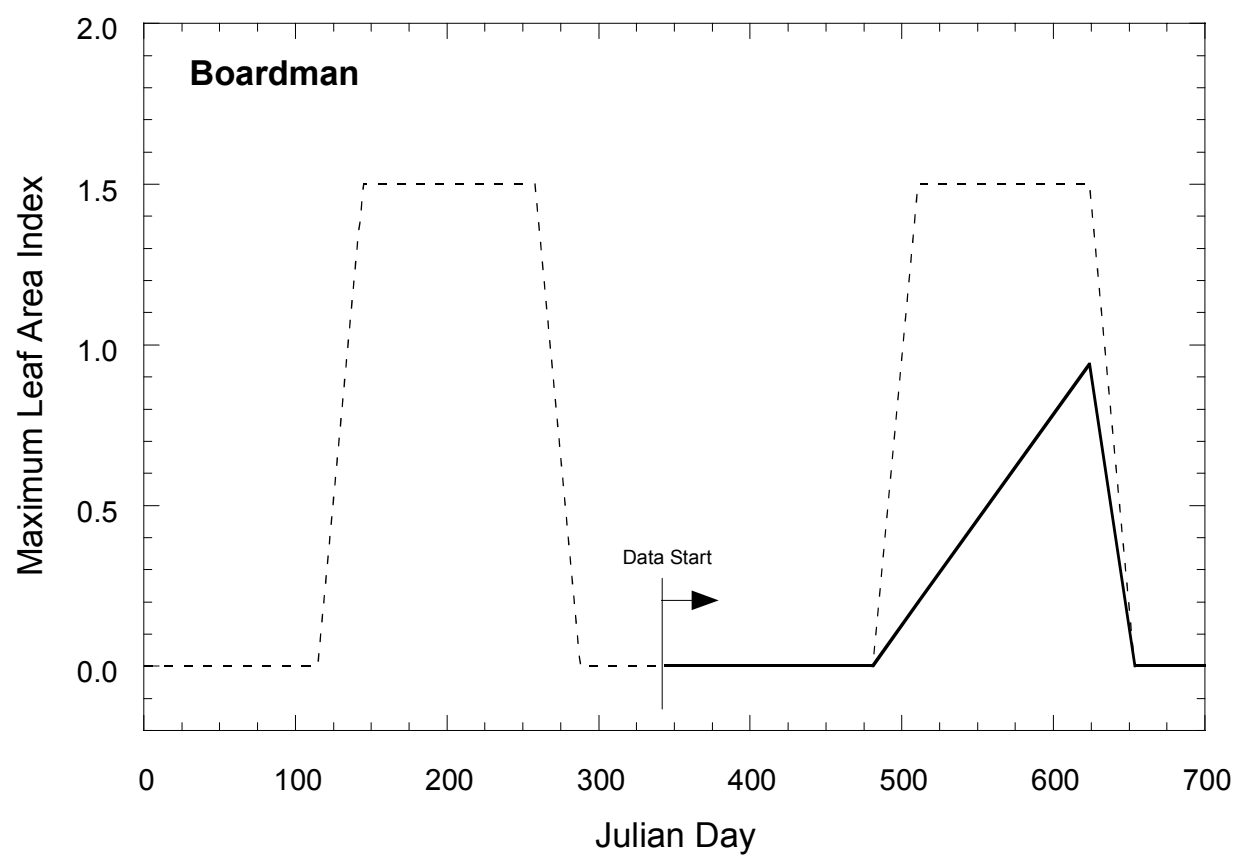


Fig.A7. LAI Plot for Boardman Site.

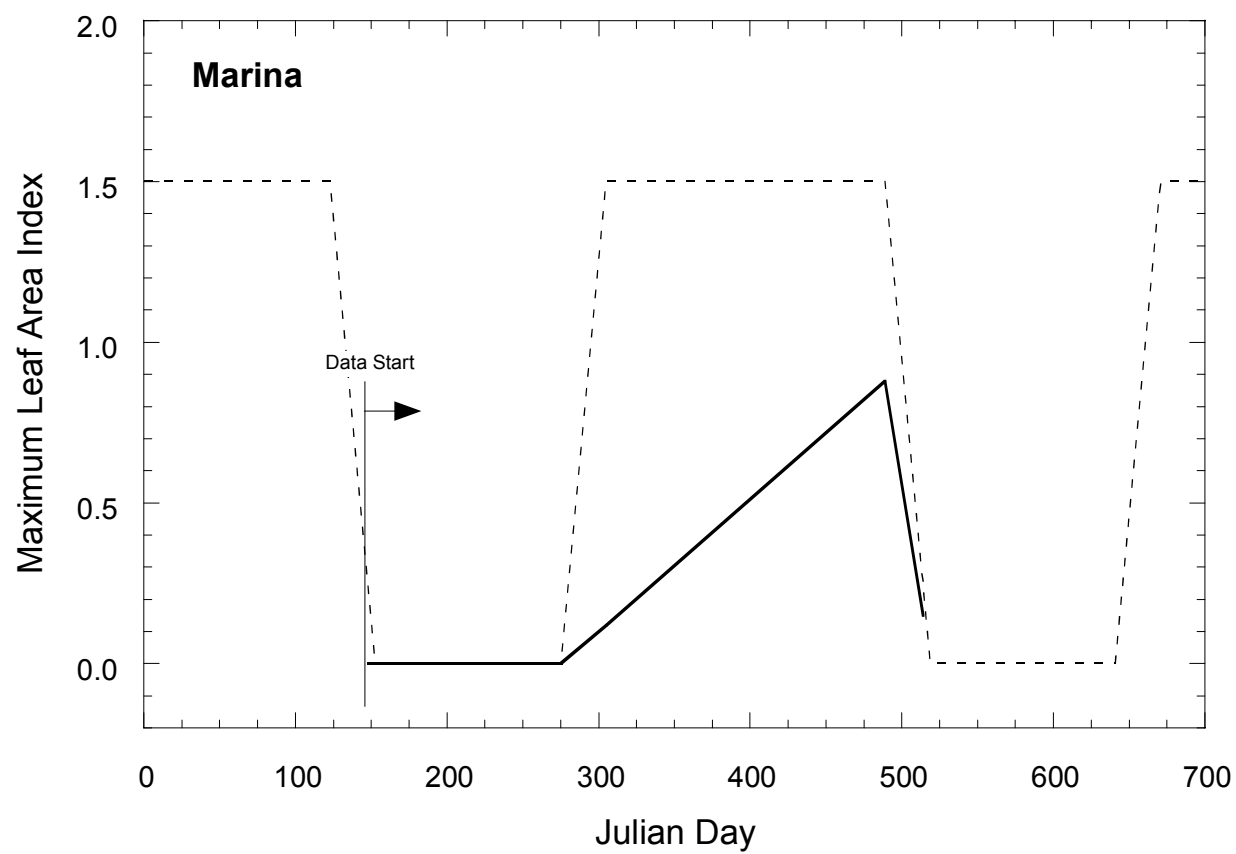


Fig. A8. LAI Plot for Marina Site.

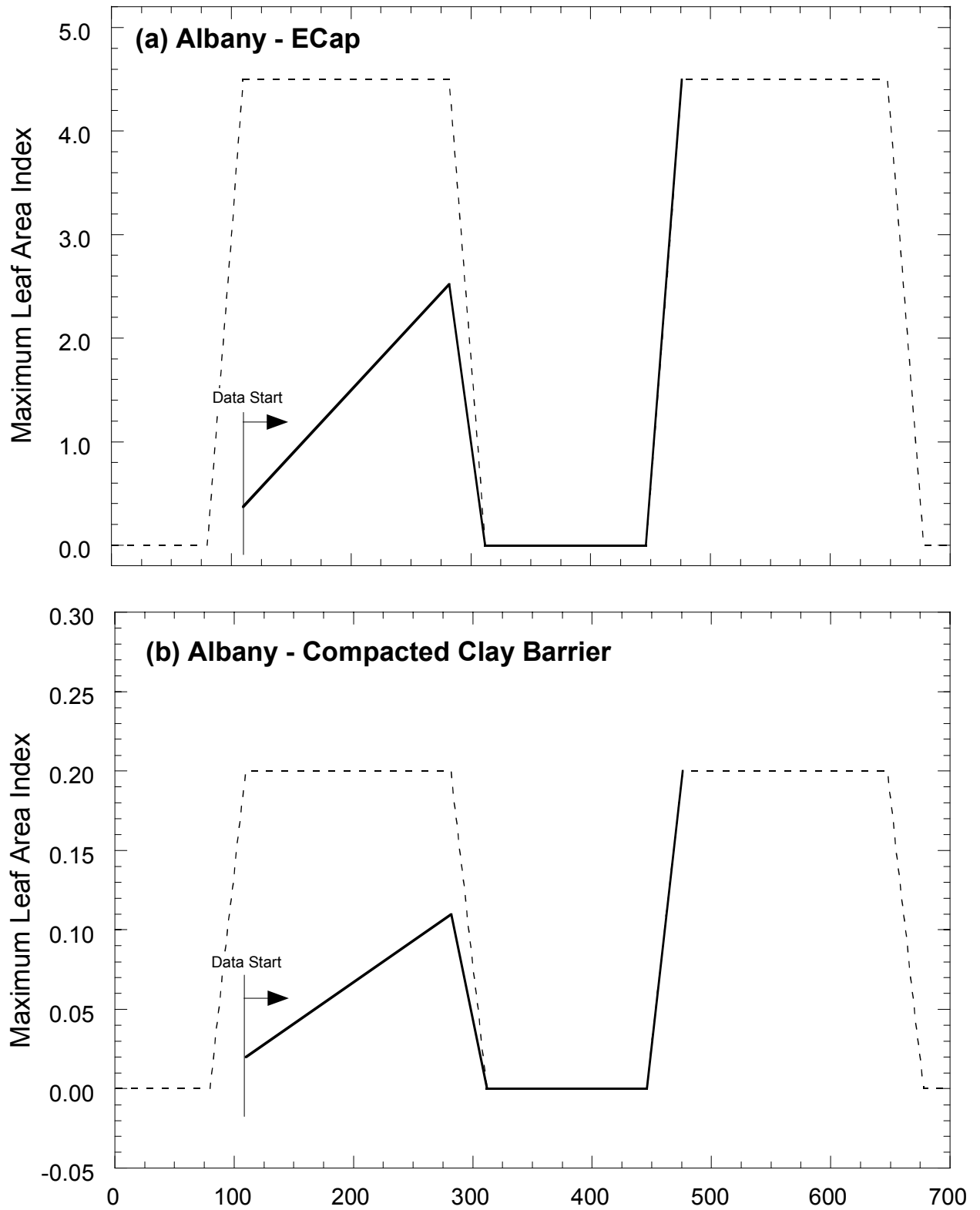


Fig. A9. LAI Plot for Albany Site: (a) ECap and (b) Compacted Clay Barrier.

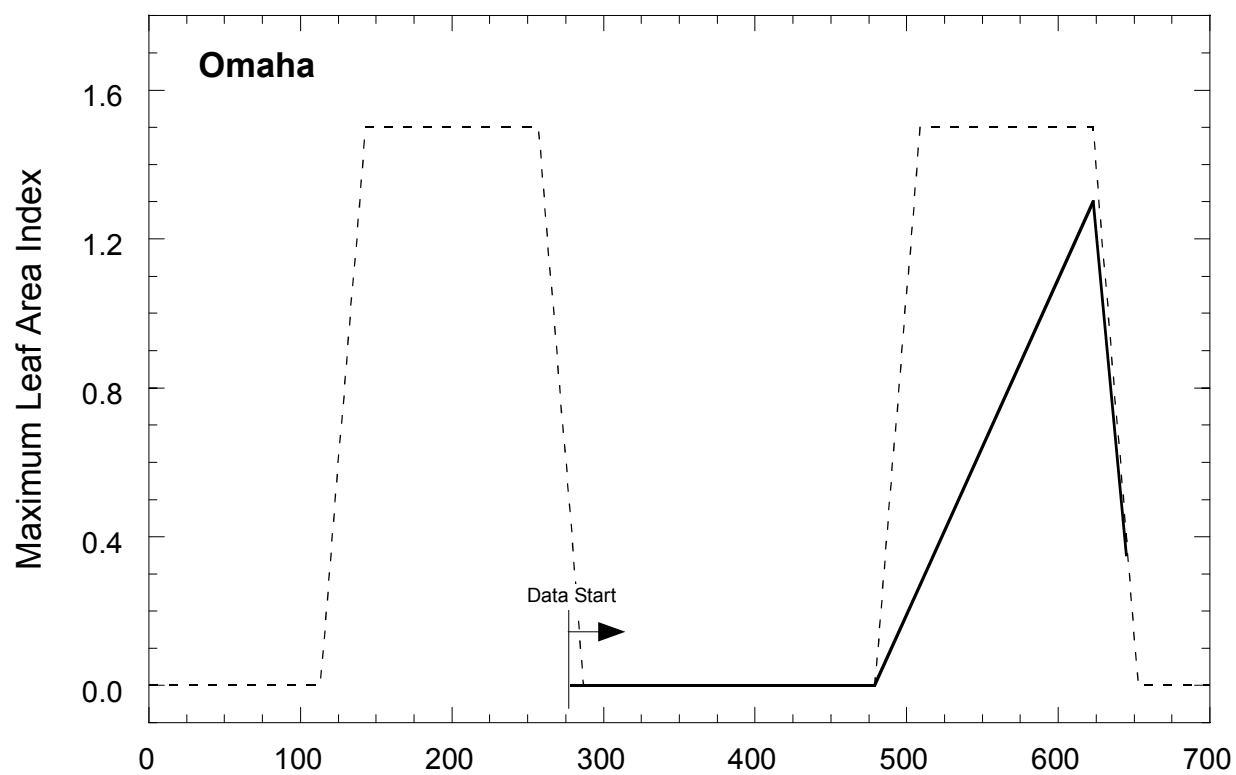


Fig. A10. LAI Plot for Omaha Site.

**APPENDIX 3**  
**FACTORS AFFECTING SURFACE RUNOFF IN FIELD**

Surface runoff from the ACAP test sections ranged between 0 and 14% of precipitation (see Table A1). There are several factors that influence surface runoff, such as rainfall intensity, slope, frozen ground conditions, and the surface layer physical and hydraulic properties. Factors that may have affected surface runoff at each ACAP site are summarized in Table A1.

Table A1. Summary of Surface Runoff Data from ACAP Study.

Climate	Site	Cover Type	Slope (%)	Tilling	Frozen Ground	Surface Runoff (% of Precip.)
Cool Semi-Arid	Boardman	"Thin" Monolithic	25	-	-	0.0
Cool Semi-Arid	Boardman	"Thick" Monolithic Barrier	25	-	-	0.0
Cool Semi-Arid	Boardman	Composite Barrier	25	-	-	0.0
Sub Humid	Marina	Monolithic Barrier	25	√ *	-	0.0
Humid Subtropical	Albany	Monolithic Barrier	5	√ *	-	0.1
Cool Humid	Cedar Rapids	Compacted Clay Barrier	5	-	√	1.9
Cool Semi-Arid	Polson	Composite Barrier	5	-	√	2.3
Cool Humid	Cedar Rapids	Composite Barrier	5	-	√	2.8
Arid to Semi-Arid	Altamont	Composite Barrier	5	-	-	3.0
Cool Semi-Arid	Polson	Capillary Barrier	5	-	√	3.1
Cool Humid	Cedar Rapids	Monolithic Barrier	5	√	√	3.5
Cool Humid	Omaha	"Thick" Capillary Barrier	25	-	√	5.0
Arid to Semi-Arid	Altamont	Monolithic Barrier	5	-	-	5.4
Semi-Arid	Sacramento	"Thick" Monolithic Barrier	5	-	-	5.9
Cool Humid	Omaha	Composite Barrier	25	-	√	6.3
Cool Humid	Omaha	"Thin" Capillary Barrier	25	-	√	6.6
Cool Semi-Arid	Helena	Capillary Barrier	5	-	√	7.4
Humid Subtropical	Albany	Compacted Clay Barrier	5	-	-	10.4
Semi-Arid	Sacramento	"Thin" Monolithic Barrier	5	-	-	10.5
Sub Humid	Marina	Composite Barrier	25	-	-	14.2

\*Includes trenching to plant trees.

**APPENDIX 4**  
**WATER BALANCE GRAPHS OF ORIGINAL UNSAT-H**  
**SIMULATIONS**



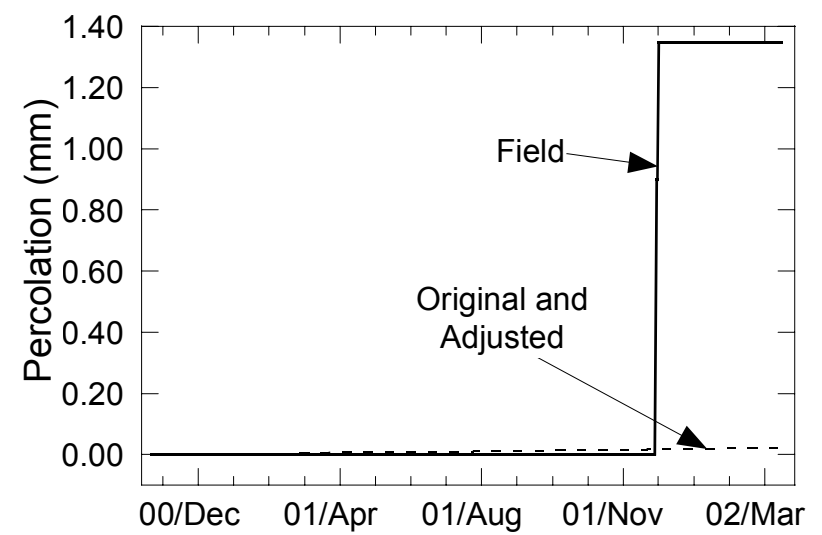
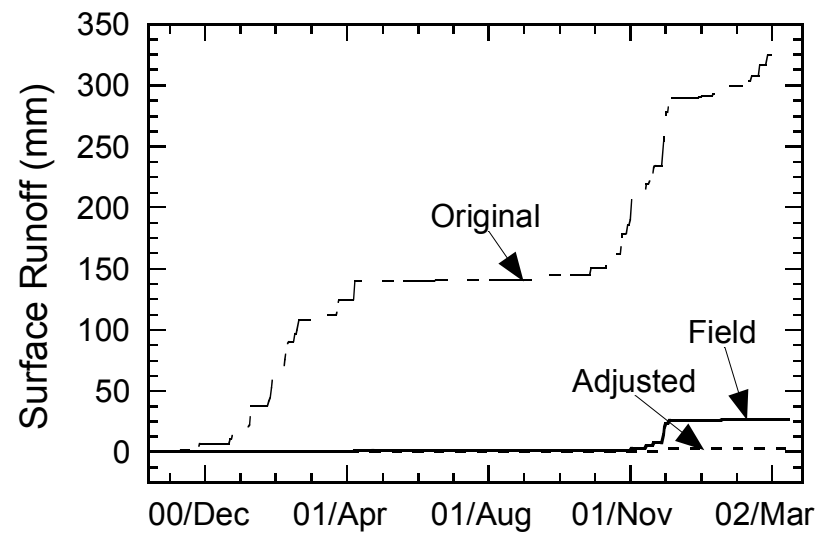
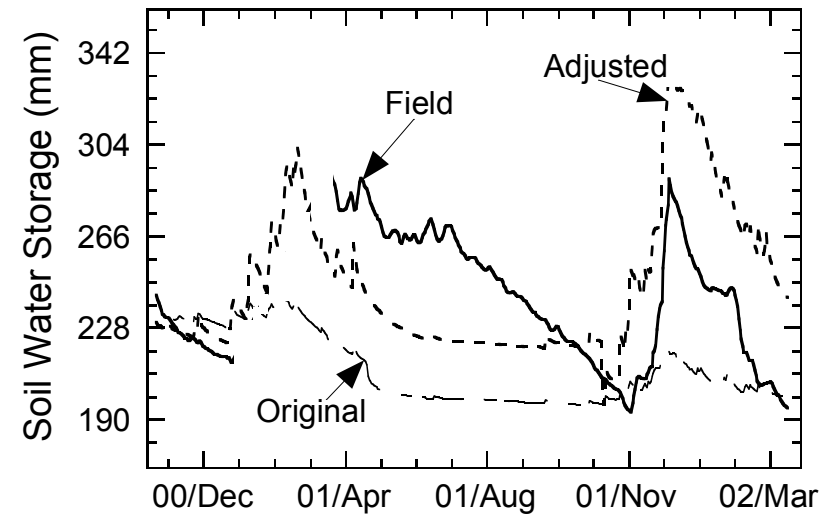
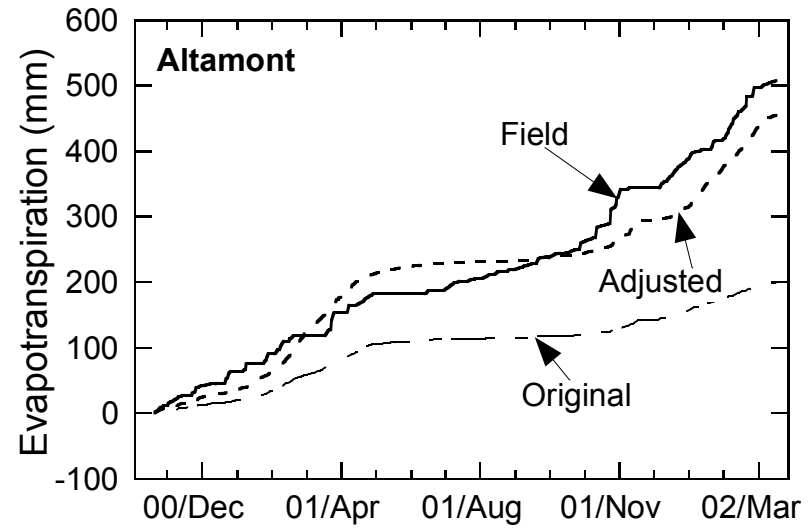


Fig. A11. UNSAT-H Comparison to Field Data at the Altamont Site.

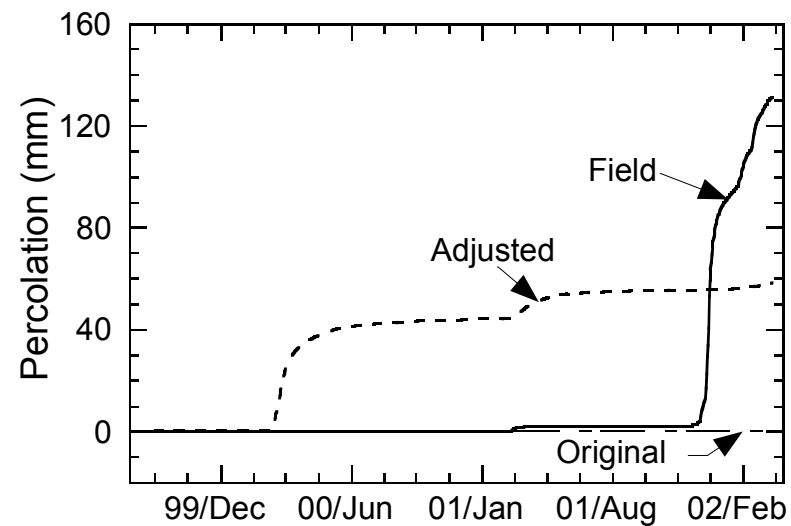
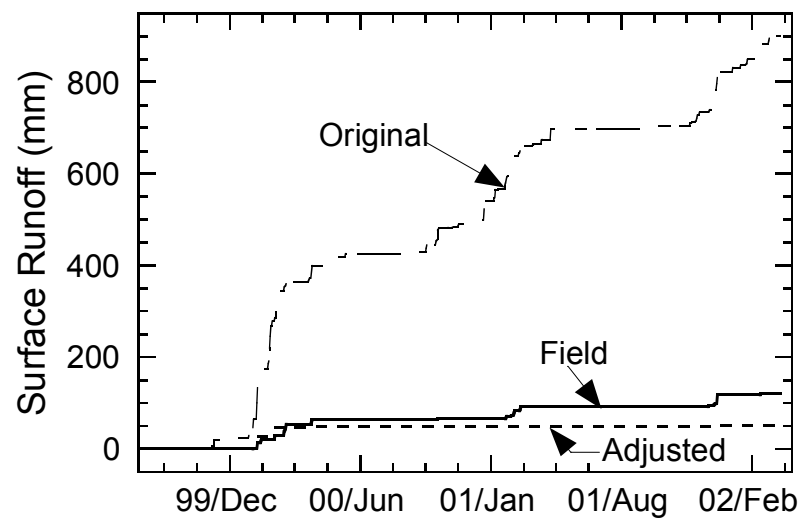
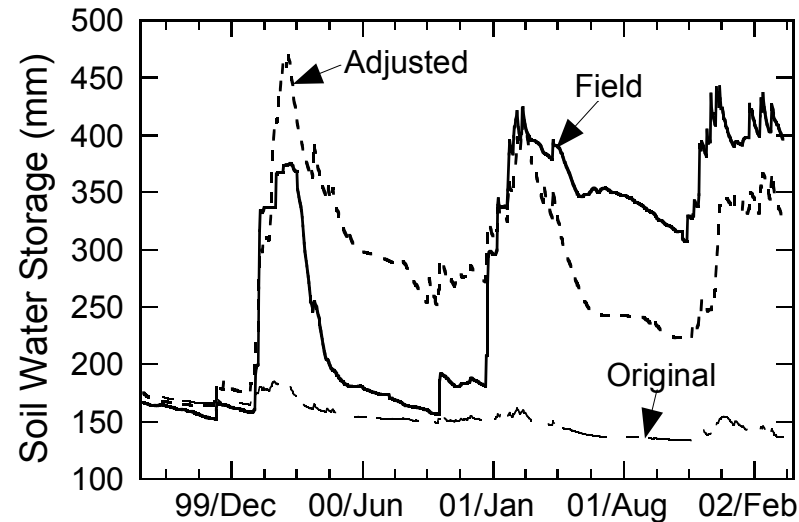
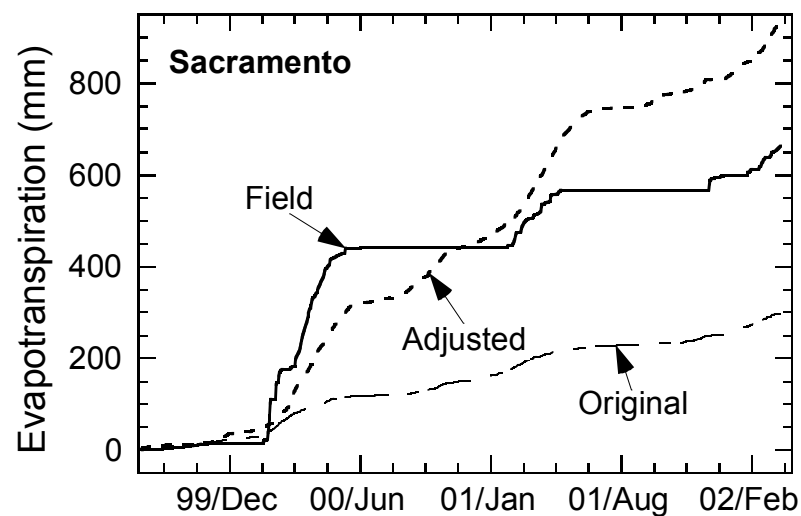


Fig. A12. UNSAT-H Comparison to Field Data for Thin Monolithic Barrier at the Sacramento Site.

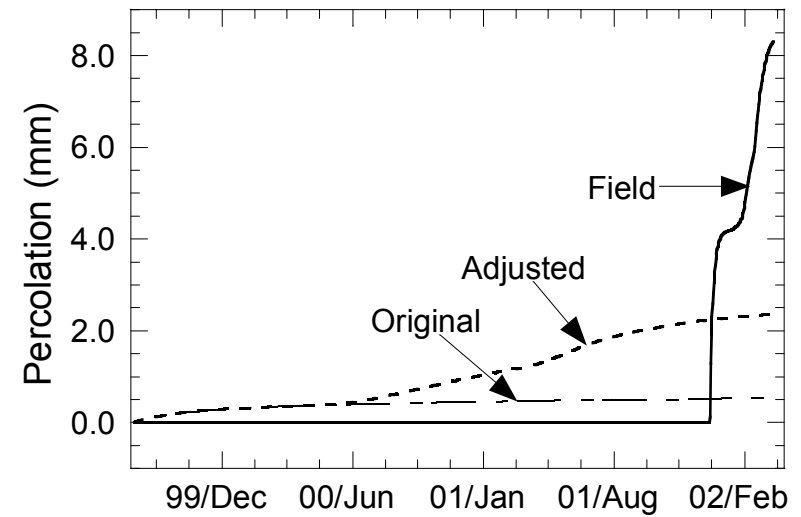
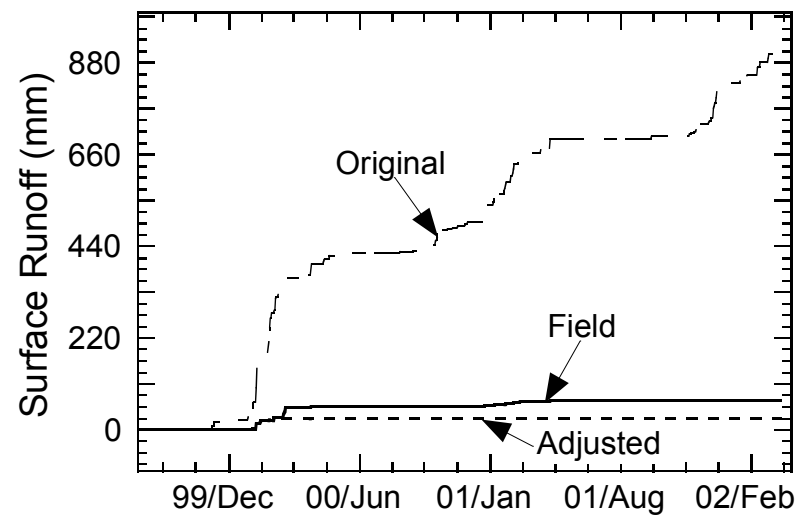
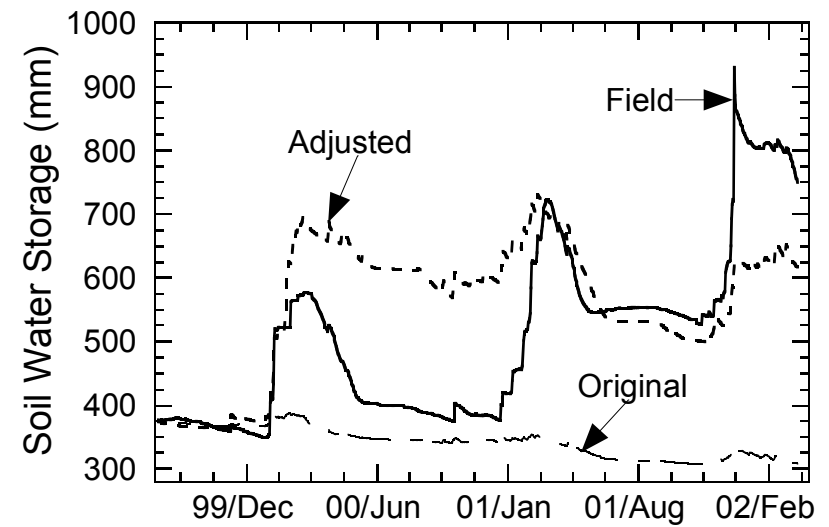
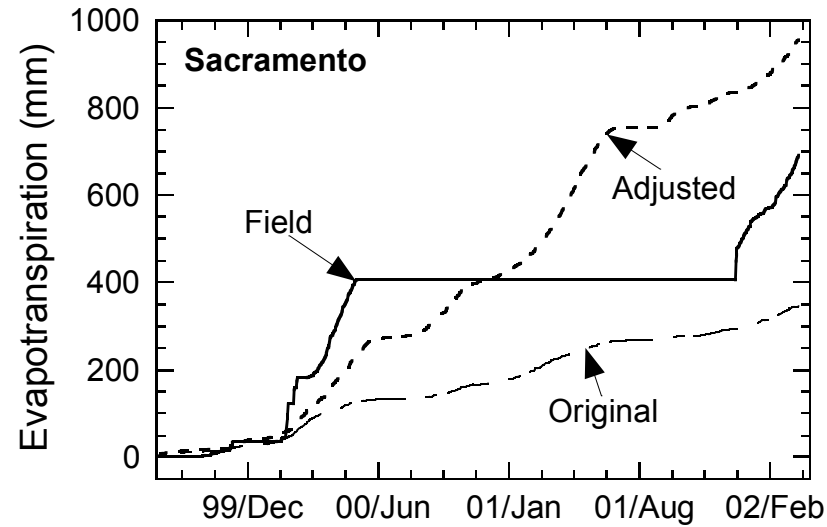


Fig. A13. UNSAT-H Comparison to Field Data for Thick Monolithic Barrier at the Sacramento Site.

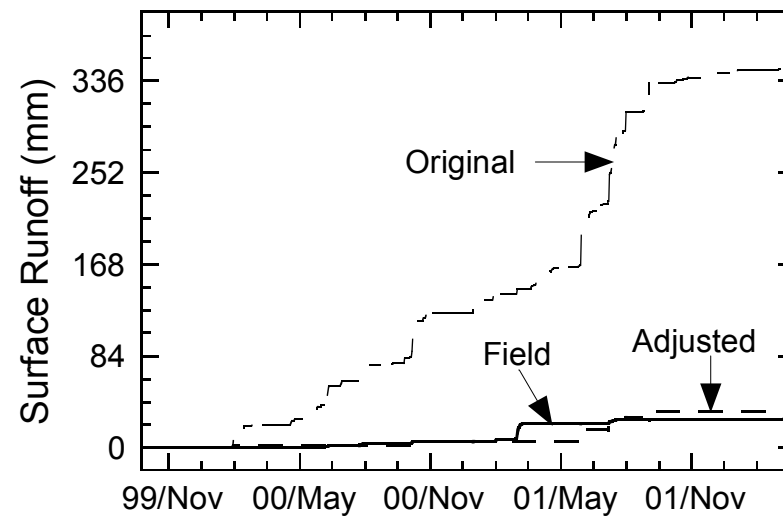
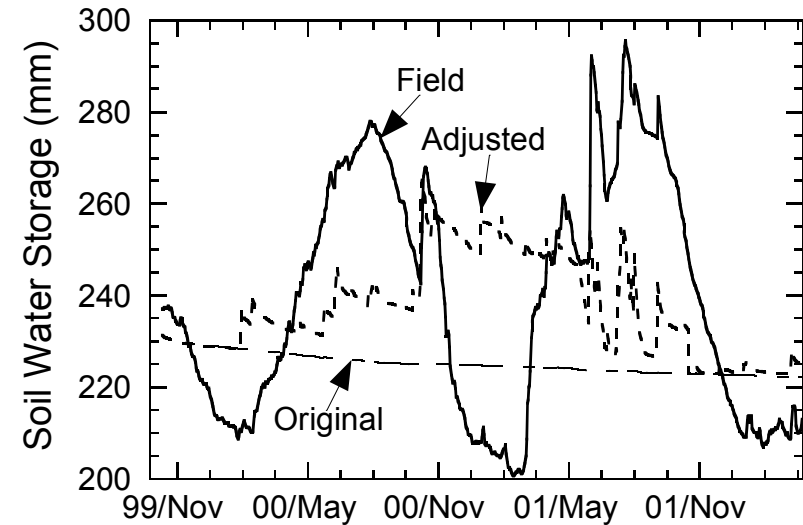
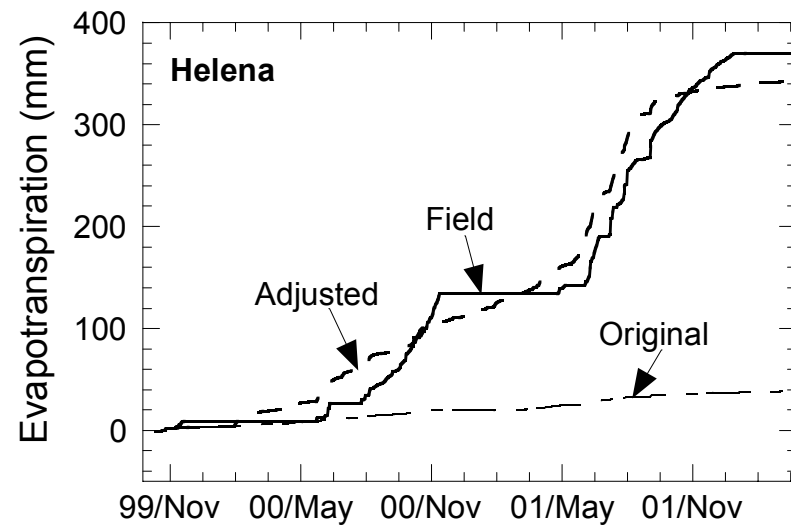


Fig. A14. UNSAT-H Comparison to Field Data at the Helena Site.

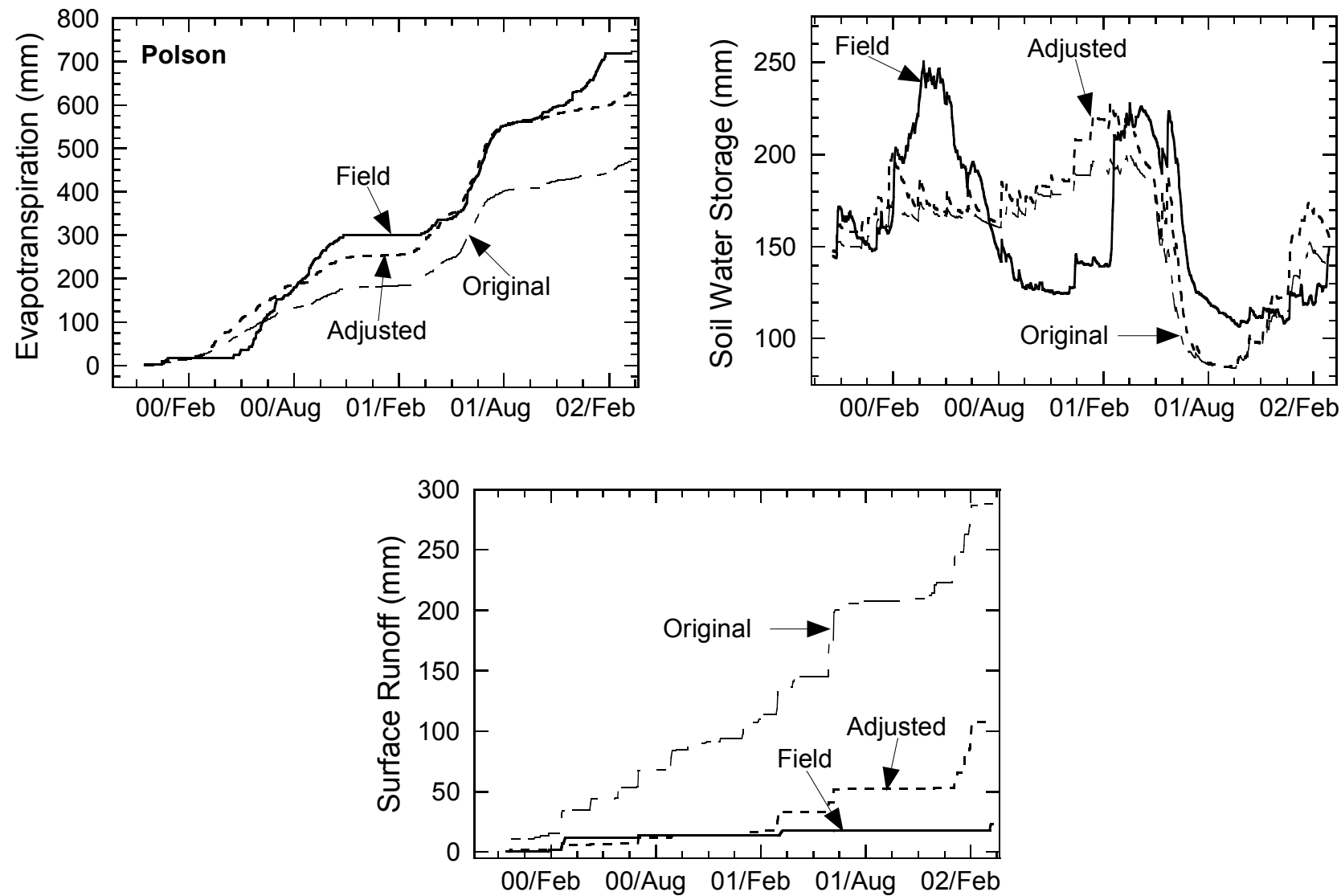


Fig. A15. UNSAT-H Comparison to Field Data at the Polson Site.

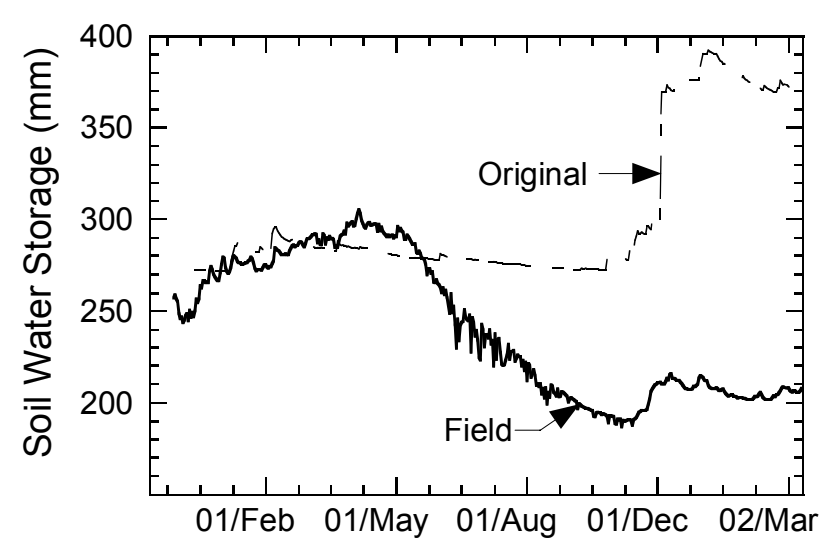
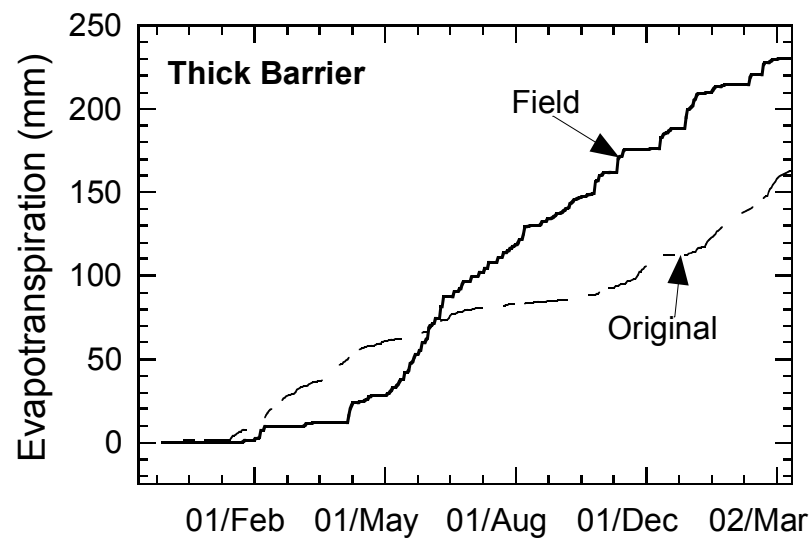
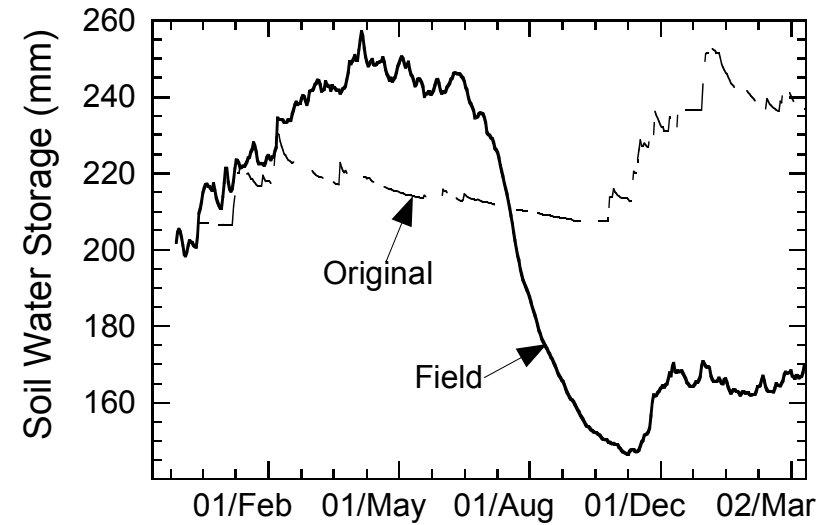
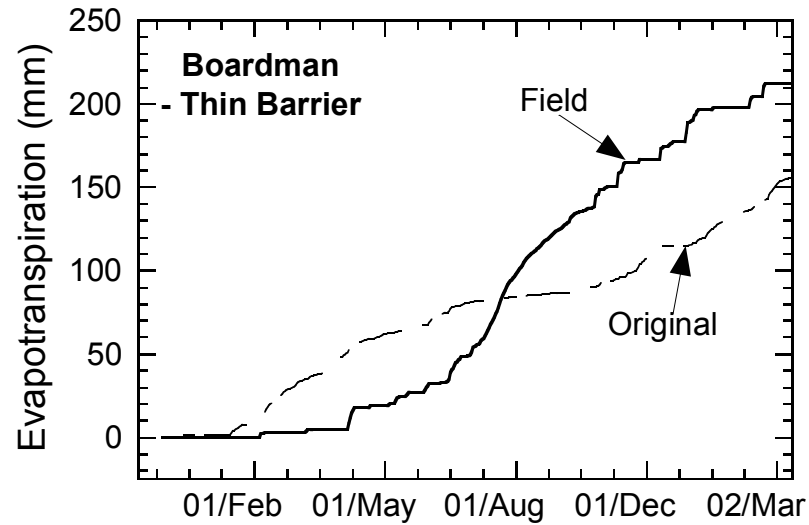


Fig. A16. UNSAT-H Comparison to Field Data at the Boardman Site.

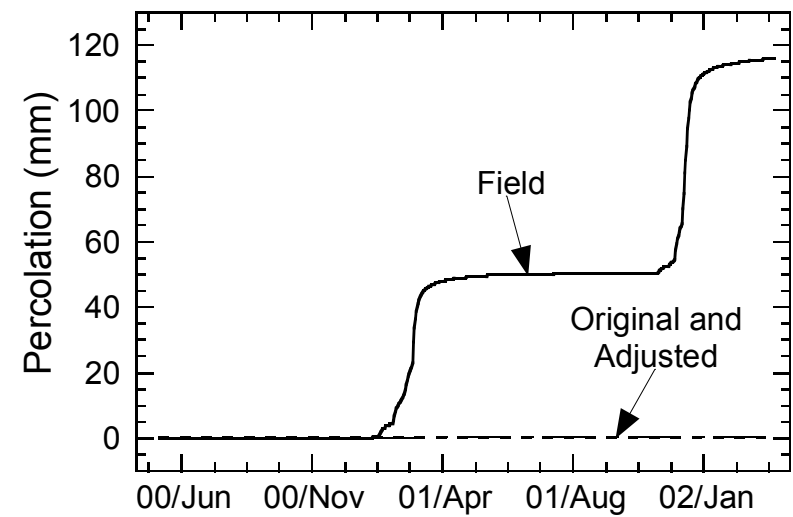
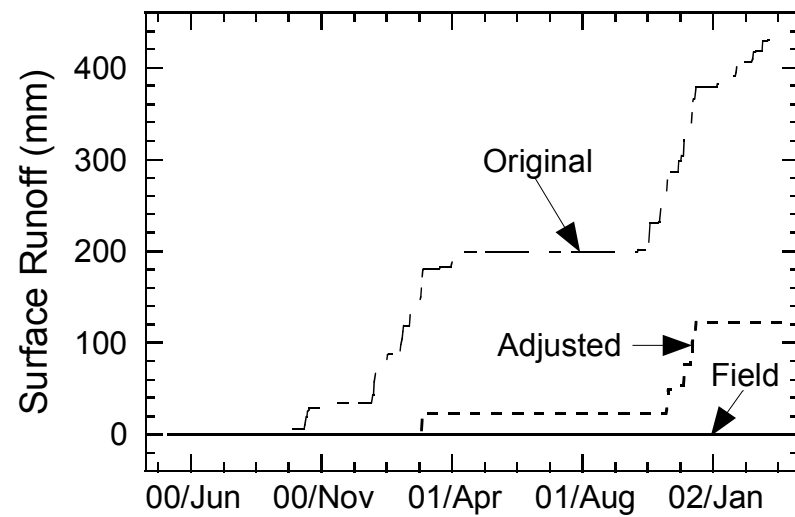
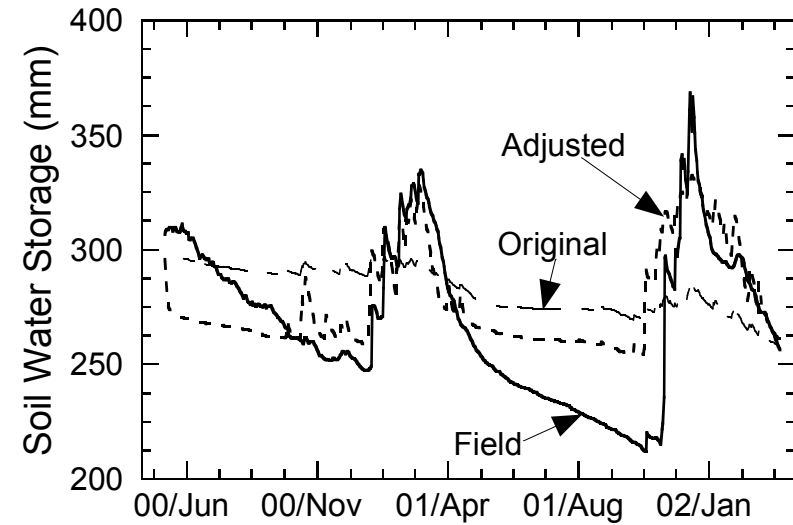
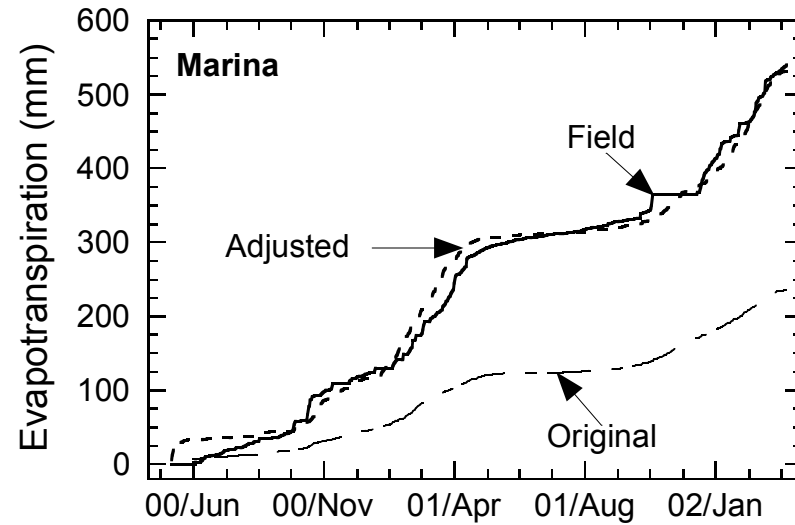


Fig. A17. UNSAT-H Comparison to Field Data at the Marina Site.

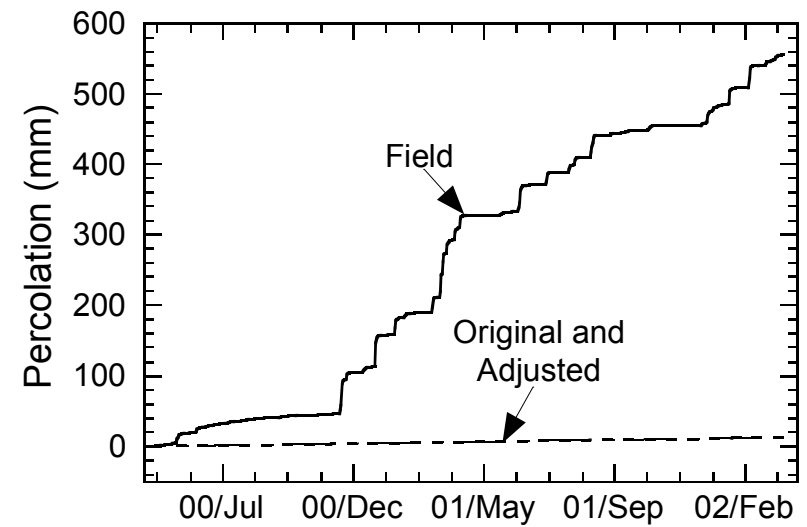
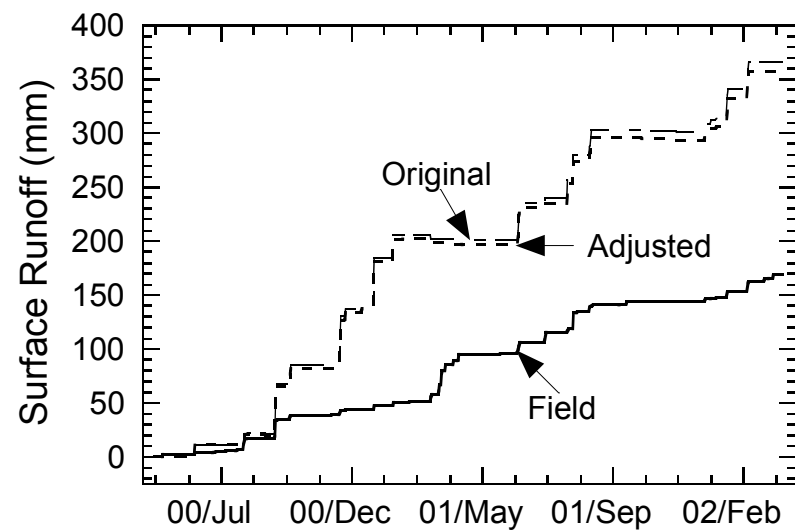
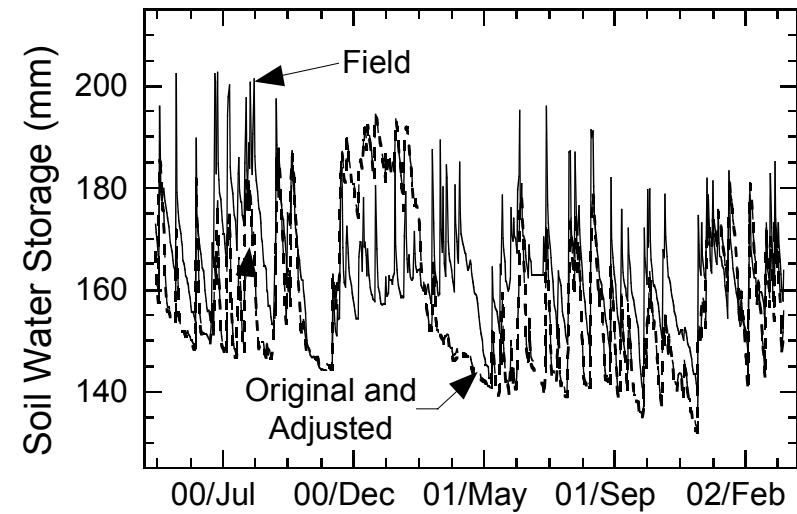
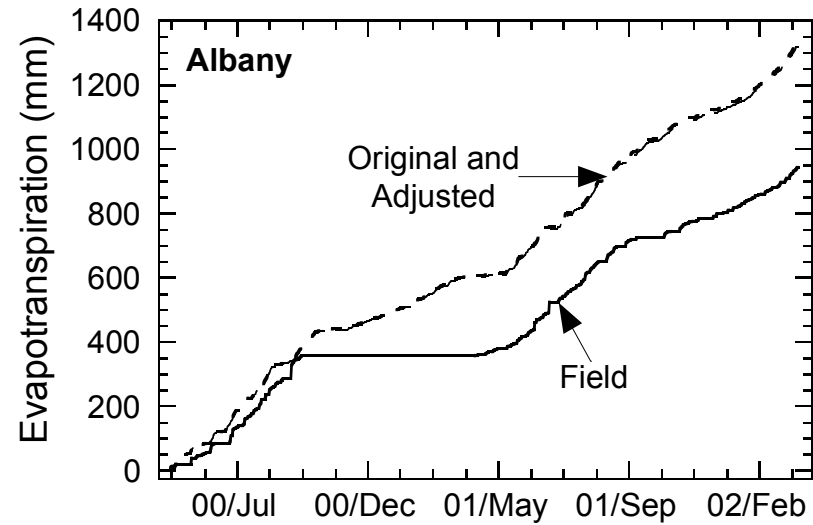


Fig. A18. UNSAT-H Comparison to Field Data for the Compacted Clay Cover at the Albany Site.



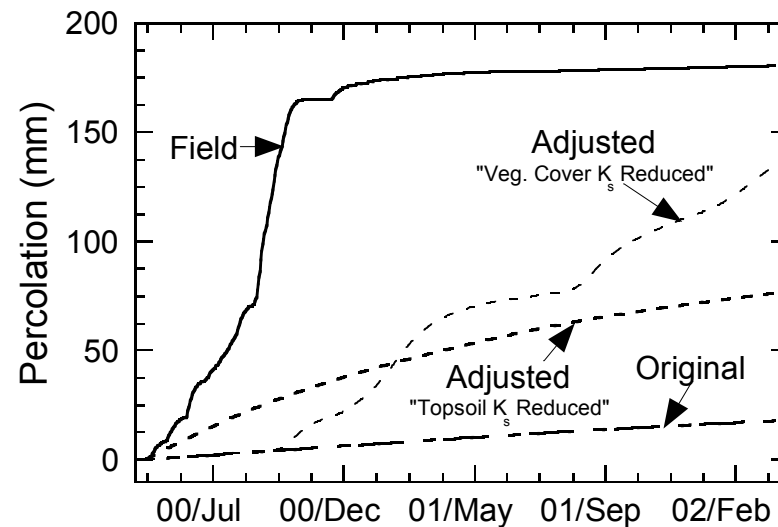
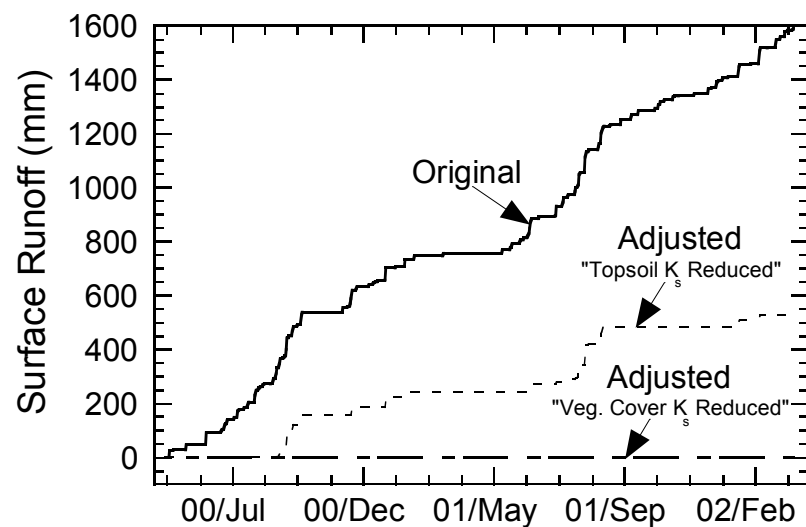
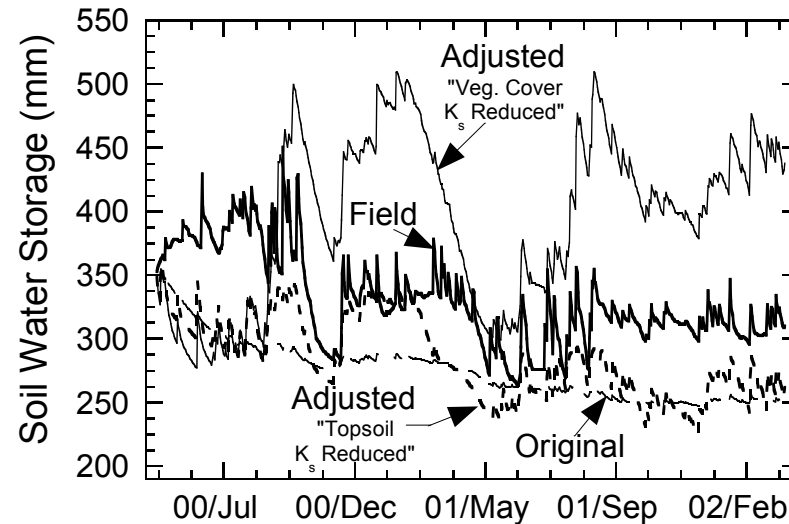
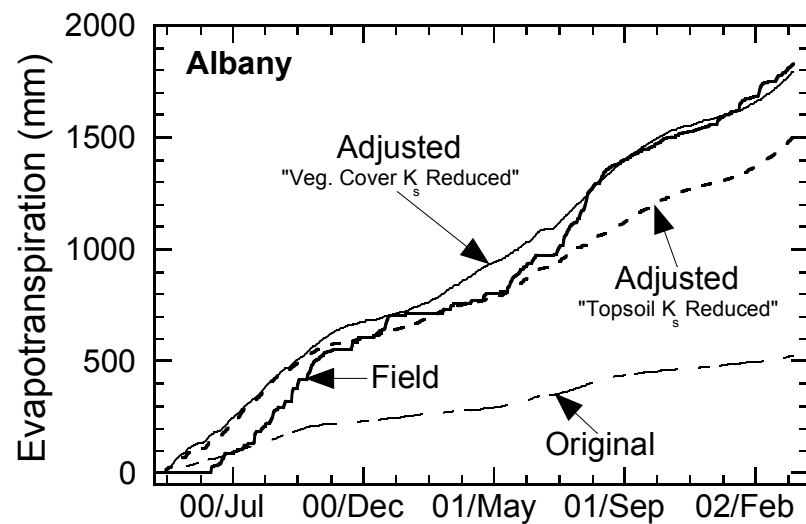


Fig. A19. UNSAT-H Comparison to Field Data for the ECap at the Albany Site.

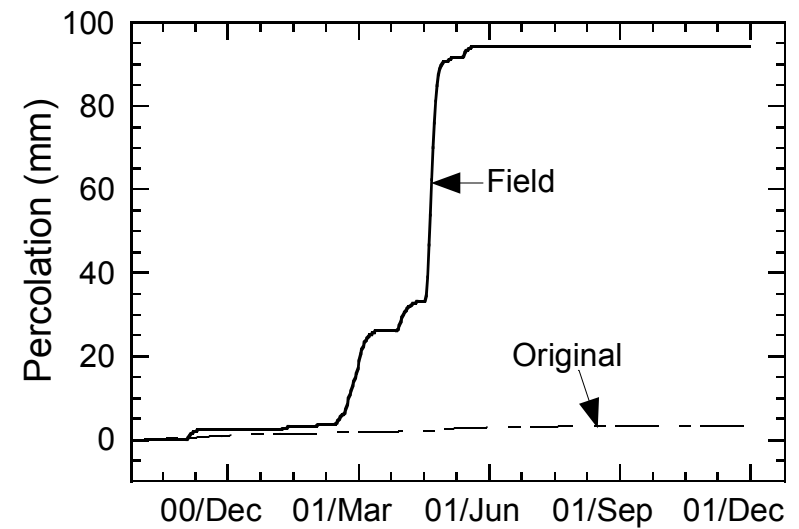
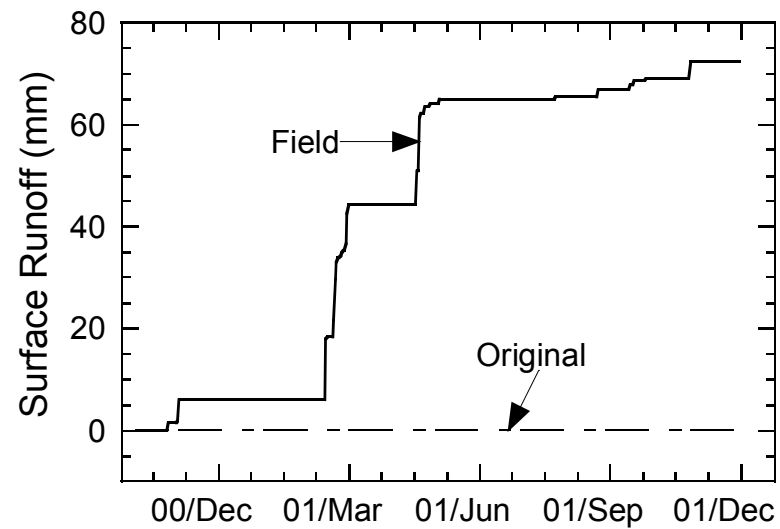
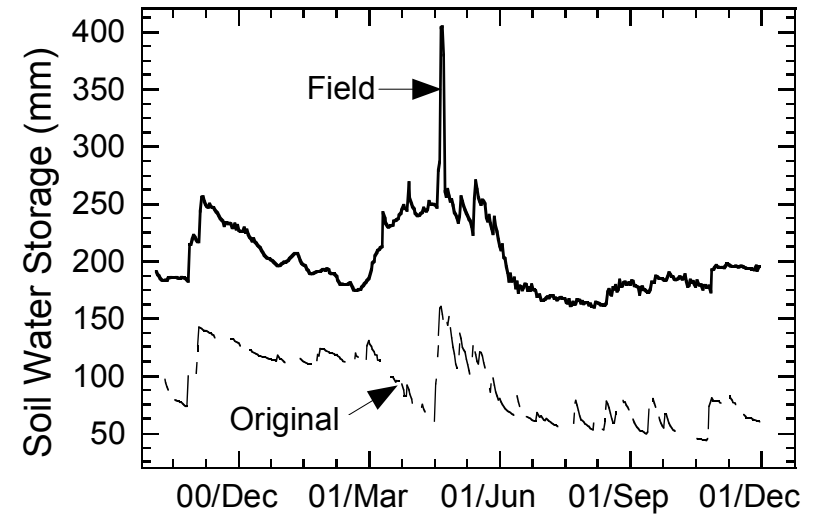
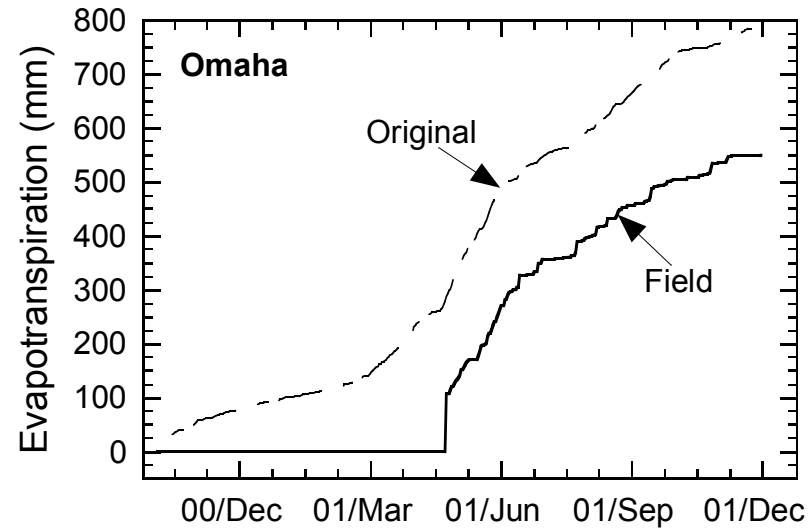


Fig. A20. UNSAT-H Comparison to Field Data for the Thin Monolithic Barrier at the Omaha Site.

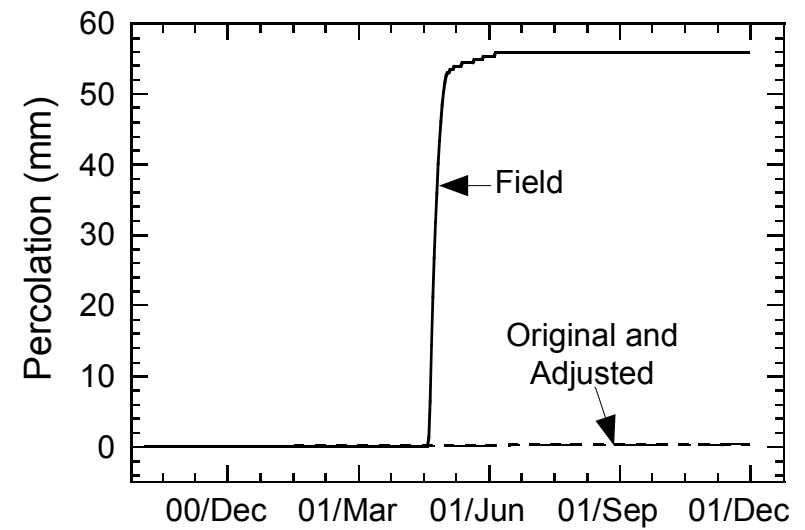
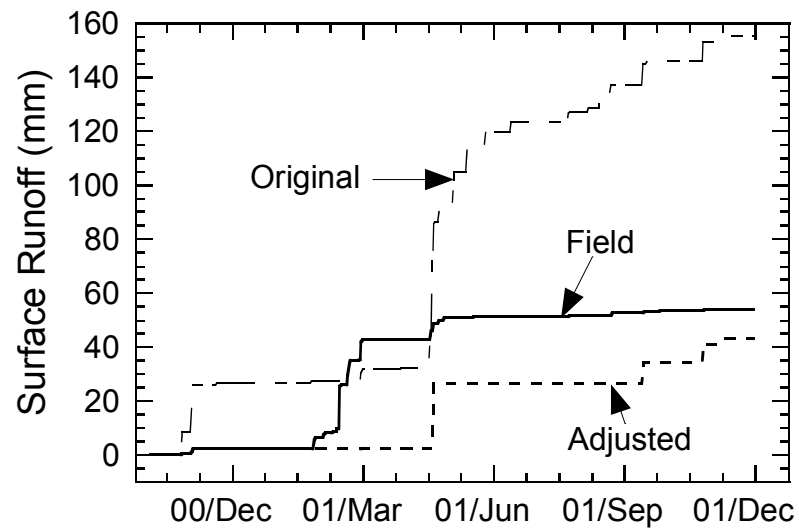
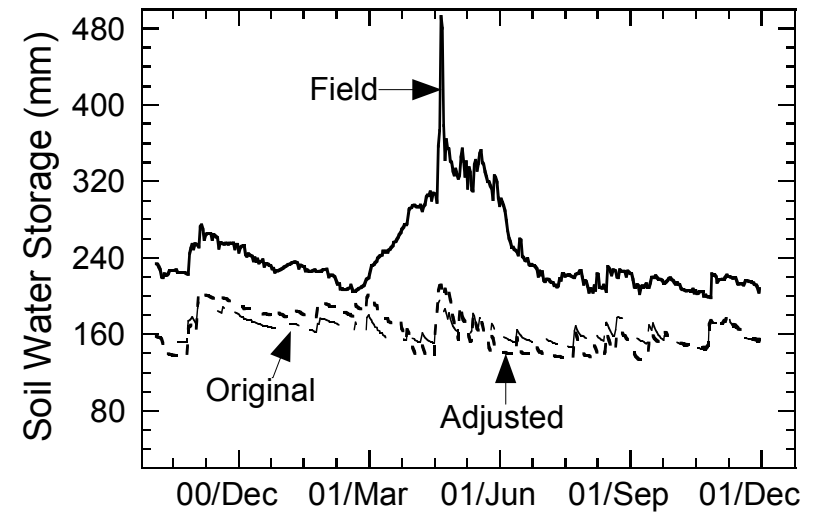
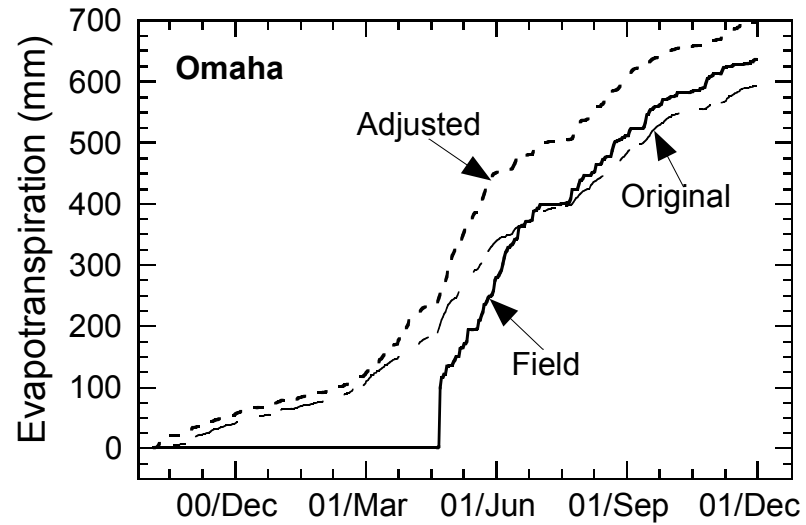


Fig. A21. UNSAT-H Comparison to Field Data for the Thick Monolithic Barrier at the Omaha Site.

**APPENDIX 5**  
**WATER BALANCE GRAPHS OF ORIGINAL HELP SIMULATIONS**

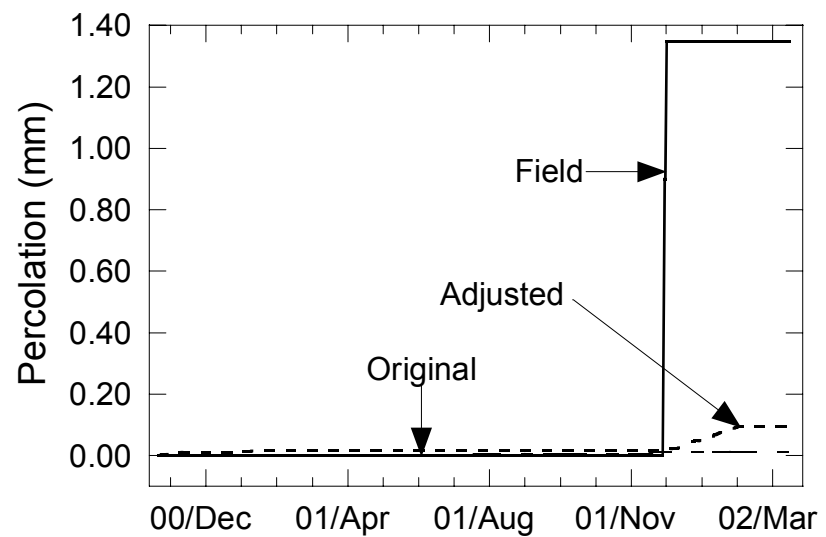
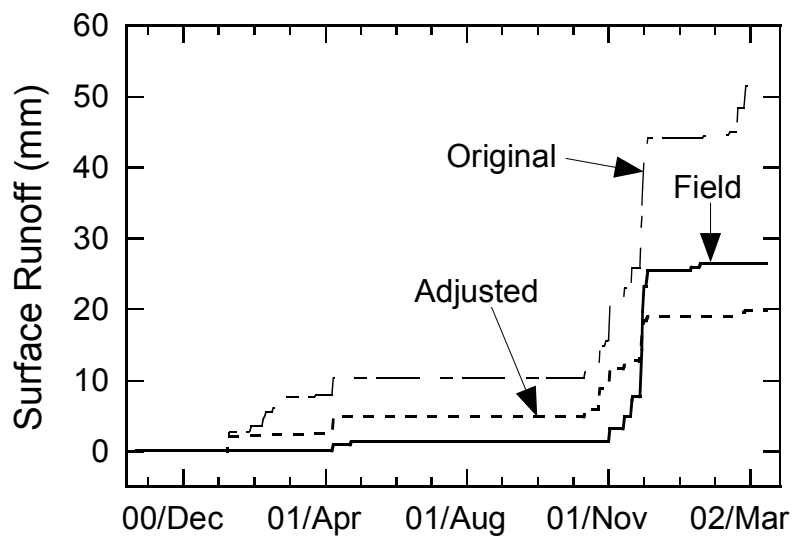
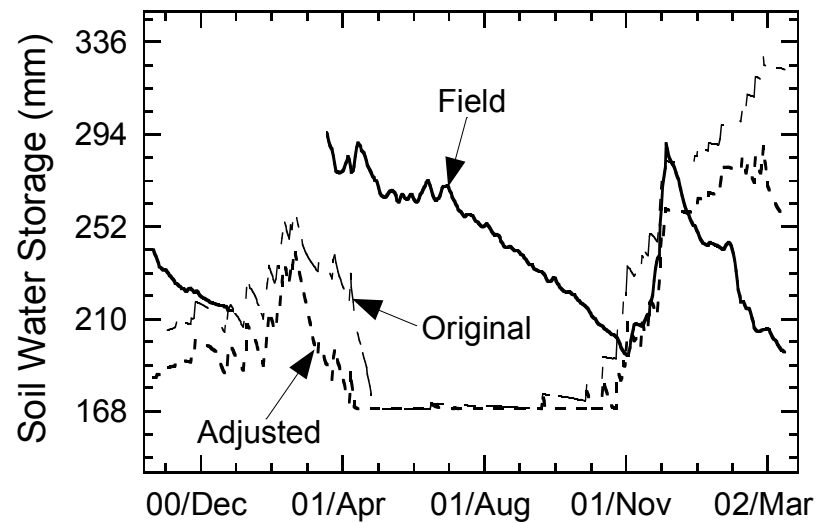
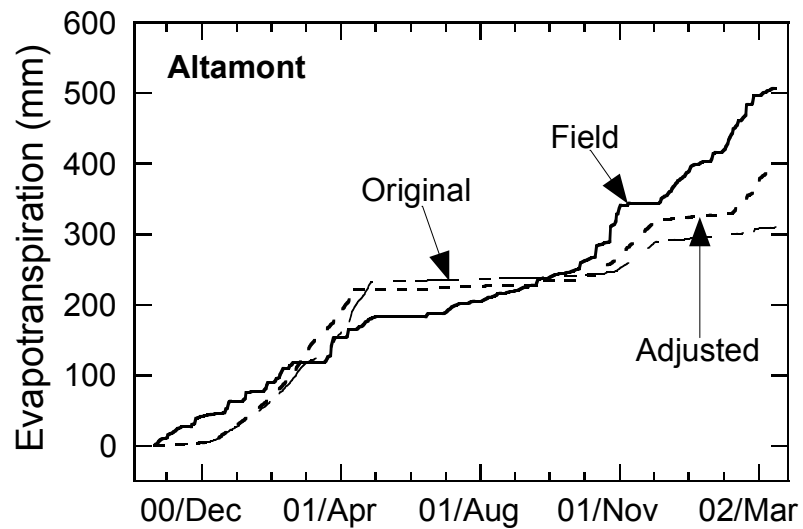


Fig. A22. HELP Comparison to Field Data for the Alternative Cover at the Altamont Site.

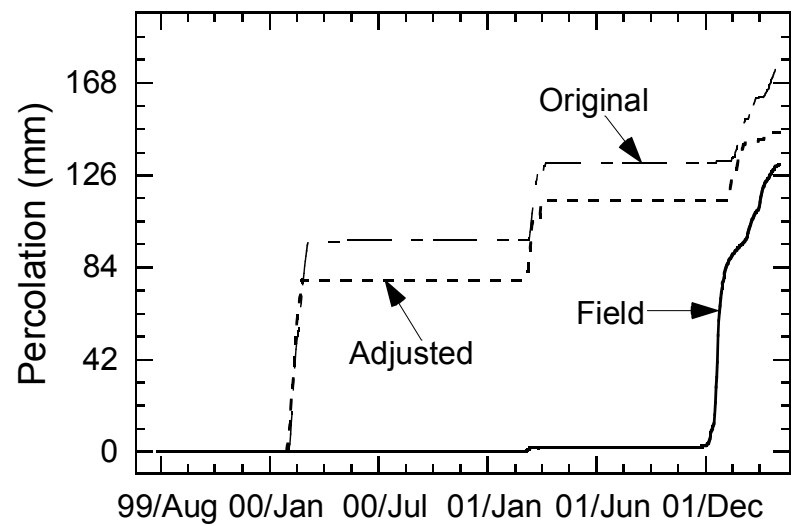
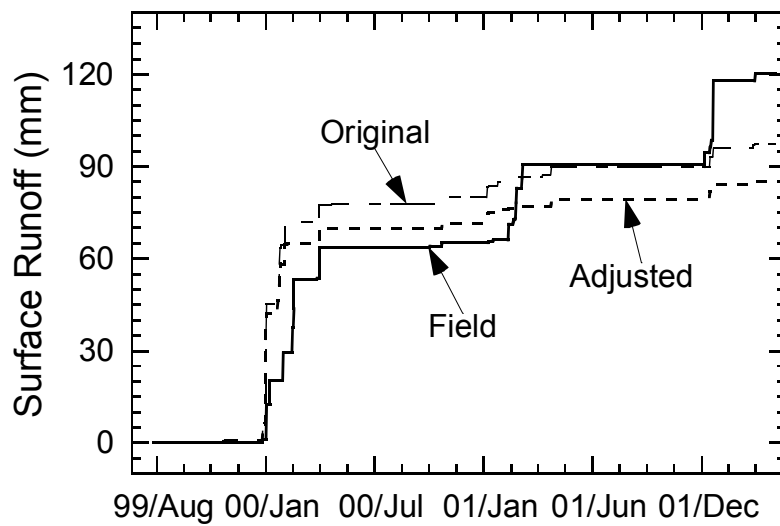
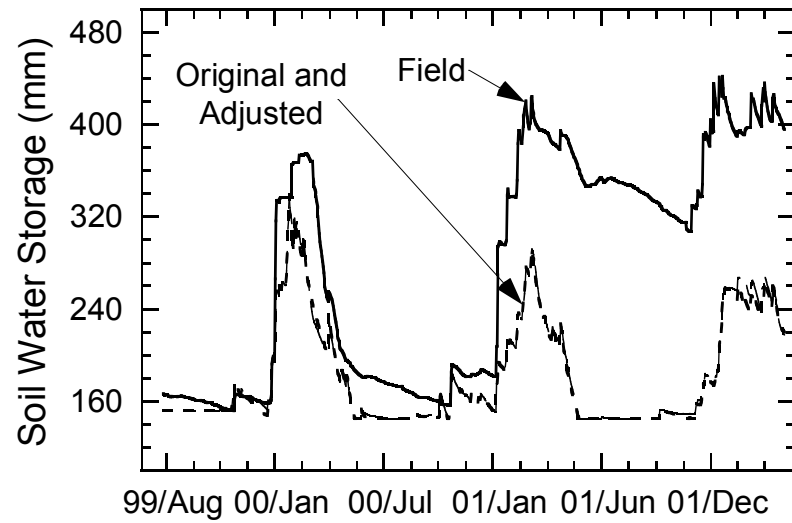
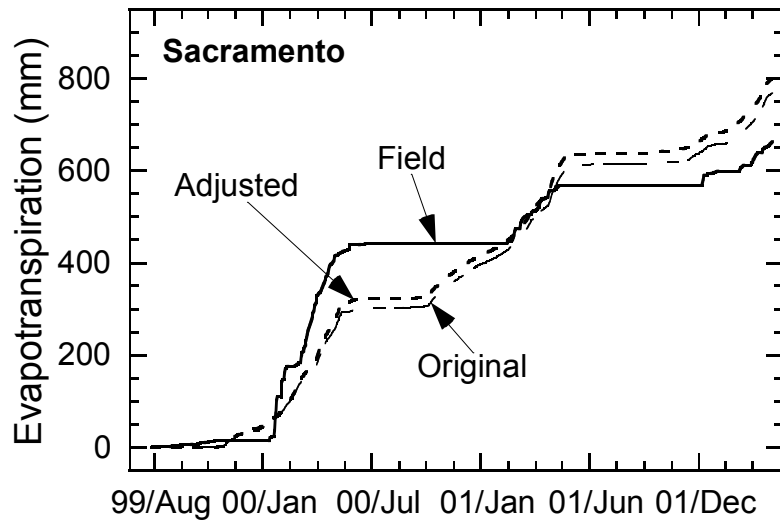


Fig. A23. HELP Comparison to Field Data for the Thin Monolithic Barrier at the Sacramento Site.

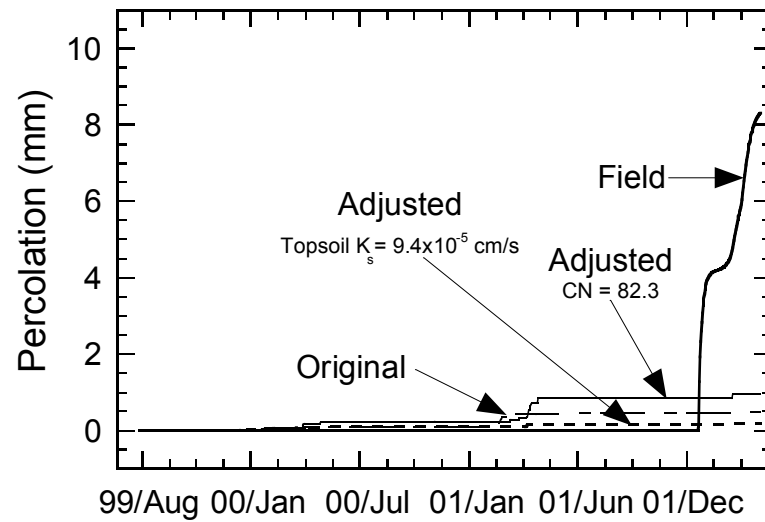
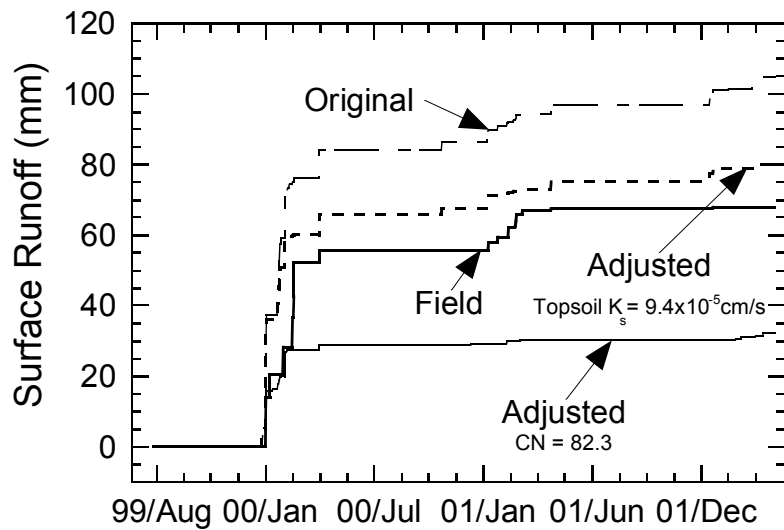
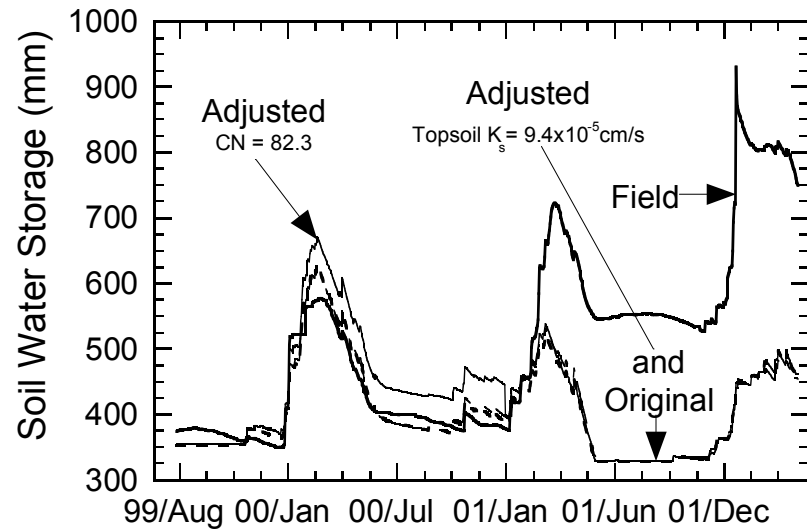
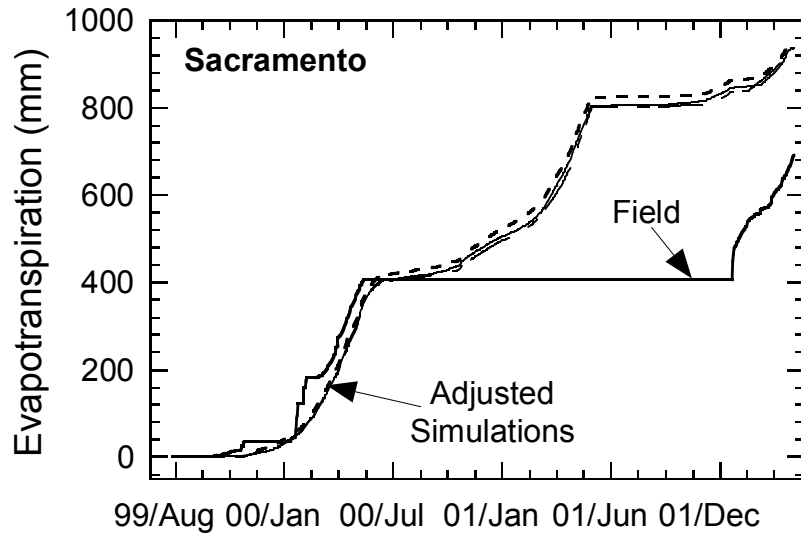


Fig. A24. HELP Comparison to Field Data for the Thick Monolithic Barrier at the Sacramento Site.

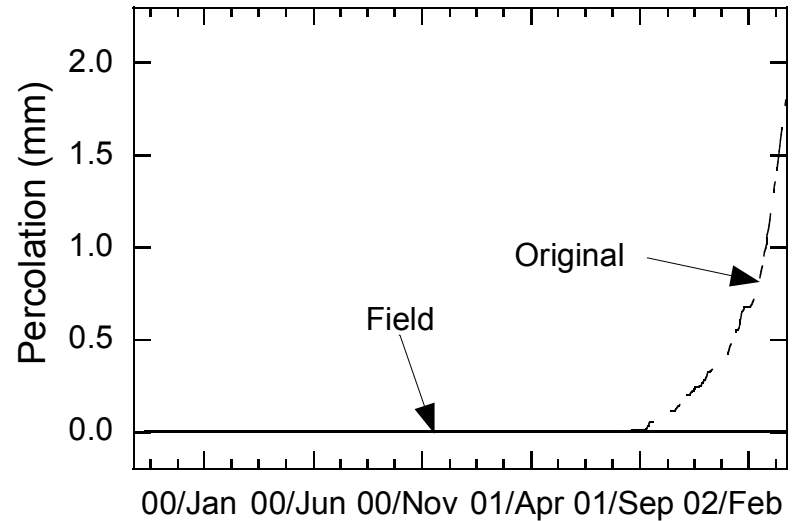
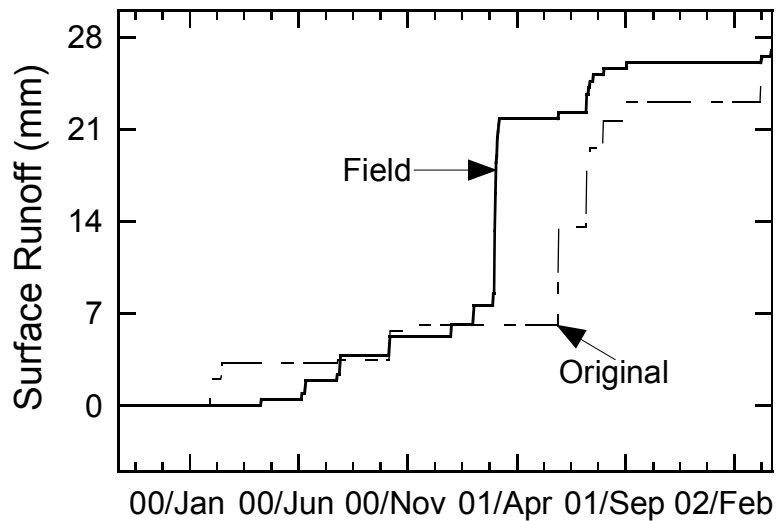
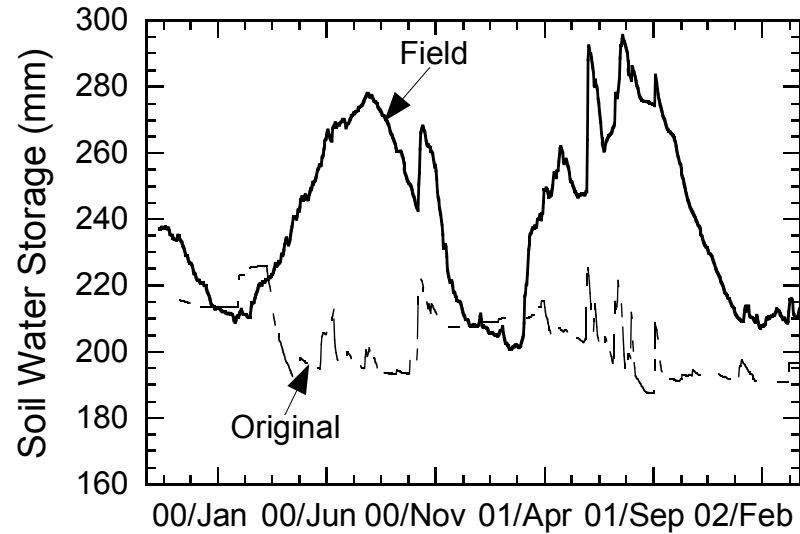
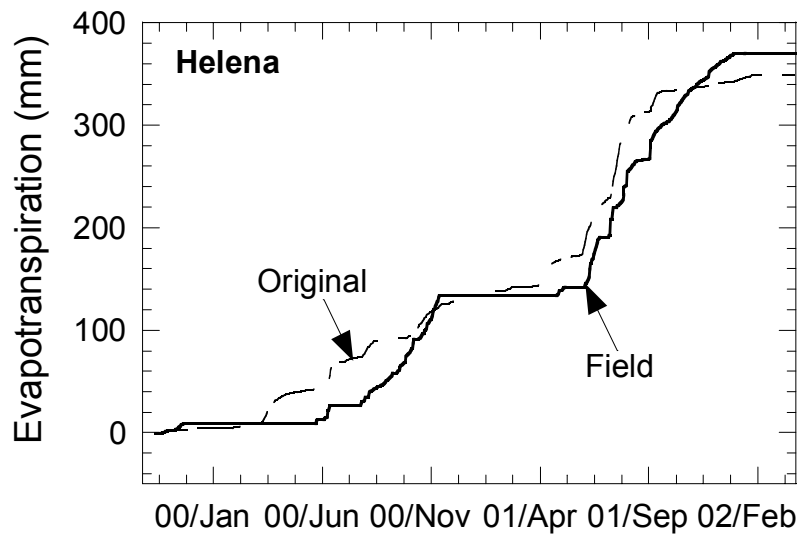


Fig. A25. HELP Comparison to Field Data for the Alternative Cover at the Helena Site.



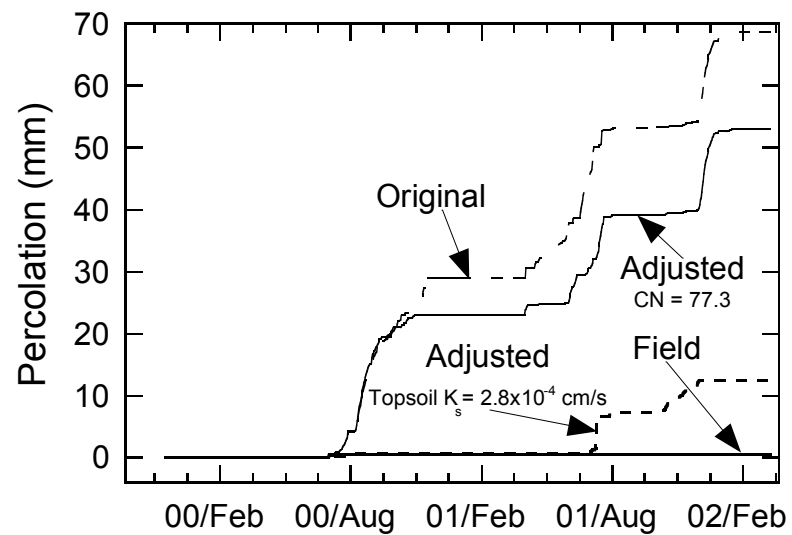
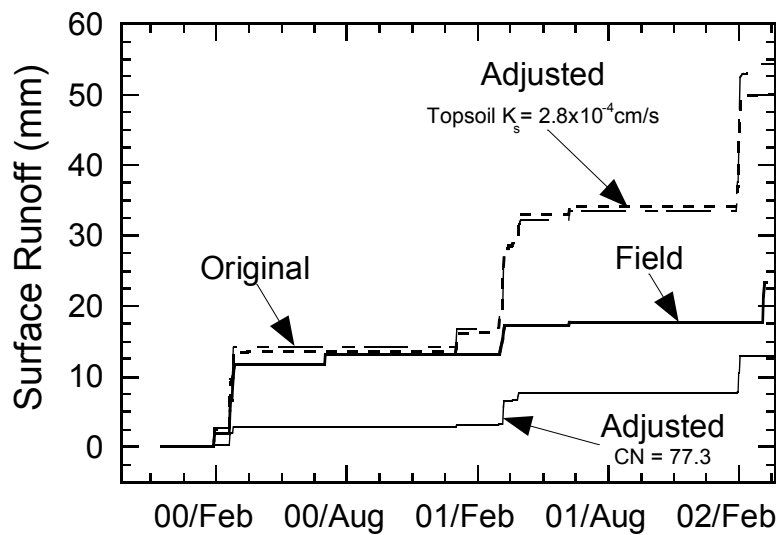
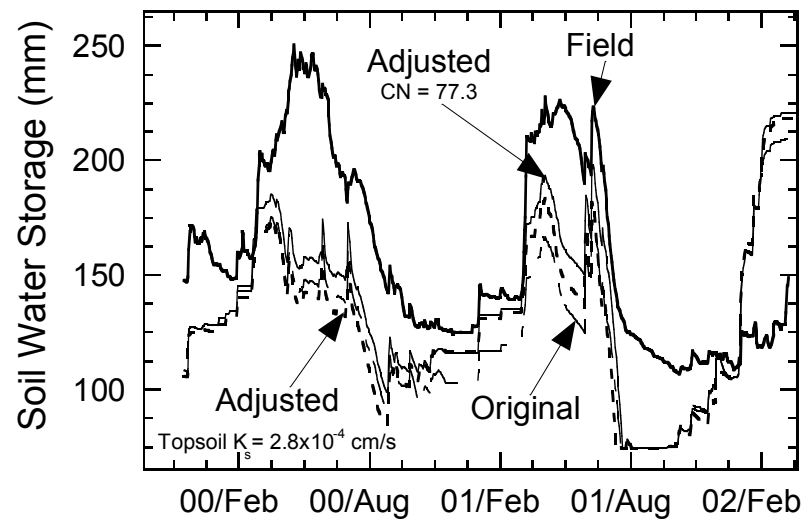
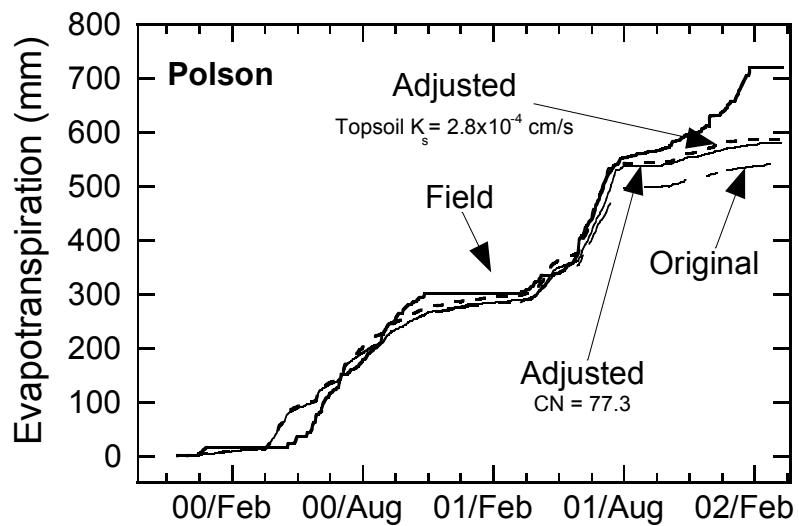


Fig. A26. HELP Comparison to Field Data for the Alternative Cover at the Polson Site.

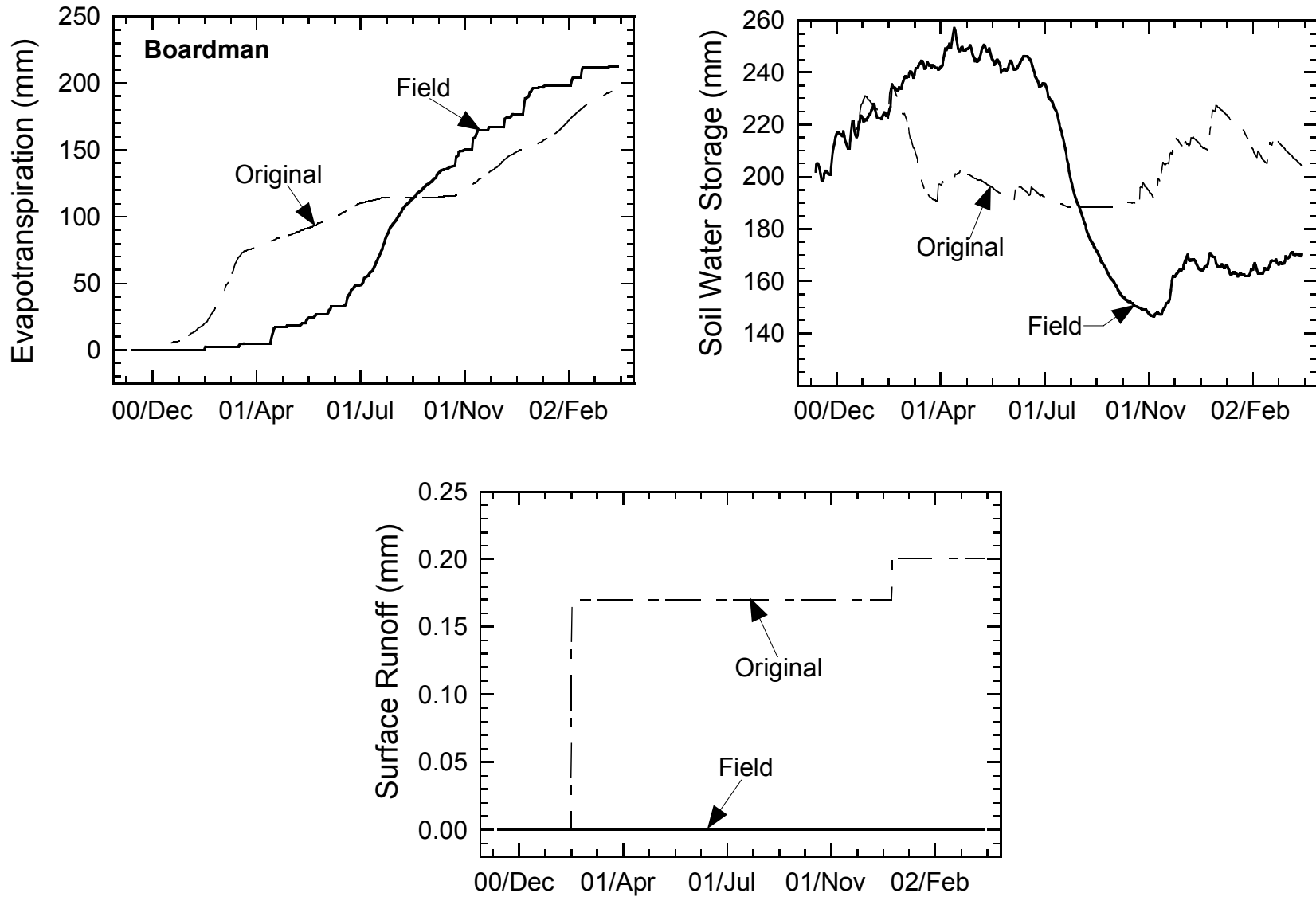


Fig. A27. HELP Comparison to Field Data for the Thin Monolithic Barrier at the Boardman Site.

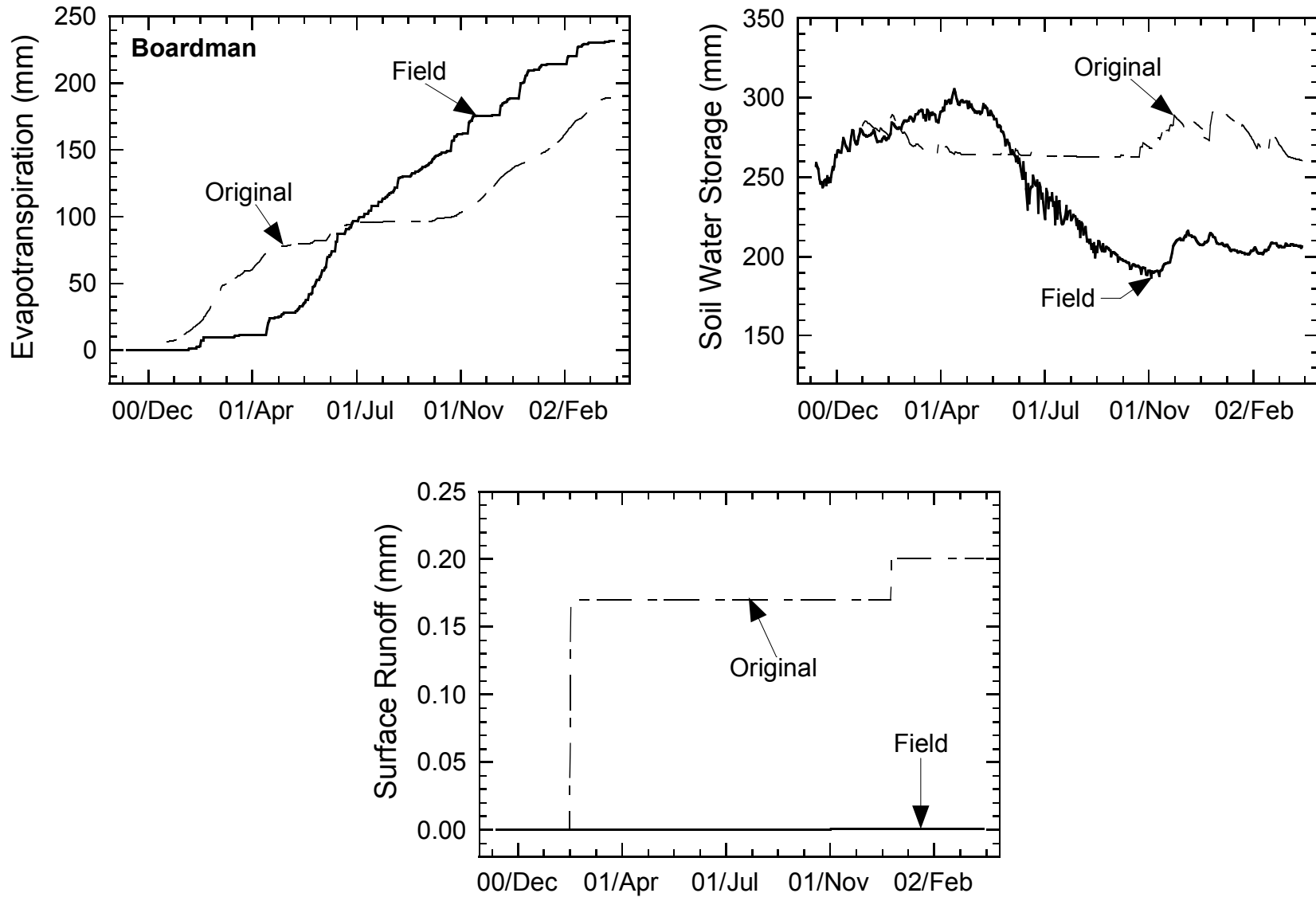


Fig. A28. HELP Comparison to Field Data for the Thick Monolithic Barrier at the Boardman Site.

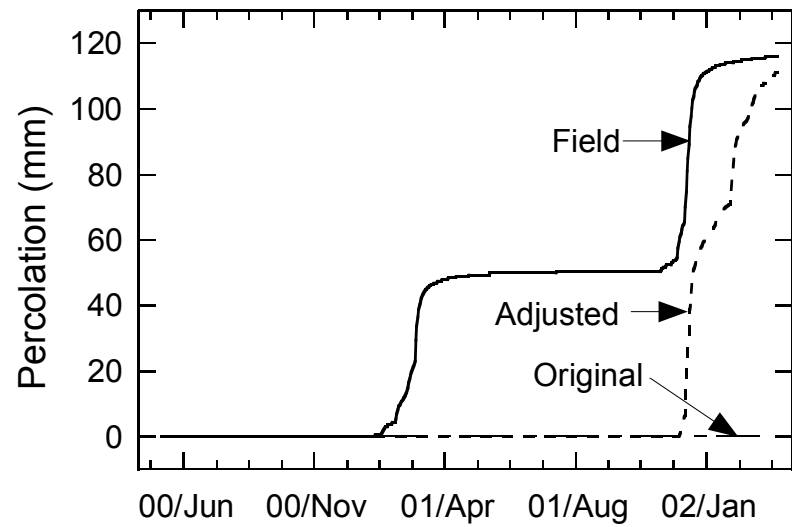
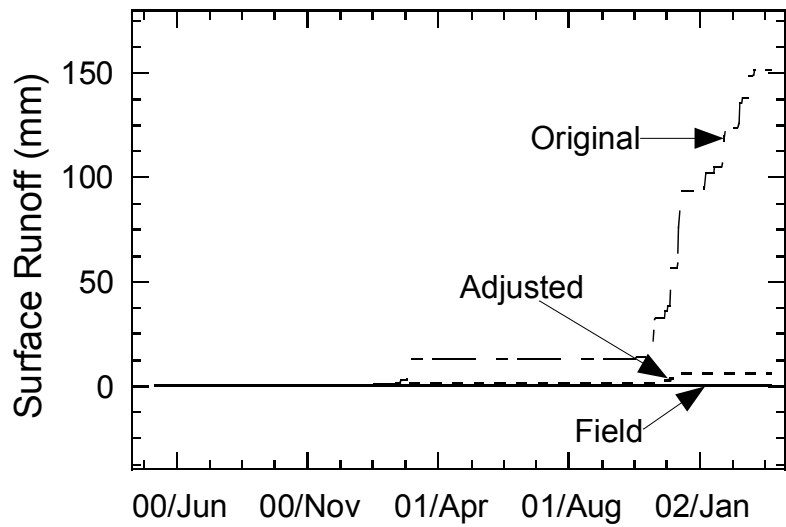
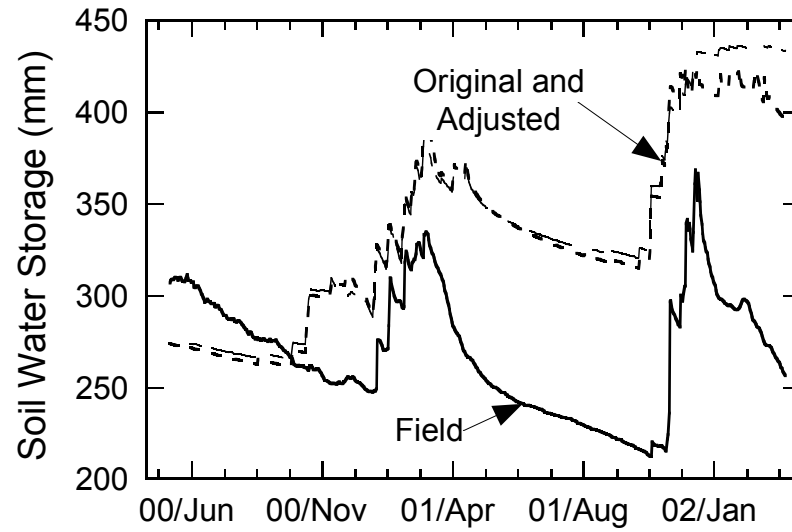
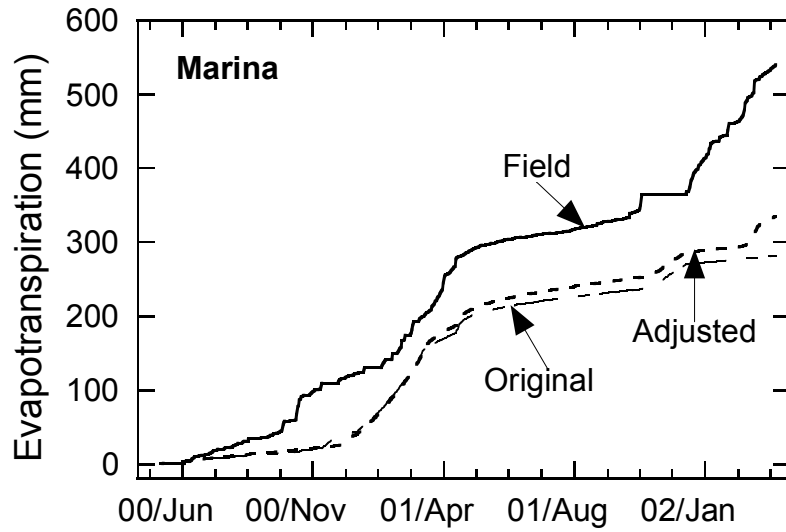


Fig. A29. HELP Comparison to Field Data for the Alternative Cover at the Marina Site.

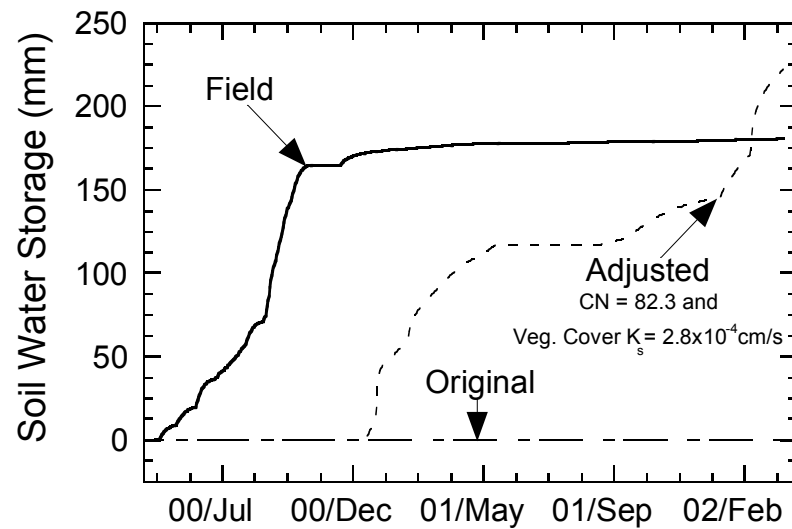
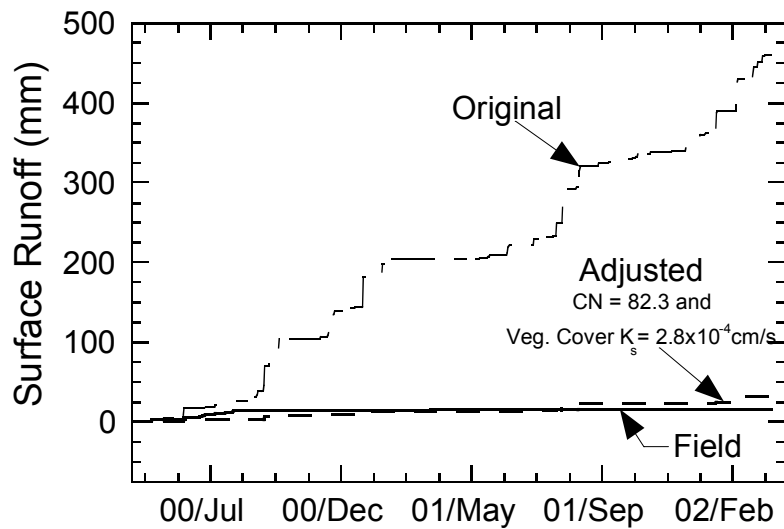
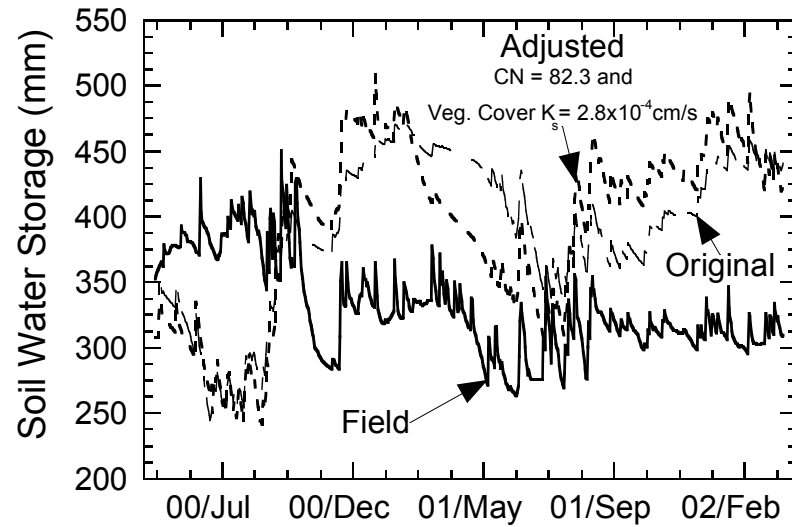
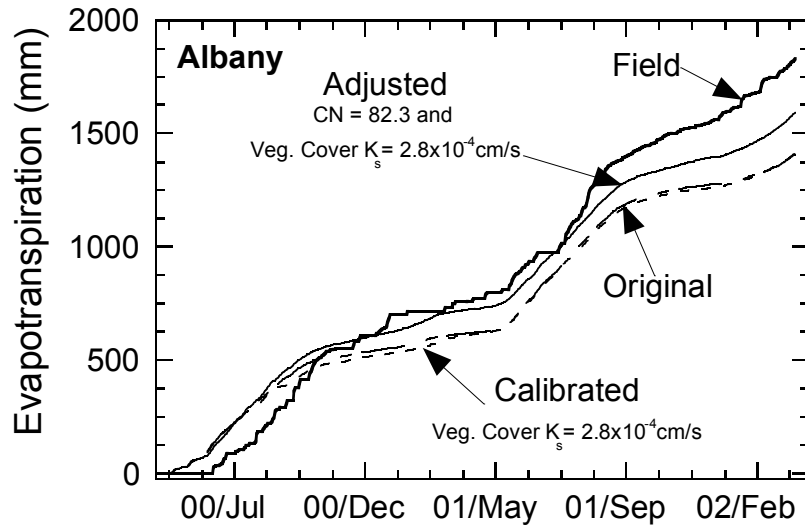


Fig. A30. HELP Comparison to Field Data for the Alternative Cover at the Albany Site.

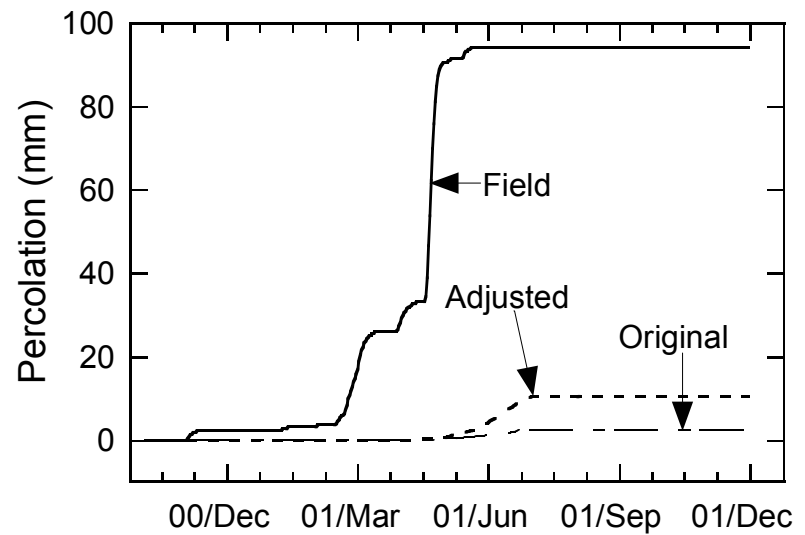
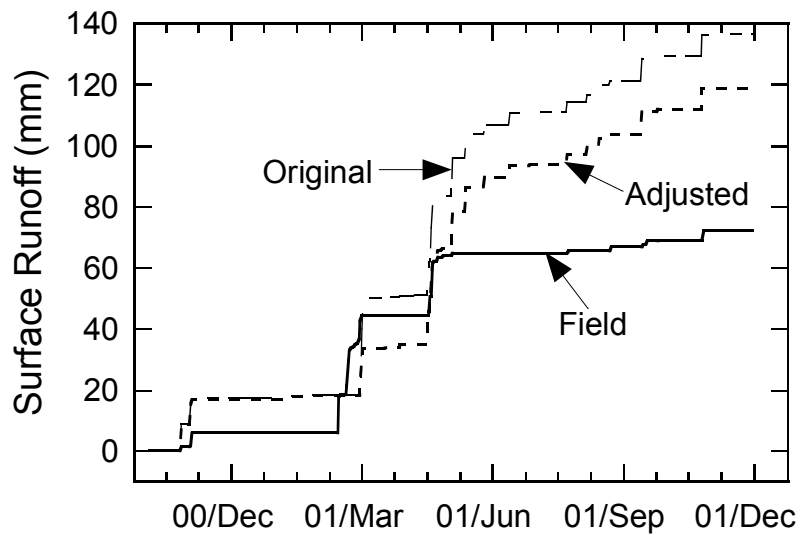
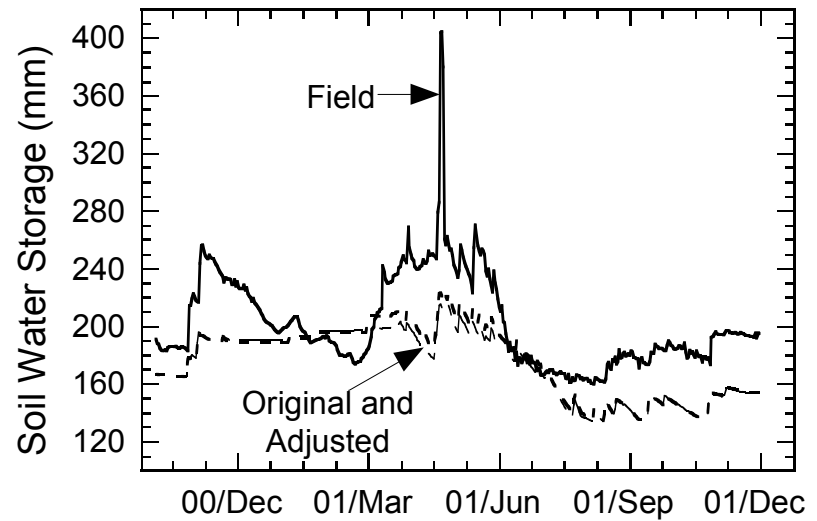
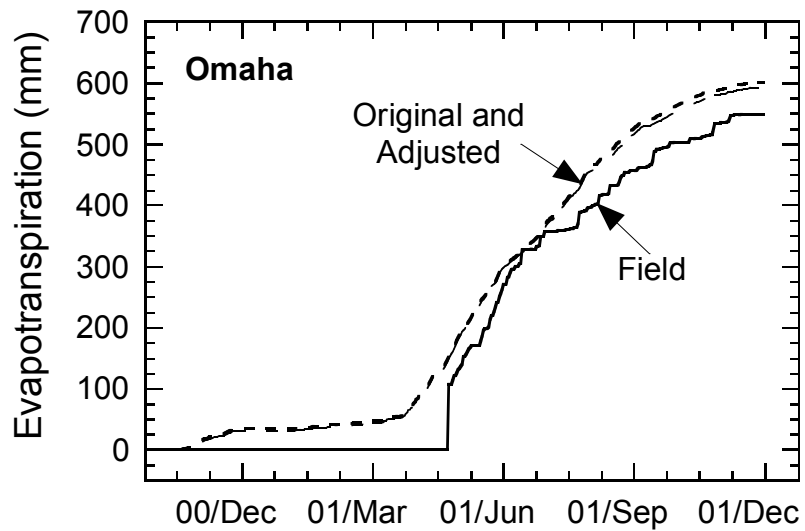


Fig. A31. HELP Comparison to Field Data for the Thin Capillary Barrier at the Omaha Site.

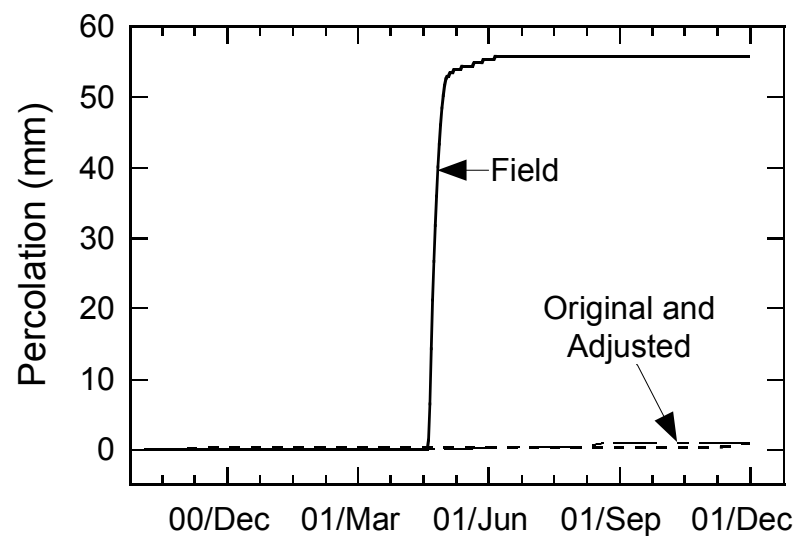
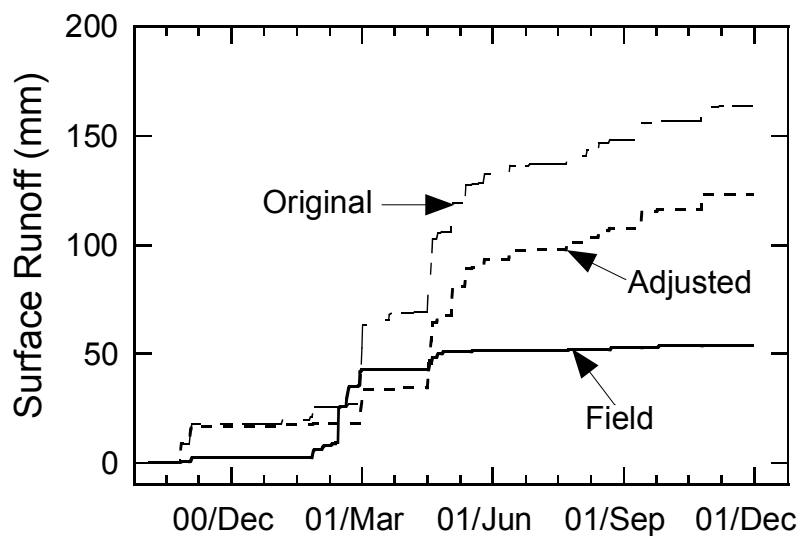
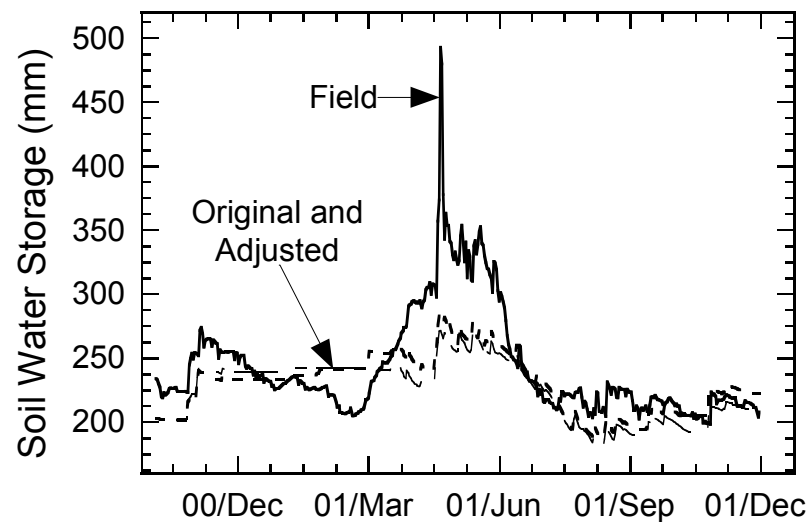
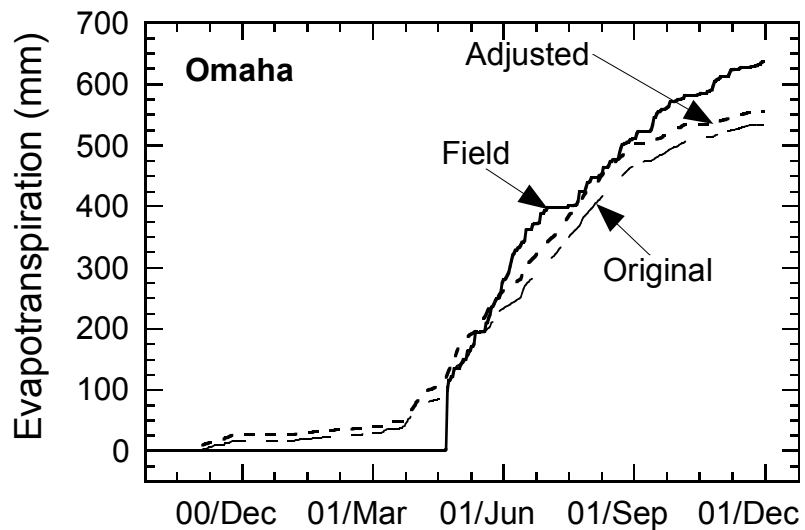


Fig. A32. HELP Comparison to Field Data for the Thick Capillary Barrier at the Omaha Site.